

**Alma Mater Studiorum – Università di Bologna**

---

**Scuola di Ingegneria e Architettura**

*D.I.C.A.M.*

*Dipartimento di Ingegneria Civile, Chimica, Ambientale e dei Materiali*

*Corso di Laurea Magistrale in Ingegneria Civile*

In collaboration with:

*Norwegian Geotechnical Institute*

*Offshore Geotechnics Section*

*Tesi di Laurea in Coastal Engineering*

**Offshore tower or platform foundations: numerical analysis of a laterally loaded single pile or pile group in soft clay and analysis of actions on a jacket structure**

Candidato:  
**Giacomo Tedesco**

Relatore:  
**Prof.Ing. Alberto Lamberti**

Correlatore:  
**Dott.Ing. Laura Tonni**

Anno Accademico 2012-2013  
Sessione III

-This page intentionally left blank-

## ABSTRACT

---

Laterally loaded piles are a typical situation for a large number of cases in which deep foundations are used. Dissertation herein reported, is a focus upon the numerical simulation of laterally loaded piles. In the first chapter the best model settings are largely discussed, so a clear idea about the effects of interface adoption, model dimension, refinement cluster and mesh coarseness is reached. At a second stage, there are three distinct parametric analyses, in which the model response sensibility is studied for variation of interface reduction factor, Eps50 and tensile cut-off. In addition, the adoption of an advanced soil model is analysed (NGI-ADP). This was done in order to use the complex behaviour (different undrained shear strengths are involved) that governs the resisting process of clay under short time static loads. Once set a definitive model, a series of analyses has been carried out with the objective of defining the resistance-deflection (P-y) curves for Plaxis3D (2013) data. Major results of a large number of comparisons made with curves from API (American Petroleum Institute) recommendation are that the empirical curves have almost the same ultimate resistance but a bigger initial stiffness. In the second part of the thesis a simplified structural preliminary design of a jacket structure has been carried out to evaluate the environmental forces that act on it and on its piles foundation. Finally, pile lateral response is studied using the empirical curves.

**Key words** P-y curves, offshore foundation, pile foundation, jacket structures, Plaxis3D 2013

## SOMMARIO

---

I pali caricati lateralmente sono situazioni comuni ove siano adottate fondazioni profonde. L'elaborato che segue tratta specificatamente di analisi numeriche di pali nelle citate condizioni di carico. Nel primo capitolo le impostazioni più performanti del modello sono esaustivamente trattate, con riguardo agli effetti dell'adozione dell'interfaccia, alla dimensione del modello e a quella della discretizzazione. Seguono tre analisi parametriche al fine di individuare la sensibilità del modello alle variazioni di: coefficiente riduttivo d'interfaccia, Eps50 e cut-off in estensione. In seguito è introdotto un modello avanzato di terreno (NGI-ADP), al fine di simulare al meglio il reale comportamento (diverse resistenze non drenate a taglio coinvolte secondo il regime tensionale, quindi del tipo di rottura, locale) di argille soggette a carichi statici impulsivi. Stabilito il modello definitivo, varie analisi hanno portato alla definizione delle curve resistenza-deflessione ottenute da Plaxis3D (2013). Risultati principali dei confronti tra curve sperimentali e curve da raccomandazioni API (American Petroleum Institute) sono: l'osservazione della medesima resistenza ultima e un'iniziale maggior rigidità delle curve empiriche ottenute da simulazioni numeriche. Nella seconda parte della tesi, è stata predimensionata una struttura jacket semplificata, valutando le sollecitazioni ambientali, quindi le azioni su jacket e fondazione. Infine, la verifica a caricamento laterale dei pali è stata eseguita con l'utilizzo delle curve P-y sperimentali.

**Parole chiave** curve P-y, fondazioni offshore, pali di fondazione, strutture jacket, Plaxis3D 2013

Bologna, 11.03.2014

Giacomo Tedesco

-This page intentionally left blank-

## ACKNOWLEDGMENTS

---

I would like to thank Senior Engineer Pasquale Carotenuto for his endless patience and help during my four months of permanence at the Norwegian Geotechnical Institute. A special thank must be listed to Thomas Langford, Head of Offshore Geotechnics Section at NGI; his positive response in June 2013 allowed me to do this amazing experience. These results have been made possible only after a series of gigantic helps constantly guaranteed to me by Khoa D.V.Huynh (Computational Geomechanics Division–NGI) and Professor Alberto Lamberti (DICAM-University of Bologna).

Professor Lamberti followed me during the development of this dissertation with attention and punctuality that must be highlighted.

A dedicated line must be written to my former flatmate, friend and (unaware) personal English teacher, Dr. Jürgen Sheibz.

No words can describe the mental support I have received from Angela, thanks for your presence fully alive.

I would like to thank my parents because they allowed me to benefit from these years of education and much more, something that only a loved son can understand. A dedication to my brother and to my grandparents for all the (unaware) relief valves that they constantly represented to me.

Giovanni and Alessandro played two important roles for this academic goal, relatively software and English grammar consulting. Mathias instead helped me with five years of pleasant conversations and cohabitation. In the end, a thought to all my friends, be they engineers, referees, scouts or simply Bortoloti'.

Dulcis in fundo Miani, I cannot forget the period passed with such a good friend. Bologna was ours.

## RINGRAZIAMENTI

---

Voglio ringraziare l'Ingegnere Pasquale Carotenuto per la sua infinita pazienza e aiuto fornitomi durante i quattro mesi della mia permanenza presso il Norwegian Geotechnical Institute. Un ringraziamento speciale va a Thomas Langford, capo della Divisione Offshore Geotechnics del NGI, che, col suo accettarmi come ospite, ha reso possibile questa formidabile esperienza. Questi risultati sono stati possibili solo grazie al costante consiglio di Khoa D.V.Huynh (Computational Geomechanics Division–NGI) e del Professor Alberto Lamberti (DICAM-Università of Bologna).

Il Professor Lamberti durante lo sviluppo di questo elaborato è stato in grado di seguirmi con un'attenzione e una puntualità davvero encomiabili.

Una riga deve essere dedicata al mio ex coinquilino e amico, nonché (inconsapevole) insegnante d'inglese, Dr. Jürgen Sheibz.

Non ci sono parole che possano descrivere il supporto mentale e affettivo datomi da Angela, grazie per la tua presenza così piena di vita.

Voglio dire grazie ai miei genitori per avermi garantito questi anni di formazione e molto di più, qualcosa che solo un figlio amato può capire. Una dedica a mio fratello e ai nostri nonni, per la loro (inconsapevole) capacità di farmi sfogare.

Giovanni e Alessandro hanno giocato due ruoli chiave in questa tesi, relativamente per consulenze inerenti software e linguistiche. Mathias invece mi ha aiutato con cinque anni di convivenza e parlate. Infine un pensiero a tutti i miei amici, siano essi ingegneri, arbitri, scout o più semplicemente Bortoloti.

Dulcis in fundo Miani, non posso scordare il tempo passato con un così buon amico. Bologna era nostra.

-This page intentionally left blank

# Index

---

ABSTRACT .....	I
Key words .....	I
SOMMARIO .....	I
Parole chiave .....	I
ACKNOWLEDGMENTS .....	III
RINGRAZIAMENTI .....	III
MODEL CONSTRUCTION.....	5
Modelling a solid pile .....	5
Cantilever verification .....	7
Solid section .....	7
Hollow section .....	10
Young modulus of the beam effect .....	12
Model dimension effect for the cantilever .....	14
Beam inertial moment effect .....	15
Full and half model .....	17
Beam position.....	20
Mesh dimension .....	21
Refinement clusters .....	26
Interface adoption.....	30
Model dimensions.....	34
PARAMETRIC ANALYSIS .....	37
Unexpected shear fluctuation .....	37
Eps50 (EpsC) .....	39
Tensile cut-off adoption .....	45
Interface reduction factor .....	49
P-Y CURVES.....	55
Matlock (1970) .....	55
Definition and use of the P-y curves .....	58
Lateral pressure calculation in Plaxis3D .....	60
Isotropic NGI-ADP soil model .....	71

- Anisotropic NGI-ADP soil model..... 82
- Experimental P-y curves ..... 95
- SIMPLIFIED ANALYSIS OF A REAL JACKET STRUCTURE ..... 99
  - International Standard ISO 19902..... 103
  - Actions calculation ..... 106
  - Piles foundation and P-y curves use..... 117
- CONCLUSIONS AND OBSERVATIONS..... 123
  
- REFERENCE ..... 127
  
- APPENDIX A – ANALYSIS OF GROUPS OF PILES ..... 129
  - Head isplacements ..... 129
  - Normalized head displacements using the maximum interaxis cases (F4-G4)..... 132
  - Normalized head displacements using SPLICE or Plaxis3D results ..... 135
  - Head displacements grouped by load ..... 138

*“Foundations can appropriately be described as a necessary evil.  
If a building is to be constructed on an outcrop of sound rock, no foundation is required.  
Hence, in contrast to the building itself which satisfies specific needs, appeals to the aesthetic sense,  
and fills its matters with pride, the foundations merely serve as a remedy for the deficiencies of whatever  
whimsical nature has provided for the support of the structure at the site which has been selected.  
On account of the fact that there is no glory attached to the foundations,  
and that the sources of success or failures are hidden deep in the ground,  
building foundations have always been treated as step children;  
and their acts of revenge for the lack of attention can be very embarrassing”*

Karl Terzaghi

-This page intentionally left blank

# INTRODUCTION

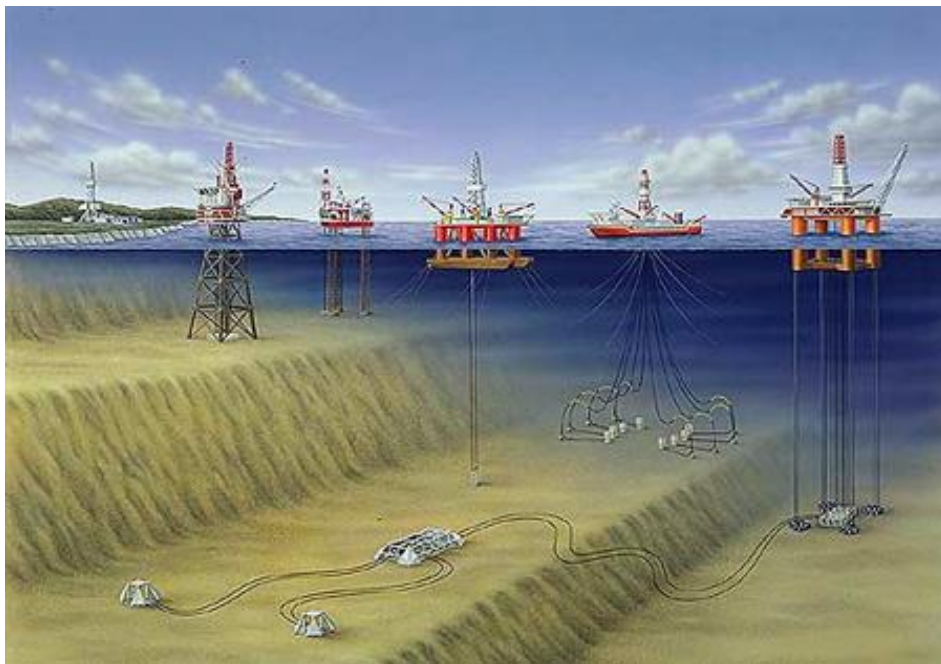
---

Since the beginning of the offshore activities, in the first half of the past century, piles have been the more diffuse technique to fix the steel structure to the seabed.

Nowadays, piles are largely used in relative shallow conditions of water depth. Fixing towers and jacket structures to the seabed is the principal role played by piling engineering today.

Development of a new type of foundation has become necessary in order to exploit oil reserves in very deep water. So, with the diffusion of floating producing system, other types of foundation have been introduced as bucket foundation or suction pile.

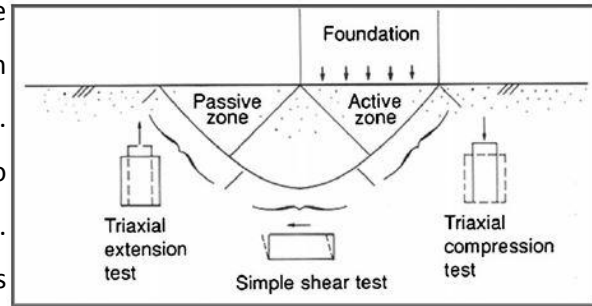
In the picture below the main offshore structure are shown, relatively from right: jacket, rig, semi-submersible, FPSO and TLP. Different types of foundation mean different peculiarities and analyses.



In the following master thesis a special attention is put upon the problem represented by laterally loaded piles in soft clay.

In order to run more realistic simulations, an advanced soil model is used. The final simulations are run adopting the NGI-ADP soil model on the optimized numerical model. The NGI-ADP soil model has been created to perform the real behaviour of clays in undrained conditions, which is the effective condition for a static short term load of a pile in cohesive soils.

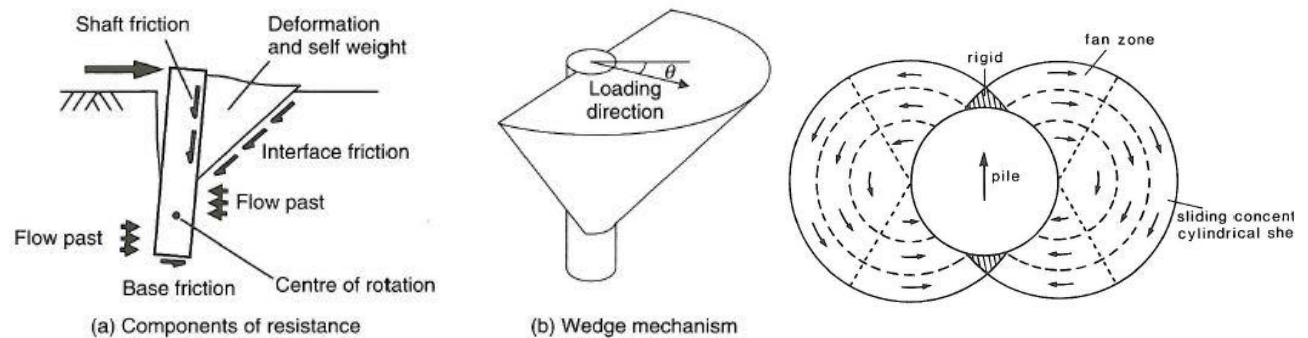
In the picture on the right, it is easy to recognize the importance of identifying clearly which resistance is interested by the resisting process. The picture reports the different tests able to furnish the correct shear strength zone by zone. Peculiarity of the NGI-ADP soil model is its capability of using all these three undrained strength in relation to the local stress regime.



Numerical simulation probably represents the future of advanced pile design but since the early 70es the most common procedure for designing laterally loaded piles has used the P-y curves. They are representative of a simple concept of non-linearity defined by Hudson Matlock into his paper of '70.

The result of this master thesis is exactly the P-y curves, calculated by Plaxis3D simulations.

The expected failure mechanism for the pile has been only partially confirmed, because the moment of a wedge of soil behind the pile is confirmed, but the displacement vectors of the integration point of the mesh do not allow defining clearly a soil flowing around the pile.



Different sensibility analysis will give an idea about the model behaviour for several parameters changing into their respective engineering range.

Defined the P-y curves, a real case is analysed; it has been possible doing that thanks to metocean data furnished by Kvaerner, a Norwegian contractor.

Performance of the pile foundation of a simplified jacket structure will be the test bench for the results just obtained.

Furthermore the preliminary structural design put in evidence a large number of aspects that must be accurately evaluated in order to guarantee a margin of safety for the platform.

Calculation of waves, wind and current actions on the structure has the indispensable passage to obtain the load acting on the foundation.

Known actions and empirical P-y curves, a comparison with curves from API recommendation is done in order to get the reliability of the method proposed.

Results will confirm some observations just found in the specific papers.

**IMPORTANT:** No space is assigned to software description, in order to report uniquely the real work personally developed. For the same reason only the indispensable theoretical concepts are listed, where strictly necessary.

-This page intentionally left blank-

## MODEL CONSTRUCTION

---

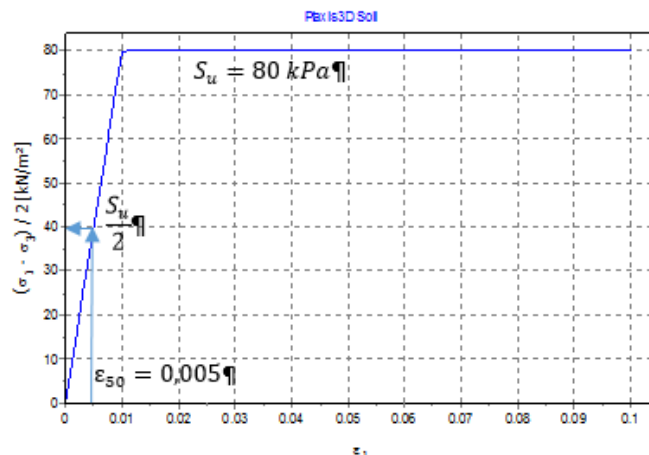
In order to allow a comparison between SPLICE and Plaxis3D, it becomes necessary to define the same soil and the same pile. This objective presents the simple problem that those softwares need in input of different setting to model a soil because SPLICE works with non-linear springs while Plaxis3D is a finite element solver, so it needs a more advanced and complicated setting.

Validation of the soil model used has been made by a soil test simulation (available in Material Setting window of Plaxis3D), confirming that the soil defined in Plaxis3D is equivalent to SPLICE soil.

In the FEA input was defined a shear modulus obtained by the following relationship:

$$G_{50} = \frac{S_u}{2} * \frac{1}{\gamma_{50}} = \frac{S_u}{2} * \frac{1}{1,5 * \varepsilon_{50}}$$

The value of shear modulus defined above from undrained strength and  $\varepsilon_{50}$  (also defined as EpsC in SPLICE, it's the strain at half the maximum stress from laboratory compression tests on clay samples. Typical values range from 0.005 to 0.02 (from 0.5% to 2%) leads to correct results, for instance below is shown a soil test run with Plaxis3D for an undrained shear strength equal to 80 kPa and Eps50 equal to 0.5%; this simple test confirm the expectation.



### Modelling a solid pile

SPLICE gives in output directly the values of the variables of interest, while there is a different situation in Plaxis3D.

Plaxis3D is a commercial software for finite element analysis of problems concerning soils and interaction soil-structure.

Normally it is not necessary to know the pressure in the contact surface pile-structure, but for the purpose of this study it is indispensable.

In order to do that, a strategy is developed to obtain the lateral pressure directly from the Plaxis3D output.

Plaxis3D has elements “embedded pile” but they are not suitable for this function because they give in output bending moment, shear and displacement with a good approximation, but they are represented by a line without thickness which means losing the soil behavior around the pile, for instance using embedded pile is not possible to observe the soil movements all around the pile shaft.

For this reason, it was decided to model the pile using soil elements with assigned properties for the pile (in the next two paragraphs the properties to use for the pile setting are largely discussed). This solution gives more representative results, of the interaction pile-soil, but presents a gigantic problem like the impossibility to obtain the structural action for each pile section.

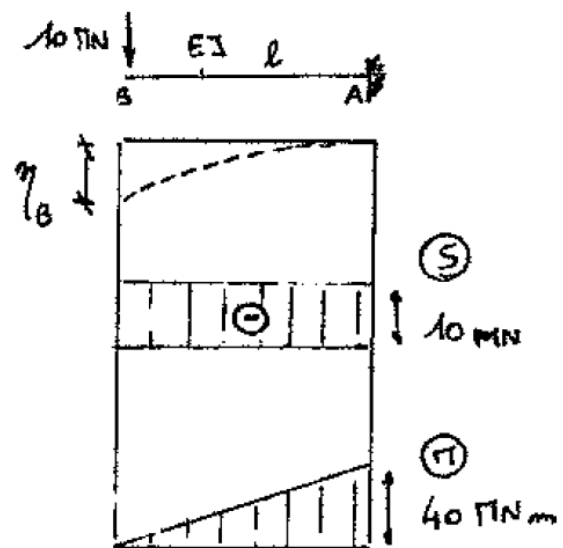
To solve this unfriendly problem there are two solutions: the first one is merely theoretical because it consists in a numerical integration of the tension on the volume elements that represent a section while the second one is the more realistic use of a “false” beam only for post-processing use.

The position for this beam is naturally the pile axis in case of full pile modeled. A different consideration about the beam position will be done in the paragraph dedicated to this problem for only half pile modeled, using the symmetric condition of the situation modeled.

Using a beam leads to obtain directly in output by Plaxis3D the displacement, bending moment and shear.

The beam must not influence the pile stiffness, but it must be representative of the pile behavior. For this reason, and in order to avoid problem related to results scaled of strange value, the beam is set with a Young modulus equal to the pile scaled one thousand times.

In the end, the calculation of lateral pressure will be treat in a specific section of the next chapter.



## Cantilever verification

### Solid section

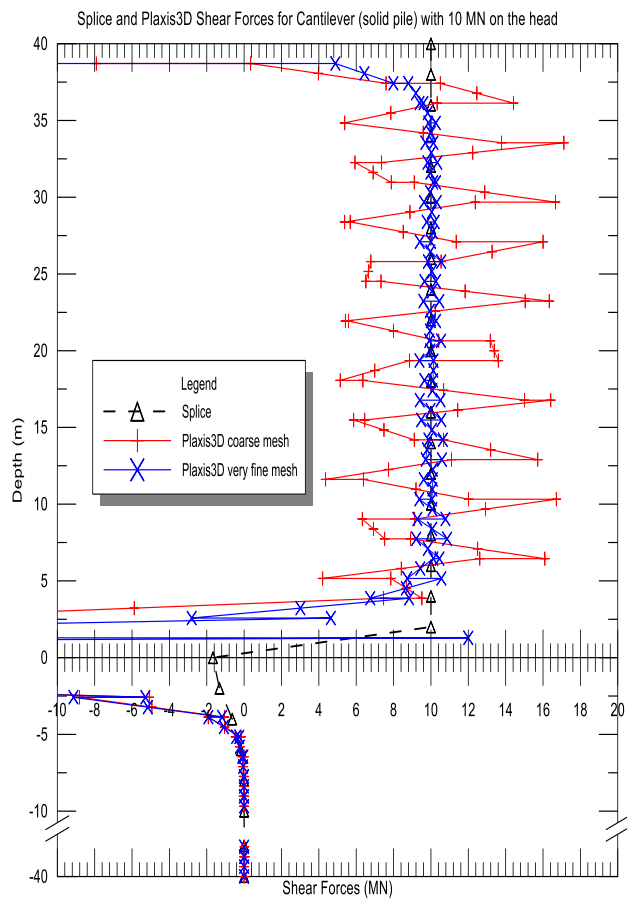
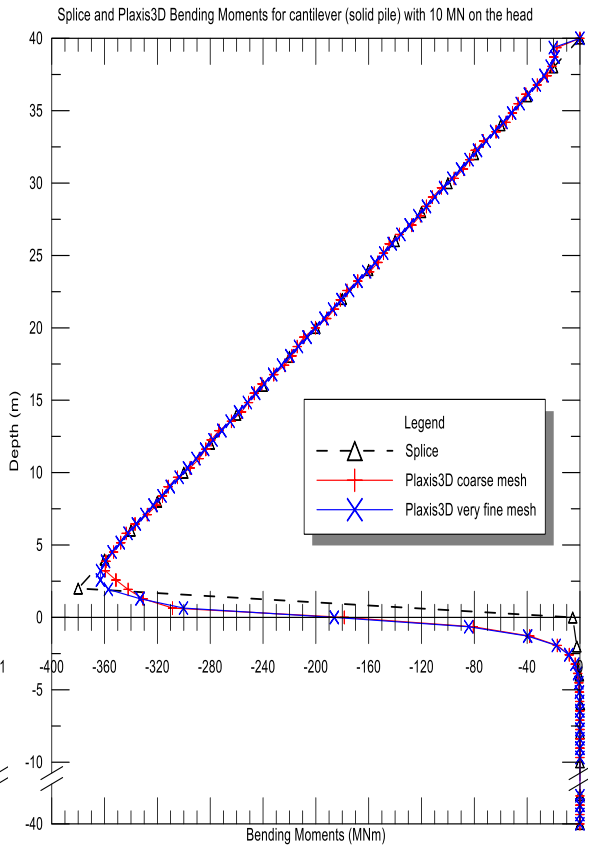
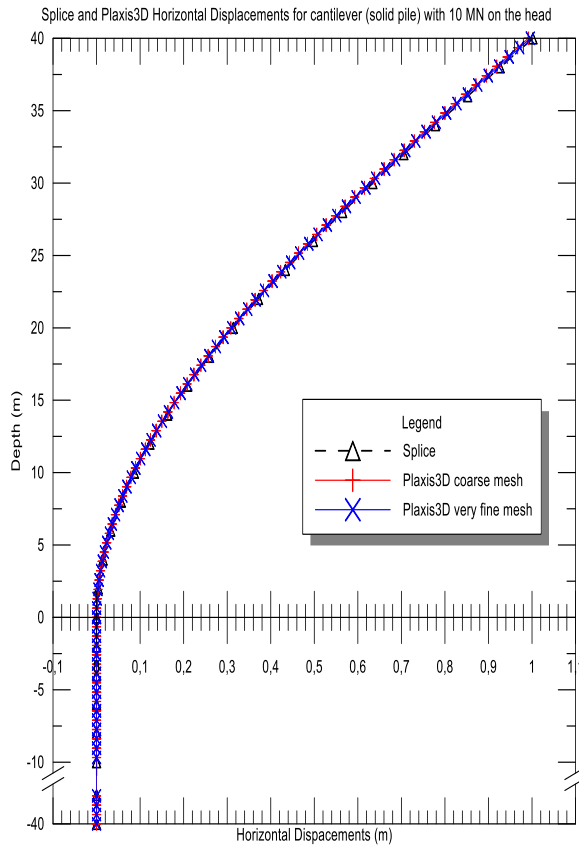
This first numerical simulation has been carried out with the objective of focus on the problem that affects the model developed to perform the behavior of a pile laterally loaded, because initially, during the first period of simulations, there were several incongruity within the results. To validate our own model, it was chosen to do a comparison between it and a note case, so the cantilever case has been chosen for the evaluation. It was chosen to work with a steel full section pile to avoid doubts about the behavior of the FE software.

The restrain condition is reached using two different tricks: very stiff soil and restrained sections; this second condition is due to the need of zero displacements and rotations at the ground level. In Plaxis3D two fixed sections has been used to model the restrain, one at the pile tip and the other at the ground level whereas in SPLICE six springs have been adopted, each one having been set with very stiff properties in order not to allow movements or rotations in the relative direction.

FE analysis (Plaxis3D model) is composed by soil (set very stiff), solid equivalent pile, beam (to get easy the post processing phase), restrained sections and point force.

In the table below the main characteristics of Plaxis3D model are shown.

PLAXIS3D			
LOAD		SOLID PILE (hollow pile equivalent)	
X-direction Point Force	10 MN	Length	80 m (40+40)
SOIL		Outside Diameter	2,134 m (84 inches)
Material Model	Mohr-Coulomb	Material Model	Linear Elastic – Non Porous
Drainage Type	Undrained (C)	Young Modulus	E_steel (210E6 kPa)
Undrained Young Modulus	self-compute from G_50	BEAM	
G_50	$S_u/(2*1,5*E_{ps\_C})$	Young Modulus (E_beam)	(E_solid_pile)E-6
Su	9E9 kPa	Section Area (A_beam)	A_solid_pile
Interface	Rigid	Inertia Moment (J_beam)	J_solid_pile
SPLICE			
LOAD		SPRINGS STIFFNESS	
X-direction Point Force	10 MN	K trasl. (rotat)	9E9 m/kN (deg/kN)
HOLLOW PILE		SOIL	
Outside Diameter	2,134 m (84 inches)	Z_bottom	50 m
Wall Thickness	1,067 m	Su	9E3 kPa
Length	80 m (40+40)	Eps_C	0,005 (-)



The comparison between the results obtained by SPLICE and Plaxis3D is herein done through bending moments, horizontal displacements and shear forces trends.

Due to zero constant value, the graphs don't show the trends between -10 and -38 meters.

For displacements and bending moments the fitting is perfect and agrees with theoretical results. A little difference can be noted at ground level for the bending moment value, probably tied to some computational "problems" of FE and it should reduce itself increasing the discretization.

Different reasons must be done for the shear forces trend, where a great dispersion affected Plaxis3D results. This behavior could be linked to beam elements Plaxis3D that compute the shear force by the bending moment derivative. An attempt to increase the shear quality was carried out by changing the modulus of elasticity of the beam. This attempt is presented in the next pages.

Next validation step is to repeat cantilever simulation for the hollow pile, in order to get possible problems connected with the new geometry of the section.

### Hollow section

Objective of this series of numerical simulation is to focus on the problem that affects the model developed to perform the behavior of a pile laterally loaded. To validate our own model, it has been chosen to do a comparison between it and a cantilever (known case).

As just explained in the last paragraph, the condition of restraint is reached using very stiff soil and restrained sections; this second adoption guarantee zero displacements and rotations at the ground level.

In the picture in the next page, the restrained section is represented by a green crown around the pile, at the pile tip and at ground level.

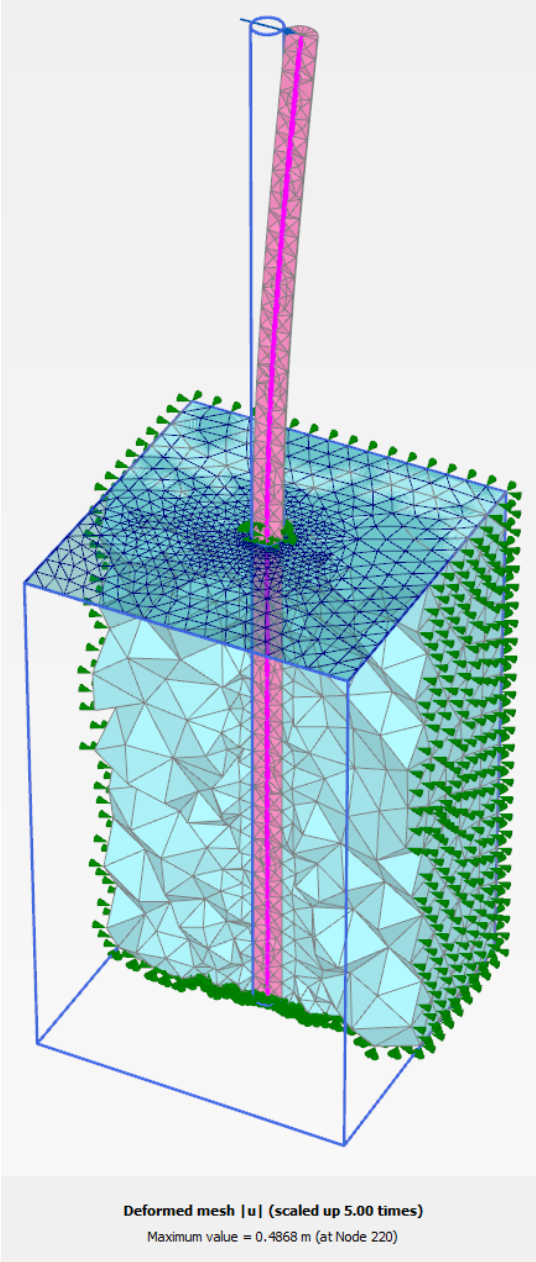
Equivalent parameters for hollow pile are calculated in the following way:

$$E_{solid\ equivalent\ pile} = \frac{E_{steel} * J_{hollow\ real\ pile}}{J_{solid\ pile}}$$

$$\gamma_{solid\ equival.pile} = \frac{\gamma_{steel} * V_{steel(hol.pile)} + \gamma_{soil} * V_{soil(inside\ hol.pile)}}{V_{total\ pile}}$$

In the table below, the main setting of Plaxis3D and SPLICE models are presented.

PLAXIS3D			
LOAD		Model Type	
X-direction Point Force	Young Modulus	Young Modulus	Linear Elastic – Non porous 43E6 kPa
BEAM		SOIL	
Young Modulus (E_beam)	(E_solid_pile)E-6	Model	Mohr-Coulomb
Section Area (A_beam)	A_solid_pile	Drainage Type	Undrained (C)
Inertia Moment (J_beam)	J_solid_pile	Undrained Young Modulus	self-compute from G_50
<b>SOLID PILE (hollow pile equivalent)</b>		<b>G_50</b>	Su/(2*1,5*Eps_C)
Length	80 m (40+40)	Su	9E9 kPa
Outside Diameter	2,134 m (84 inches)	Interface	Rigid
SPLICE			
LOAD		SPRINGS STIFFNESS	
X-direction Point Force	1 MN	K trasl. (rotat)	9E9 m/kN (deg/kN)
HOLLOW PILE		SOIL	
Outside Diameter	2,134 m (84 inches)	Z_bottom	50 m
Wall Thickness	6 cm	Su	9E3 kPa
Length	80 m (40+40)	Eps_C	0,005 (-)



**Young modulus of the beam effect**

Herein, the comparison of the results came out from Splice and Plaxis3D is done through bending moments, horizontal displacements and shear forces trends. Beam Young modulus is set small in order to avoid a false stiffness increase.

As in the last chapters, the graphs do not show the curve trends between -10 and -38 meters.

For displacements and bending moments, the fitting is perfect and it agrees with theoretical results calculated by hand.

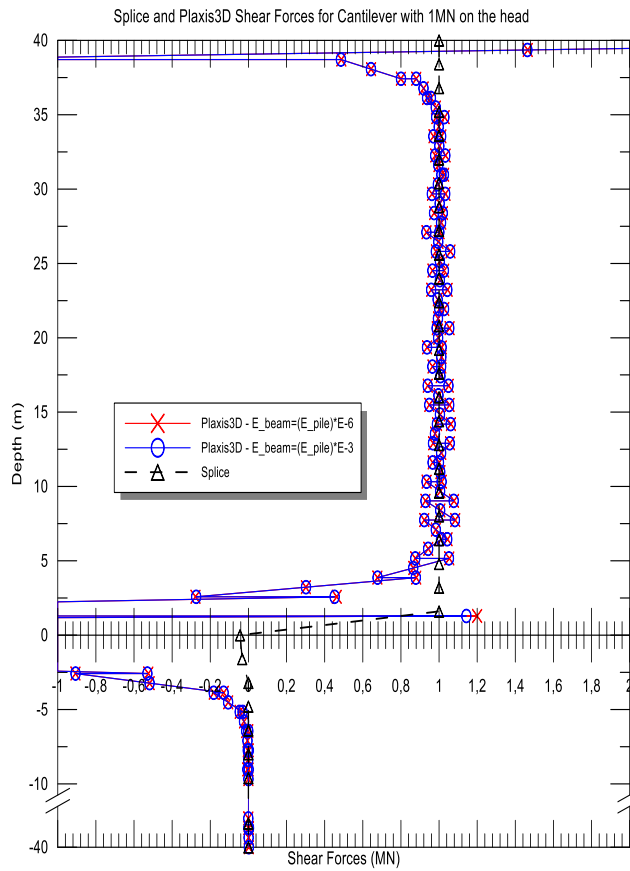
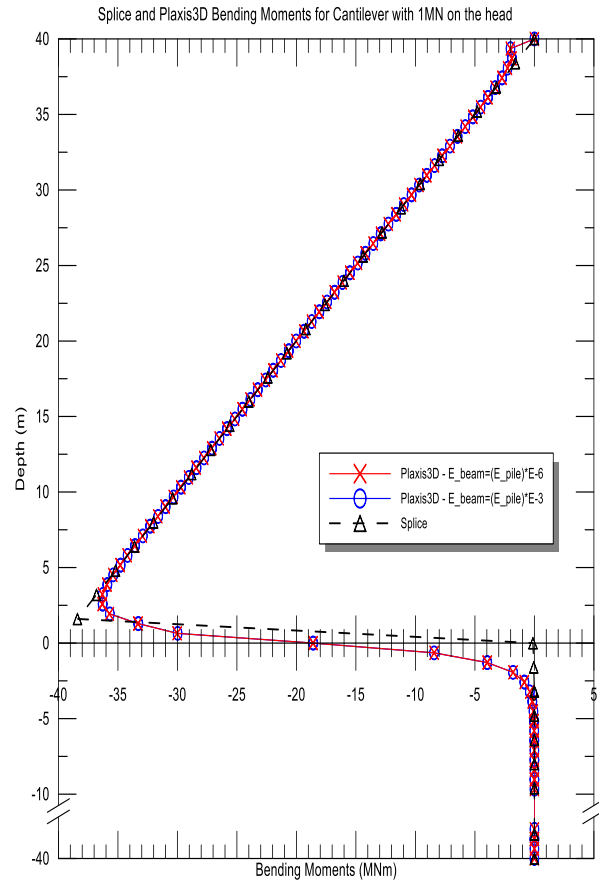
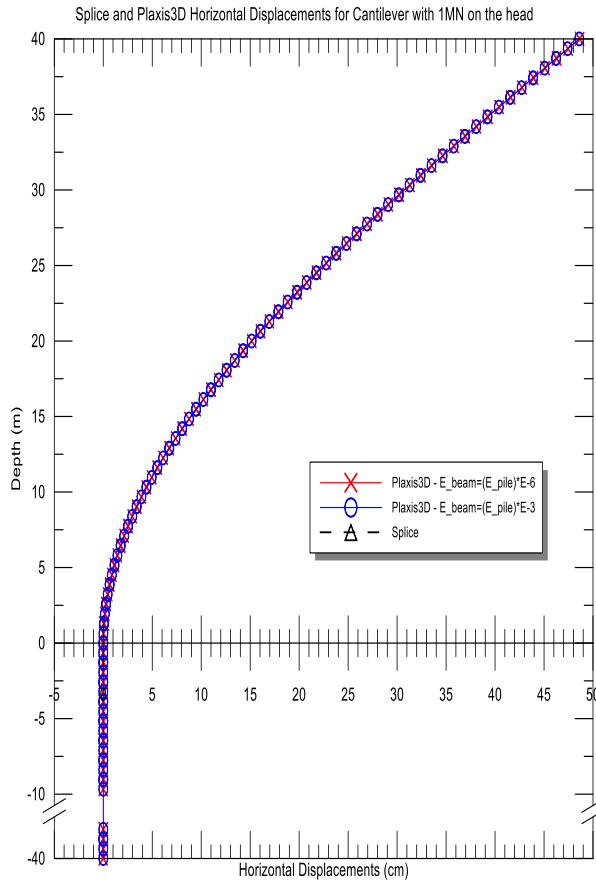
A little difference can be noted at ground level for the bending moment value, probably tied to some computational "problems" of FE, a behavior just observed into others numerical simulations.

Different reasons must be elaborated for the shear forces trends, where a great dispersion affects Plaxis3D results.

This behavior could be linked to the one for beam elements Plaxis3D that computes the shear forces by the bending moment derivative. We obtained moment data from the false beam for post processing; we had assigned to it a very small Young Modulus (reduced by a million times). This means that bending moments computed by Plaxis3D, shown in the graphs herein reported, have multiplied by about one million times from the original output data, meaning that a very little fluctuation of moment can involve a strong shear variation.

This problem is partially reduced adopting the beam Young modulus scaled only  $E-3$  times. Furthermore, this is a great help for the engineer, because the Plaxis3D output values are along these lines just in MN and MNm (output in kN and kNm but scaled  $E-3$  times means that the value is just in mega Newton).

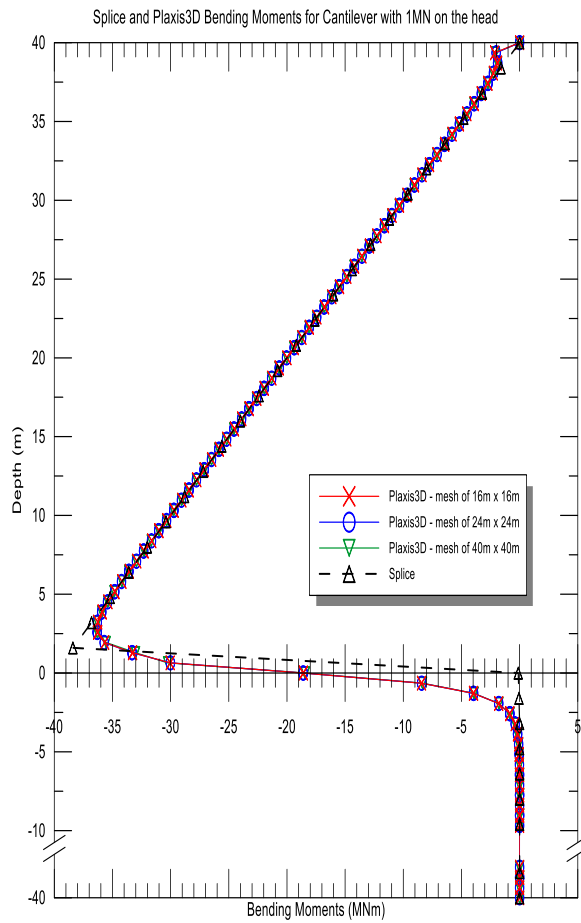
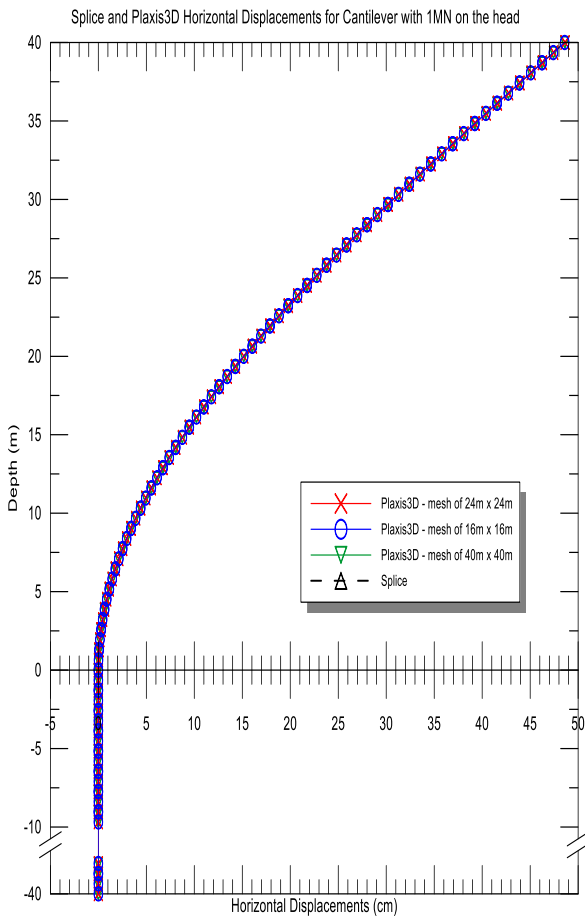
With this Young modulus increasing, the stiffness of the system pile-beam is governed by the pile stiffness, so a beam modulus of elasticity scaled a thousand times from the true value (pile modulus of elasticity) gives absolutely negligible effects.

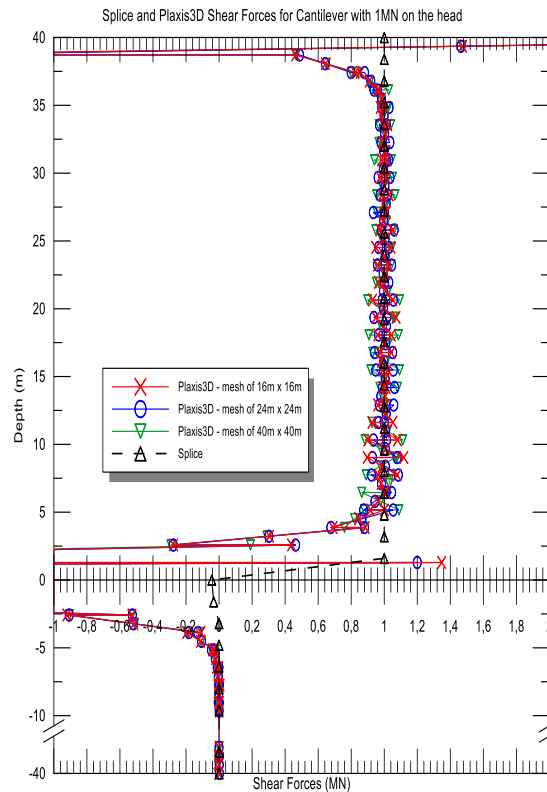


**Model dimension effect for the cantilever**

Down below here, the results comparison is presented, by Splice and Plaxis3D, for the same problem, i.e. hollow pile cantilever, with different base dimensions for Plaxis3D model.

In agreement with our own previsions, there are not differences. Indeed, the cantilever is used in order to investigate the pile behavior and the soil must not influence the results. The restrained sections block the pile into the soil in order to obtain a cantilever.





**Beam inertial moment effect**

It's interesting to note that the model response for the beam inertial moment is set equal to the inertial moment for a hollow section: results obtained for bending moment and shear force are completely wrong (blue curves into below). It is explained by the simple reason that those trends do not respect the equilibrium condition (bending moment and shear must be equal to 40MNm and 1MN respectively at the first restrained section). Instead, the displacements are correct.

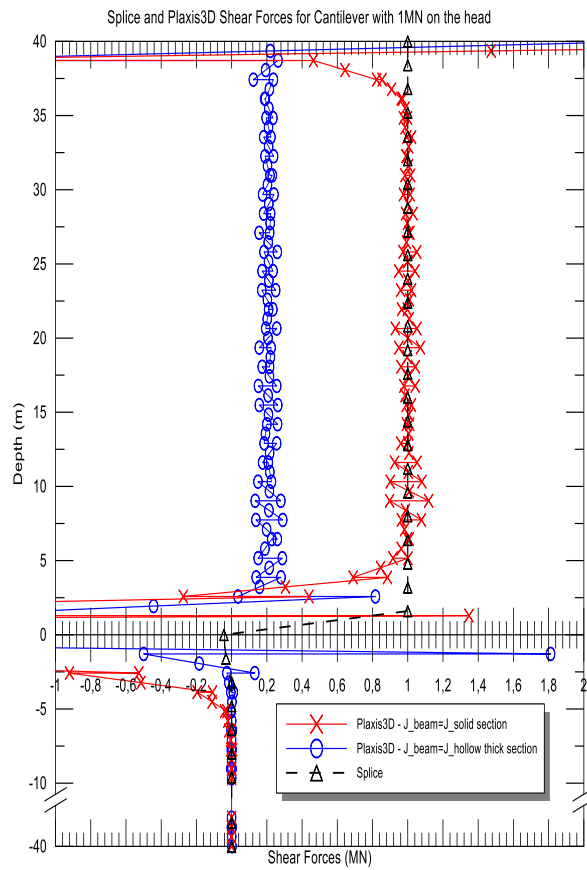
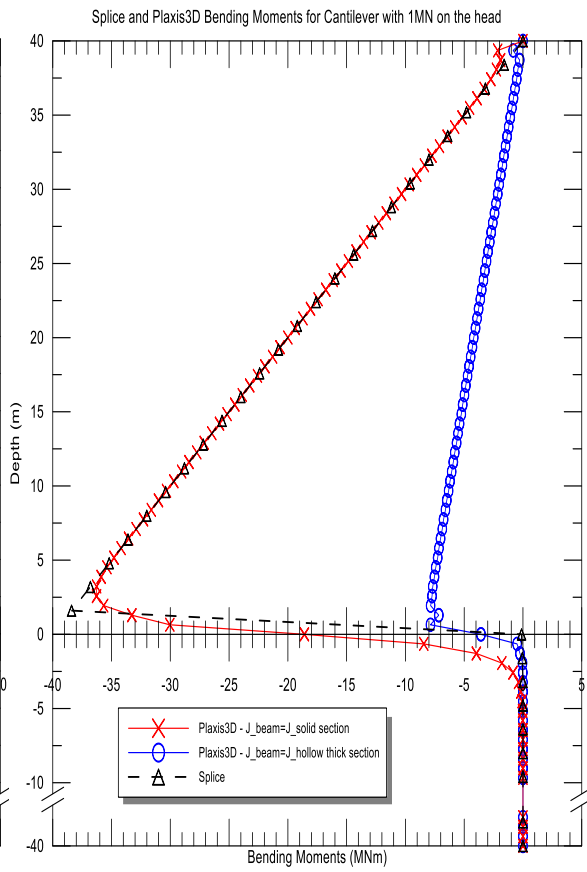
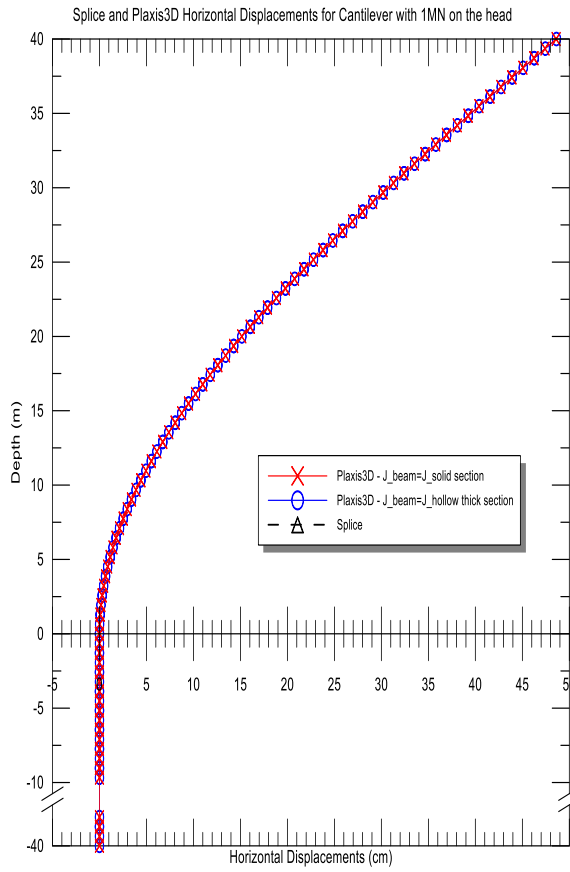
The motivation of that erroneous behavior could be due to a kind of surplus of "information" about section properties, because they are just "included" into the displacement value where displacements are function of  $E^*$ , i.e.  $E_{beam}$ , is function of inertial moment of hollow real pile section. Displacements calculation does not use  $E_{beam}$ , so displacements are not affected by this kind of information redundancy.

This means that assigning to the beam an inertial moment of hollow section (real pile) produces a superabundance of information, in facts bending moment and shear trends are scaled of the ratio between hollow section and solid section inertial moments. For the bending moment:

$$M_{beam} = E_{beam}J_{beam}\chi = E_{beam}J_{beam} \frac{d^2u_{beam}}{dz^2}$$

$$u_{beam} = u_{pile} \quad u_{pile} \equiv u_{pile}(E^*) \quad T_{beam} = \frac{dM_{beam}}{dz}$$

$$E^* \equiv E^*(J_{hollow\ real\ pile}, J_{solid\ equivalent\ pile}, E_{steel}) \quad \text{but} \quad E_{beam} = 10^{-6}E^*$$



## Full and half model

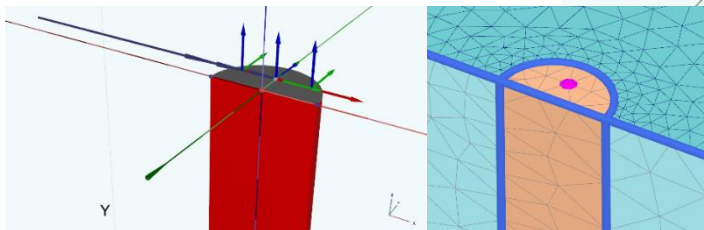
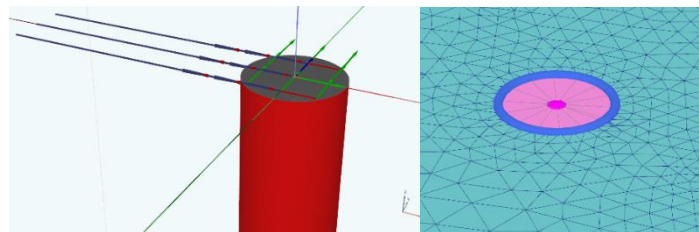
In order to reduce the computational costs for FEA, it was decided to work with only a half model. This means a substantial time reduction for each PLAXIS3D run for an equivalent fine discretization. Using this trick it became possible to spend the same time for a run with a finer mesh in the correct place. It has to be kept in mind that a "surface load against a point load" adjustment has already been used to reduce the local effects on the highest beam elements. This has been done in order to reduce local effects related to tension diffusion on the pile head, but the results showed that the problem is only reduced but not avoided. This will be discussed in a specific section of the next chapter.

PLAXIS3D			
FULL MESH		HALF MESH	
<b>DIMENSIONS (x/y/z)</b>			
40m/40m/50m		40m/20m/50m	
<b>LOAD</b>			
X-direction force (surface load)	10 MN (2796 kN/m <sup>3</sup> )	X-direction force (surface load)	5 MN (2796 kN/m <sup>3</sup> )
<b>POST PROCESSING BEAM</b>			
Position (in plan)	Pile Axis	Position (in plan, from pile axis)	Y_beam/Radius=0,2804
Young Modulus (E_beam)	(E_solid_pile)E-3	Young Modulus (E_beam)	((E_solid_pile)E-3)/2
Section Area (A_beam)	A_solid_pile	Section Area (A_beam)	A_solid_pile/2
Inertia Moment (J_beam)	J_solid_pile	Inertia Moment (J_beam)	J_solid_pile/2
<b>SOIL</b>			
Model	Mohr-Coulomb	Model	Mohr-Coulomb
Drainage Type	Undrained (C)	Drainage Type	Undrained (C)
Undrained Young Modulus	self-compute from G_50	Undrained Young Modulus	self-compute from G_50
G_50	Su/(2*1,5*Eps_C)	G_50	Su/(2*1,5*Eps_C)
Su	80 kPa	Su	80 kPa
Interface	NO	Interface	NO
<b>SOLID PILE (hollow pile equivalent)</b>			
Section	Circular	Section	Semicircular
Length	40 m	Length	40 m
Outside Diameter	2,14 m (84 inches)	Outside Radius	1,07 m (42 inches)
Model Type	Linear Elastic – Non porous	Model Type	Linear Elastic – Non porous
Young Modulus	43E6 kPa	Young Modulus	43E6 kPa
<b>SPLICE</b>			
<b>LOAD</b>			
X-direction Point Force		10 MN	
<b>HOLLOW PILE</b>		<b>SOIL</b>	
Outside Diameter	2,134 m (84 inches)	Z_bottom	50 m
Wall Thickness	6 cm	Su	80 kPa
Length	40 m	Eps_C	0,005 (-)

In this report three different solutions to compute the lateral pressure (fundamental to estimate of P-Y curves) from different Plaxis3D data are shown (results into the graph of lateral pressure in the next page).

The first way to calculate the lateral pressure needs to fit the bending moment trend with a six order polynomial trendline, then a second order derivative of the trendline equation must be done. Finally, to obtain a force the previous result is divided by the pile diameter. The second way to calculate the lateral pressure is conceptually the same as the first one and the only difference is that shear curve is fit with a fifth order polynomia and so a first order derivative is sufficient.

Finally this “empirical” derivative (calculated “by hand”): shear variation is divided by depth and then divided by the pile diameter.

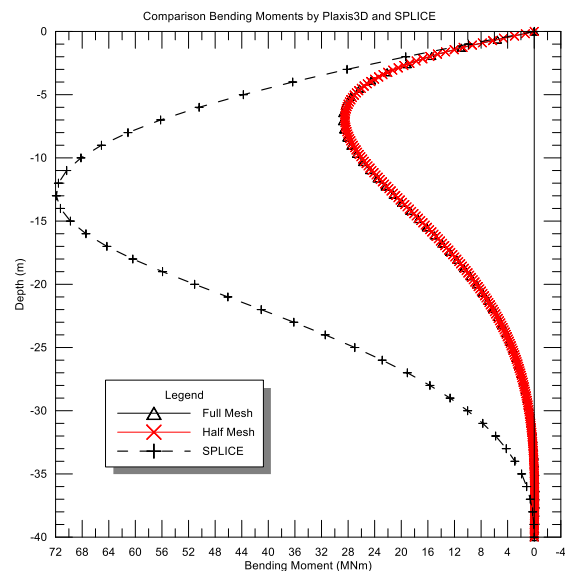
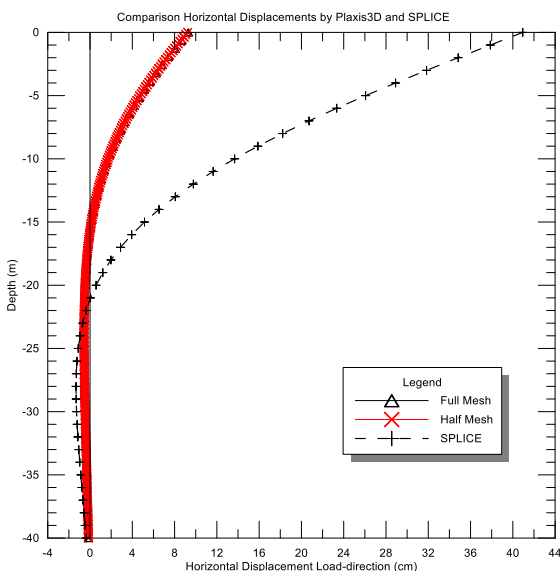


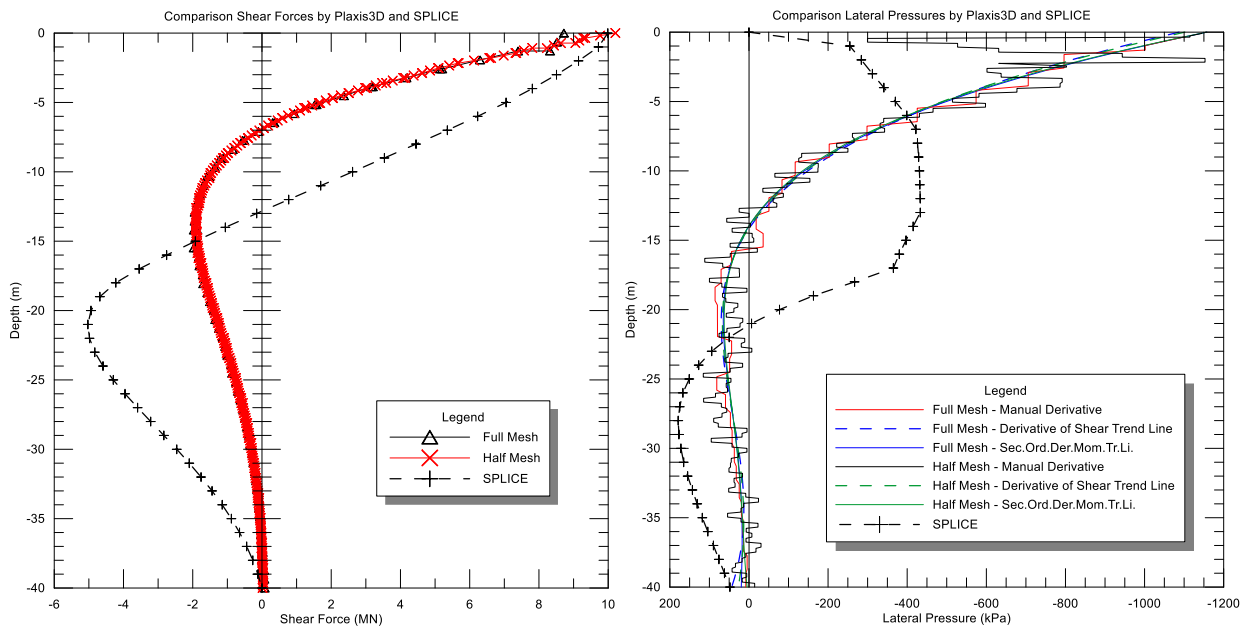
Expressed in a formula:

$$Lateral\ Pressure_{manual\ derivative} = \frac{Shear_i - Shear_{i+1}}{(Depth_i - Depth_{i+1})D}$$

Lateral pressure calculation will be largely discussed in a dedicated section.

To avoid local phenomena which do not fit with the corresponding trendline, an intersection value for shear (equal to load) and bending moment (zero) was set on the pile head. In this way, the first beam element is bypassed.





As it can be seen in the graphs above, the work with half a full mesh have same behavior. In detail: shear distributions show that Plaxis3D computes a lower maximum negative value than SPLICE (2.5 times less) and therefore the peak of the curve is localized 7 meters deeper for SPLICE. The same application is valid for the peak reduction and relocation of the bending moment trends. The horizontal displacements from Plaxis3D are 4.5 times lower than from SPLICE and the point of zero displacement is moved up by around five meters for Plaxis3D.

Last observations have been done on wrong results, because the model length used in Plaxis3D was too small and for this reason the model response is too stiff.

Lateral pressure graphs show that the analytical derivative method gives equal results while the manual derivative results get an important dispersion around the trend read from the analytical derivative. The fluctuation magnitude increases with a fine beam discretization (half mesh). Near the pile tip this behavior is due to a little and slow shear variation with the depth. At the pile tip all curves show a very little value but none as low as zero. On the pile head: SPLICE computes zero while Plaxis3D gives the maximum lateral pressure value. Through an approximate evaluation all curves include an equivalent area.

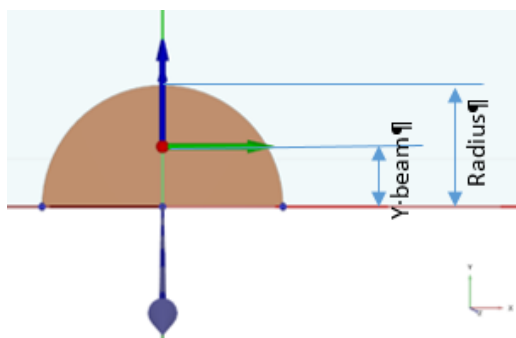
A stiffer response from Plaxis3D was expected (2) but not so stiff. The next step will be a new approach for a better match between SPLICE and Plaxis3D, using an interface or a coaxial layer of soil with weak properties (with an equivalent effect to an interface).

### Beam position

The use of half a mesh has entailed a sensible time reduction for each run but at the same time a problem's started due to the beam position.

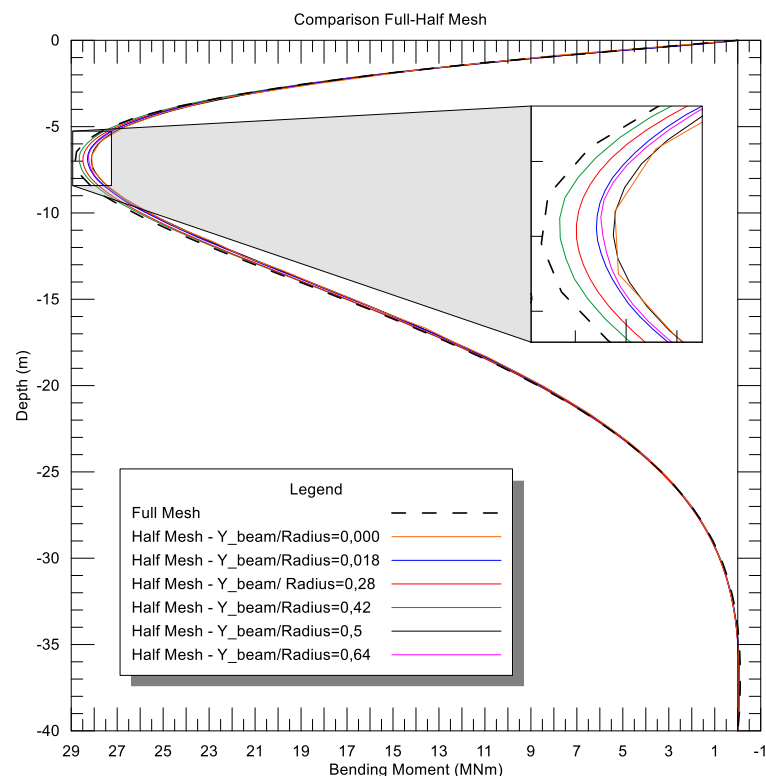
The beam is used only for helping the engineer during the post processing phase i.e. against several difficult volume integrations on the equivalent pile volume, using the beam became possible to obtain all the interesting variables (mainly bending moment and horizontal displacement than shear) directly from Plaxis3D. Below are shown results for different beam positions: coinciding with the pile axis (that for half mesh used model is part of the mesh border).

Herein are reported only bending moment data, for the simple reason that is the unique trend with a



sensible variation with the beam position. For exam cases the maximum bending moment variation peak has been found in the order of 3,4% (against full mesh value). In case of horizontal displacement analysis (not reported herein) this error is halved.

Different changing beam positions run give a clear result: the best match between a half and a full mesh is found for a beam position equal to the sectional barycenter. In this case, there is a relevant reduction against full mesh value (2%). This could be due to some effect in the solid pile related with the tangential stresses diffusion, maybe something like a torsional effect.



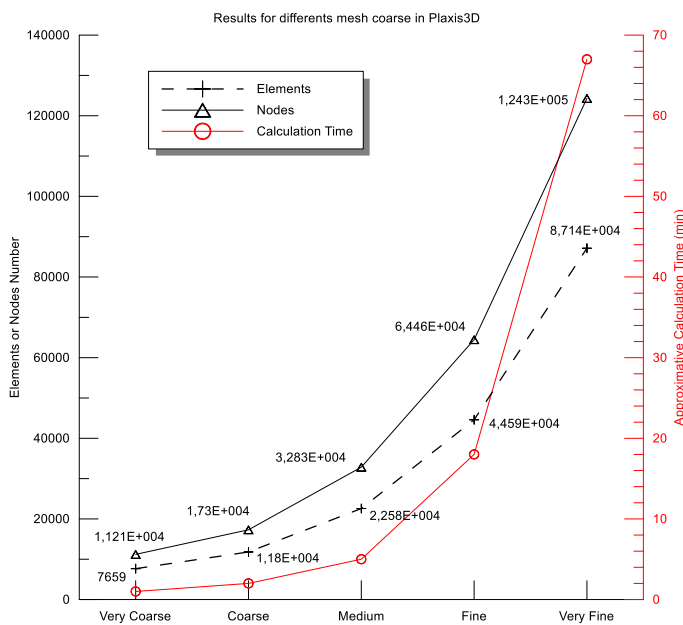
### Mesh dimension

Objective of the study herein reported is to show the trend changing for bending moments, shear force and horizontal displacements computed for different coarse of mesh elements.

Adopting the best compromise for the element size in a finite elements analysis is the main choice for the engineer.

Mesh Type	Approx. Time (min)	TOTAL		BEAM		Max.Displacements		Max.Sheer		Max.Moment	
		Elements (-)	Nodes (-)	Elements (-)	Nodes (-)	Value (cm)	Rel.Err. (%)	Value (MN)	Rel.Err. (%)	Value (MNm)	Rel.Err. (%)
Very Coarse	1	7659	11206	60	180	8,664	13,038	9,96	3,2318	27,06	11,4528
Coarse	2	11799	17298	74	222	9,076	8,9029	9,73	0,8493	28,18	7,78795
Medium	5	22575	32829	74	222	9,258	7,0761	9,63	0,1657	28,66	6,21727
Fine	18	44586	64460	74	222	9,725	2,3888	9,72	0,7250	29,9	2,15968
Very Fine	67	87143	124307	74	222	9,963	0	9,65	0	30,56	0

it's noticeable that the known error in the first beam element (a wrong value for bending moment and shear force) hasn't been corrected in order to evaluate the behavior of that element in different mesh condition.



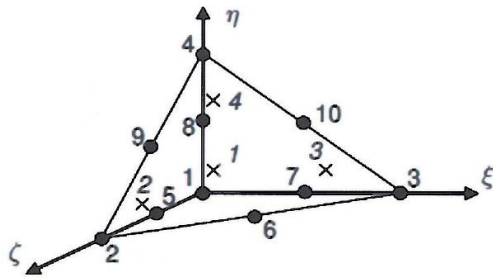
On the left are shown nodes and elements number for each global coarseness adopted.

In the graphs below it can be noted that for a very coarse discretization the shear behavior has several skips around the (supposed) correct value.

The number of the beam elements (and node) increase only between "very coarse" and "coarse". After that, it is constant although the model precision

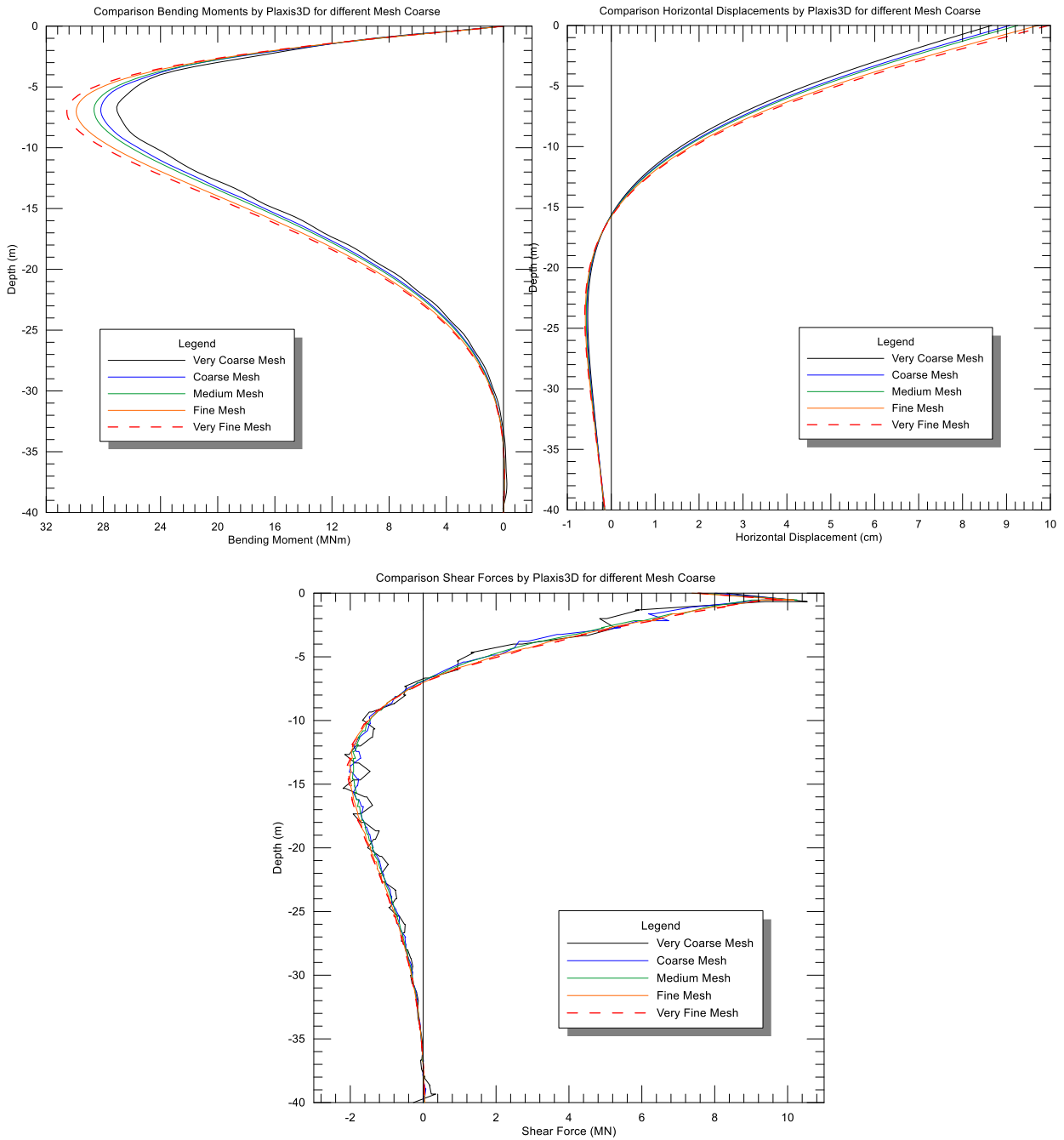
continues to grow, so different mesh coarseness increase only the soil discretization.

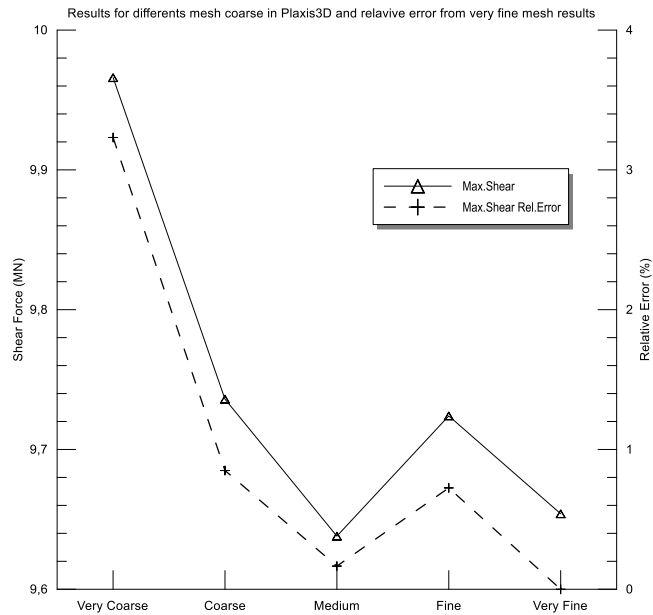
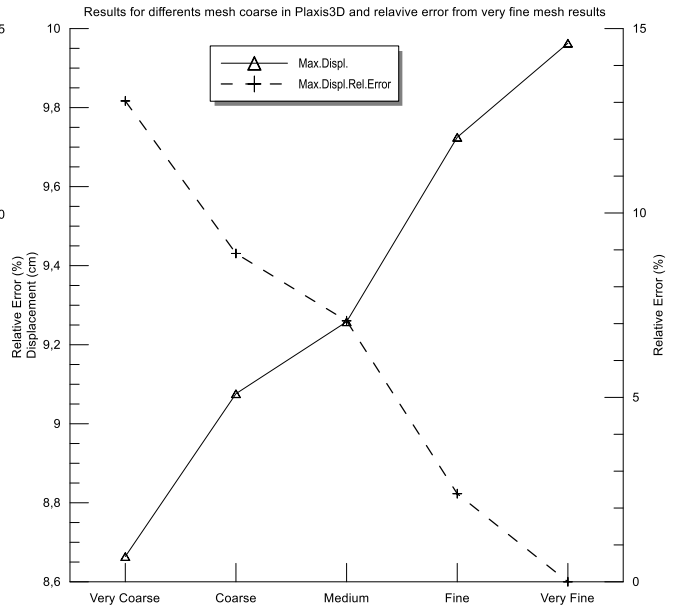
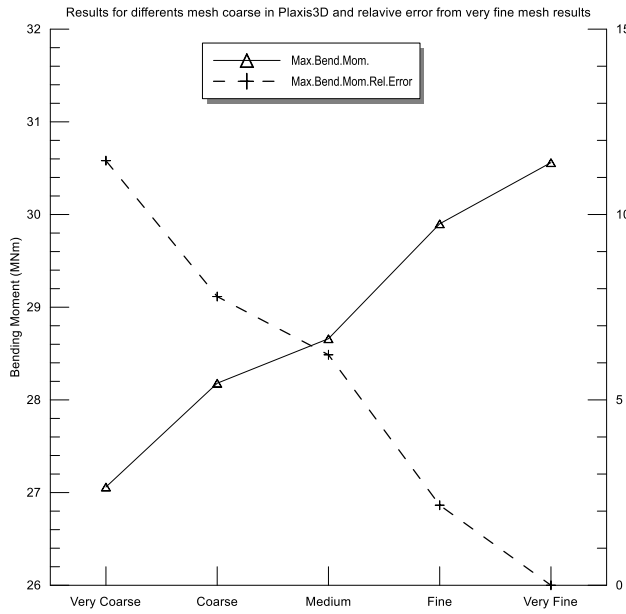
It has been supposed that results are more precise when computed by very fine mesh coarse.



In line with this assumption, the relative error for each coarse condition and each variable has been calculated referred to very fine results.

On the right a Plaxis3D soil element detailed (10-nodes tetrahedrons):

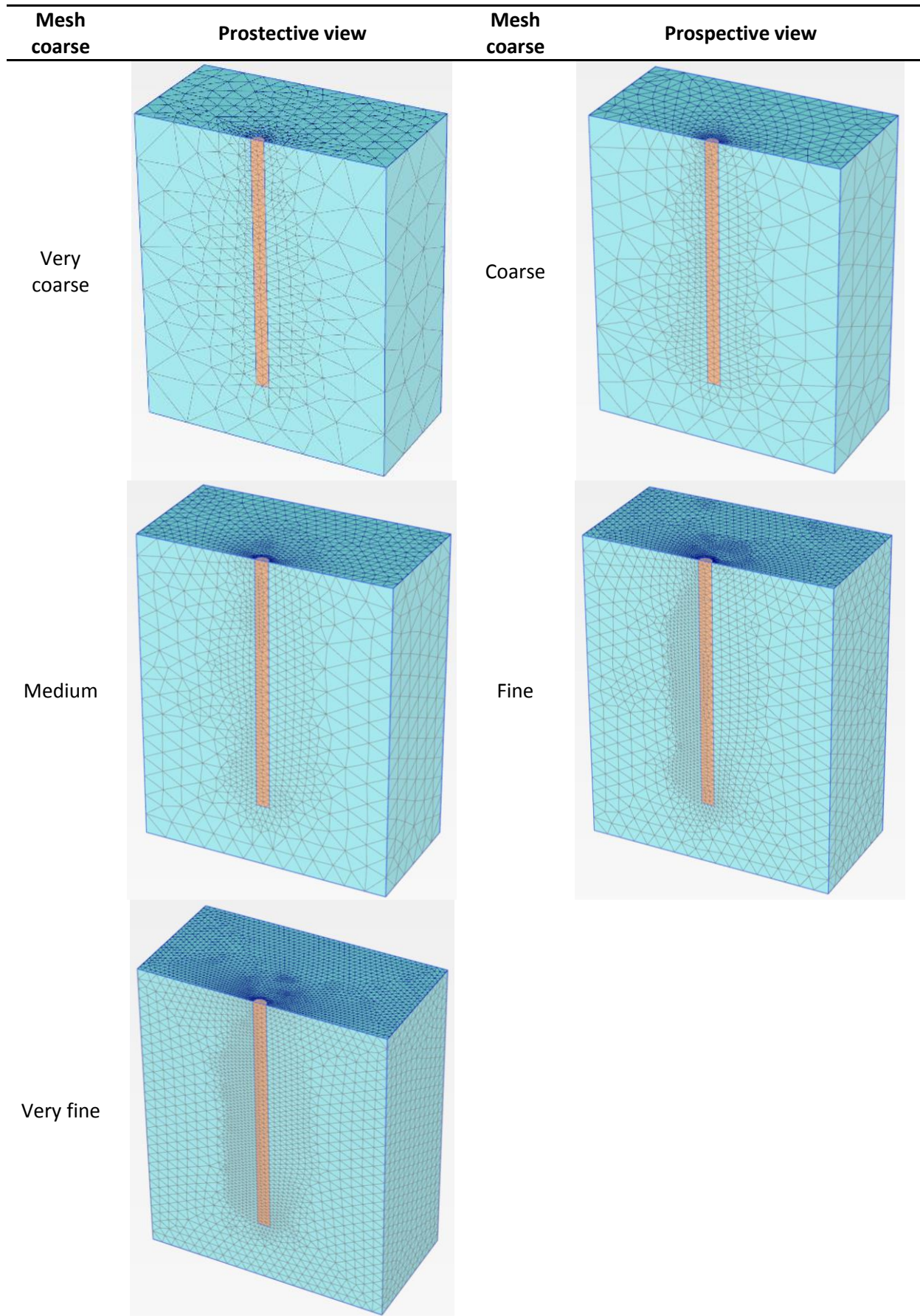


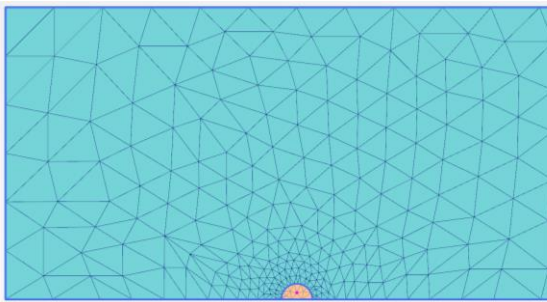
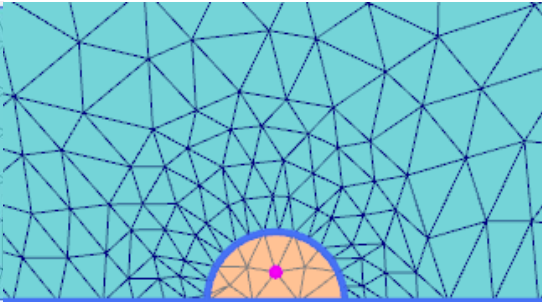
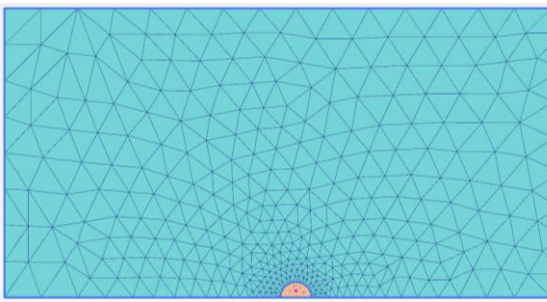
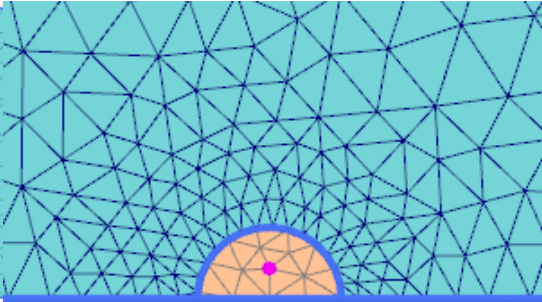
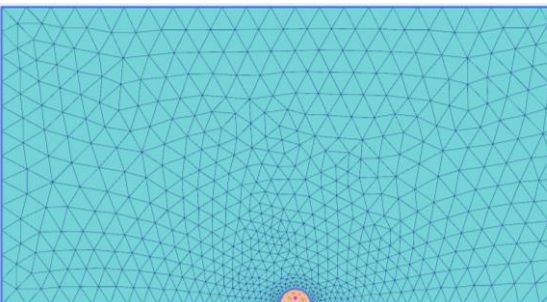
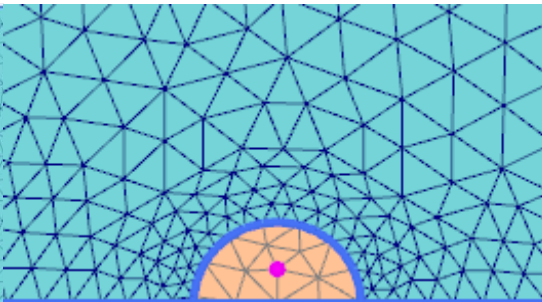
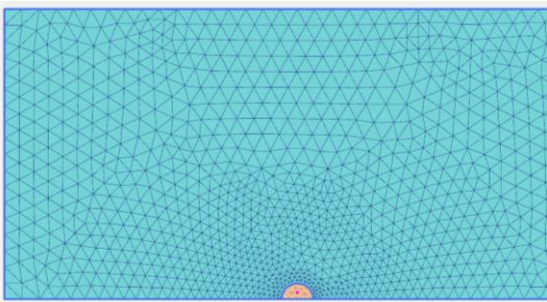
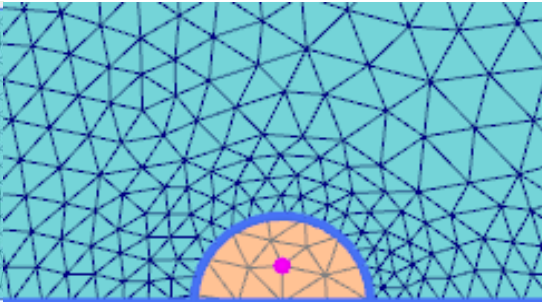
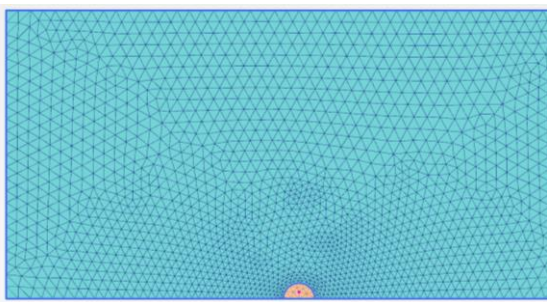
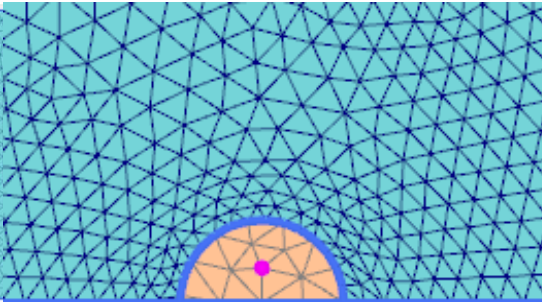


For a mesh elements dimension bigger or equal to "coarse", shear trends show a very small variation, less than 1%.

Bending moments and horizontal displacements exhibit an equal trend: a relative error reduction as finest mesh and an variation minor than 2% between "fine" and "very fine" elements.

In the next two pages are plotted three sketches for each coarse condition in order to allow an easy visual recognition for the engineer.



Mesh coarse	Top view	Pile detail (top view)
Very coarse		
Coarse		
Medium		
Fine		
Very fine		

## Refinement clusters

In this section, Plaxis3D results are shown for different cluster shapes around the pile. These proves are done in order to increase locally the mesh refinement, consequently to the results quality, in a defined zone of interest, as the upper half pile subjected to great displacements and stress.

It had been chosen to use a "coarse" mesh setting for the global model and to refine every cluster of interest with different fitness factors. A simple model properties summary is shown in the table below:

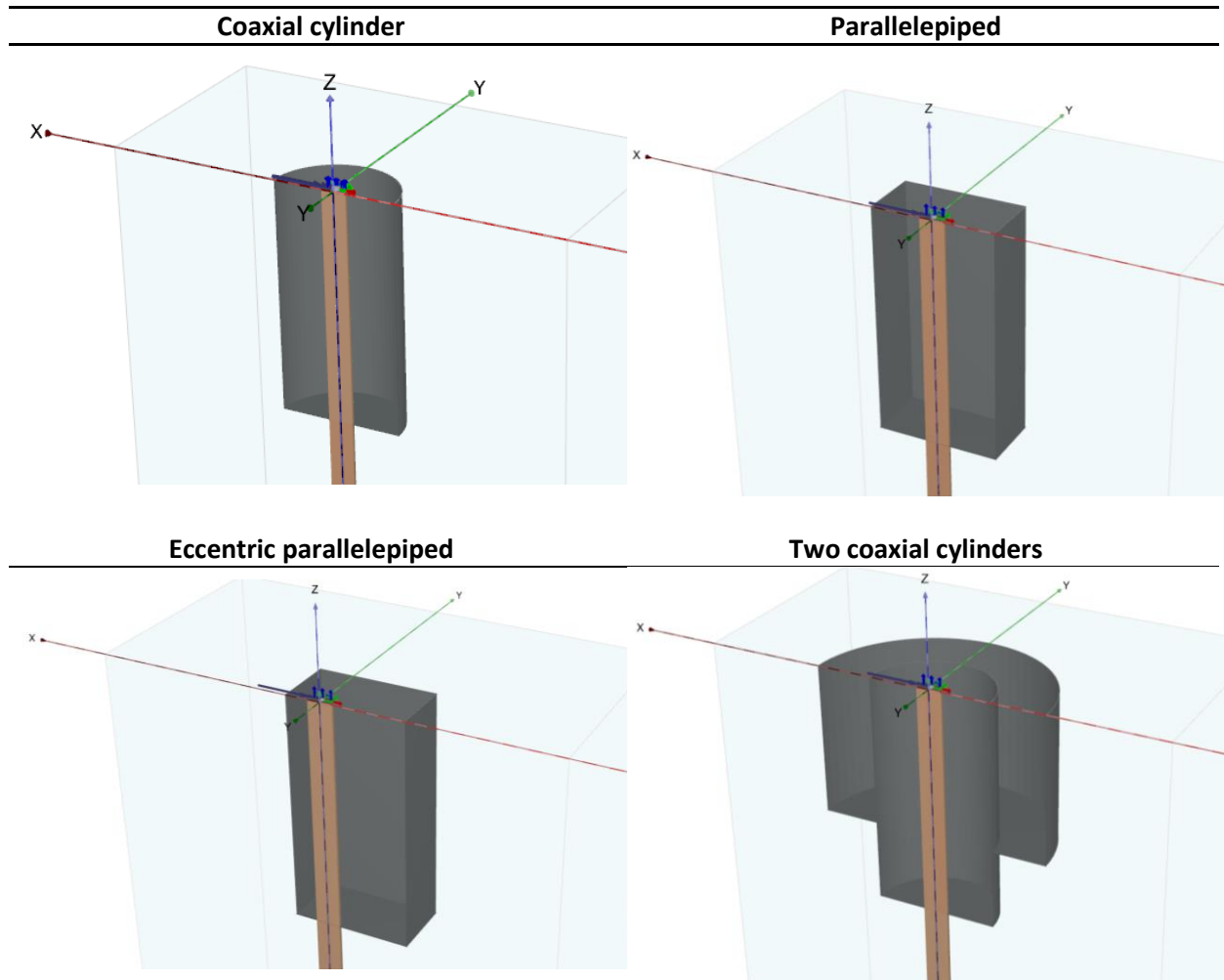
Curve ID	Mesh coarse		Cluster	Pile	
	Type	$r_e$	Dimensions (m)	Fitness Factor	Fitness Factor
Very fine	very fine	0,7	-	-	1
Coaxial cylinder	coarse	1,5	R5,3 L20 Z20	0,2	0,5 (0,2 up)
Parallelepiped	coarse	1,5	L10,6 B5,3 Z20	0,2	0,5 (0,2 up)
Eccentric parallelepiped	coarse	1,5	L10,5 B5,3 Z20 (2,05 ecc.X-dir.)	0,2	0,5 (0,2 up)
Two coaxial cilindrs	coarse	1,5	R5,3 Z20 (R10 Z13)	0,2 (0,5)	0,5 (0,2 up)

Where the Fitness factor (FF) is a coefficient of reduction for the target element dimension, calculated with this formula:

$$l_e = \frac{r_e}{20} \sqrt{(x_{max} - x_{min})^2 + (y_{max} - y_{min})^2 + (z_{max} - z_{min})^2}$$

$$l_{e \text{ (cluster) MODIFIED}} = l_e * FF$$

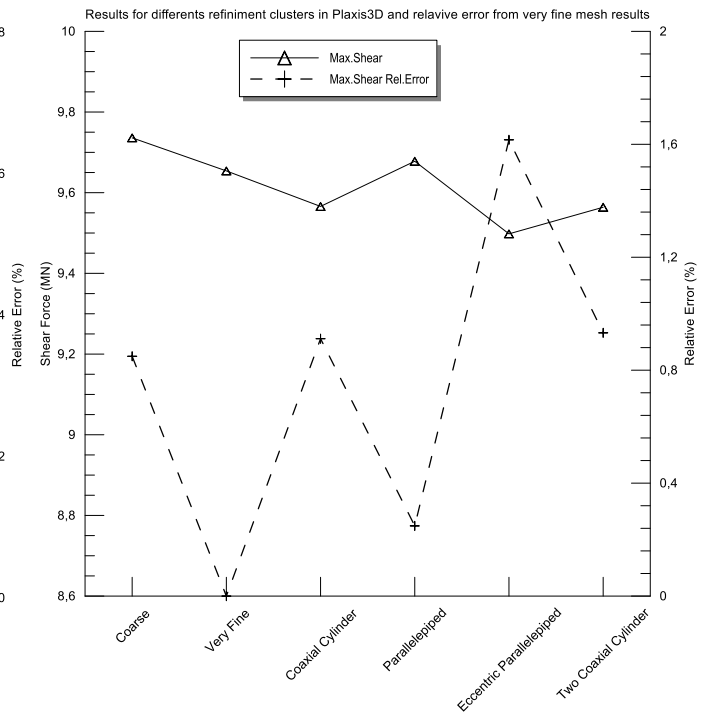
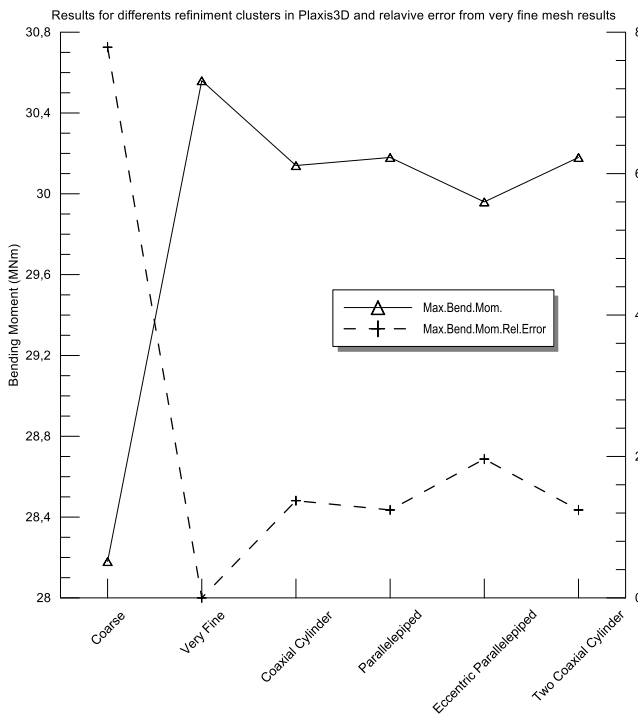
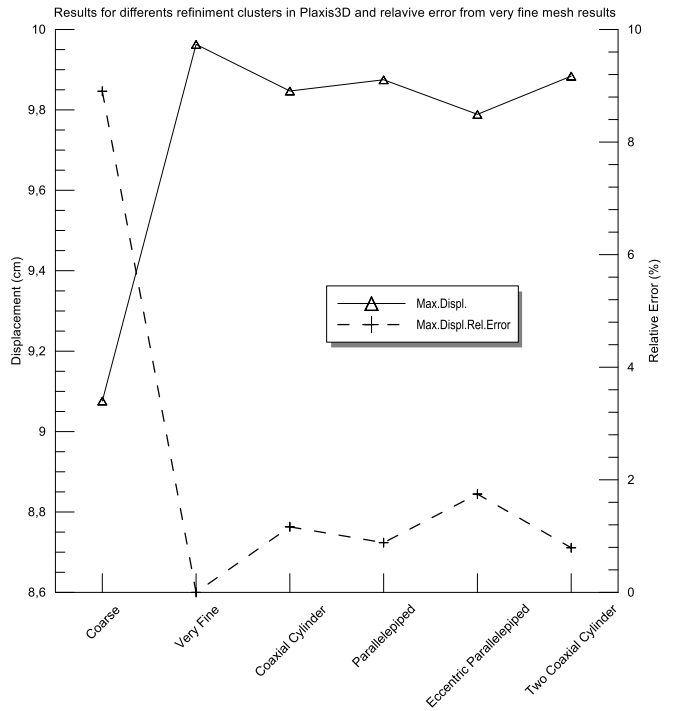
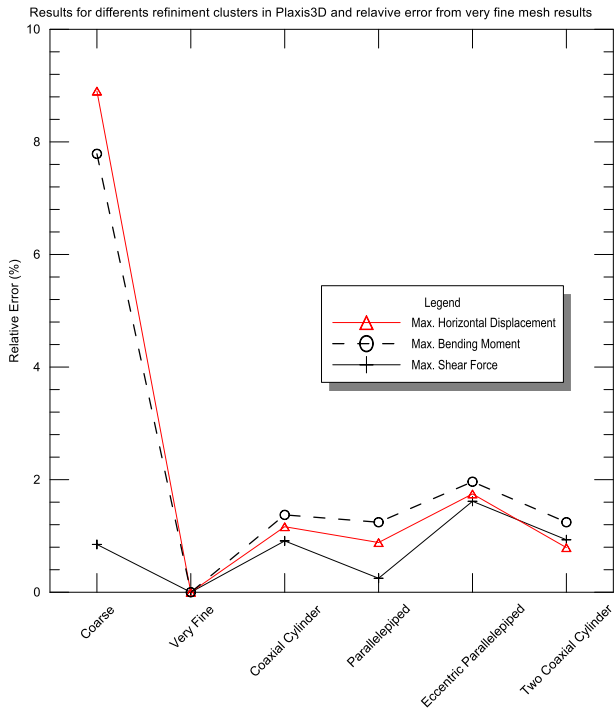
During the meshing phase, when each element dimension is lower than the value of the target element dimension, the subdivision process is stopped. The fitness factor role is ever the same: reducing for a single cluster or structural element the target element dimension. In this way it becomes possible to lighten the model discretization in zones where a low precision is required.

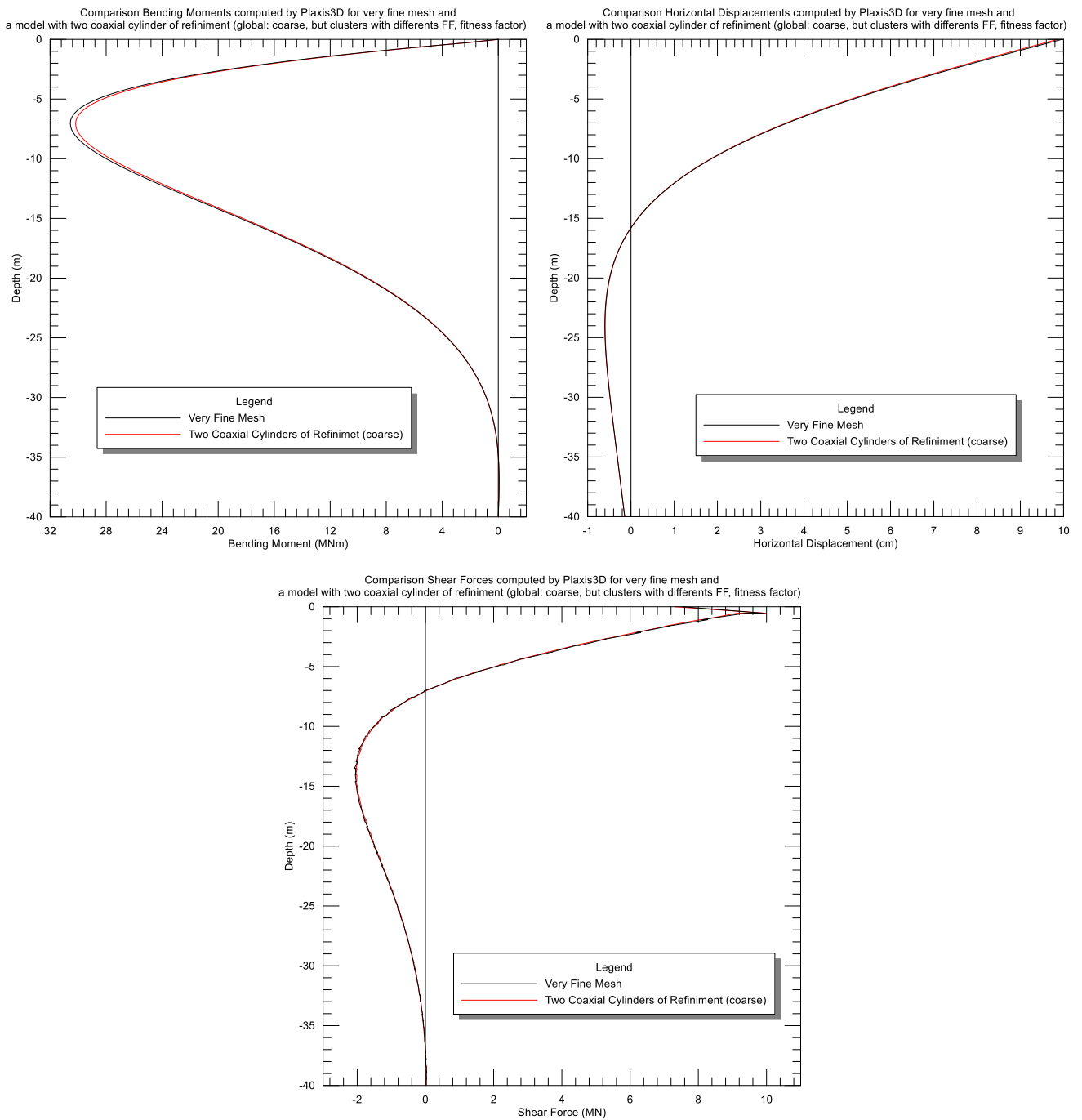


Here below is shown the relative error for each variable and for each refinement cluster shape adopted.

The model with the smallest difference with the very fine mesh condition, is the model with two coaxial cylinder.

Moreover, it's clear that each shape of refinement cluster gives good results, with only a little percentage variation to each other.



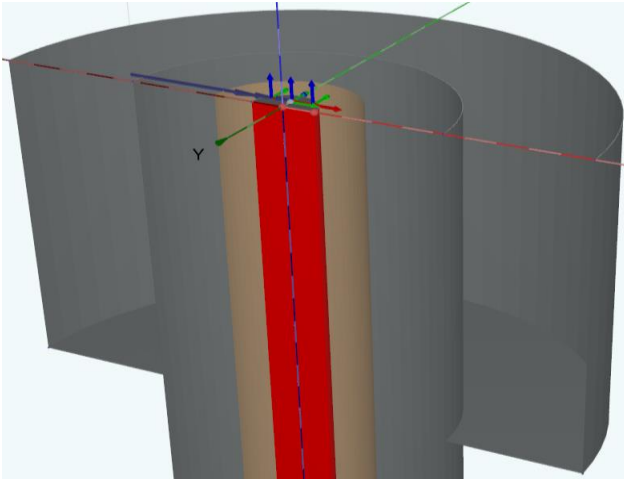


Herein are shown the trends for the interest variables computed by a very fine element subdivision and a coarse mesh with two coaxial cylinder of refinement around the pile.

It's simple to check an equal behavior for each variable in both cases. Only the bending moment peak is reduced of 2%, and this is perfectly acceptable in reason of an important computational time reduction.

## Interface adoption

The following paragraph treats a sequence of analyses run in order to: understand the real need for adopting an interface, its usefulness and then (next chapter) the results depending from its parameter R, a kind of reduction coefficient with a clear role stated by the name itself: interface reduction factor.



In input, Plaxis3D demands to create a positive or negative interface; the sign is subjected to the local Z-axis for the original surface, so it does not have to change behavior and therefore the results.

After meshing process interface is composed by 12-node elements, each element consists of 6 couple of nodes (compatible with the 6-noded triangular side of a soil element or plate element). On the monitor, and then on the plot, the interface has a finite thickness, but in the finite elements formulation, each nodes pair has the same coordinates, which means that the element has zero thickness.

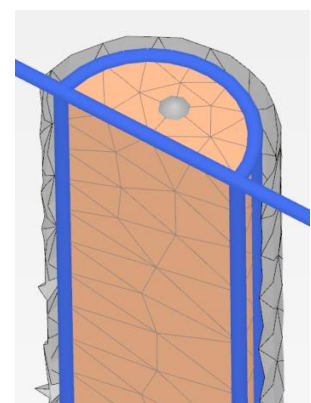
However, Plaxis3D assigns a virtual thickness in order to calculate the stiffness properties of the interface. This virtual thickness is calculated on the average elements size that surrounds the interface (check "target element dimension" in next chapter) scaled by a virtual thickness factor. This factor is set at a value of 0,1 and the user cannot modify it.

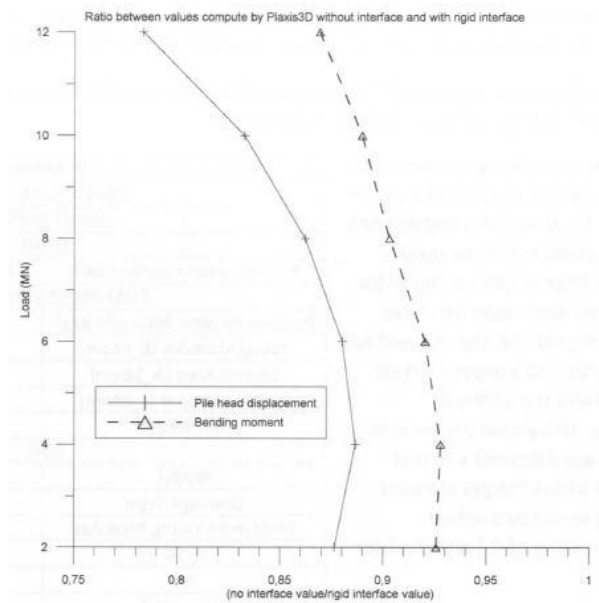
In this chapter the model behavior is analyzed in relation with different load steps of a model both with and without interface.

It could be interesting to note that at the interface ends every interface element nodes pair "degenerates" to a single node.

In this section, the simulation run with the interface reduction factor equal to one is used as benchmark for the calculation of the variables variation. For the interface reduction factor equal to one is common to use the definition: rigid interface, in that case only the Poisson coefficient change (automatically set equal to 0.45).

Above two image to explain the interface position, first during input phase and then after the mesh construction.

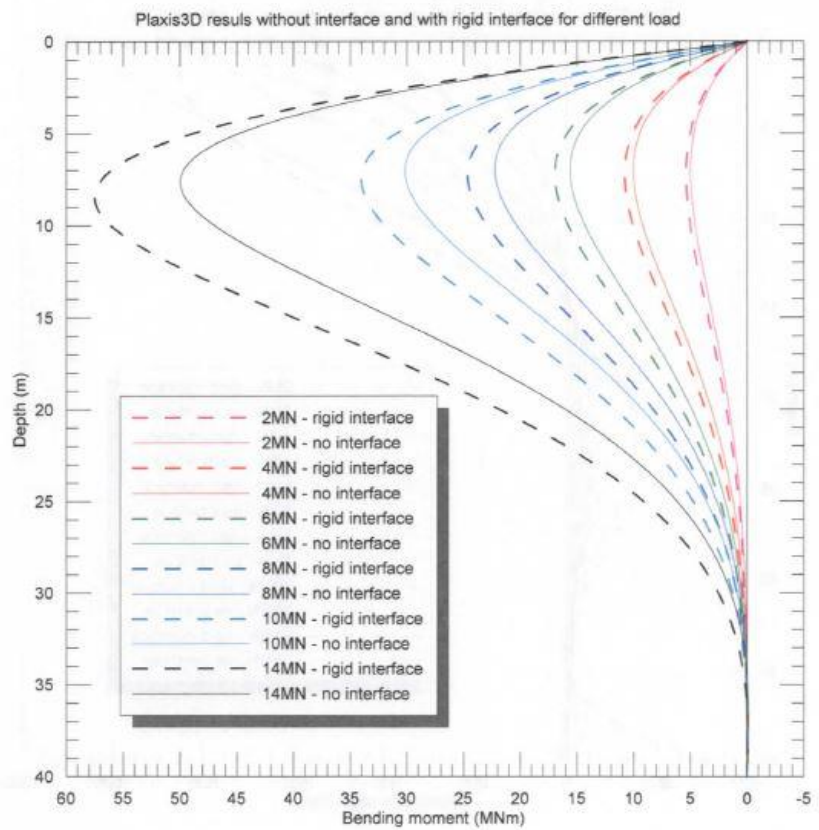
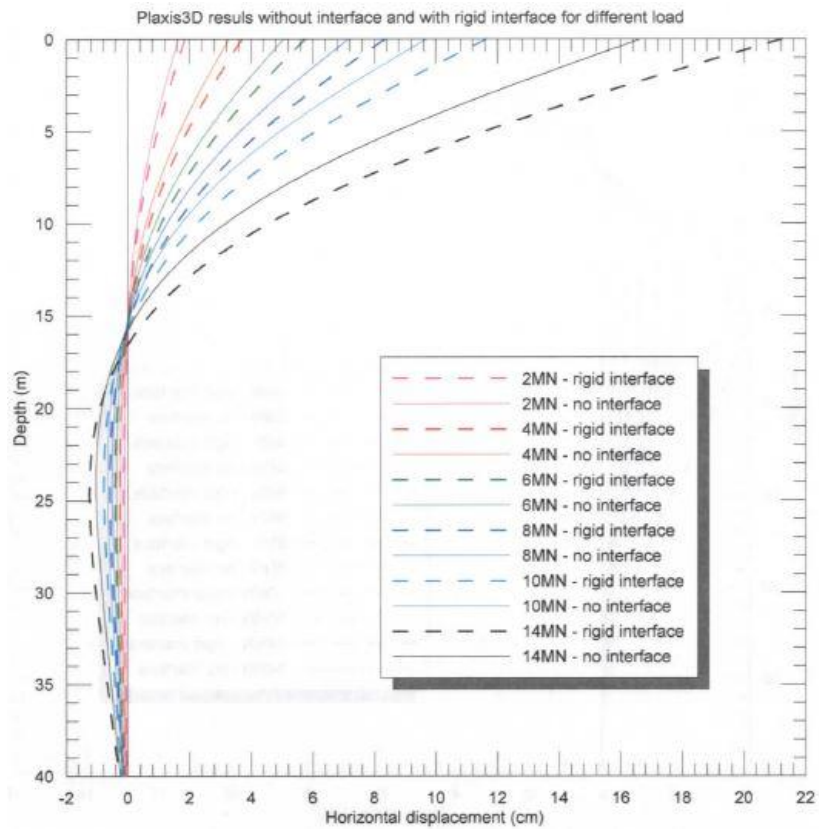


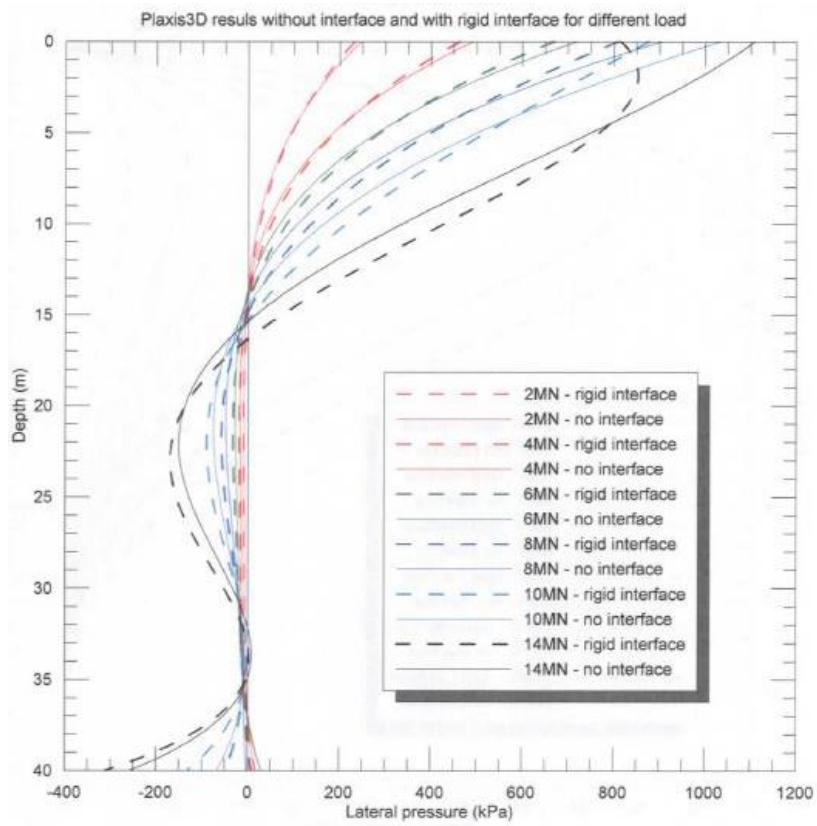
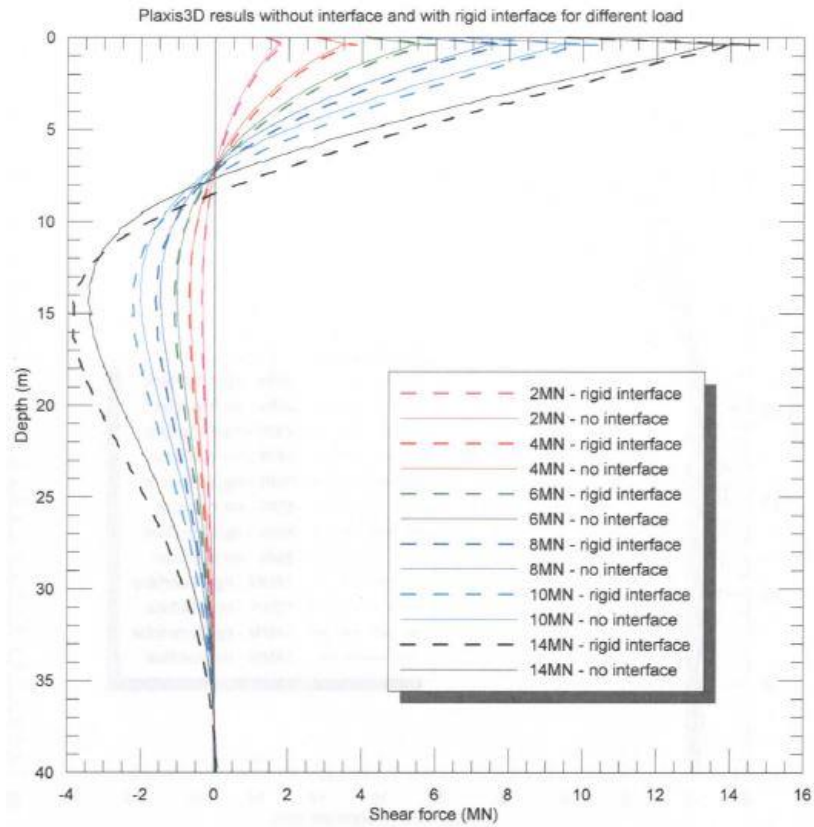


On the left side, a summary graph with bending moment and head displacement from a model with rigid interface normalized by values computed. For high load level, in this case higher than 8MN, the difference between the two situations became relevant; instead, for low load the difference is almost constant and equal to 5% for the bending moment and 8% for the pile head displacement.

The shear force, bending moment, pile displacement and lateral pressure are plotted for both the examined configurations (without and with rigid interface) for 2, 4, 6, 8, 10 and 14MN. This series of loads is chosen in order to evaluate if exists a function in the variables behavior between load and interface adoption.

From the graphs below it is clear that the interface adoption leads to a general increase in shear force, bending moment and pile head displacement.





## Model dimensions

Herein, the results of simulations run for three different model (mesh) dimension are presented.

It was chosen to investigate the mesh dimension effects in order to adopt the best engineering solution for the analysis on the definitive model.

It has been changed only the dimension parallel to the load, which means the main direction of displacement and deformation.

Model ID	u_x max	%u_x max	M_3 max	%M_3 max
D1A_100m	1,7643	0,9760	60,1186	1,0010
D1B_120m	1,7881	0,9893	60,0966	1,0007
D1C_150m	1,8076	1,0000	60,0562	1,0000

The model dimensions adopted are 100m, 120m and 150m.

Above, the table presents the maximum values of the main variables of interesting i.e. bending moment and horizontal displacement. In the same table are presented the same data described above but normalized by the value assumed as final i.e. from D1C\_150m; this is done in order to show clearly the variables' variation.

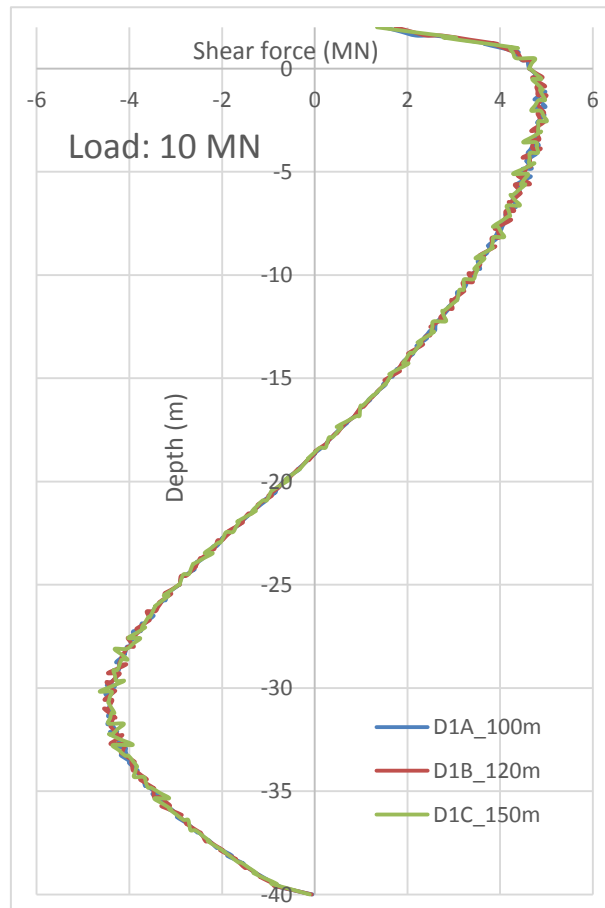
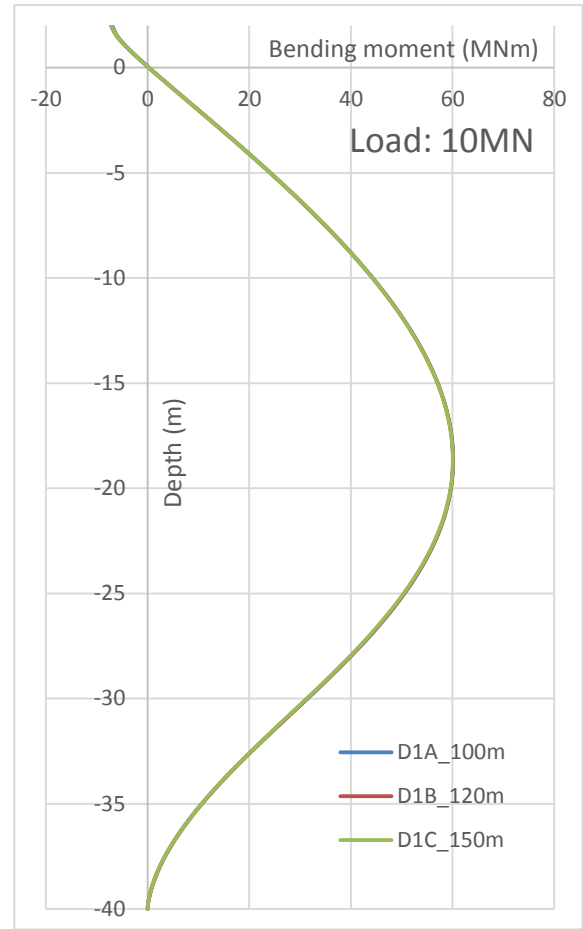
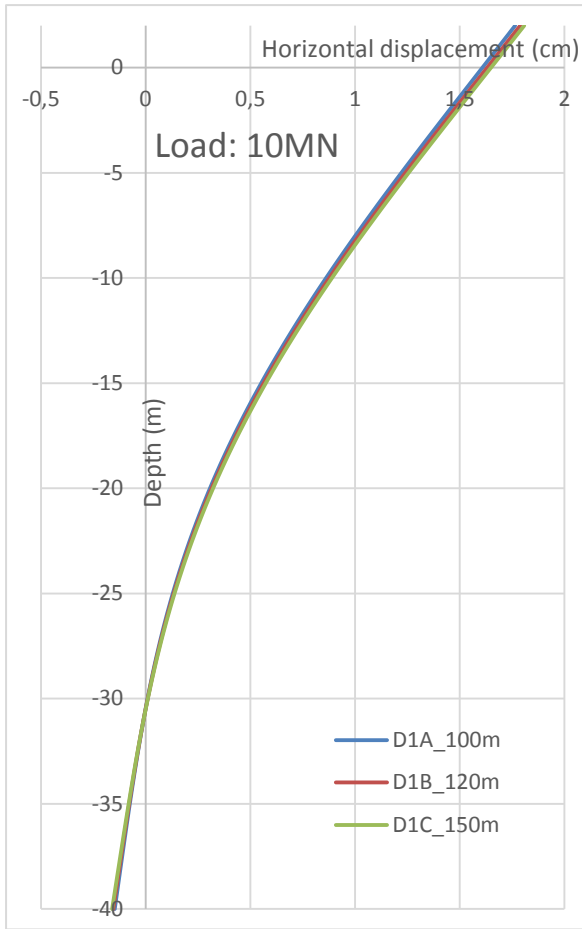
Bending moment is absolutely constant (fluctuation of 0.1% between 100m and 150m).

Horizontal displacement instead, has a little variation: 2.4% (less) between 100m and 150m and 1.1% between 120m and 150m.

The conclusion of this tests is that 100m as model side is a good assumption, because it adopts a larger side length. This means better results but it also means adopting a larger number of elements in order to maintain the indispensable relatively small element coarseness.

Briefly: a little bit better results do not justify such a large increase of time consumption.

In the following pages, are shown trends for shear, bending moment and horizontal displacement for pile with and without a surrounding interface.



-This page intentionally left blank-

## PARAMETRIC ANALYSIS

---

In the following paragraphs, a parametric study of the model defined in the last chapter is presented.

These sensibility analyses cover three variables of primary importance that must be defined in the input phase for each numerical model representative of soil behavior.

The model construction has just been described in the previous chapter, where each choice and assumption is largely explained. Now it has become necessary to know which input parameter has major effect on the behavior of numerical model of a pile laterally loaded in soft clay.

In order to evaluate the major capability of influence on the model, it is tested:

- Eps50 (EpsC in SPLICE), because it is the unique parameter that allows us to set an equivalent material into Plaxis3D and SPLICE, so both analyses are run with the software;
- Tensile cut-off, it is investigated the effect of its global adoption and then some configuration with activation localized. This second series of simulation is run in order to evaluate which possible layer subdivision best match the real soil behavior, especially back the pile. It's important to know that SPLICE allows gap opening, so only Plaxis3D results changing during these tests;
- Interface reduction factor, the model response for this parameter is studied in reason to get the sensibility of the model in relation with this variable that can be seen like arbitrary in some case, especially in merely academic exercise where none field or laboratory data are available.

If the interface role and operation in Plaxis3D are clear, not so clear is the correct value to assign to it. The presence of a highly reworked layer all around the pile is demonstrated and intuitive, but a unique theory-rule does not exist to define the correct value of the interface reduction factor. So in several scientific papers it is possible to find different values for it, but everyone it is representative of a specific site condition only. From literature the unique indication that crops out is that the interface reduction factor depends essentially on the soil type and pile type (technology used to construct or drive it) i.e. on the level of the coaxial layer material reworking with the pile.

### **Unexpected shear fluctuation**

In each analysis done up to now exists a large fluctuation that affects the shear distribution calculated by Plaxis3D on the pile top, at seabed level.

This problem could come from: numerical problem due to the great difference of stiffness between pile and soil or numerical problem connected with the load application on the deformed structure (top section rotated but load defined only in horizontal direction).

In order to try to remove this annoying problem it has been attempted to:

- change the beam Young's modulus (E-6 and E-3 than pile elasticity modulus);
- decrease the single elements size near the top part of the pile;
- use different ways of loading, like point force, line load and surface load;
- maintain the load on the seabed pile section increasing the pile length above the seabed.

Every test carried out has been affected by the same inconvenience.

For the models later used, two tricks have been adopted in order to reduce the shear fluctuation: adopting a stiff plate on the pile head (Young modulus is a thousand times stiffer than pile Young modulus) and increasing the pile length above the seabed. Load was applied upon the rigid plate with a couple of forces that balance the residual bending moment in order to have zero moment at the seabed pile section (like in the original situation).

Several tests were run to find out the best solution (none of these are reported) and eventually it was chosen to work with: plate activated and the pile length increased two meters above the seabed (four meters) led to even better results. But it had a problem too: a too large number of elements were needed for a good discretization and in that case it became too important the bending moment effect connected with the arm of the load.

Disturbing phenomena were also present but reduced, which meant an increased lateral pressure study quality.

The next chapter presents a possible explanation for the strange behavior of lateral pressure in the top part of the pile; moreover, the problem due to the shear variation has been briefly explained above.

### Eps50 (EpsC)

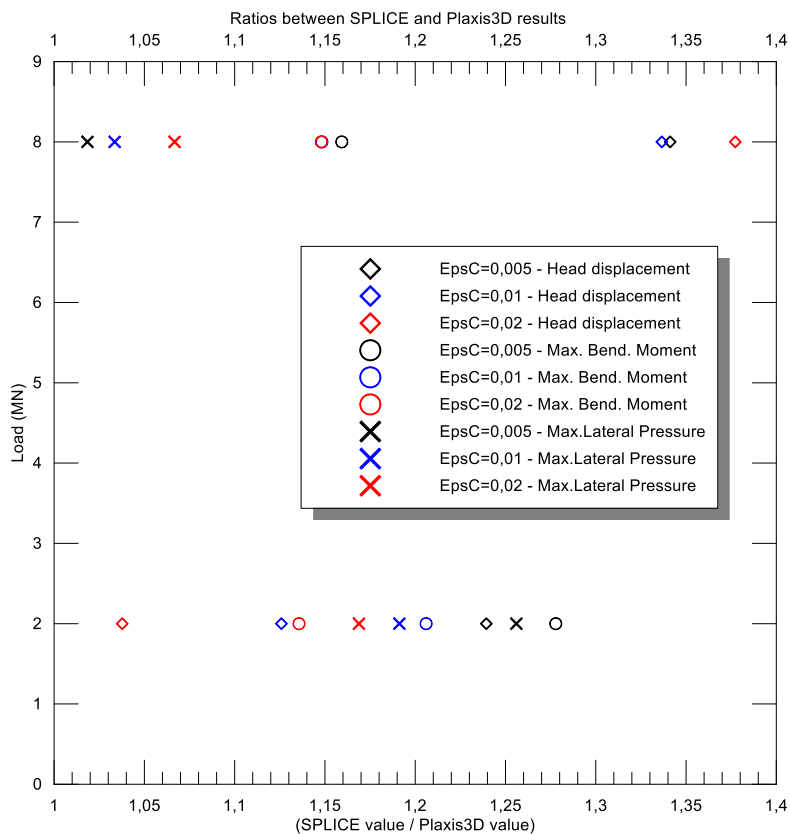
In this section are presented the effects of Eps50 on the soil response for our model of single pile in soft clay.

It has been chosen to run these series of analyses for 2 and 8 MN because 8 MN is the maximum load allowed by SPLICE solution for Eps50 equal to 1% and 2% (for 0,5% it's a little bit more: 9MN), so a comparison with SPLICE is possible.

Calculation results by Plaxis3D are compared with SPLICE output. This has been done in order to investigate a possible law in the relationship between variables of interesting and Eps50.

It's important to know that the Eps50 definition, also here adopted, is: the strain at half of the maximum stress from laboratory compression test on clay.

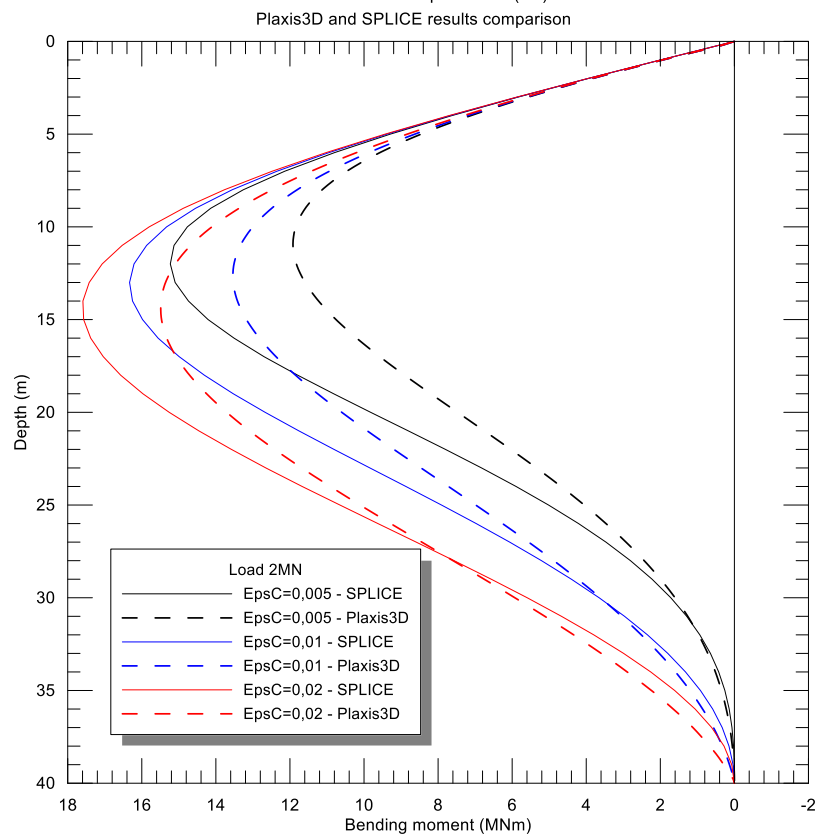
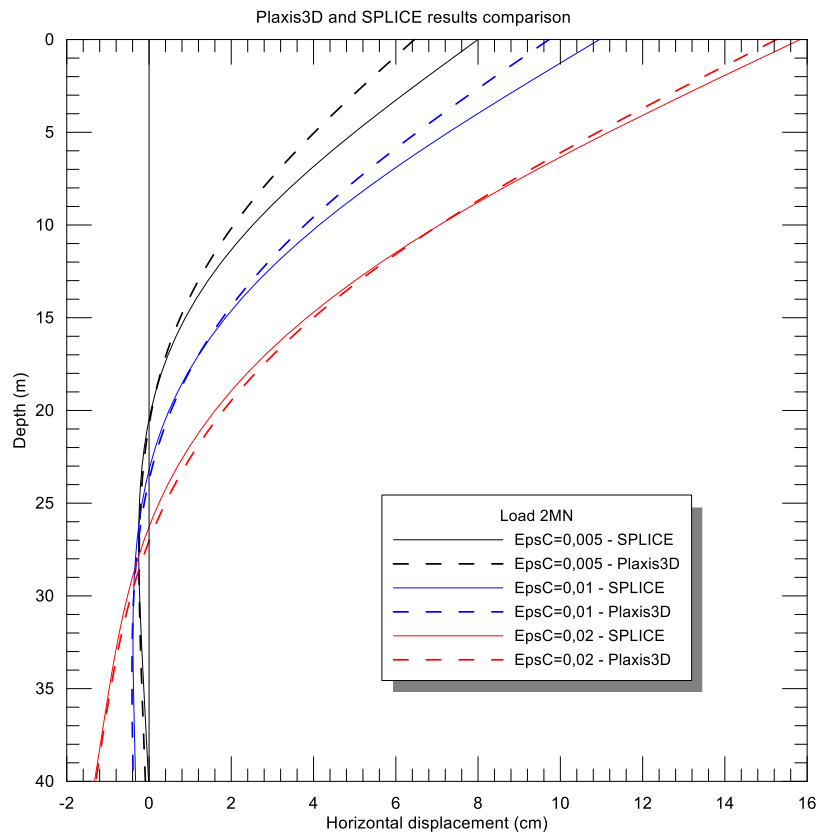
Below are shown the results for different Eps50. SPLICE results are normalized by Plaxis3D values in order to estimate the percentage variation.

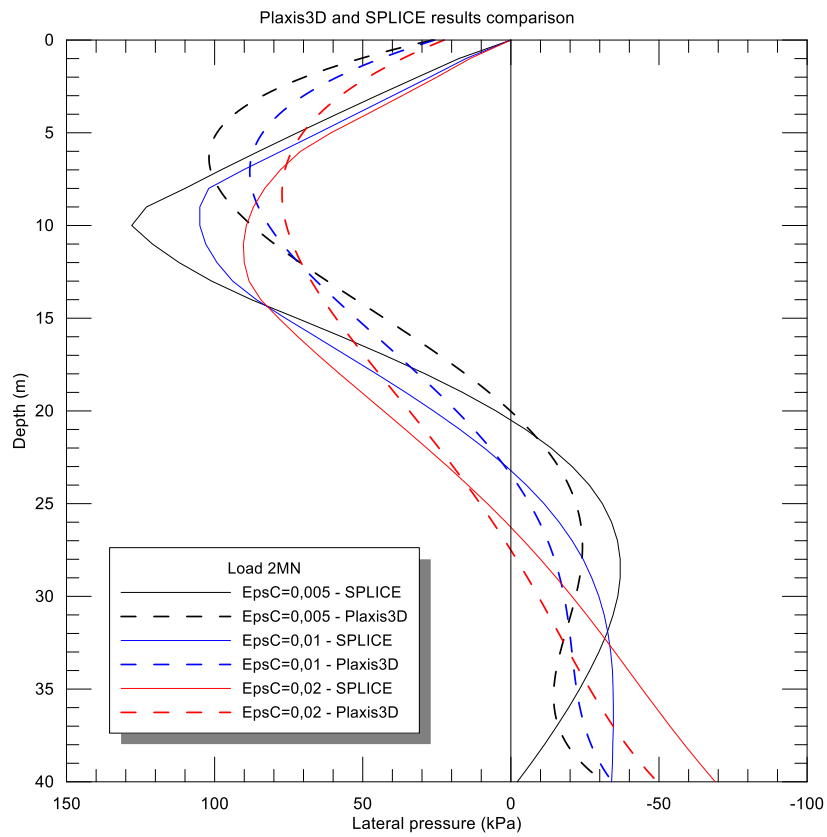
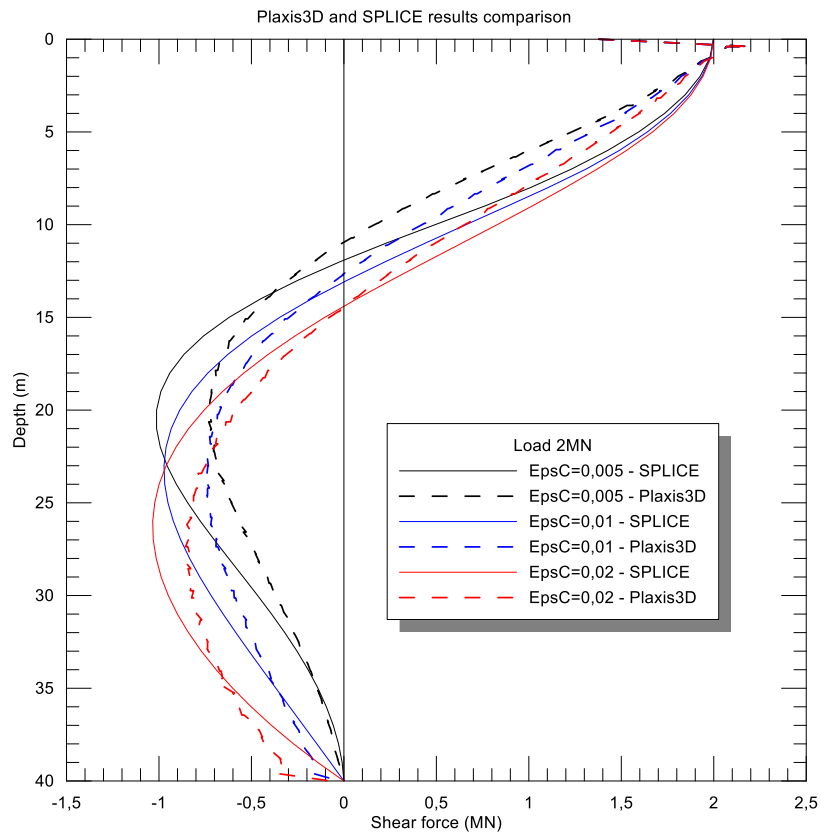


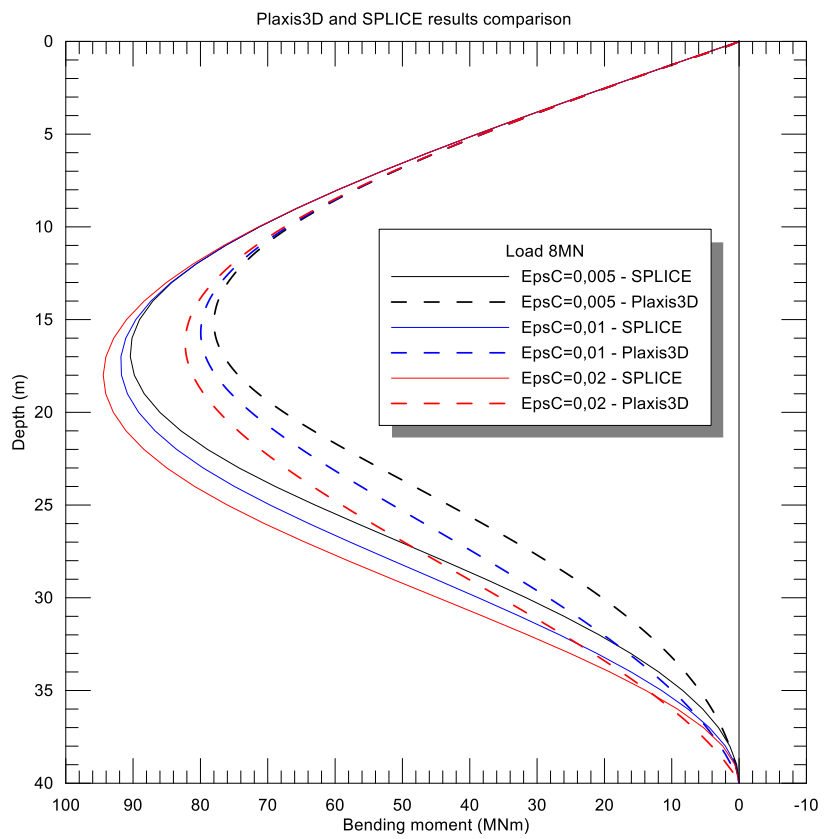
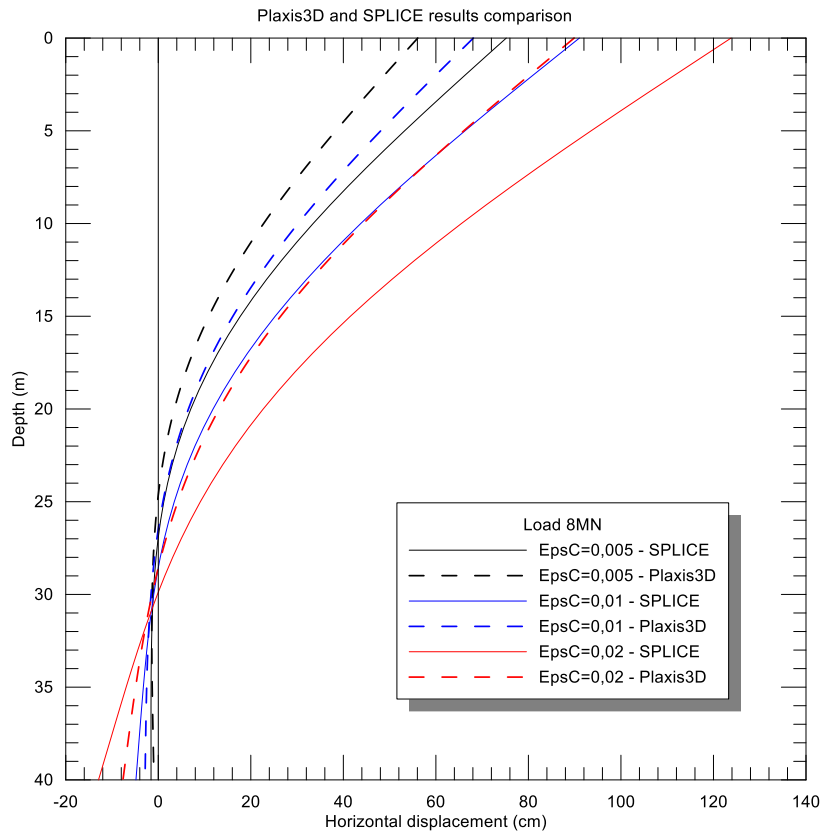
It seems clear to observe that for a low load like 2 MN exists a fluctuation of every variable larger than for 8 MN. For the highest load condition each variable is grouped by type (maximum bending moment, horizontal displacement and lateral pressure), and the elements of this whole "family" stay in a range of 5% or less (approximately 2% for the maximum bending moment).

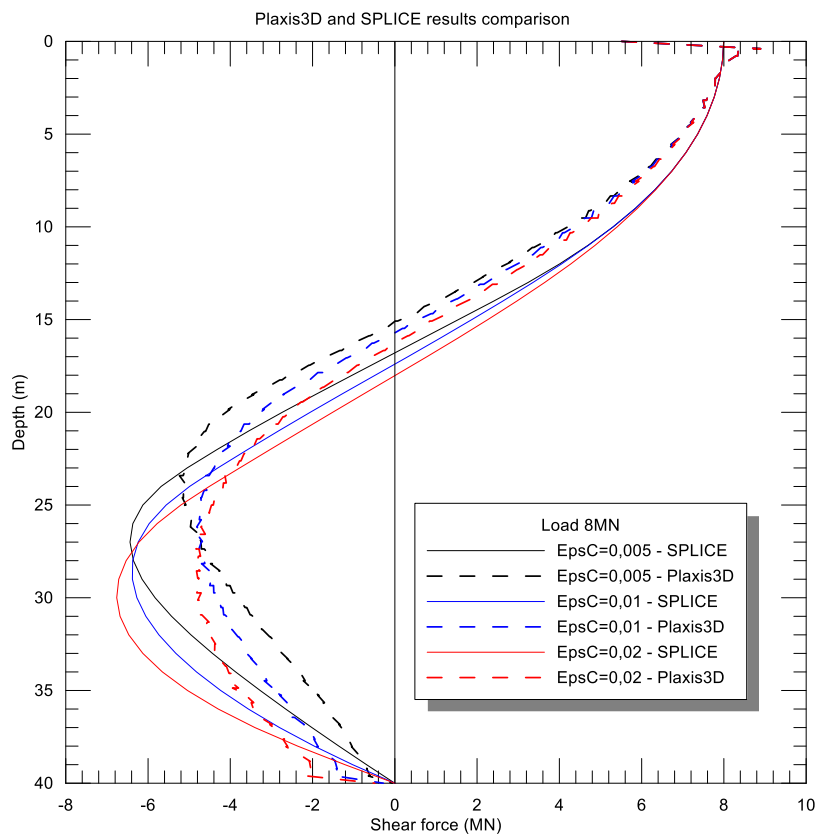
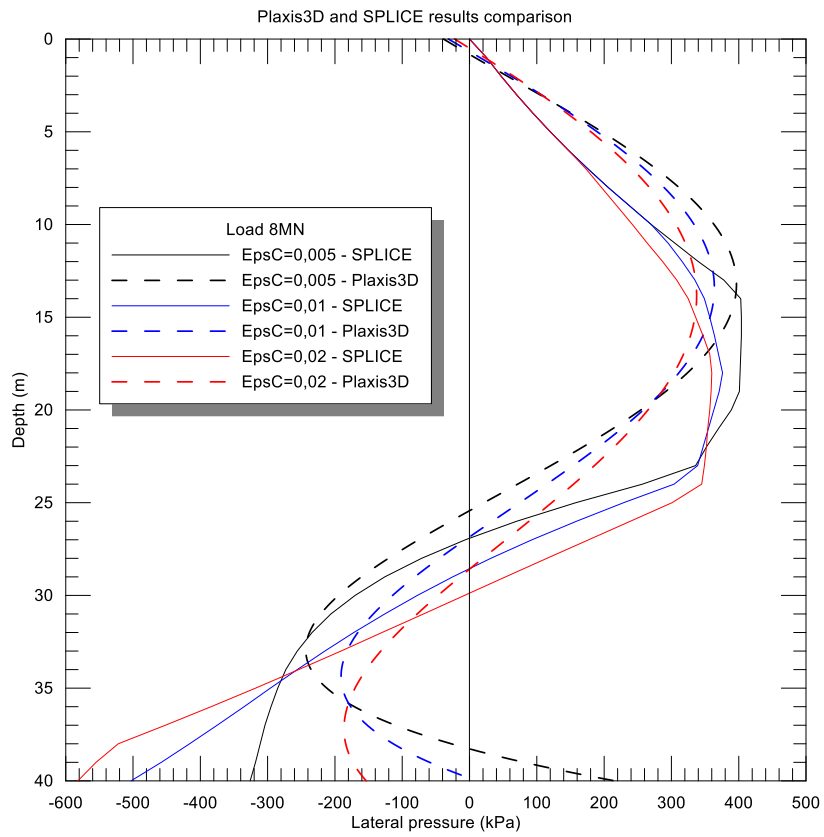
For 8 MN the difference between SPLICE and Plaxis3D results are set on: around 30% for the pile head displacement, 15% for the maximum bending moment and 4% for the maximum lateral pressure.

This behavior of the lateral pressure is very “friendly” because confirm us that once reached the maximum strength (undrained), the soil can only increase the involved (plasticized) volume i.e. bearing capacity factors are almost the same.









### Tensile cut-off adoption

It has been decided to run analyses with different extension of tension cut-off zone.

These were done in order to investigate the effects of tension cut-off activated in different configurations of the shallow layer to find the best compromise between tension cut-off adoption and computational time required per each analysis.

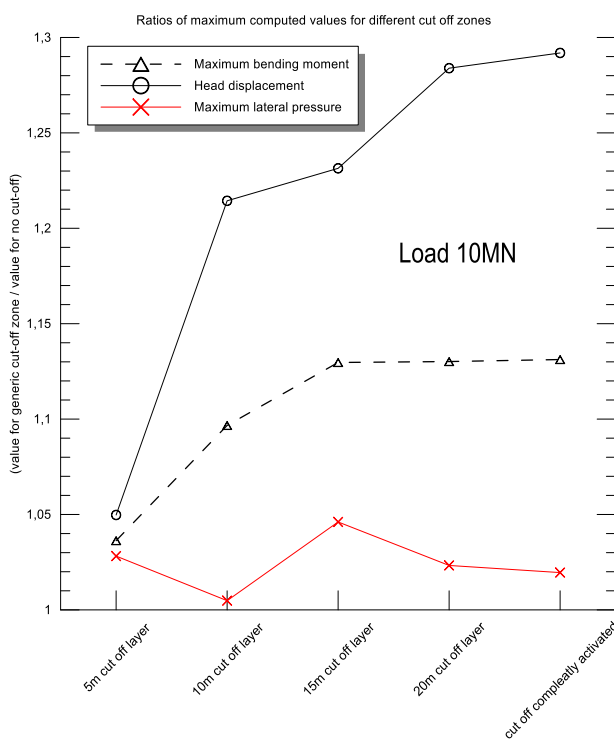
Model case with tension cut-off deactivated is used as benchmark for the following results comparison, in order to present clearly the effects concerning this study.

From the model with tension cut-off completely activated, it has been possible to figure out that around 30 meters is the maximum extension of the zone in tensile cut-off condition, which means that every test has to be carried out for a layer with tension cut-off shallower than 30 meters depth.

It was chosen to test the following cut-off zone depth: 5-10-15-20 meters and furthermore, the “extreme” cases with tension cut-off completely activated and deactivated.

Each model needs to re-run its meshing phase; this was caused by the new layering conditions i.e. new geometry. Anyway, elements and nodes numbers are only subjected to a slight variation and the extreme situations, both with a unique layer, have lower elements and nodes number.

It was run only the load condition of 10 MN, which means a high load i.e. near failure condition. It was established that a lower load would not bring more information than that severe load. For these



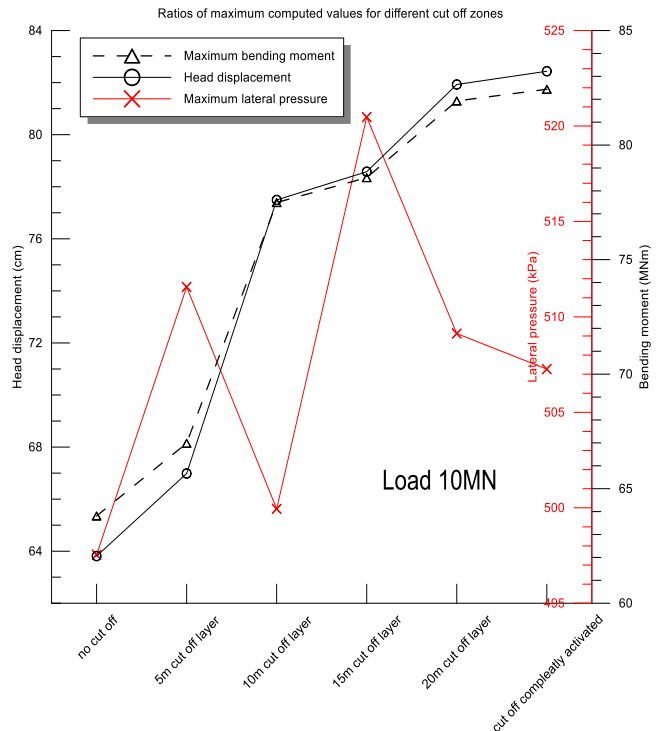
sensitivity analyses were defined two soil materials: equal in all their properties except for the tension cut-off activation and set equal to zero for one of these.

The graph on the left side clearly presents the percentage variation of the maximum bending moment and pile head displacement for different cut-off zones normalized by the case results with tension cut-off completely deactivated. Maximum bending moment presents a variation by about 25% between 5m and all activated; for the pile head displacement this variation is lower, around

10% complexly.

The largest difference is in the passage through 5 and 10 meter of cut-off zone. This fact confirms the logic thinking that the cut-off effect is more important in that region subjected to a great tensile stress like the soil in the pile backward.

Above, the effects of different cut-off zones have been explained but it was also found that each layer subdivision means an increase of the computational time requested by Plaxis3D to run each model phase.



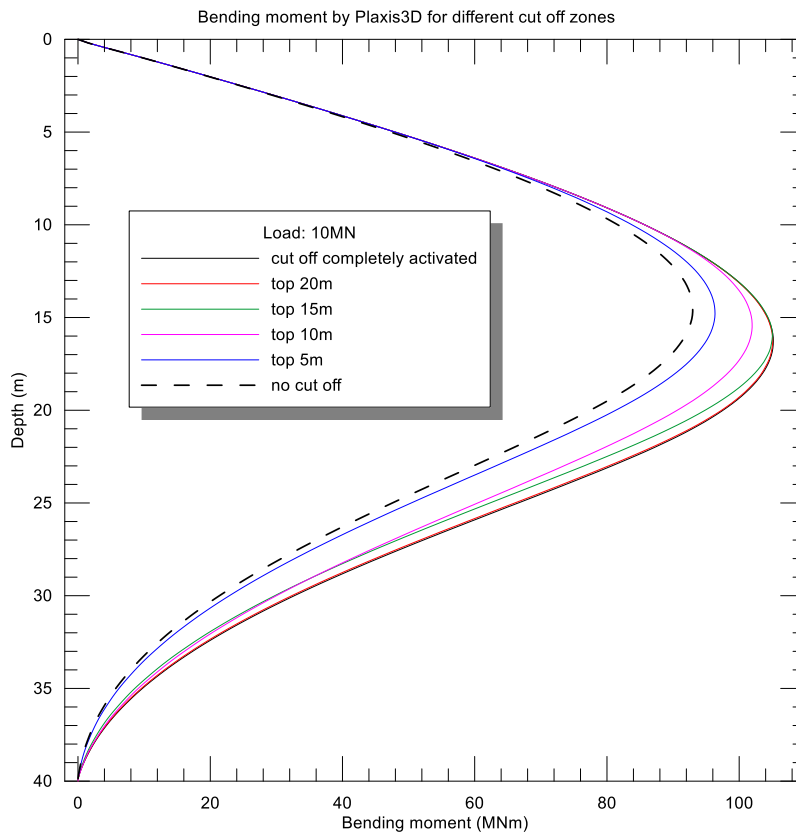
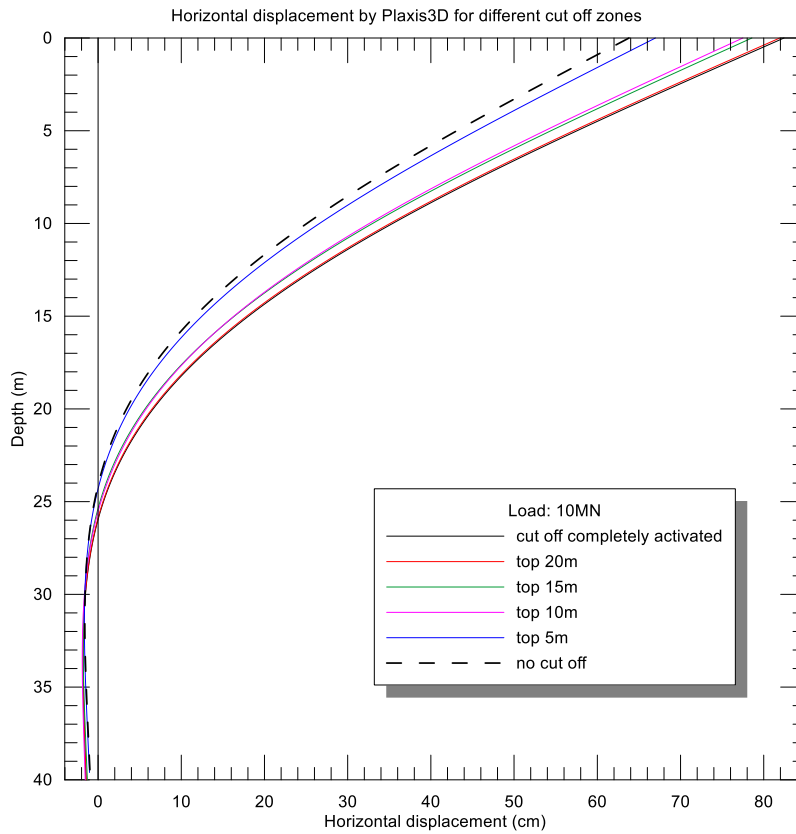
Finally, it is possible to declare that the best solution for our purpose will be using the tension cut-off completely activated this in order to consider the tension cut-off effects because none of the proposed solutions showed a computational time reduction or at least an increase of it.

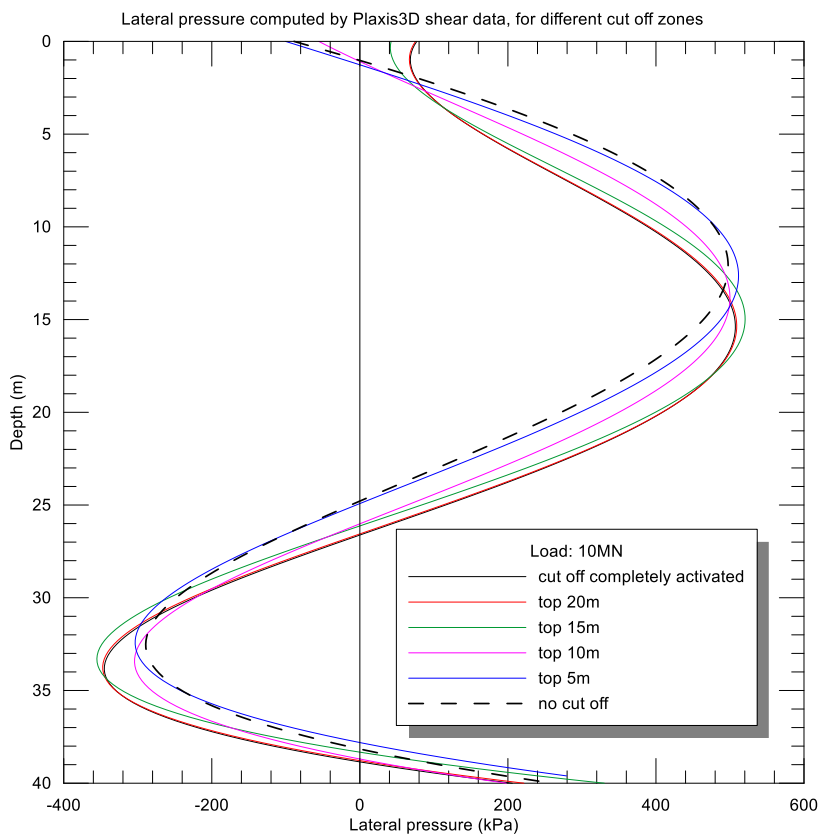
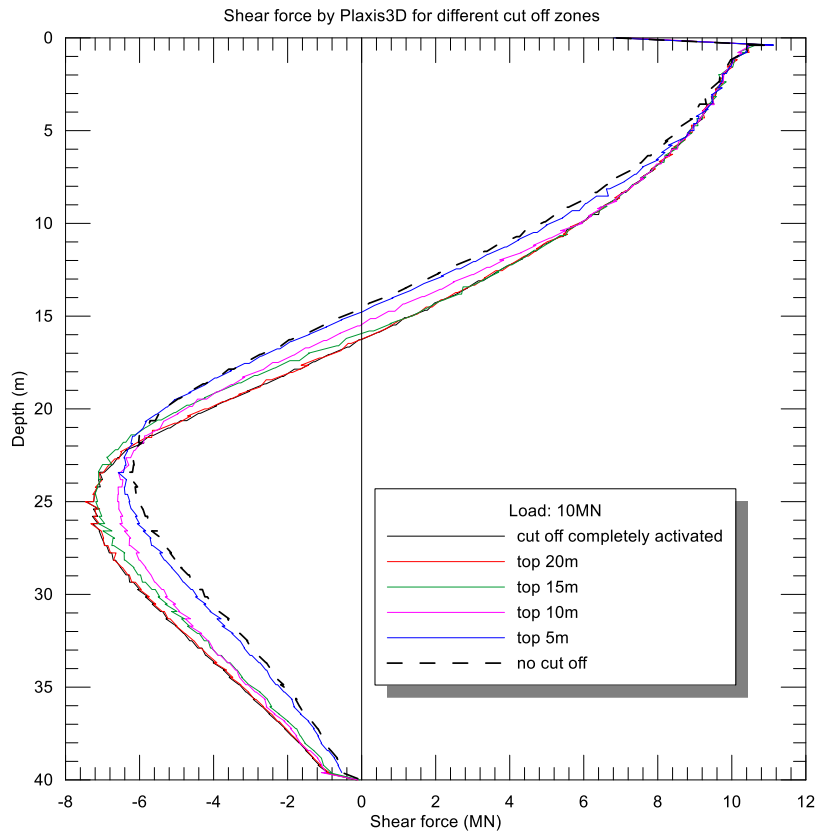
Anyway, some uncertainties about a real physical meaning of tension cut-off adoption remains, because a gap opening of 30 meters depth is not real.

Bending moment, horizontal displacement, shear force and lateral pressure trends have shown the same behavior for every different condition tested.

Correctly, the case with only the top layer of 5m presents a trend similar to the situation with tension cut-off deactivated. 10 and 15 meters have very similar results both converging to the "all activated" value. The best match with "all activated" has been found for 20 meters depth of cut-off zone; in that case, the results are almost equivalent.

Below are plotted the trends of every variable object of this study.





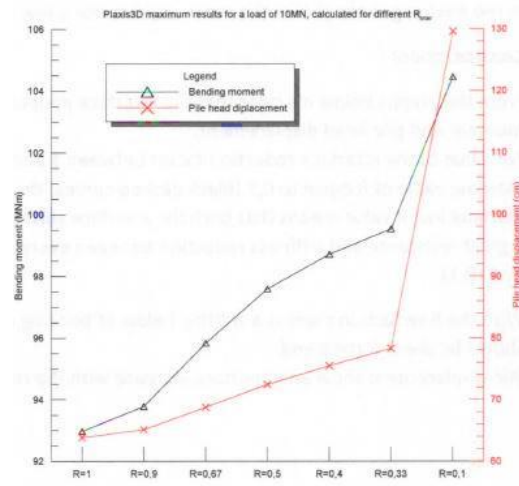
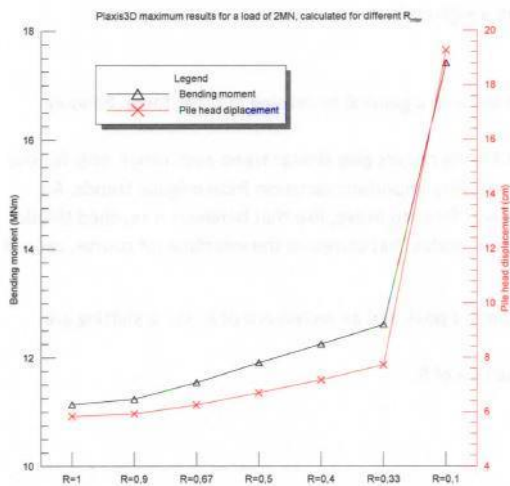
### Interface reduction factor

The important role played by the interface reduction factor has been just explained in the intro part of this chapter.

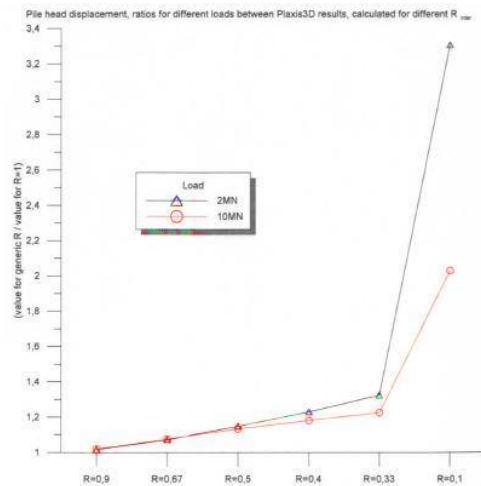
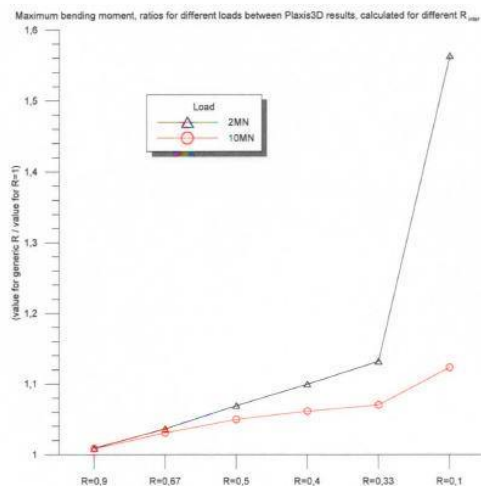
Adopt and interface in a Mohr-Coulomb soil model require to define a value for the interface reduction factor, which is the setting that define the interface behaviour.

For two load conditions are tested different values of the parameter object of study in order to define clearly the relation between model responses and interface. It is used a load of 2 and 10 MN.

Below the maximum value for each variable is plotted for different interface reduction factor, these graphs allow to write that for a reduction of the interface parameters between 0.90 and 0.33, the shears are linear and the same behaviour is shown by the bending moment.



Above summary graphs with the maximum values for each R tested. Below the same graph normalised.



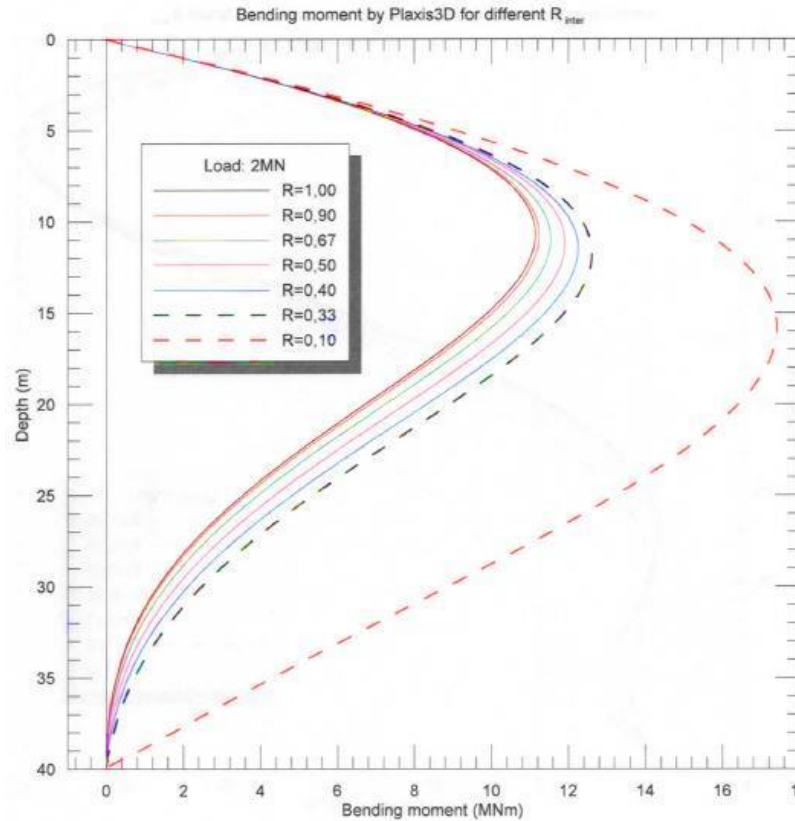
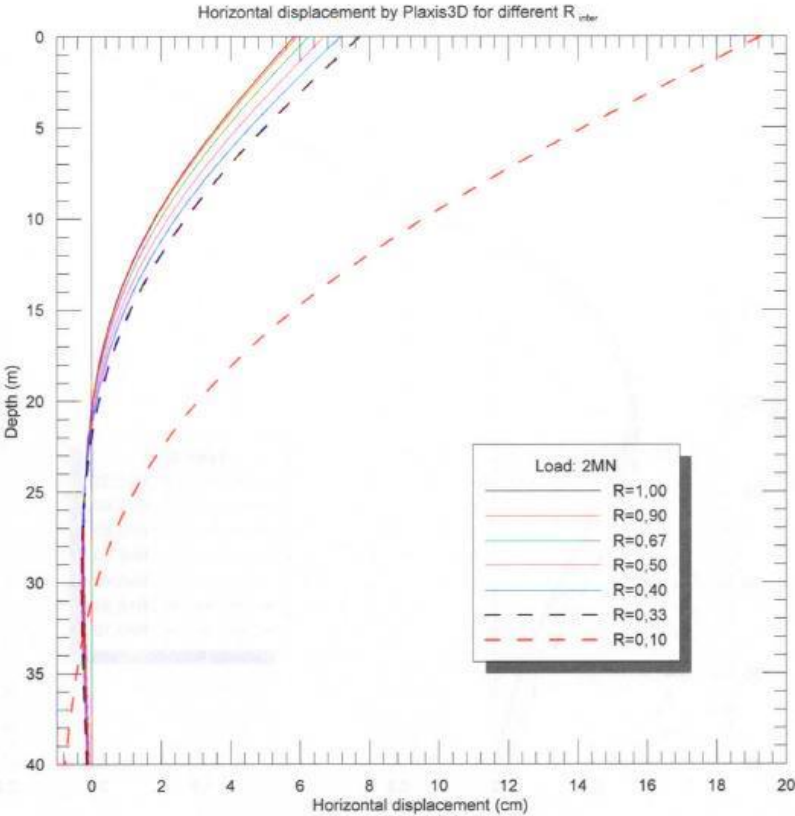
Below are reported graphs of displacement, bending moment, shear and later pressure for both the load conditions tested for different interface reduction factor.

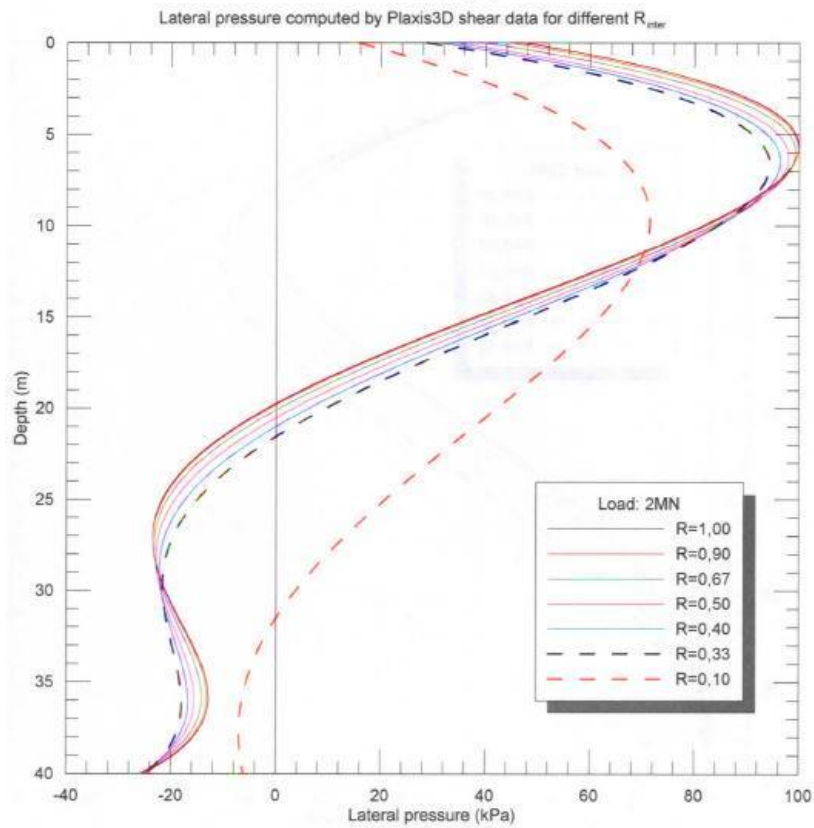
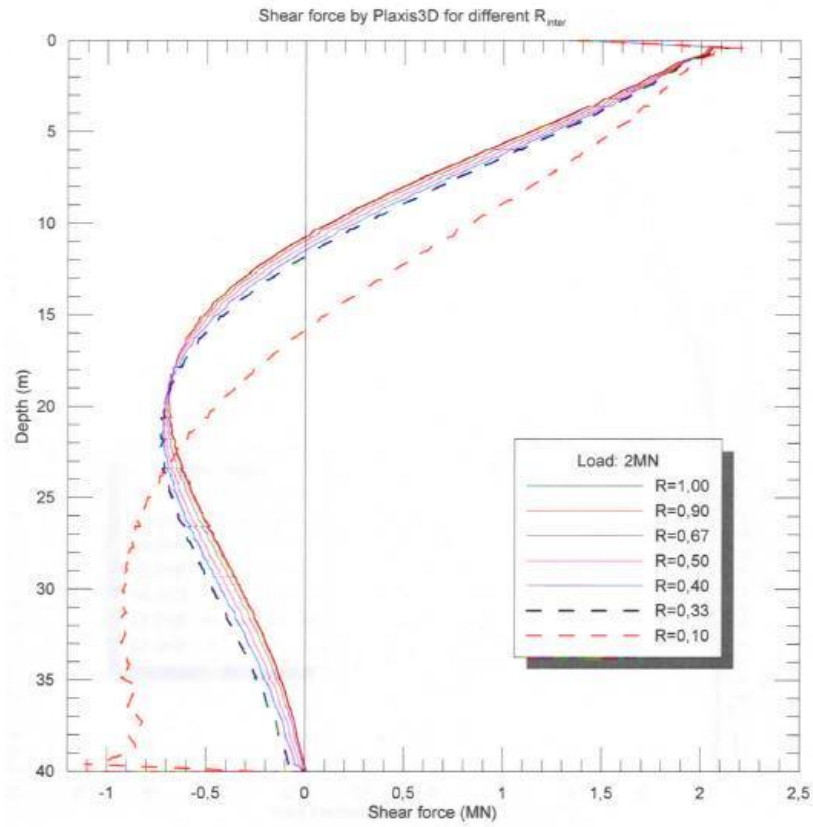
From the graphs below it is clear that the interface adoption leads to a general increase of the variables of interest.

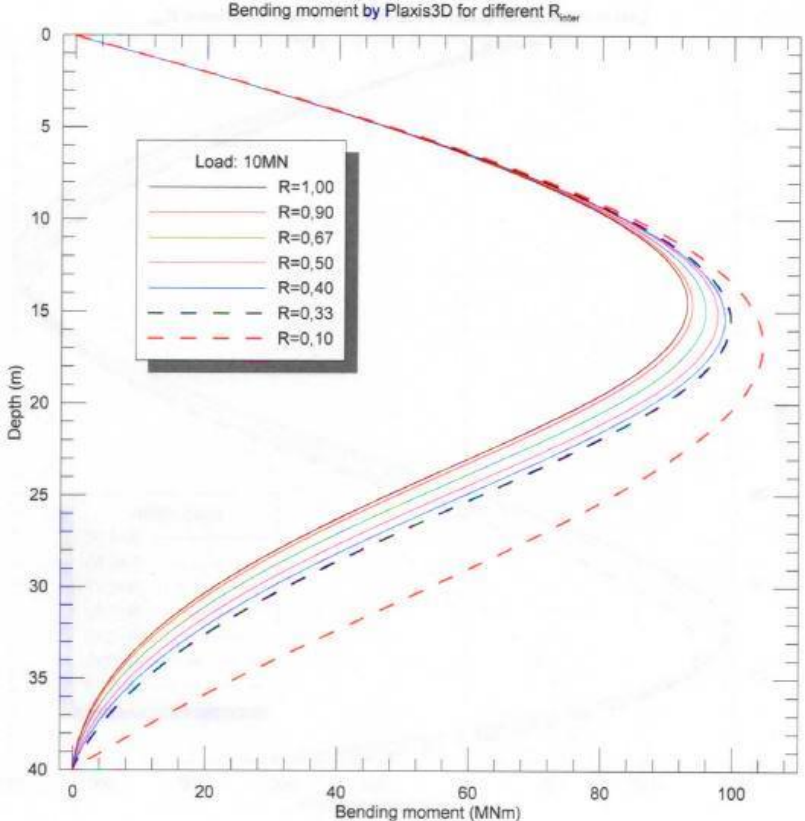
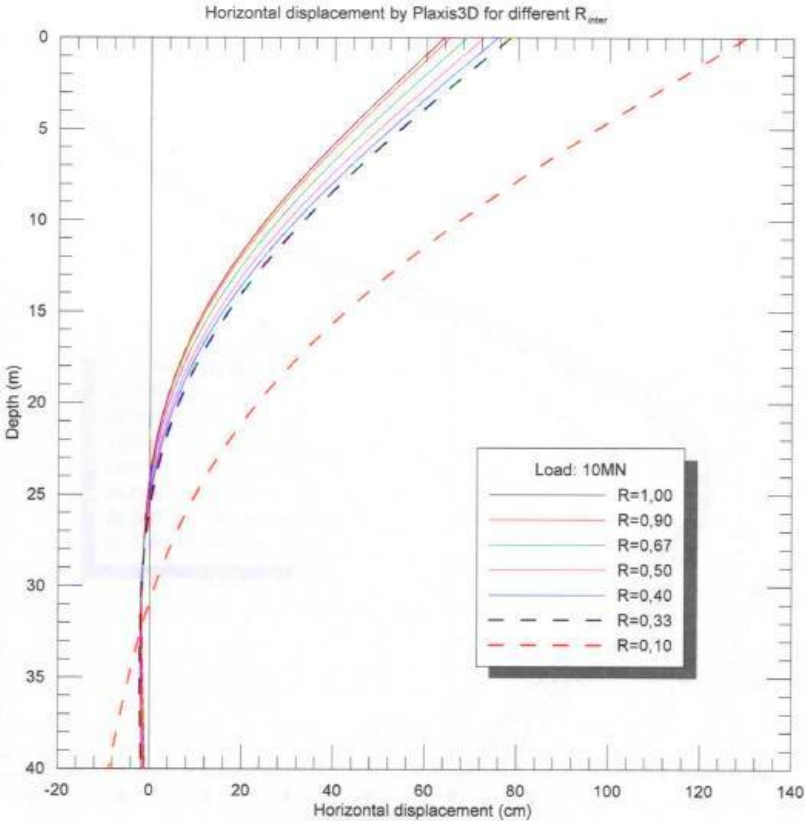
For a value of the interface reduction factor between 1 and 0.33, the results give a similar linear trend to each other, and only for the extreme value of 0.10 (black dashed curve) there are very important variations from the original trends. An extremely low value of the interface reduction factor means that both the interface surfaces are “free” to move. That behaviour is reached thanks to a great reduction of resistance and stiffness between each pair of nodes that compose the interface (of course, caused by 0.10 like reduction factor).

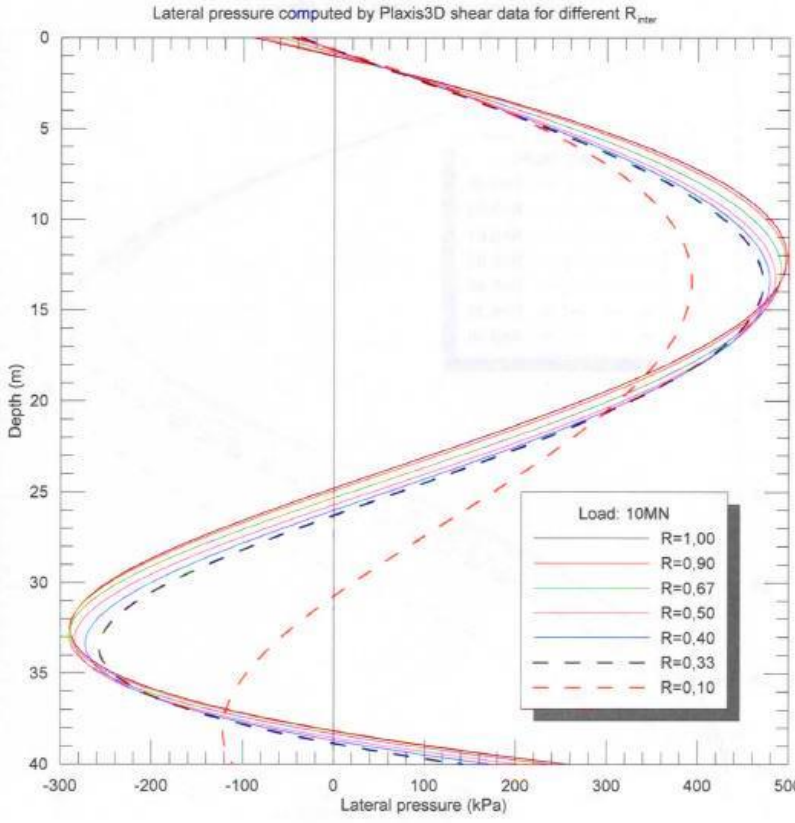
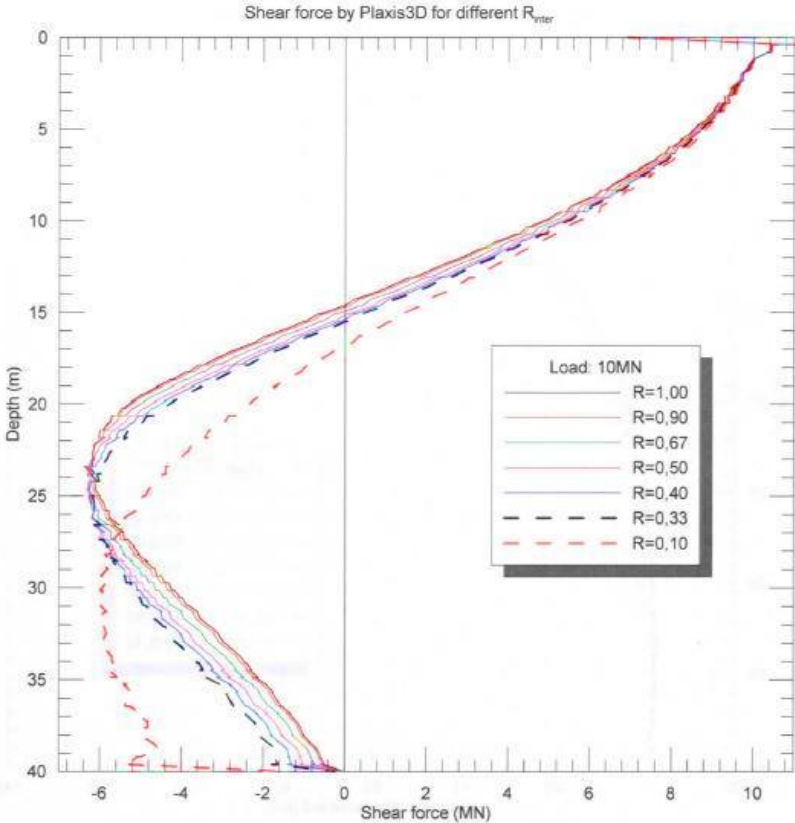
A decrease of the reduction factor leads to a shift of the bending moment peak and at the same time an increase of the maximum value; the same shift is shown by shear force trend.

Pile displacement increases with the reduction of the interface reduction factor.









## P-Y CURVES

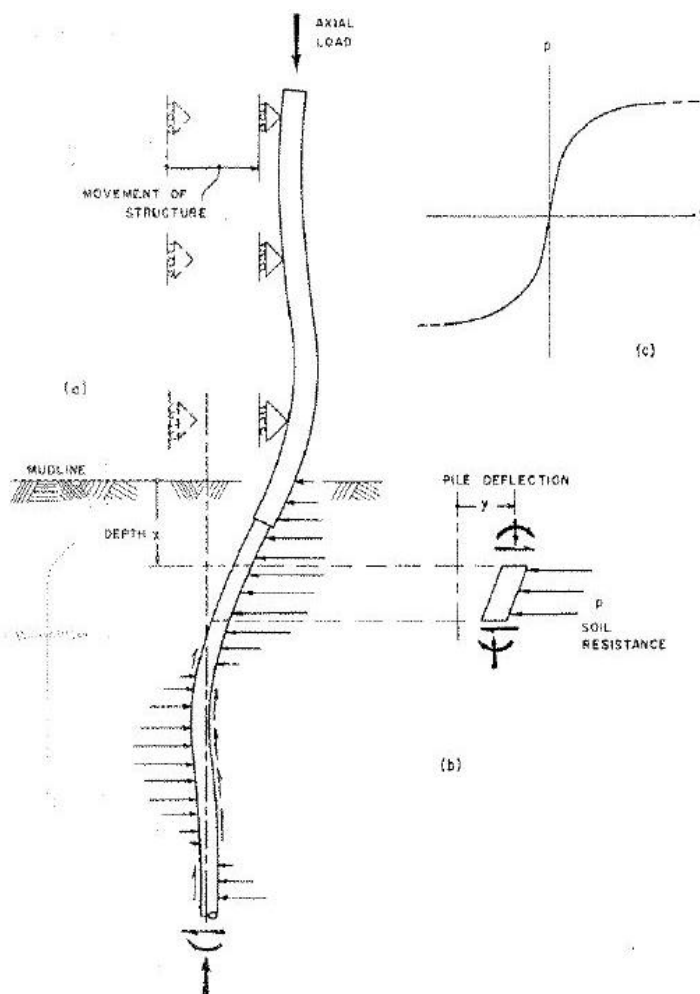
The ability to do a reasonable estimate of the behaviour of laterally loaded piles is an important consideration in the design of many offshore installations.

To perform an analysis for the design, it must be possible to reduce the soil behaviour at each depth to a simple p-y curve.

### Matlock (1970)

In the paper "correlation for design of laterally loaded piles in soft clay" published in 1970, Hudson Matlock wrote the most widespread approach for that typology of problems. Below, parts of that paper are reported.

He ran three load conditions pertinent with laterally loaded pile design: short-time static load, cyclic loading (like a storm) and reloading with a force less than the previous maximum.



Some problematic effects were present but Matlock neglected it explaining his choice with its low final effect.

Matlock studied the behaviour of laterally loaded piles in the Gulf of Mexico, where, like other seas, large lateral forces are produced by wind and waves associated with hurricanes and where the foundation materials in the critical zone near the mudline are often weakly clayey.

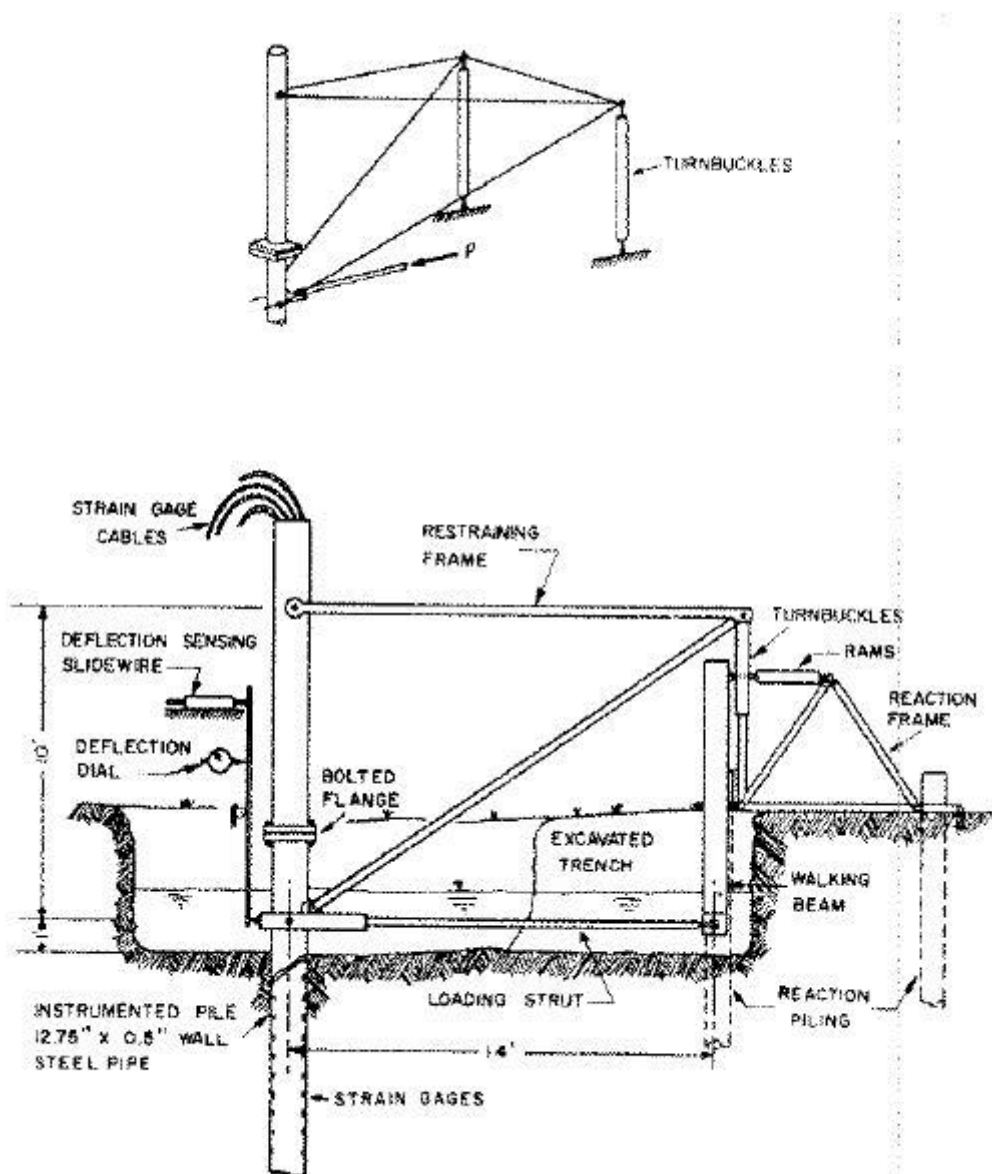
The structural analysis problem consists of a complex beam-column on an inelastic base. For piles separated by spacing of several diameters or more, the Winkler assumption is useful

to facilitate the analysis.

Soil is considered as a series of independent layers in providing resistance ( $p$ ) to the pile deflection ( $y$ ).

Soil resistance may be a highly non-linear function of the deflection. Only few versions of this problem, with simple configurations and elastic behaviours, can be solved by closed-form mathematics. Somewhat more complicated cases may be handled by non-dimensional curves or tables.

The steel tested pile presents a diameter of 12.75 inches and a length of 42 foot. The pile was calibrated in order to provide extremely accurate determinations of the bending moment.



Free-head tests were done with only lateral applied to the mudline. Fixed-head tests were done using a framework to simulate the effect of jacket structure. The load from the hydraulic rams was transferred to the pile by a walking beam and a loading strut.

Precise determination of the pile bending moment, during the static loading, allows differentiation to obtain curves of the soil reaction along the pile to a high degree of precision. Integration of the bending moment diagram provides the deflected shape of the pile. Load were increased by increments and for any selected depth the soil reaction ( $p$ ) mat be plotted as a function of the pile deflection ( $y$ ).

These experimental p-y curves are the main basis for the development of this design procedure.

Principal conclusion from Sabine River and Lake Austin (Matlock, 1970) were:

- The resistance-deflection (p-y) characteristics of the soil are highly non-linear and inelastic;
- Within practical ranges, the fundamental resistance-deflection characteristics of the soil appear to be independent of the degree of pile head restrain;
- A principal effect of cyclic loading appears to be permanent physical displacement of the soil away from the pile in the direction of loading. It is not clear what contribution to this effect was provided by loss in strength within the soil volume;
- The cyclic shear reversals in the soil mass may have caused some structural deterioration in the clay;
- Permanent displacement of the soil created a slack zone in the resistance-deflection characteristics;
- Although significant changes occurred with continued repetitions of load cycles, at any given magnitude of lateral load (except for the highest) the behavior of the pile-soil system tended to stabilize.

Then it becomes possible to define a static ultimate resistance.

In soft clay soil is confined so that plastic flow around a pile occurs only in horizontal planes, the ultimate resistance per unit of length of pile may be expressed as:

$$P_u = N_p c d$$

Where  $c$  is the soil strength ( $S_u$ ),  $d$  is he pile diameter and  $N_p$  is a non-dimensional ultimate resistance coefficient. For soft clay soils flowing around a cylindrical pile at a considerable depth below the surface, the  $N_p$  factor should be 9. Very near the surface the soils in front of the pile will

fail by forward and upward and so the corresponding value of  $N_p$  reduces to the range of 2 to 4. For a cylindrical pile a value of 3 is believed appropriate.

The resistance increase with the distance from the free soil surface. The following equation describes this variation:

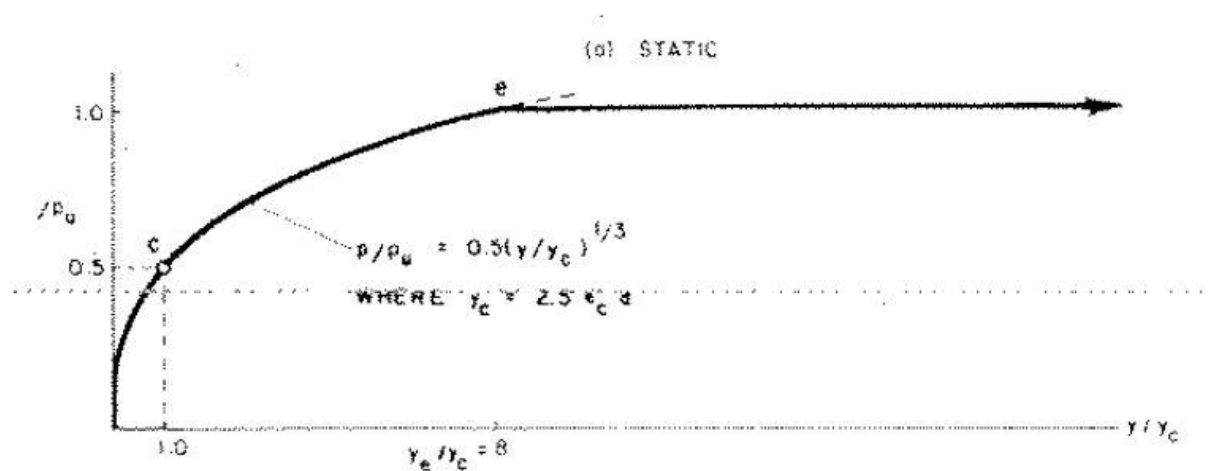
$$N_p = 3 + \frac{\sigma'_x}{S_u} + J \frac{x}{d}$$

Where the first term expresses the resistance at the surface, the second term gives the increase with depth due to overburden pressure, and third term may be thought of as geometrically related restraint that even a weightless soil around the pile would provide against upward flow of the soil.

$J$  is an empirical factor obtained by field data, for instance on Sabine River is approximately 0.5

### Definition and use of the P-y curves

P-y curve is the most widespread relation adopted to design laterally loaded piles. The curve represents the non-linear behaviour of the soil at a certain depth. Each curve is representative of a spring at a specific depth.



Exist several correlations to improve the quality of original p-y curves thought by Matlock or to define a relation resistance-deflection for cyclic load, also in the original paper this design is considered.

P-y curves for static and cyclic loading is part of American Petroleum Institute standard today.

The proper form of the p-y relation is influenced by many factors:

- Natural variations of soil properties with depth;
- General form of the pile deflection;

- Corresponding state of stress and strain throughout the affected soil zone;
- Rate, sequence and history of the cyclic wave loadings.

To perform an analysis for the design, it must be possible to reduce the soil behavior at each depth to a simple p-y curve.

The curves are in non-dimensional form with the ordinates normalized according to the static ultimate resistance  $P_u$  determined like above described for each average depth of the sub-layer. The horizontal coordinate is the pile deflection divided by the deflection at the point where the static resistance is one-half of the ultimate.

The form of the pre-plastic portion of the static resistance curve is based on semi-logarithmic plots of the experimental p-y curves, which fall roughly along straight lines at slope yielding the exponent of one-third.

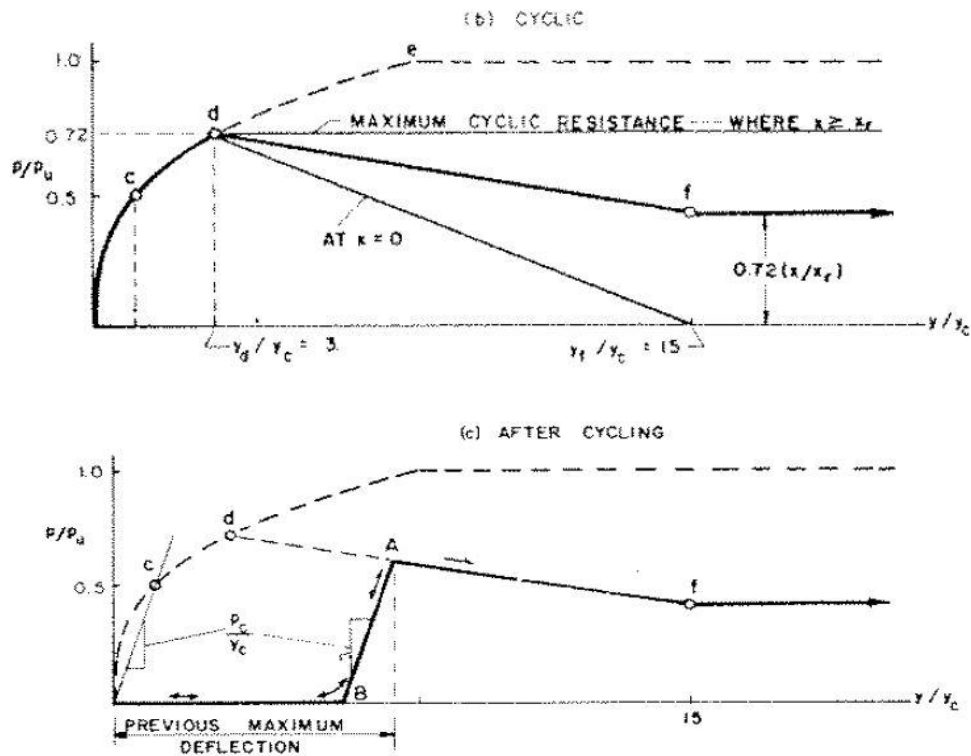
Equation of the resistance-deflection curve by Matlock is:

$$\frac{P}{P_u} = 0.5 \left( \frac{y}{y_c} \right)^{1/3}$$

The value of the deflection at the point where the static resistance is one-half of the ultimate, is based on concepts given by Skempton by which he combines elasticity theory, ultimate strength methods and laboratory soil properties to estimate the short-time load-settlement characteristics of buried strip footings in clay soils. The strain  $E_{ps50}$  ( $E_{psC}$  in the original paper) is defined like the strain that occurs at one-half of the maximum stress on a laboratory stress-strain curve. It may be determined by dividing the shear strength  $c$  ( $S_u$  for us) by an estimated secant modulus of elasticity ( $E_c$ ) or it may be taken directly from stress-strain curves.

Using the relation proposed by Skempton, the deflection sought is defined like:  $y_c = 2.5 d E_{ps50}$ . Complete loss in resistance is assumed to occur at the soil surface when deflections at the point reaches  $15y_c$ .

P-y curves for cyclic load and re-load, are not part of this study.



### Lateral pressure calculation in Plaxis3D

Since the first analysis, there was the problem of choosing the most accurate way to calculate the lateral pressure i.e. the contact pressure between soil and laterally loaded pile.

A real and accurate value of lateral pressure is essential to build the p-y curves that is the objective of these series of analysis.

In the first part of this section are presented the lateral pressure obtained for two different degree of fitting polynomial (5<sup>th</sup> and 6<sup>th</sup> order), then are tested different intersection values for those curves at seabed level (depth equal to zero).

For both, the polynomial degrees are tested by the following intersection values: the load applied (like boundary condition), the value of Plaxis3D shear at seabed and without fixing an intercept.

In the graph below, lateral pressure trends are shown; it is clear that below 5 meters depth all these different polynomials compute the same lateral pressure.

Problems are localized on the pile tip and, more dangerously, on the top 5 meters.

Lateral pressure has been calculated like the first order derivative of the shear. Note that it was chosen to fit the trend of Plaxis3D shear with a polynomial to obtain a continuous function, then it was done the analytical derivative of first order of that function. In order to calculate the lateral

pressure, the shear derivative is also divided by pile diameter, this to obtain dimensionally a pressure.

In the end, it was done also a test with the lateral pressure calculated by a trend line with intercept set equal to the average of load applied and Plaxis3D shear at the seabed section.

In all this proves were obtained too variable results in the shallows (5 meter depth).

For this reason, it has been decided to "solve" the problem by hand calculation based on the simple and, at the same time, sure concept of force equilibrium.

It's important to highlight that this method modifies the lateral pressure, on the top part of the pile, working on the lateral pressure trend computed like above explained.

The first step consists in choosing a depth where the results are assumed as correct so in this case it is chosen a depth of 5 meters. In these pages the expression "sure depth" is used with reference to the depth just above defined. Known the shear variation (calculated like the difference between Plaxis3D shear at the sure depth and the load applied on the pile head), this value is divided by the corresponding depth variation (sure depth subtracted seabed level) and divided by pile diameter. The pressure, in this way calculated, is the constant pressure value able to guarantee the force equilibrium on the top part of the pile. Note that the lateral pressure value at sure depth it's known, which means the possibility of create a linear trend between that point and the seabed level, this because it's already known the constant value of lateral pressure that equilibrates the system. Now, fixed one point more, to create a linear trend becomes simple, i.e. same area (force) but linear distribution of pressure against constant.

With this method are obtained approximate but plausible results for the shallow part of the problem that alternatively is affected by problems connected with the weakness of adopting a fitting curve. The idea of using a polynomial fitting curve (trend line) was found in several technical papers.

Using the "manual" derivative (shear variation divided by depth variation and diameter, point by point) was left aside because every typical (little) shear fluctuation into Plaxis3D data output produces a gigantic and senseless variation of lateral pressure.

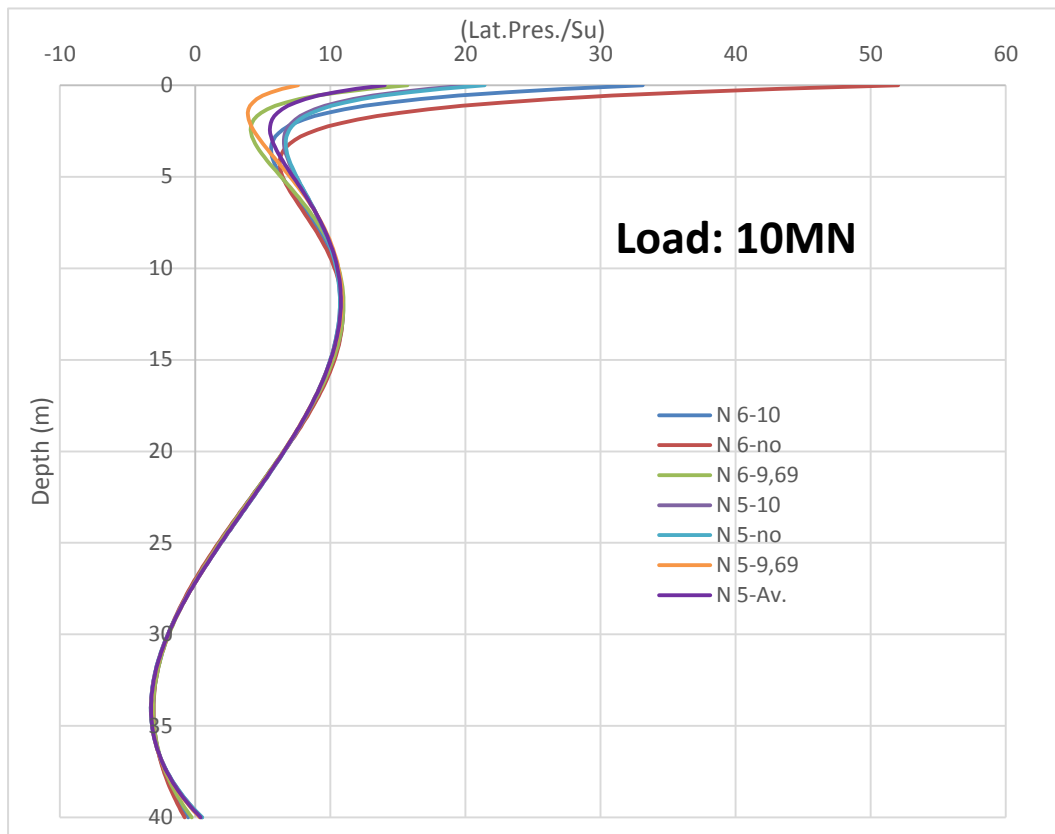
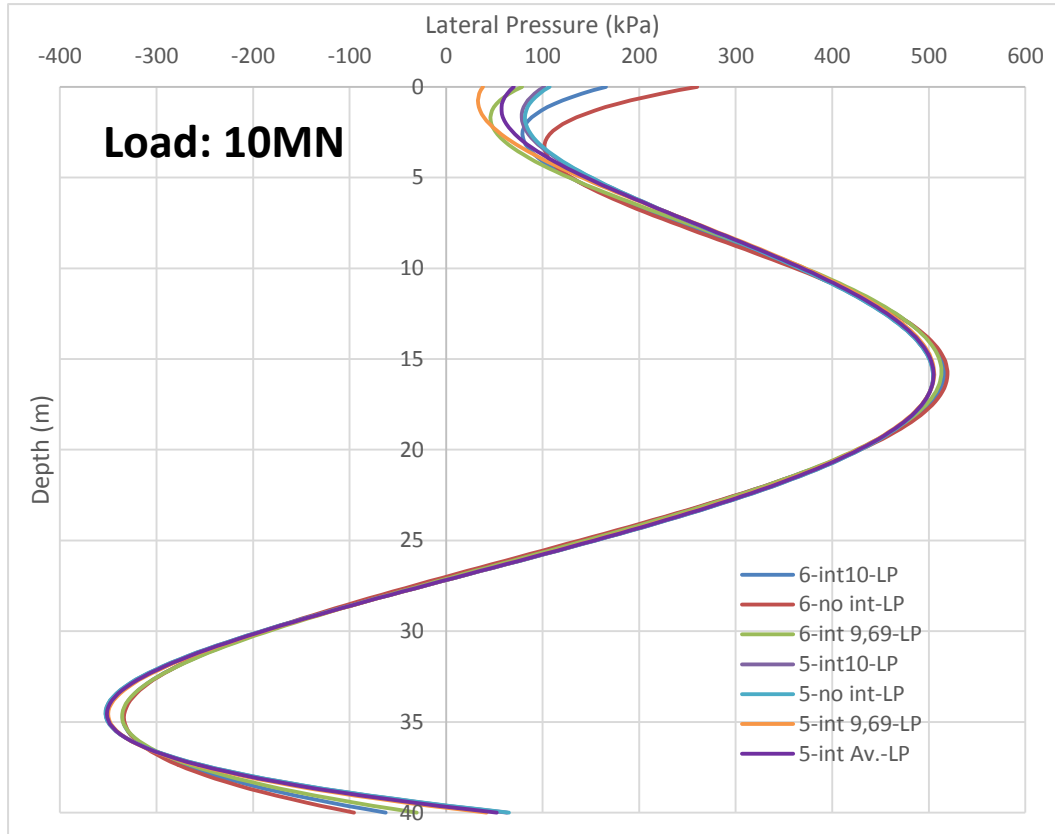
In the end, the pile tip problem, i.e. in some case a value slightly negative related with the pile displacement, it should be connected with a kind of boundary condition for the pile shear with the pile tip friction against the soil that produces a resistance force able to restrict the pile tip movement. In order to reduce it, a rigid interface is adopted on the pile tip. Another solution consists

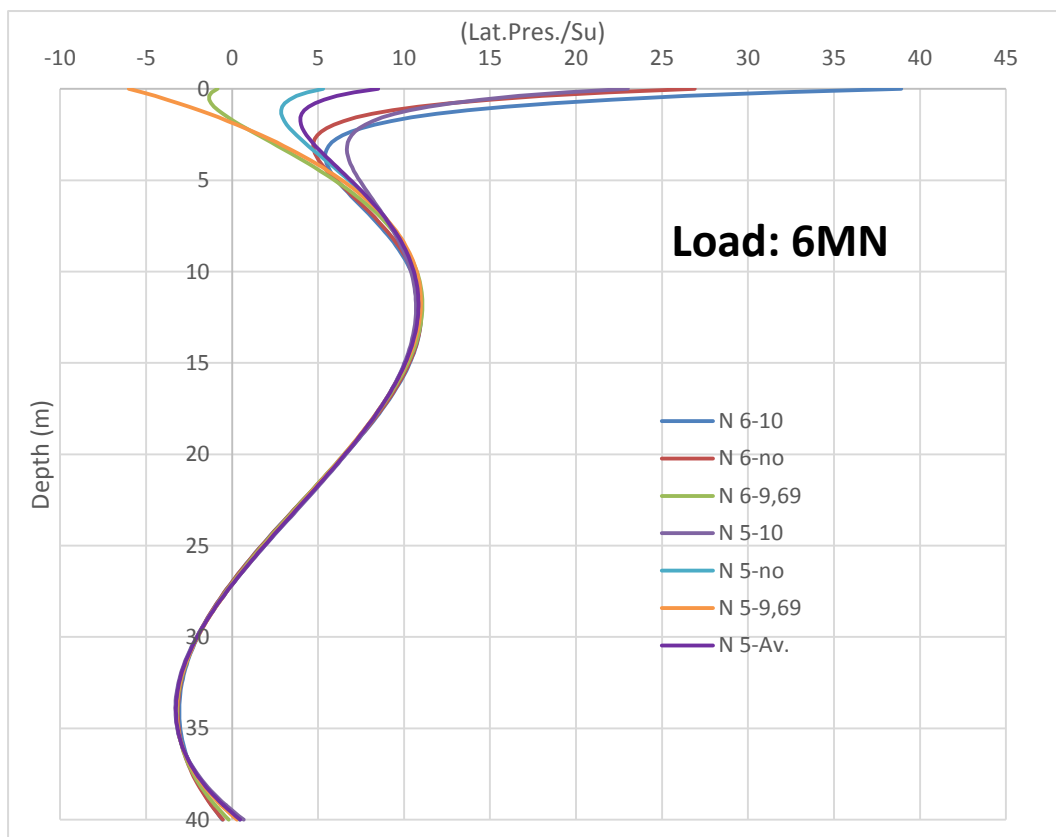
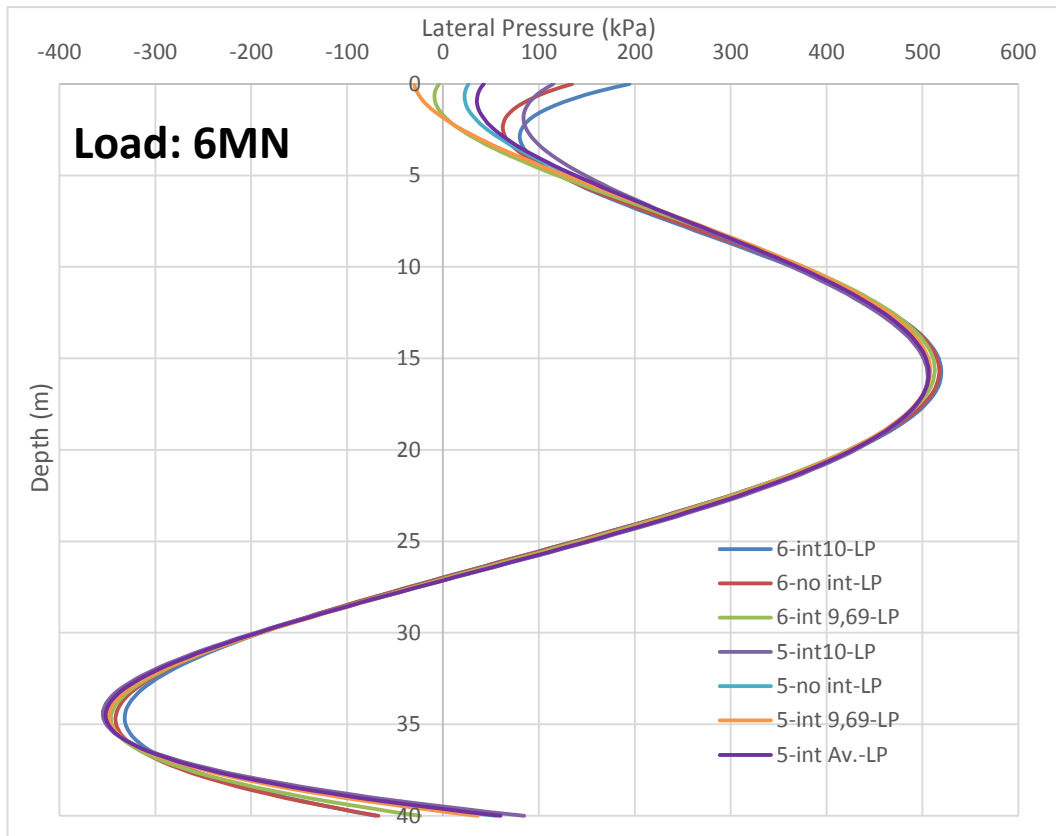
in defining a thin layer at the pile tip level, where a very fine discretization must be set in order to allow the tip movement and to evaluate it with an acceptable precision.

Note that only for the definitive model the lateral pressure at shallow depth will be calculated by equilibrium like above described.

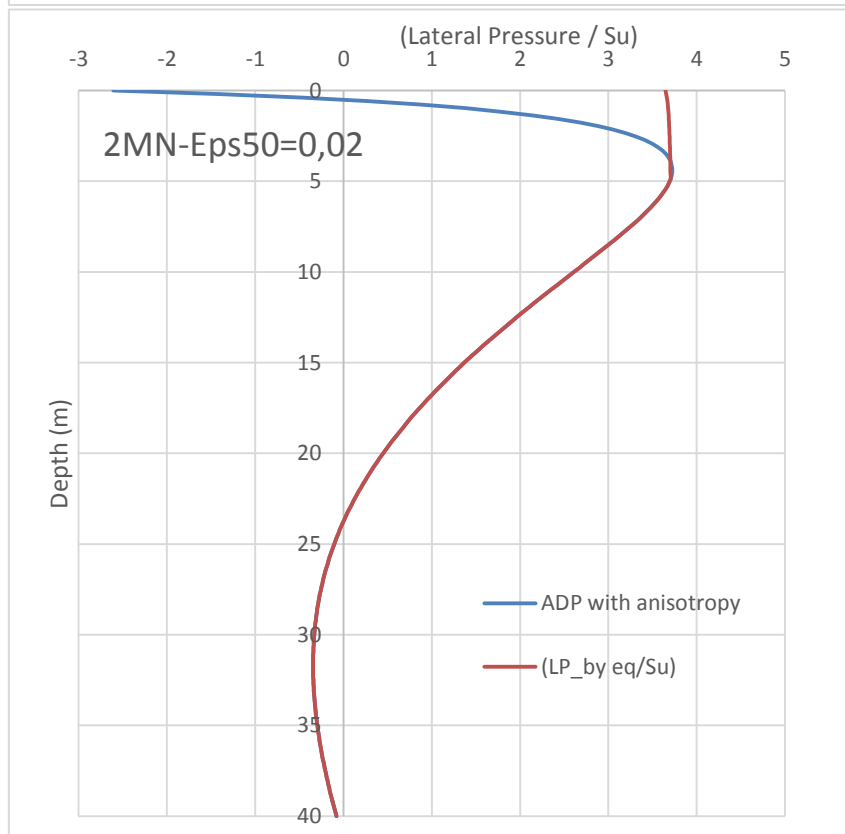
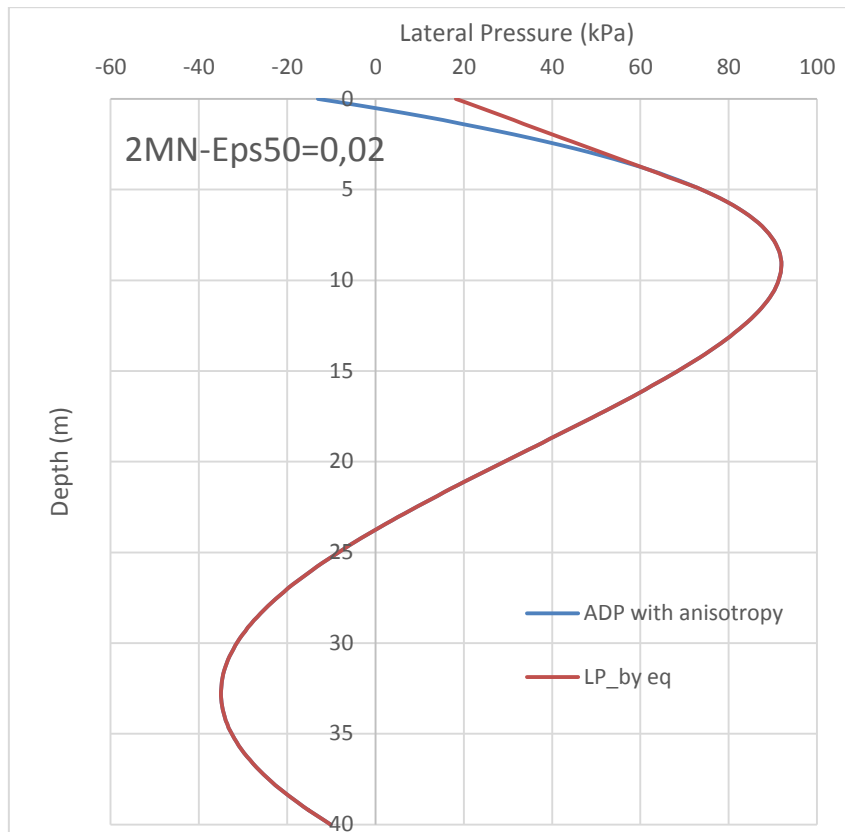
From the graphs below, it is clear that using a trend line is a comfortable way of working, but at the same time it is a weak solving methods.

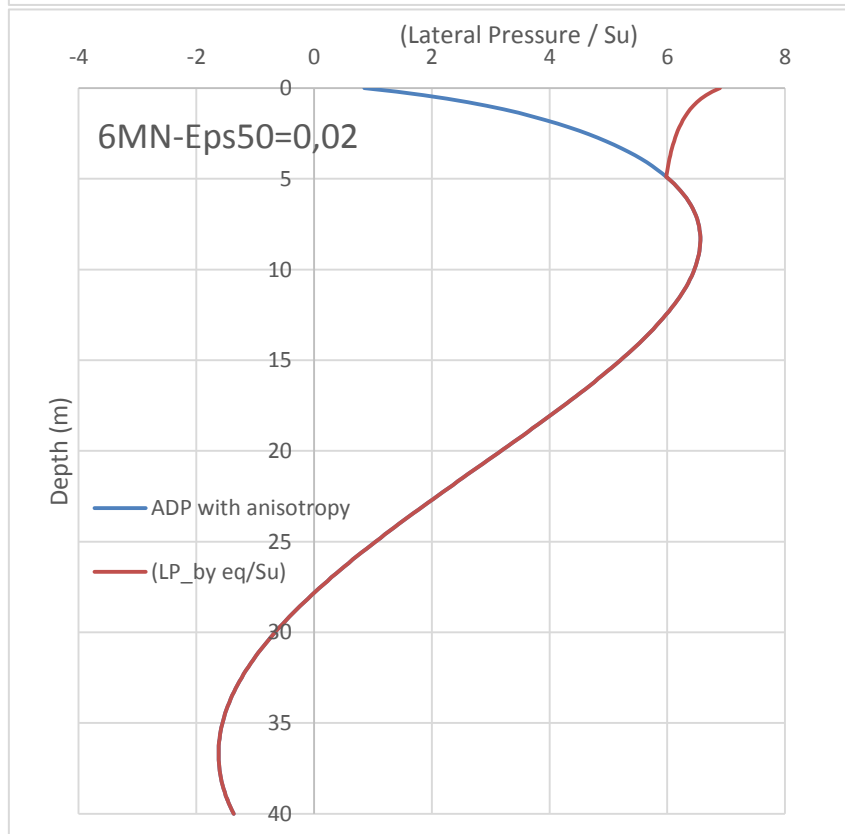
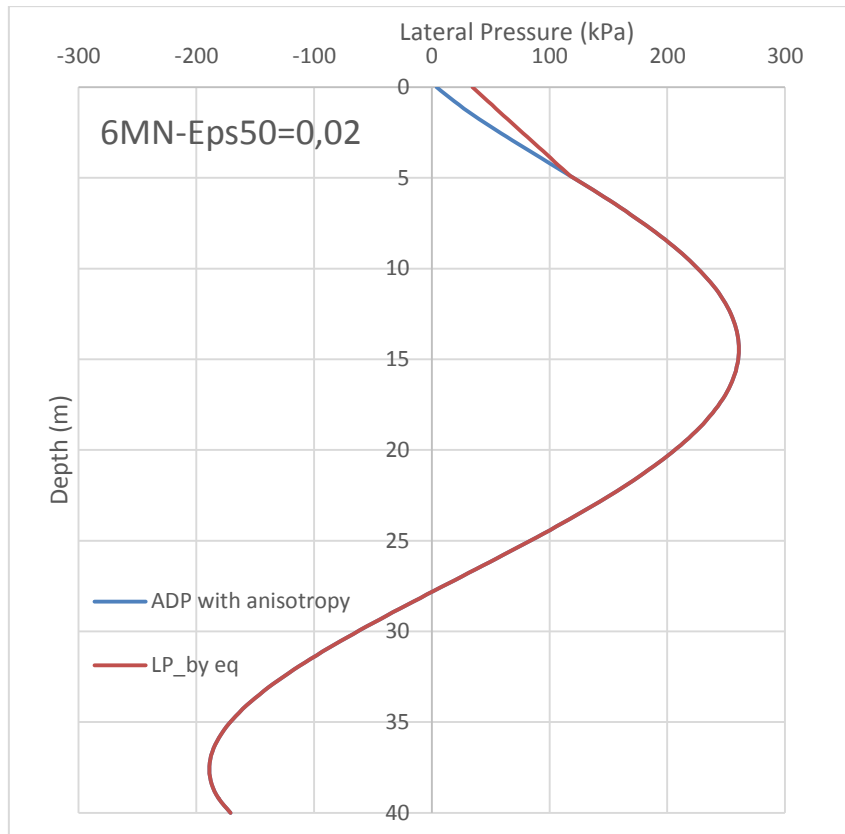
A negative value for the lateral pressure has not sense near the pile tip, or positive near the pile head. Where it happens, it is due to some numerical wrong approximations of the fitting curve, that is amplified by the second order derivative.

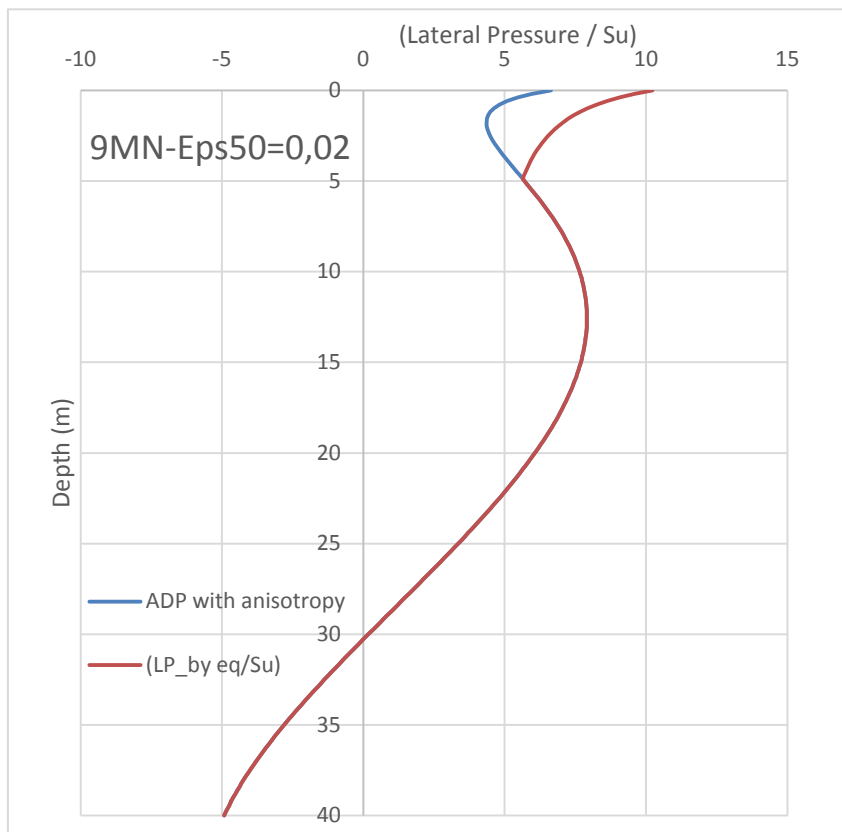
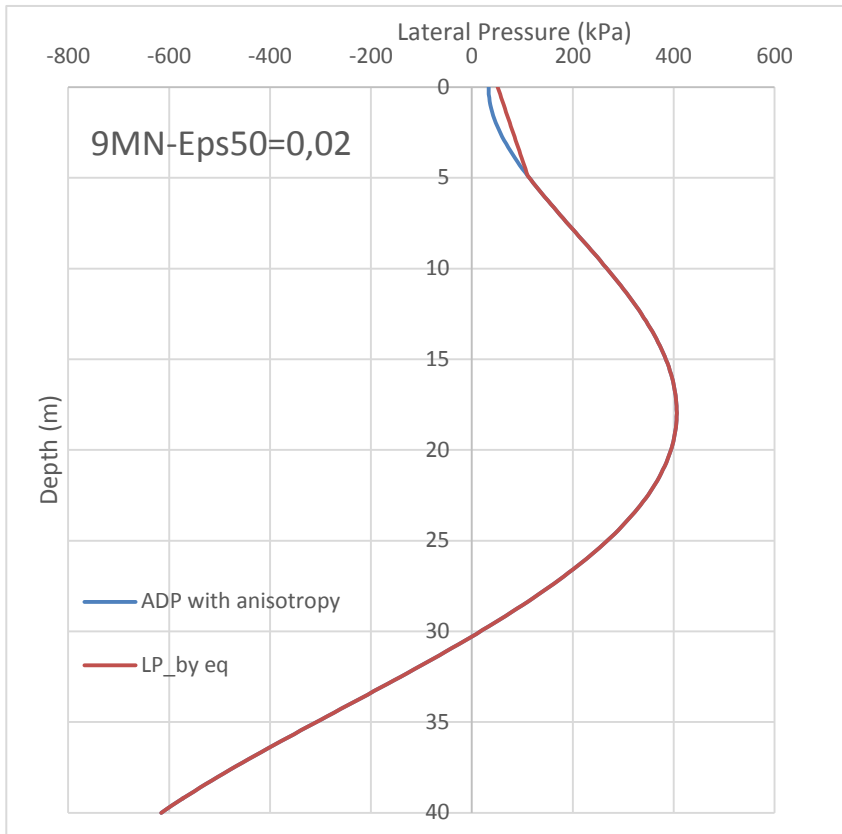


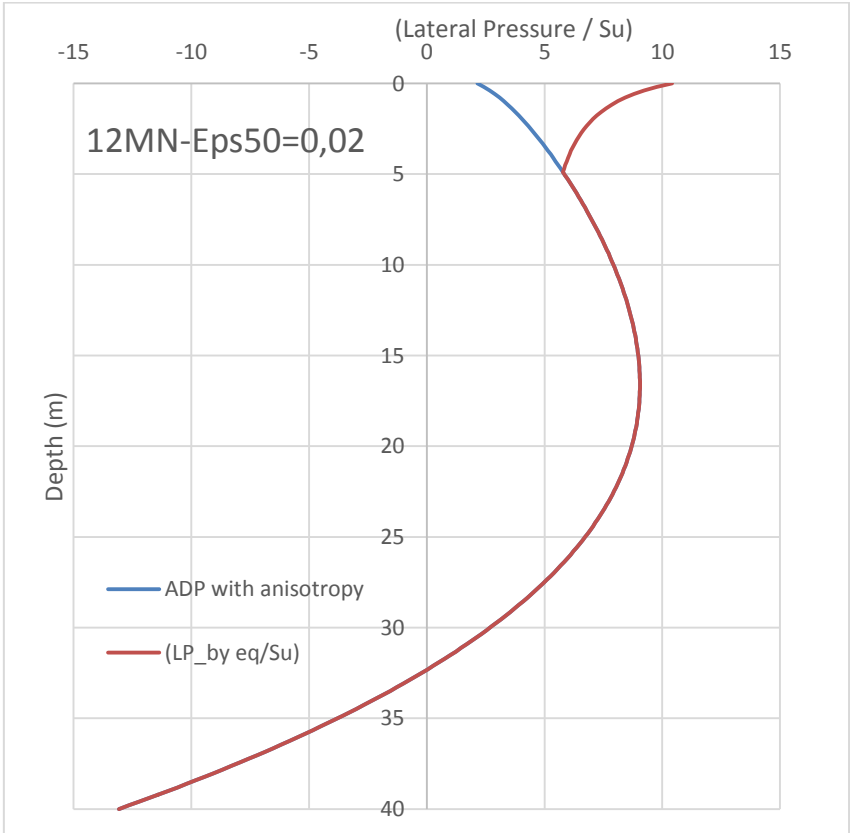
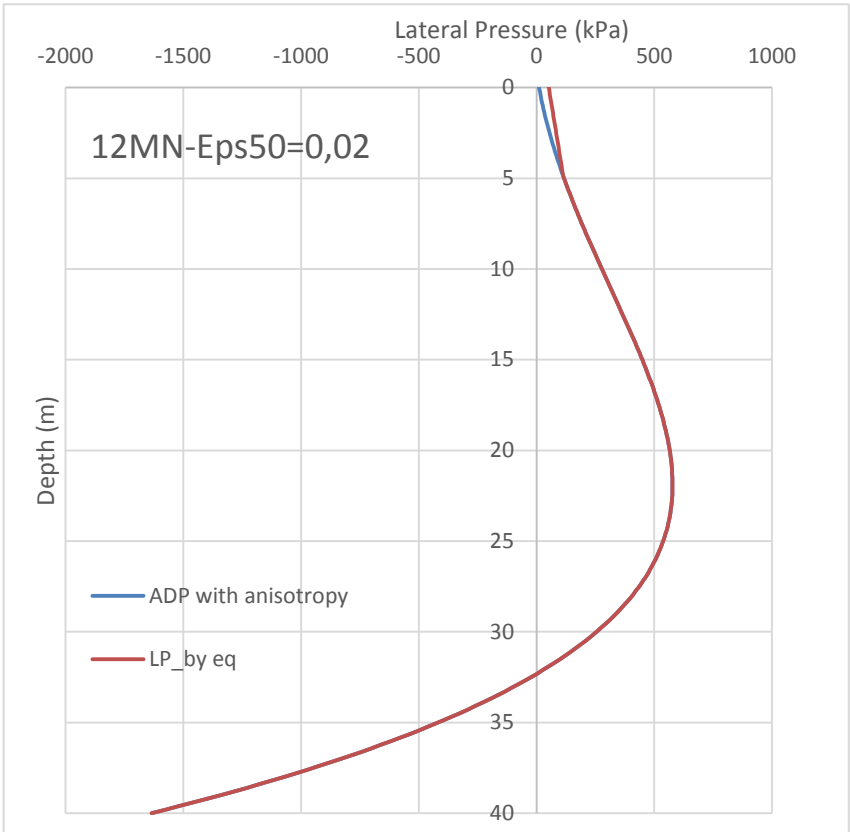


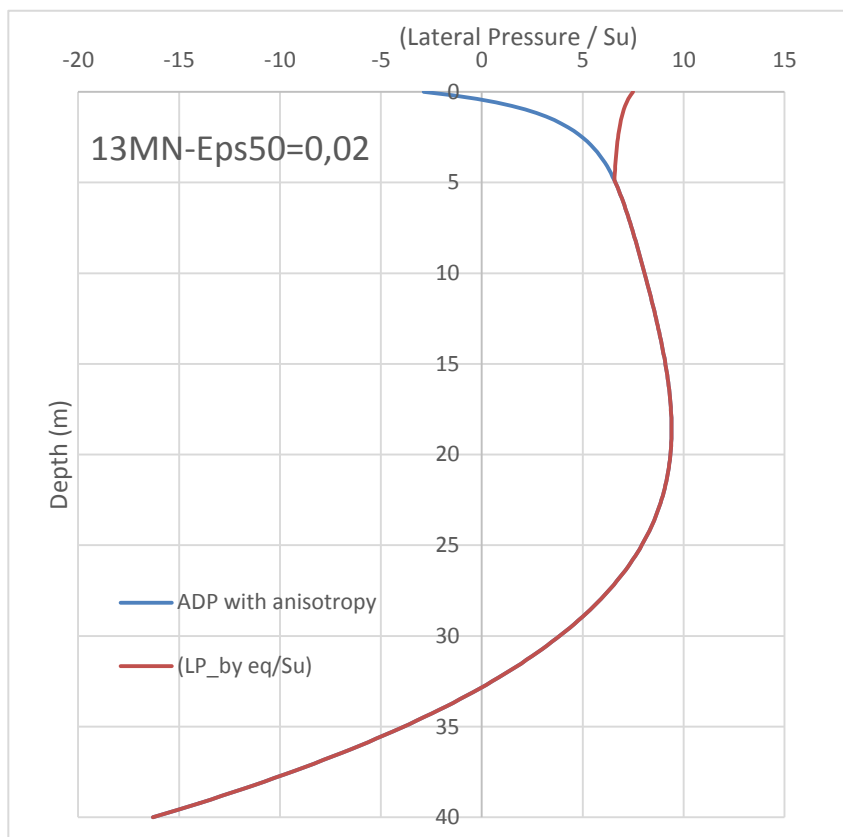
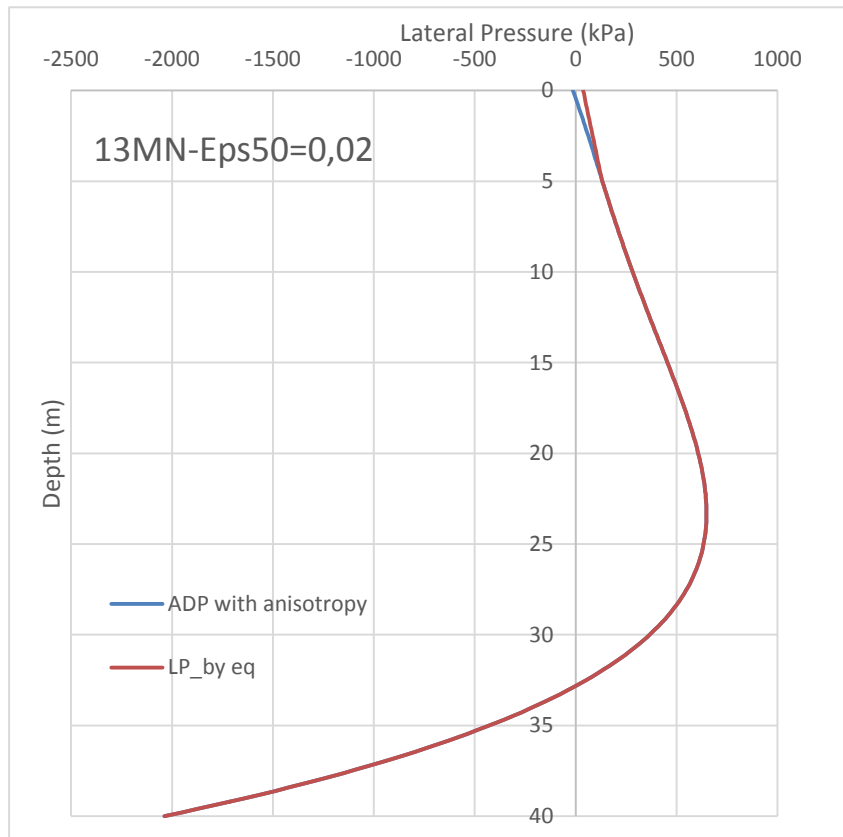
Model (series ID: D1) with lateral pressure corrected by equilibrium above the node at a 4,88m depth:

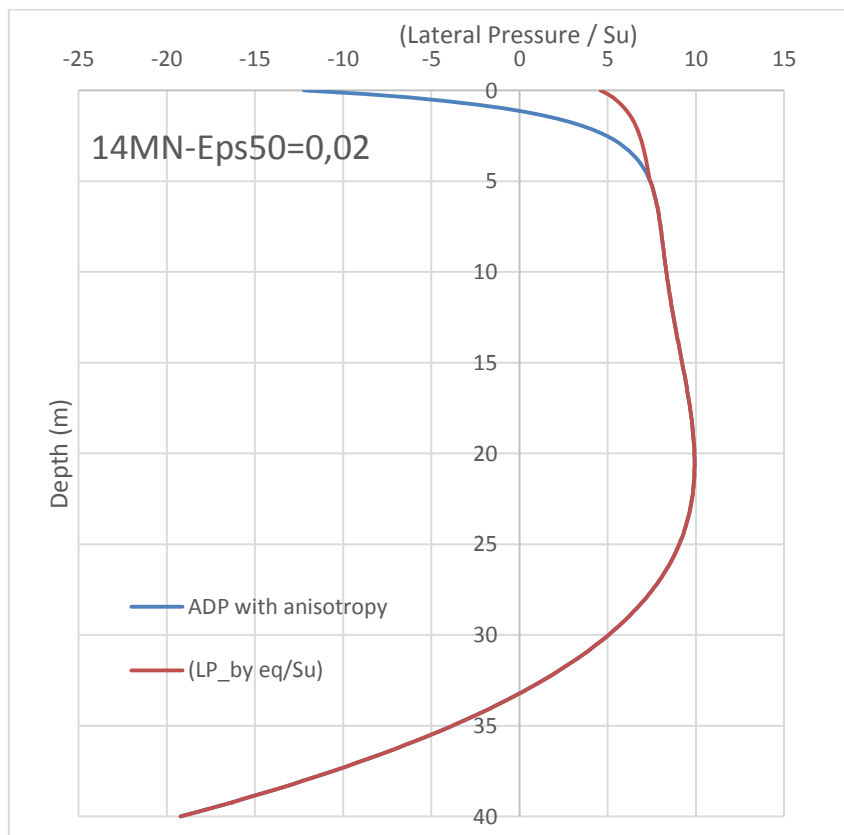
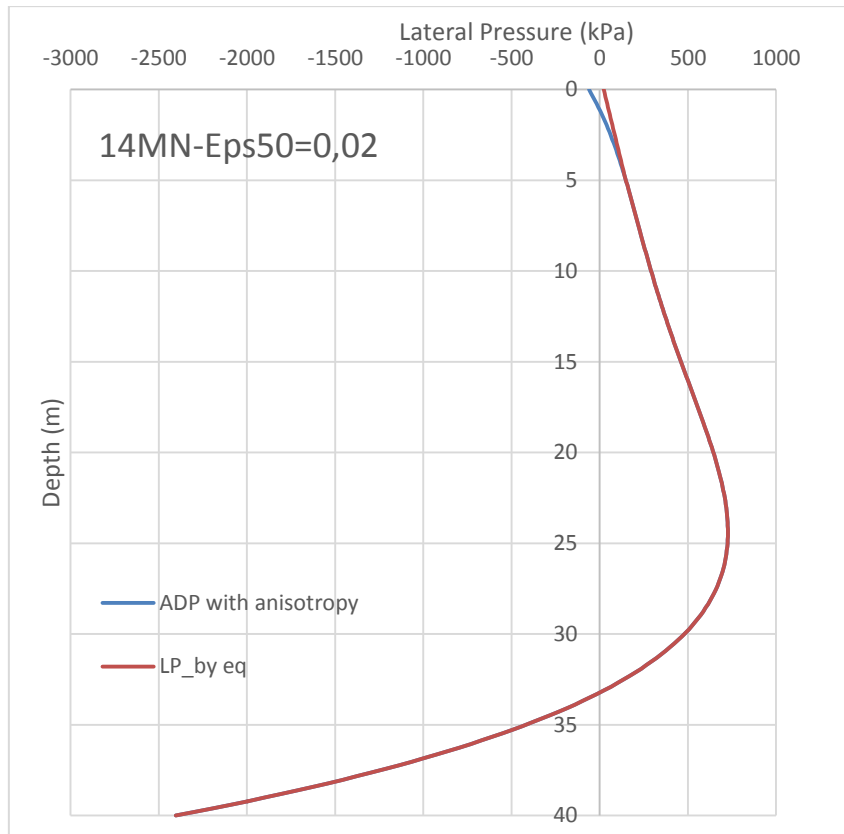












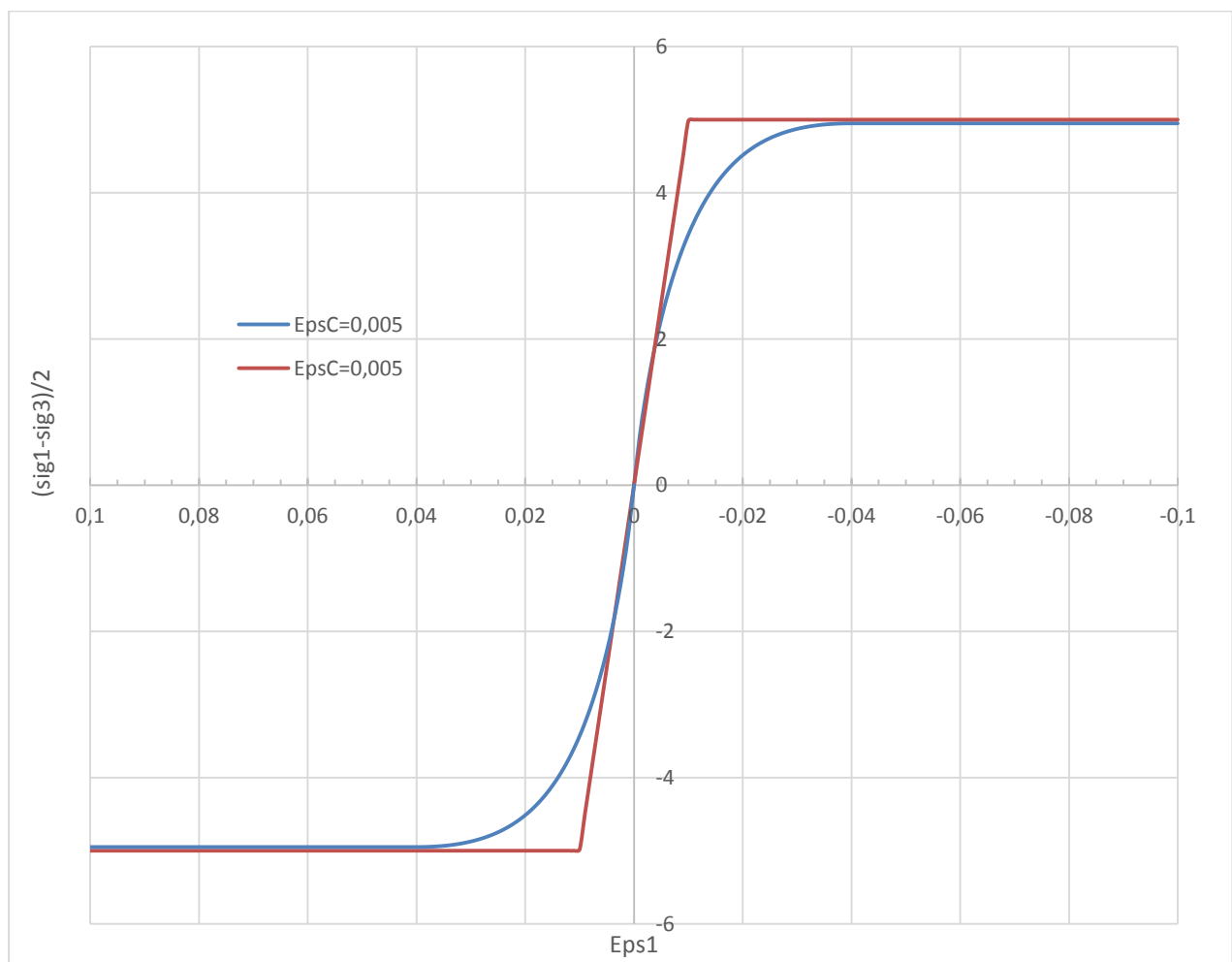
In the last pages, for each load step is presented a couple of graphs: lateral pressure and ratio between it and undrained shear strength. This ratio is comparable with the Matlock N factor, but only in the areas where the soil is totally plasticized i.e. where the ultimate pressure is reached. This parameter for the heaviest load condition presents a good trend. It starts around 4 and it reaches a maximum of 10. Matlock range of values starts from a minimum of 3 to a maximum of 9 (other papers propose different values of the bearing factor, but in any case no more than 12).

### Isotropic NGI-ADP soil model

After all, the sensibility analysis for the soil, just run for different variables, that adopts a Mohr-Coulomb model was chosen to pass at ADP soil model.

This new model increases the quality of the numerical simulation response thanks to its affinity observed to perform the real behavior of clay in undrained condition.

Using ADP soil model means defining a larger range of parameters than Mohr-Coulomb, like the ratios between  $Su_{DSS}$  and  $Su_{AVERAGE}$ ,  $Su_{TX-COMPRESSION}$  and  $Su_{AVERAGE}$ ,  $Su_{TX-EXTENSION}$  and  $Su_{AVERAGE}$ .



Note that in the use of ADP soil model, the assignation of a different interface material has been preferred to the definition of the interface reduction factor ( $R_{inter}$ ) in the surrounding soil (adopting ADP). The interface adopts Mohr-Coulomb as soil constitutive model and 0.67 is the value set for the interface reduction factor in agreement with the value suggested by Plaxis3D manual for situations without specific indication or available test data.

It is very important to note that until now it has been used a very low Young's elasticity modulus, something which cannot be now changed or the comparison with older data will not be correct. This is a problem because, in Plaxis3D, the minimum acceptable value of the ratio between  $G_{ur}$  and  $Su_{AVERAGE}$  is 100 whereas unfortunately the real values are 66.7 for  $Eps50=0.5\%$ , 33.3 for 1% and 16.7 for  $Eps50=2\%$ . Therefore, it has been chosen to work adopting 100 (minimum input recognized) for that ratio.

Note that also the definition of shear modulus is different through ADP and Mohr-Coulomb. Indeed, Mohr-Coulomb defines in input  $G_{50}$  at half of the maximum stress instead in ADP soil model  $G_{ur}$  is defined like the shear modulus of the initial part of stress-strain curve.

Note that NGI-ADP is adoptable only in Plaxis3D 2013 VIP package, but it is not possible to run soil tests in the 3D input phase. Fortunately, it is possible to do them in 2D input phase.

It has been found a matching between ADP and Mohr-Coulomb changing the failure strain in ADP model (failure strain is equal to 1.5 times  $Eps50$ ).

It was also chosen to work with two extreme values of the typical  $Eps50$  strain at half of the ultimate stress range, relatively 0.5% and 2%.

These analyses were run in reason to investigate essentially the response differences using ADP compared with a soil model elastic perfectly plastic until now used.

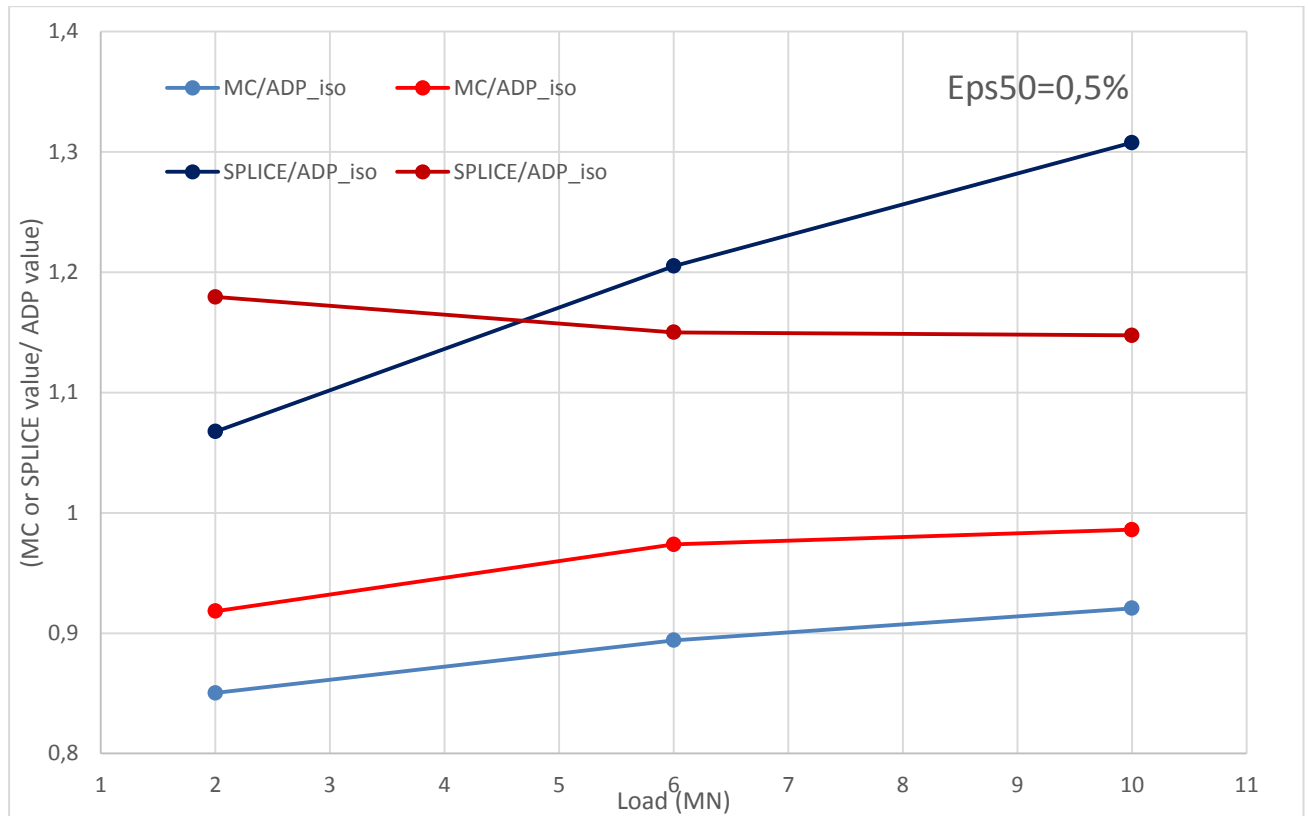
It's fundamental to know that to obtain an ADP soil equivalent to Mohr-Coulomb it has been necessary to set every  $Su$  equal to  $Su_{AVERAGE}$ . It means every  $Su$  ratio equal to 1. In order to avoid annoying numerical problems it was preferred to adopt 0.99 as ratio between  $Su_{COMPRESSION-TX}$  and  $Su_{AVERAGE}$ .

For  $Eps50$  equal to 0.5% and 2.0% it was set the failure strain relatively equal to 2% and 22% into ADP soil model (input phase).

Below, the ratios between SPLICE and Plaxis3D results are plotted (Mohr-Coulomb and isotropic ADP), then: shear force, lateral pressure, bending moment and horizontal displacement, only for the

case with Eps50 set equal to 0.5% in three load conditions (2/6/10 MN, where 10 MN is the maximum value able to guarantee convergence in SPLICE for this Eps50 value.

Below, in recapitulative graphs, the values are normalized with isotropic ADP results. In blue are plotted the maximum bending moment trends, instead in red the displacement trends of the pile head. Dark tones are adopted for SPLICE, soft for Mohr-Coulomb.



It's interesting to note that for a low load like 2 MN, SPLICE gives a displacement trend very similar to isotropic ADP results, but the bending moment peak for ADP is substantially different from SPLICE peak (15% ca).

For low load, the differences between ADP and Mohr-Coulomb are considerable, increasing the load, especially near the failure, that behavior change, so ADP and Mohr-Coulomb give approximately the same results.

This trend could be explained by the fact that the soil behavior is governed by the soil stiffness for low load, instead for high load the ultimate strength governs the problem. Indeed, looking at the strain-stress curve it is simple to note that the difference between isotropic ADP and Mohr-Coulomb behavior is localized in the first part of that curves, i.e. the stiffness, then, for large strain, both the curves converge to the assigned  $S_u$ .

Finally, it's important to highlight that for a load near the failure (10 MN) the ratio between lateral pressure and undrained strength has a maximum of 9 in SPLICE (in agree with Matlock paper, where this ratio is named  $N_p$ ) instead Plaxis3D leads to a value near to 10.5.

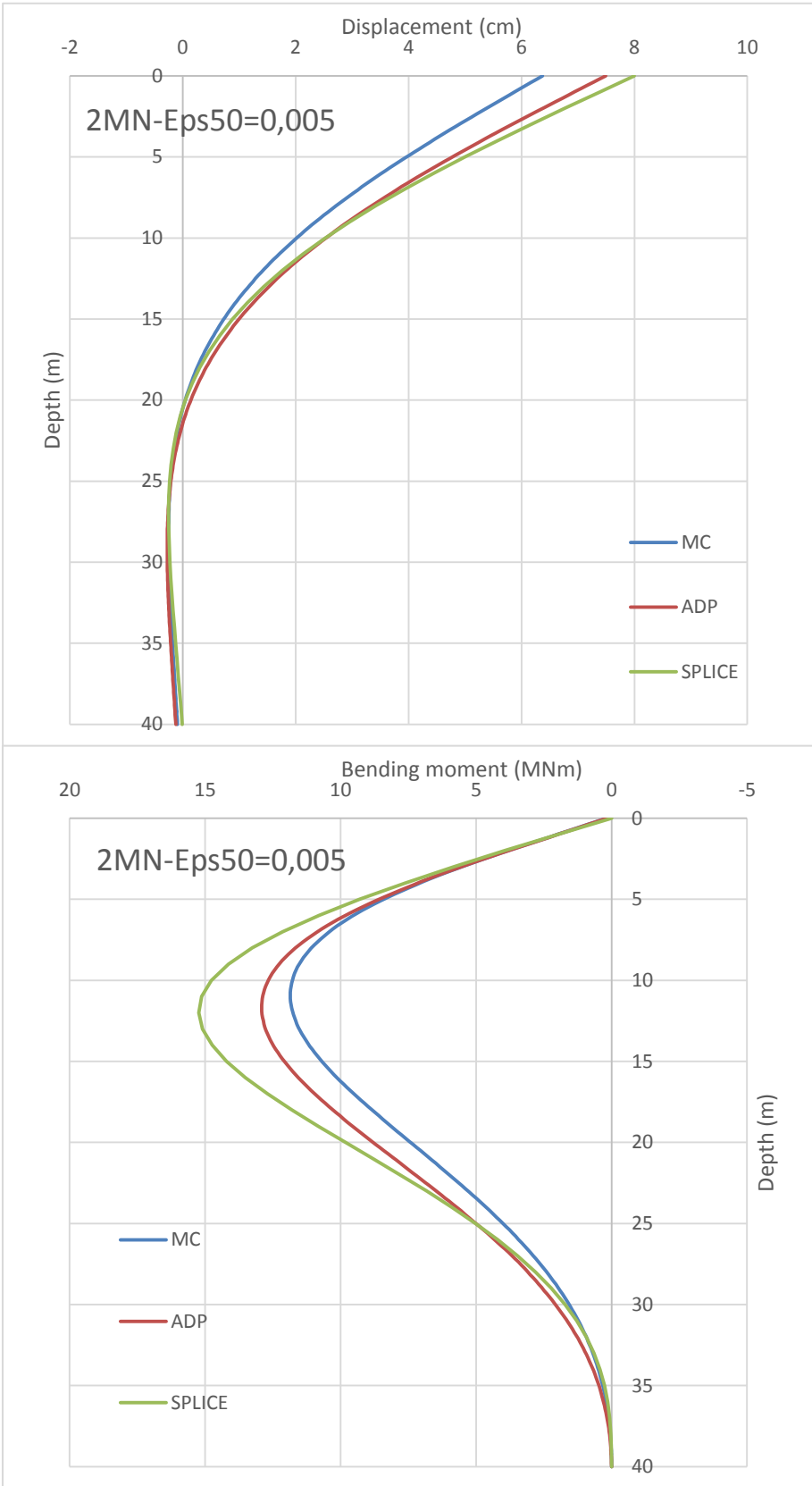
Consideration just done for SPLICE and Plaxis3D result differences, are also now working.

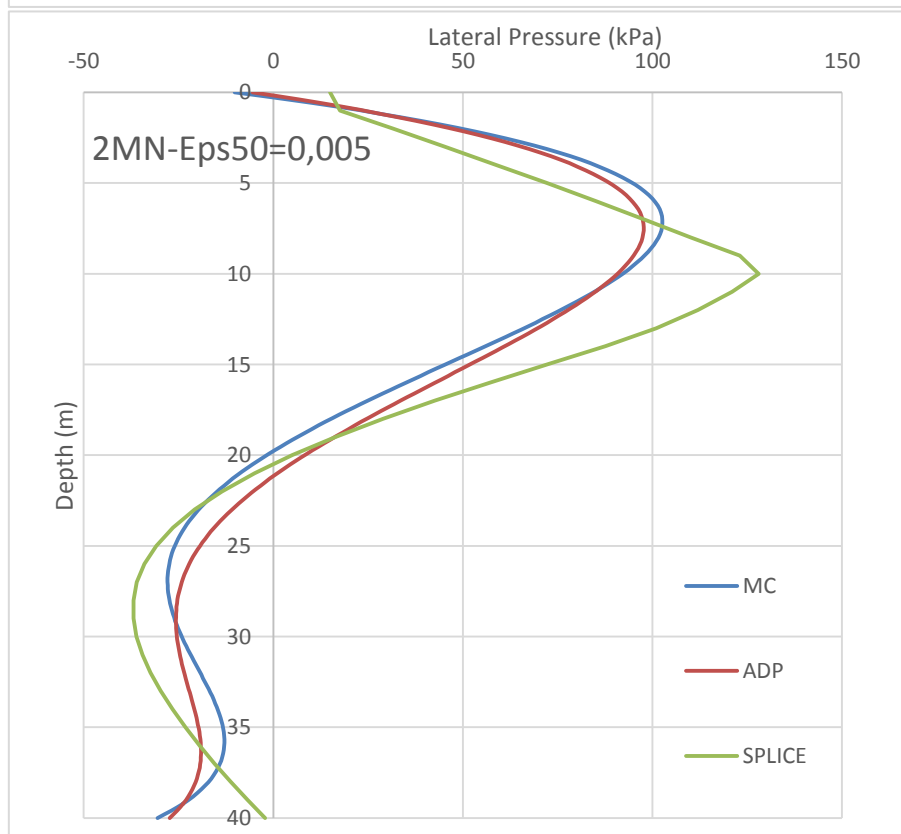
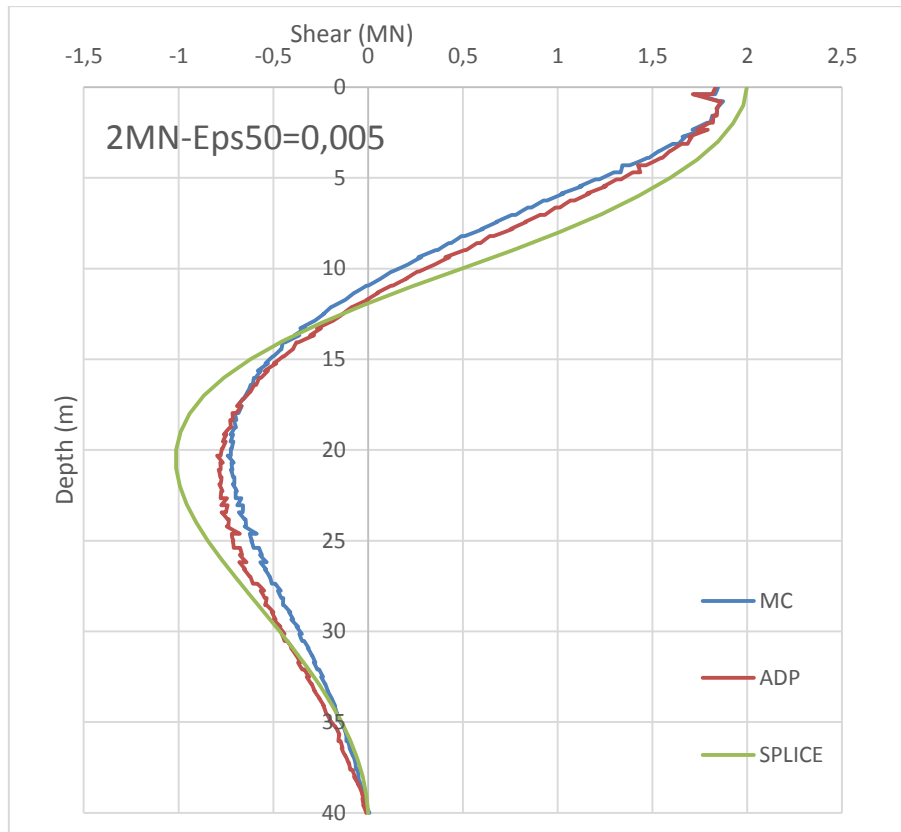
Results for Eps50=2% are reported in the next paragraph, in order to avoid repetitions.

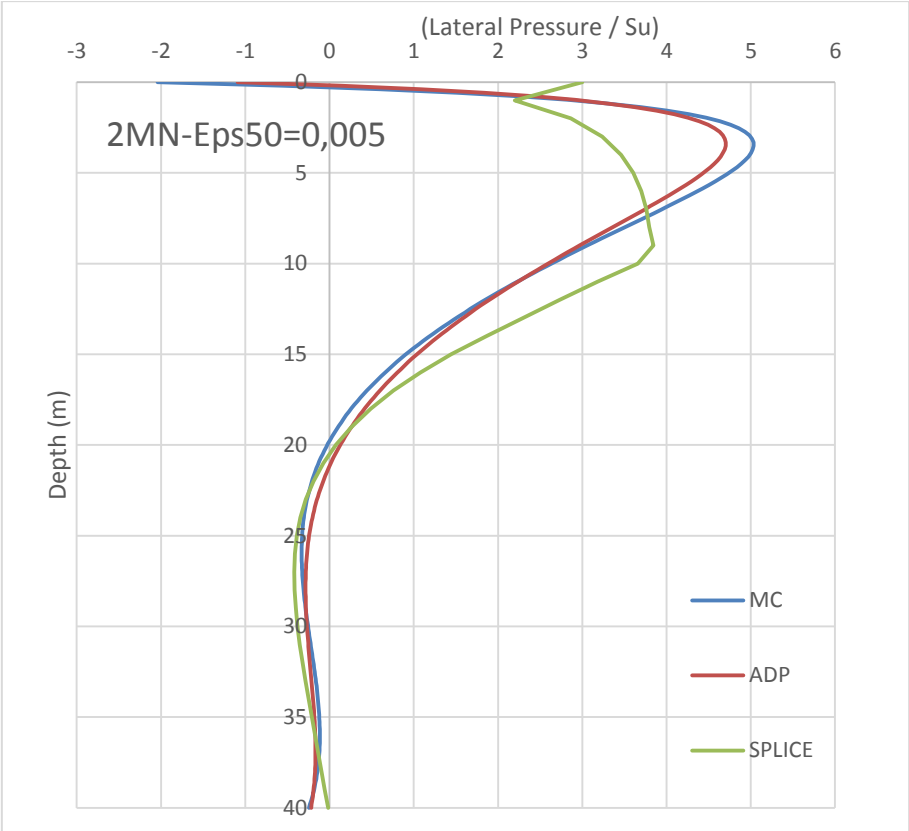
All new parameters are reported in the table below.

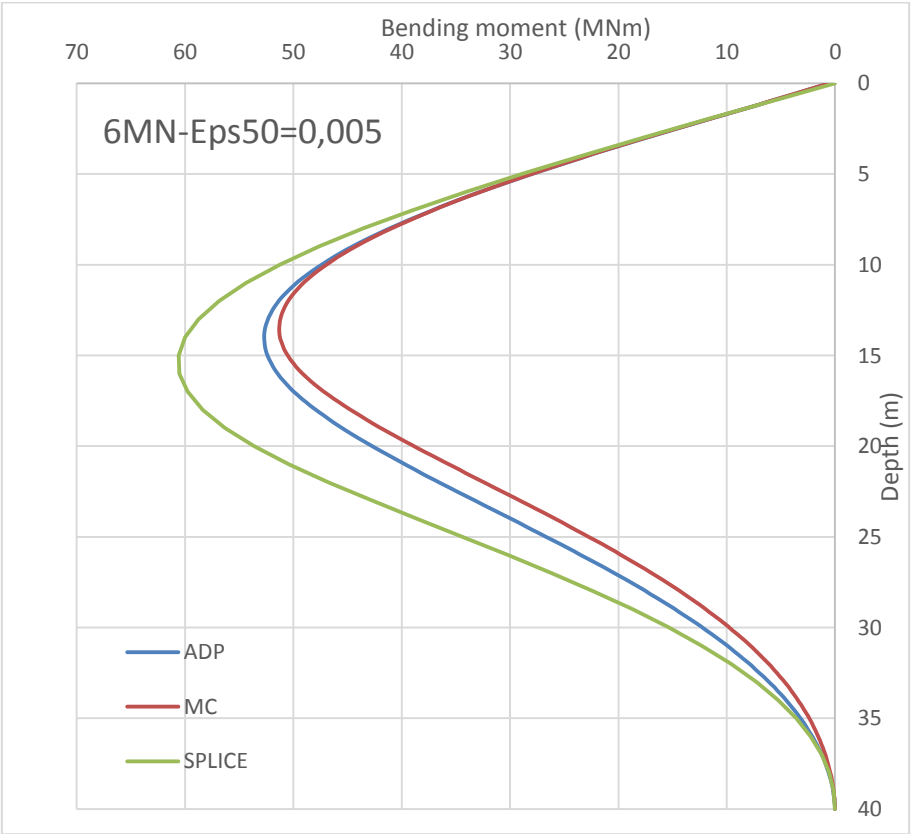
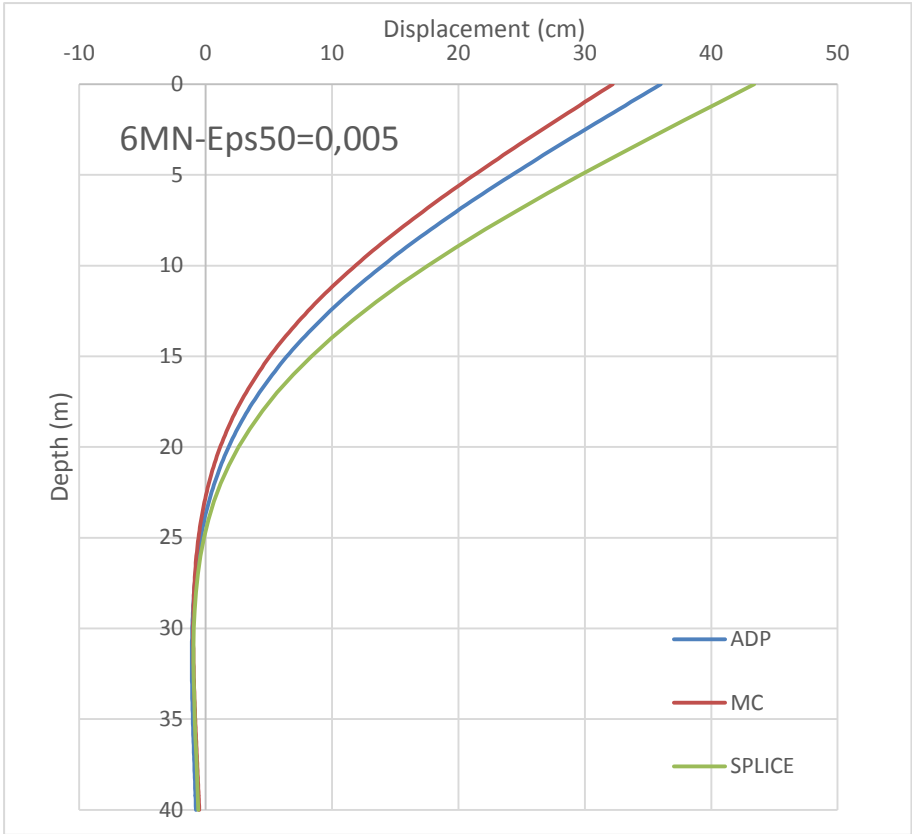
NGI-ADP (C2A)			Mohr-Coulomb (C1C)					
<b>Identification</b>	Soil ADP EpsC 0,5%		<b>Identification</b>	Interface EpsC 0,02		<b>Identification</b>	Soil	
<b>Identification number</b>	4		<b>Identification number</b>	1		<b>Identification number</b>	1	
<b>Material model</b>	User-defined		<b>Material model</b>	Mohr-Coulomb		<b>Material model</b>	Mohr-Coulomb	
<b>Drainage type</b>	Drained		<b>Drainage type</b>	Undrained (C)		<b>Drainage type</b>	Undrained (C)	
<b>Colour</b>	RGB 134, 234, 162		<b>Colour</b>	RGB 161, 226, 232		<b>Colour</b>	RGB 161, 226, 232	
<b>Comments</b>			<b>Comments</b>			<b>Comments</b>		
<b><math>\gamma_{unsat}</math></b>	kN/m <sup>3</sup>	10	<b><math>\gamma_{unsat}</math></b>	kN/m <sup>3</sup>	10	<b><math>\gamma_{unsat}</math></b>	kN/m <sup>3</sup>	10
<b><math>\gamma_{sat}</math></b>	kN/m <sup>3</sup>	10	<b><math>\gamma_{sat}</math></b>	kN/m <sup>3</sup>	10	<b><math>\gamma_{sat}</math></b>	kN/m <sup>3</sup>	10
<b>Dilatancy cut-off</b>	No		<b>Dilatancy cut-off</b>	No		<b>Dilatancy cut-off</b>	No	
<b>e_init</b>		0,5	<b>e_init</b>		0,5	<b>e_init</b>		0,5
<b>e_min</b>		0	<b>e_min</b>		0	<b>e_min</b>		0
<b>e_max</b>		999	<b>e_max</b>		999	<b>e_max</b>		999
<b>Rayleigh <math>\alpha</math></b>		0	<b>Rayleigh <math>\alpha</math></b>		0	<b>Rayleigh <math>\alpha</math></b>		0
<b>Rayleigh <math>\beta</math></b>		0	<b>Rayleigh <math>\beta</math></b>		0	<b>Rayleigh <math>\beta</math></b>		0
<b>DLL file</b>	usrmod_adp.dll		<b>E</b>	kN/m <sup>2</sup>	249,1	<b>E</b>	kN/m <sup>2</sup>	996,6
<b>Model in DLL</b>	NGI-ADP		<b>v (nu)</b>		0,495	<b>v (nu)</b>		0,495
<b>G<sub>ur</sub>/s<sub>u</sub><sup>A</sup></b>		100	<b>G</b>	kN/m <sup>2</sup>	83,3	<b>G</b>	kN/m <sup>2</sup>	333,3
<b>s<sub>u</sub><sup>C,TX</sup>/s<sub>u</sub><sup>A</sup>(,PS)</b>		0,99	<b>E<sub>oed</sub></b>	kN/m <sup>2</sup>	8413	<b>E<sub>oed</sub></b>	kN/m <sup>2</sup>	3,37E+04
<b>y<sub>ref</sub></b>	m	0	<b>c<sub>ref</sub></b>	kN/m <sup>2</sup>	5	<b>c<sub>ref</sub></b>	kN/m <sup>2</sup>	5
<b><math>\Delta s_{uA}/\Delta y</math></b>	kN/m <sup>2</sup>	3	<b><math>\phi</math> (phi)</b>	°	0	<b><math>\phi</math> (phi)</b>	°	0
<b>s<sub>u</sub><sup>A</sup><sub>ref</sub></b>	kN/m <sup>2</sup>	5	<b><math>\psi</math> (psi)</b>	°	0	<b><math>\psi</math> (psi)</b>	°	0
<b>s<sub>u</sub><sup>DSS</sup>/s<sub>u</sub><sup>A</sup></b>		1	<b>V<sub>s</sub></b>	m/s	9,035	<b>V<sub>s</sub></b>	m/s	18,07
<b>s<sub>u</sub><sup>P</sup>/s<sub>u</sub><sup>A</sup></b>		1	<b>V<sub>p</sub></b>	m/s	90,8	<b>V<sub>p</sub></b>	m/s	181,6
<b><math>\tau_0</math>/s<sub>u</sub><sup>A</sup></b>		0	<b>Set to default values</b>	No		<b>Set to default values</b>	No	
<b><math>\epsilon_1</math><sup>f</sup><sub>C,TX</sub></b>		4	<b>E<sub>inc</sub></b>	kN/m <sup>2</sup>	152,8	<b>E<sub>inc</sub></b>	kN/m <sup>2</sup>	598

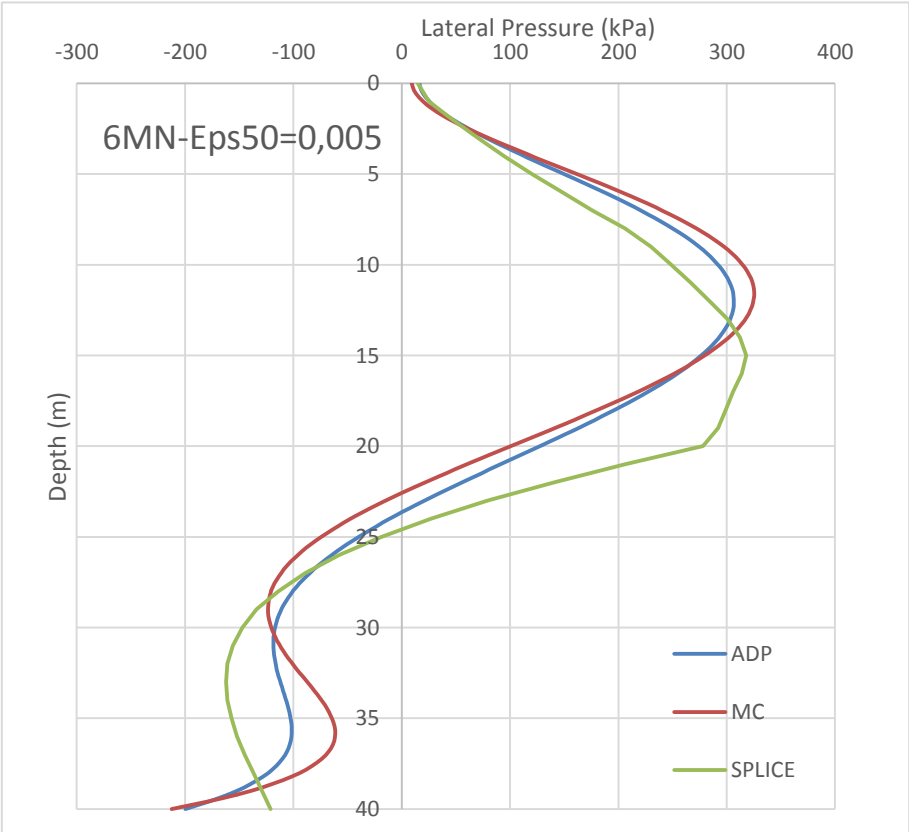
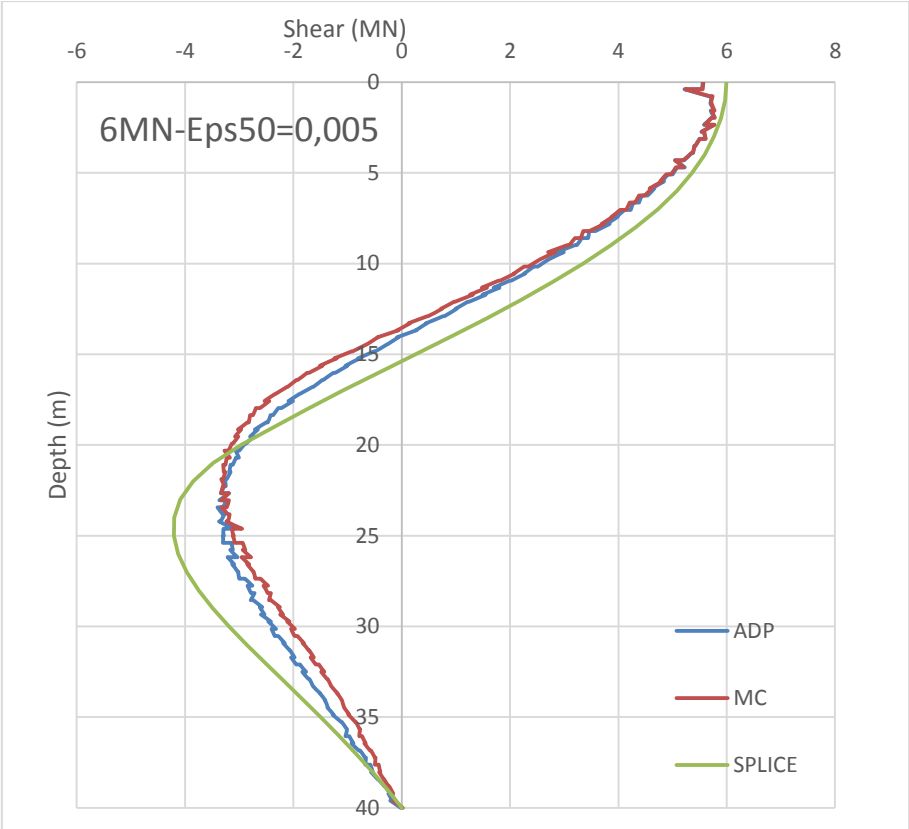
<b>y_f^DS</b>	6	<b>z_ref</b>	m	0	<b>z_ref</b>	m	0
<b>S</b>							
<b>ε_1_f^E, TX</b>	4	<b>c_inc</b>	kN/m <sup>2</sup> /m	3	<b>c_inc</b>	kN/m <sup>2</sup> /m	3
<b>v</b>	0,495	<b>z_ref</b>	m	0	<b>z_ref</b>	m	0
<b>v_u</b>	0,495	<b>Tension cut-off</b>	Yes		<b>Tension cut-off</b>	Yes	
<b>a_2</b>	0	<b>Tensile strength</b>	kN/m <sup>2</sup>	0	<b>Tensile strength</b>	kN/m <sup>2</sup>	0
<b>Check input? Y=0, N=1</b>	1	<b>C_v,ref</b>	m <sup>2</sup> /day	0	<b>C_v,ref</b>	m <sup>2</sup> /day	0
<b>tom</b>	0	<b>Strength</b>	Manual		<b>Strength</b>	Manual	
<b>tom</b>	0	<b>R_inter</b>	0,67		<b>R_inter</b>	0,67	
<b>tom</b>	0	<b>Consider gap closure</b>	Yes		<b>Consider gap closure</b>	Yes	
<b>tom</b>	0	<b>δ_inter</b>	0		<b>δ_inter</b>	0	
<b>tom</b>	0	<b>K_0 determination</b>	Automatic		<b>K_0 determination</b>	Automatic	
<b>tom</b>	0	<b>K_0,x = K_0,y</b>	Yes		<b>K_0,x = K_0,y</b>	Yes	
<b>tom</b>	0	<b>K_0,x</b>	1		<b>K_0,x</b>	1	
<b>tom</b>	0	<b>K_0,y</b>	1		<b>K_0,y</b>	1	
<b>tom</b>	0	<b>k_x</b>	m/day	0	<b>k_x</b>	m/day	0
<b>tom</b>	0	<b>k_y</b>	m/day	0	<b>k_y</b>	m/day	0
<b>tom</b>	0	<b>k_z</b>	m/day	0	<b>k_z</b>	m/day	0
<b>tom</b>	0	<b>e_init</b>	0,5		<b>e_init</b>	0,5	
<b>DEBUG</b>	0	<b>c_k</b>	1,00E+15		<b>c_k</b>	1,00E+15	
<b>Strengt h</b>	Rigid						
<b>R_inter</b>	1						
<b>Consider gap closure</b>	Yes						
<b>δ_inter</b>	0						
<b>E_oed^ref</b>	kN/m <sup>2</sup>	10					
<b>c_ref</b>	kN/m <sup>2</sup>	1					
<b>φ (phi)</b>	°	0					
<b>ψ (psi)</b>	°	0					
<b>UD-Power</b>		0					
<b>UD-P^ref</b>	kN/m <sup>2</sup>	100					
<b>K_0 determination</b>	Automatic						
<b>K_0,x = K_0,y</b>	Yes						
<b>K_0,x</b>	1						
<b>K_0,y</b>	1						
<b>k_x</b>	m/day	0					
<b>k_y</b>	m/day	0					
<b>k_z</b>	m/day	0					
<b>e_init</b>	0,5						
<b>c_k</b>	1,00E+15						

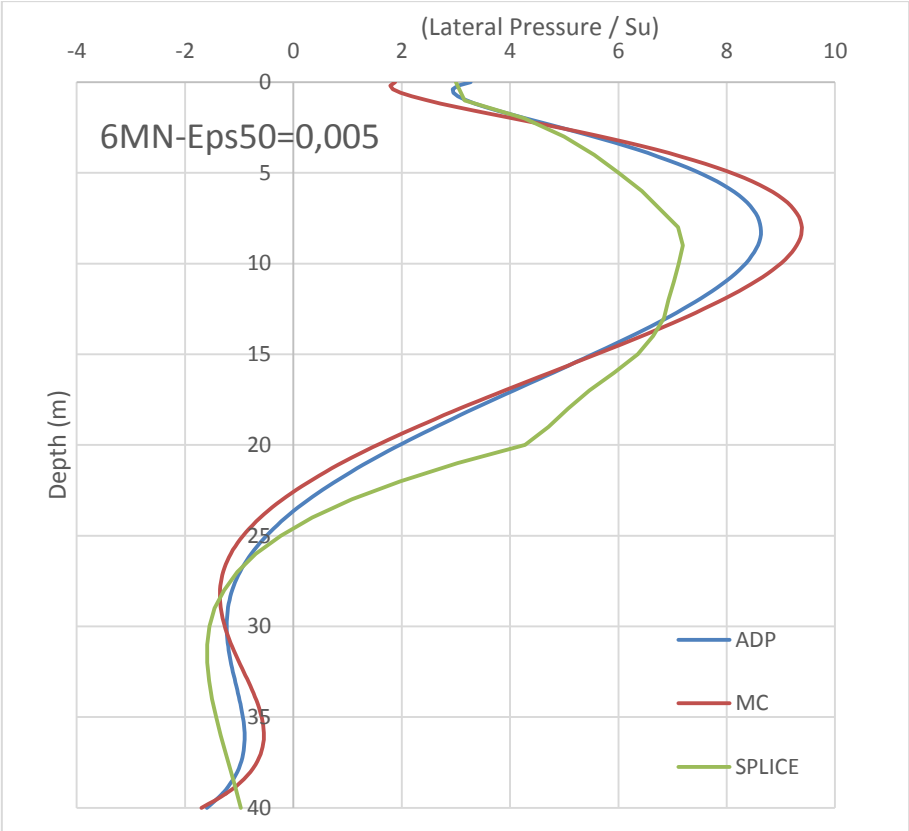












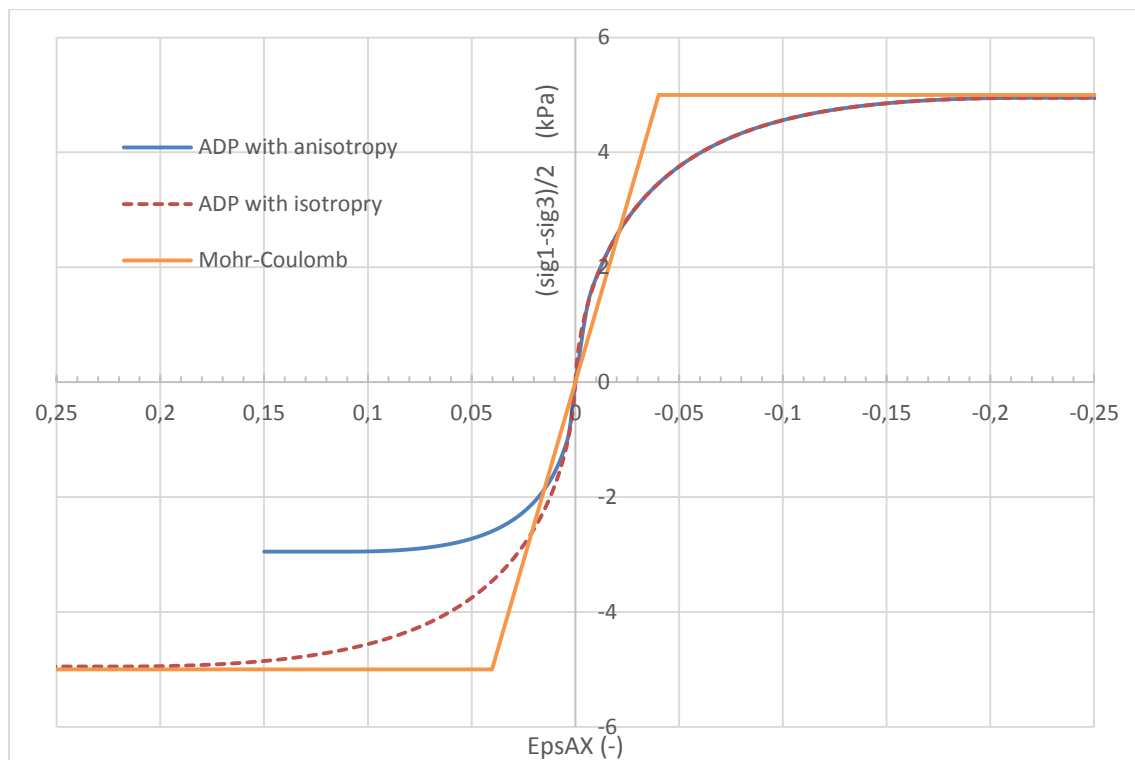
### Anisotropic NGI-ADP soil model

Herein, the results of finite elements simulation done with anisotropic ADP soil model are presented.

In the last paragraph was presented a comparison between SPLICE and Plaxis3D data in reason to highlight the different behavior of the same problem simulated with different soil models. in this paragraph instead is presented a simulation that use the ADP capability of describing an anisotropic behavior, typical for a soil.

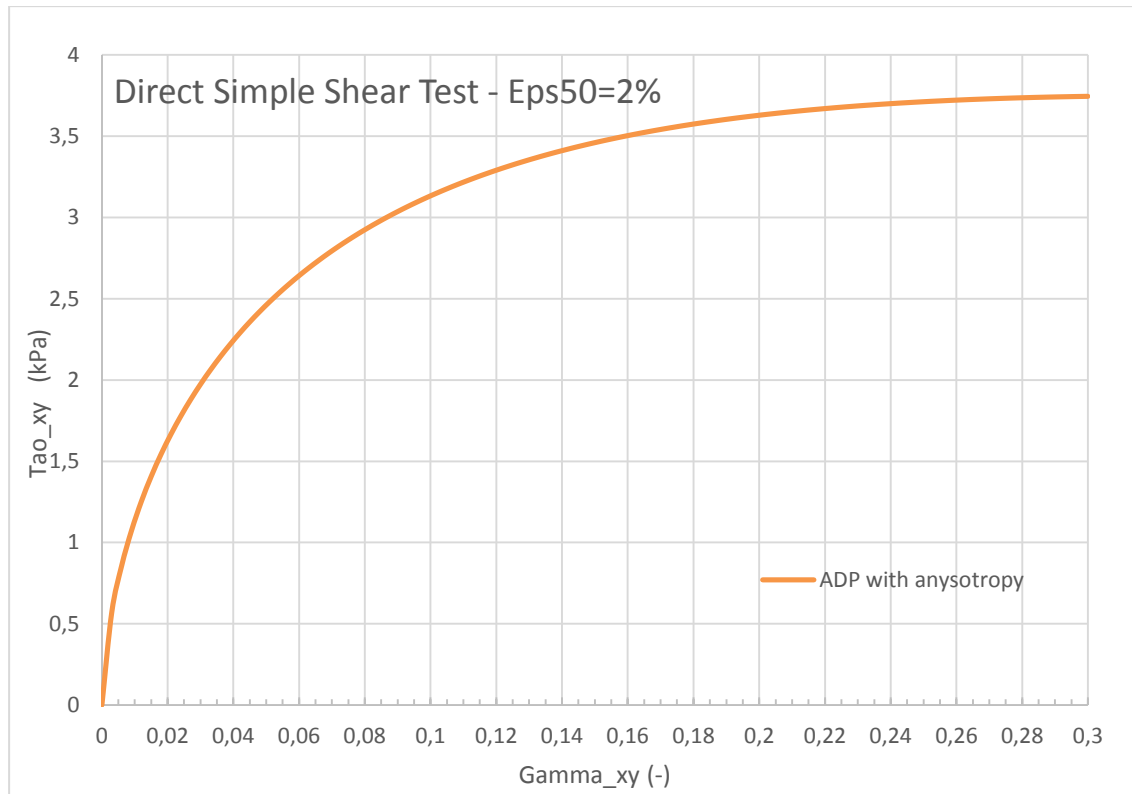
In order to define the anisotropy the following parameters are defined:  $Su_{DSS}/Su_{AVERAGE}=0.75$ ,  $Su_{TX-EXTENSION}=0.60$  and  $Su_{TX-COMPRESSION}/Su_{AVERAGE}=0.99$  (0.99 is used instead of 1 to avoid numerical problem).

Soil tests have been carried out with Plaxis3D, in 2D input phase and the results are plotted below.



The above graph presents a series of triaxial tests simulated with the specific Plaxis3D function, tests run for ADP soil with and without anisotropy; the soil has been tested in compression and extension both.

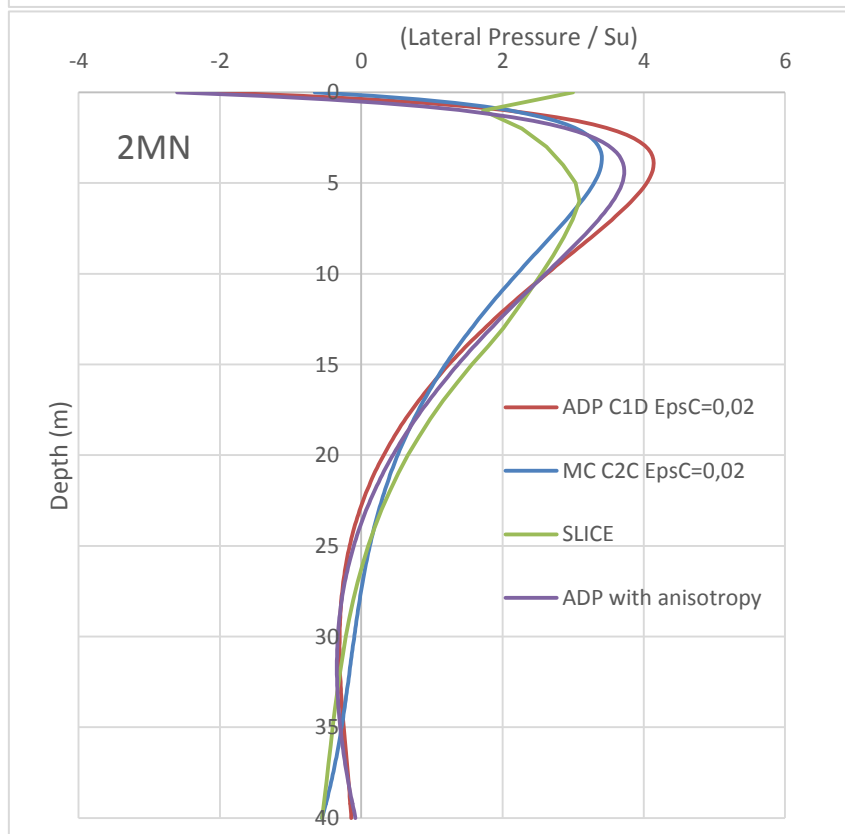
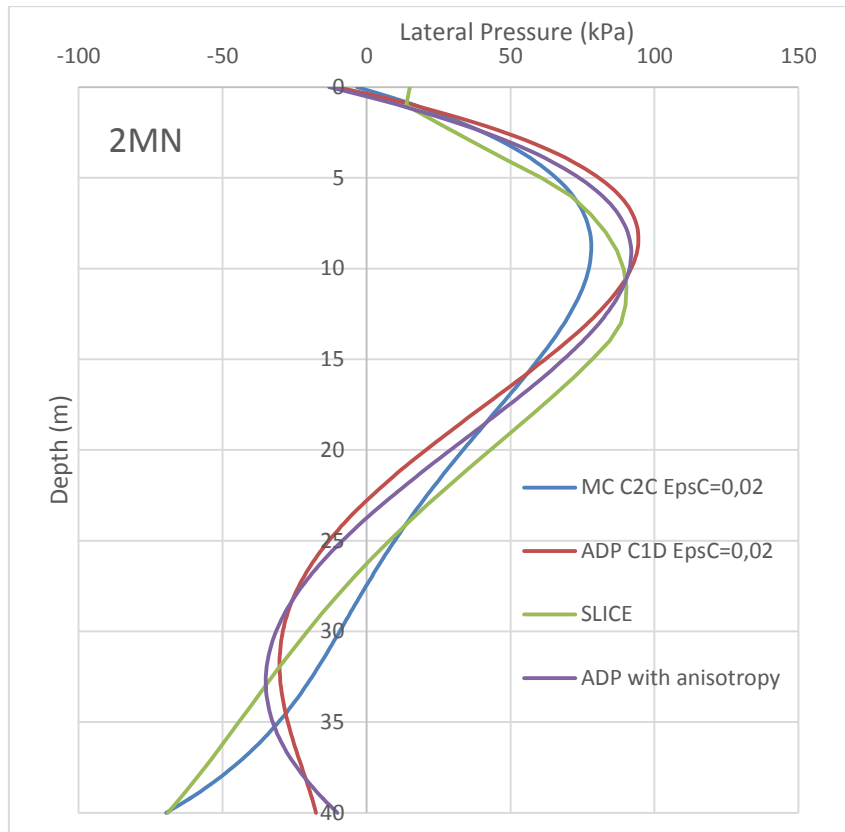
The second graph below instead shows the results of a direct simple shear test. These graphs confirm that the input parameters, used in order to define anisotropy, effectively give the expected behavior.

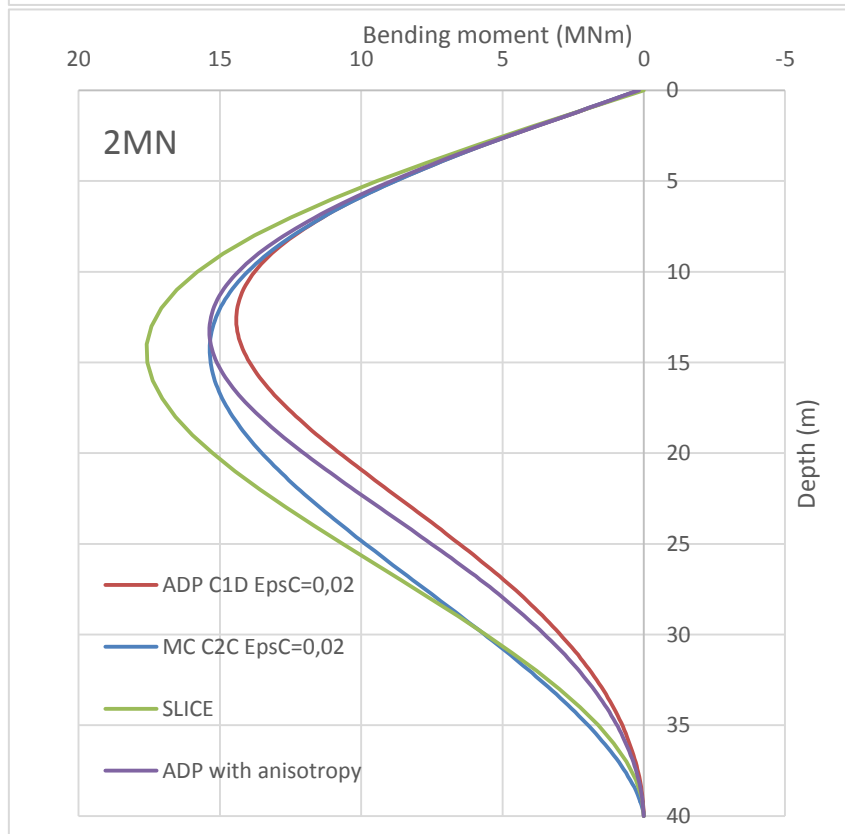
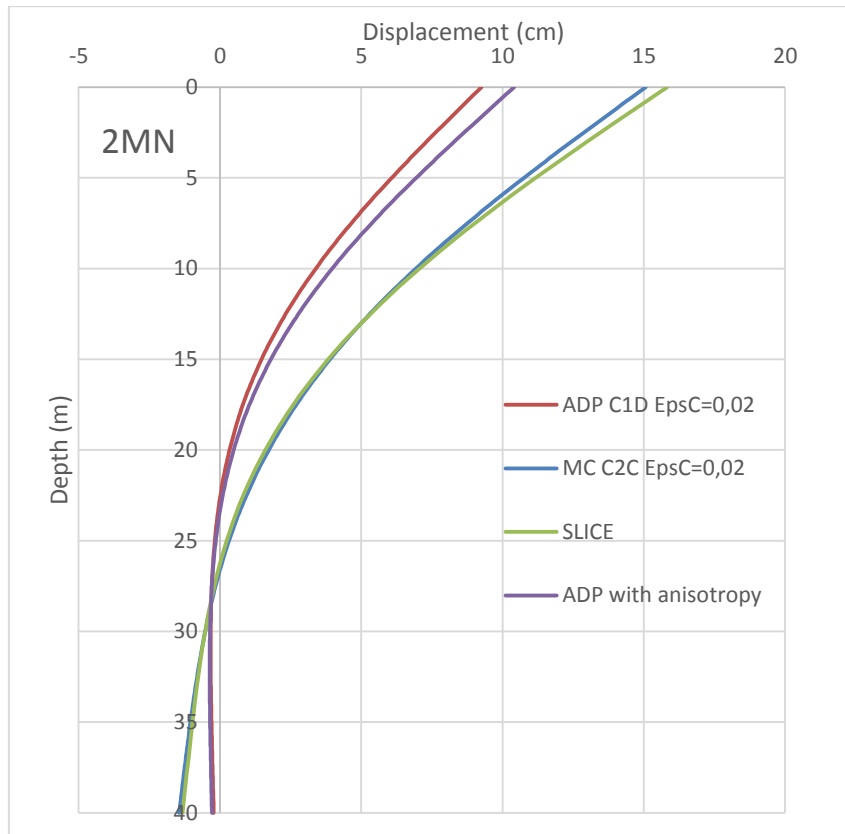


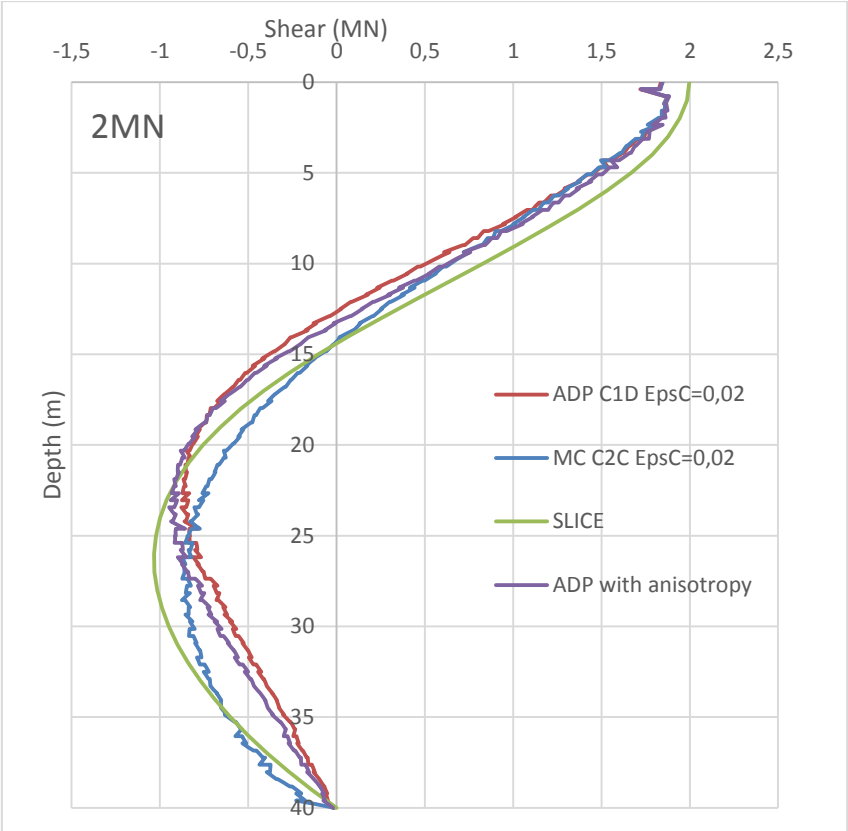
Then, are presented trends of: horizontal displacement, bending moment, shear force, lateral pressure and ratio between lateral pressure and undrained shear strength.

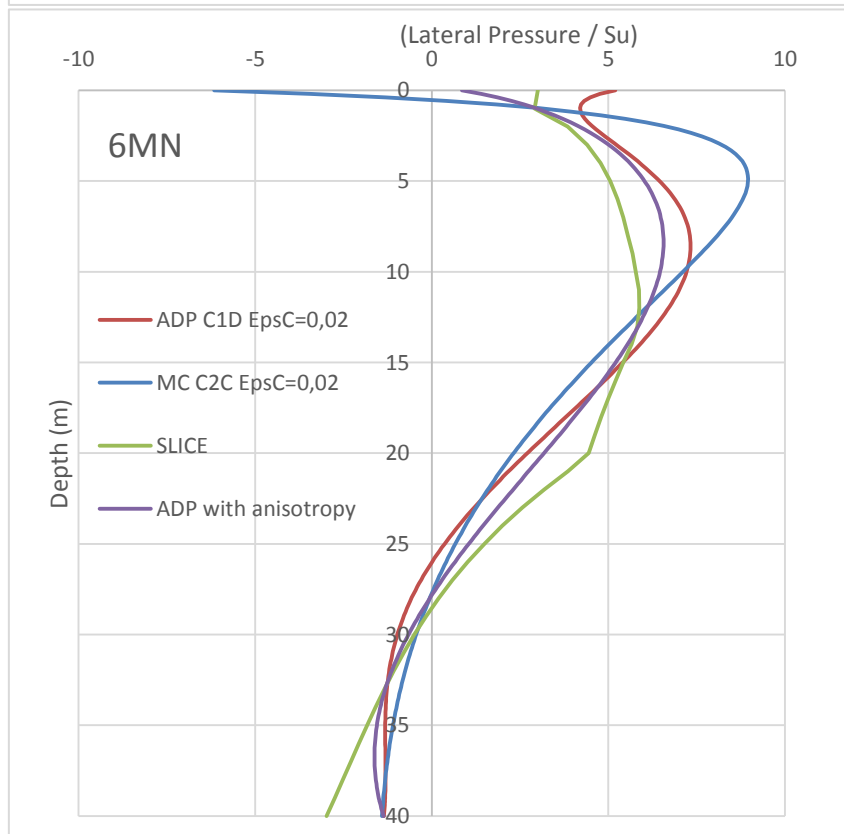
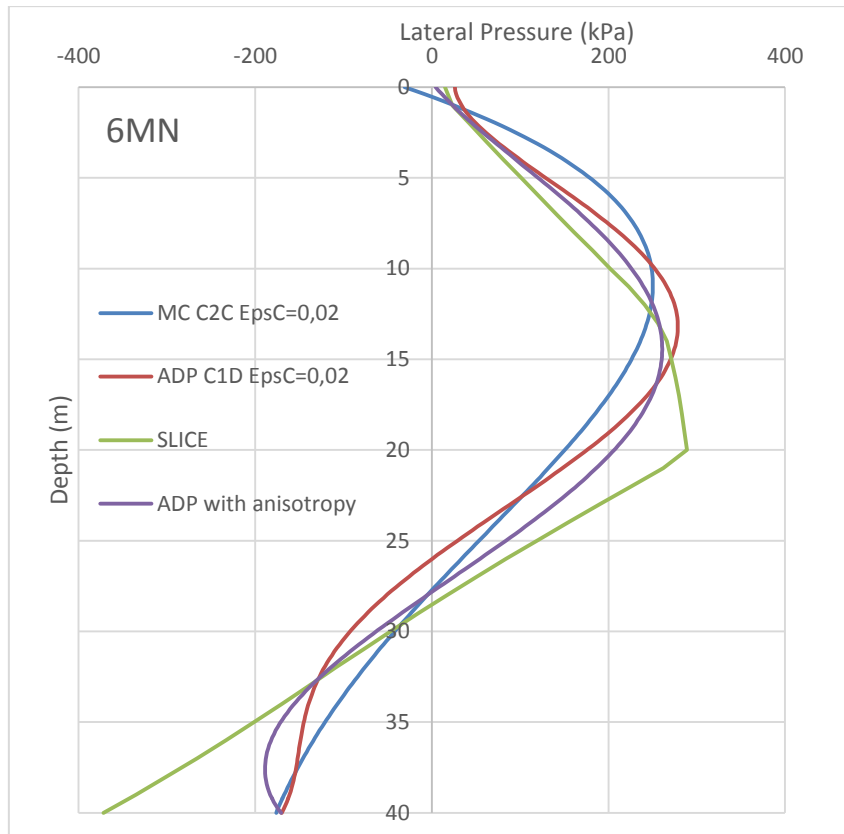
These analyses are carried out for different load condition (2, 6, 9 and 12 MN) in reason to put on evidence every possible different relation between load level and variables of interest (especially bending moment and horizontal displacement).

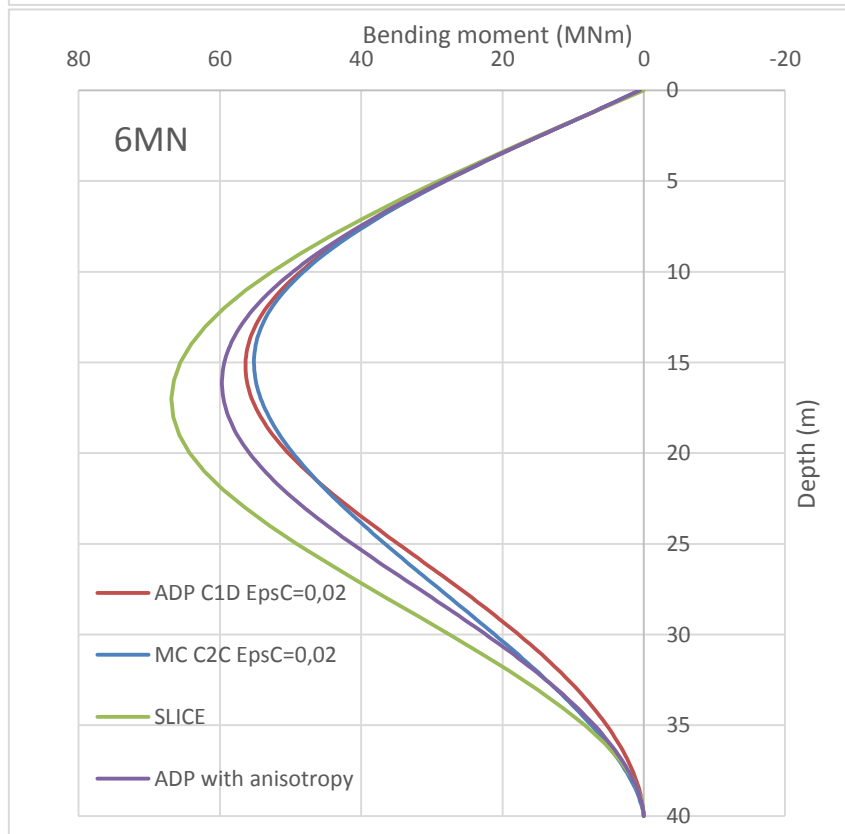
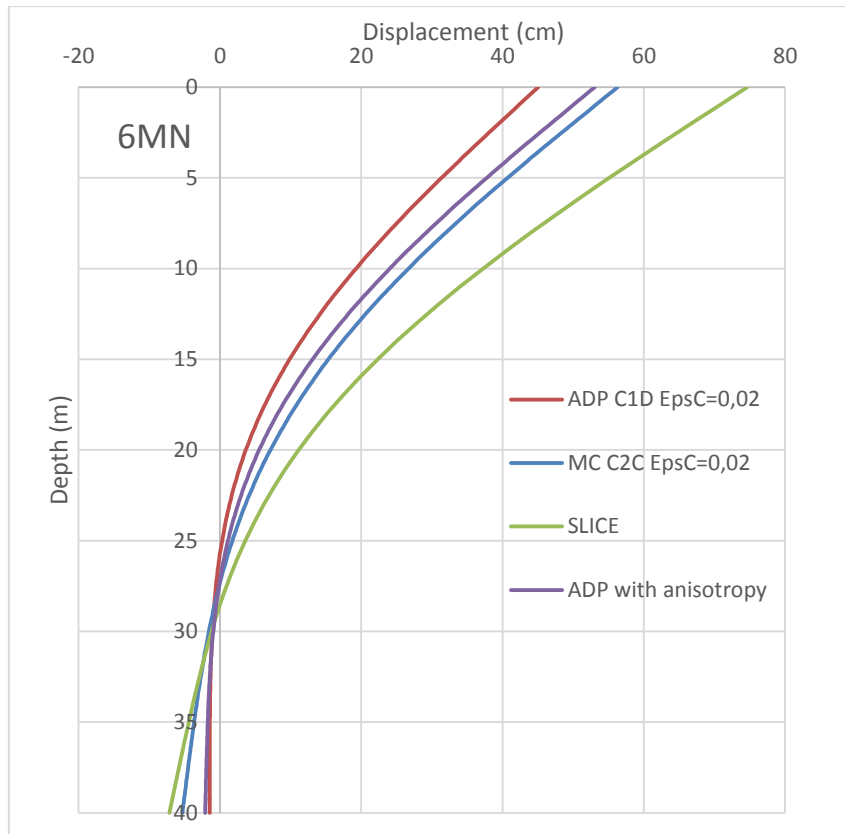
For Eps50 bigger than 0.5%, in SPLICE ultimate load is 9 MN, for a load larger than this there is not convergence, i.e. solution. Instead, with Plaxis3d has been carried out an analysis for 12 MN also in reason to be sure that the failure is reached into the pile model simulation.

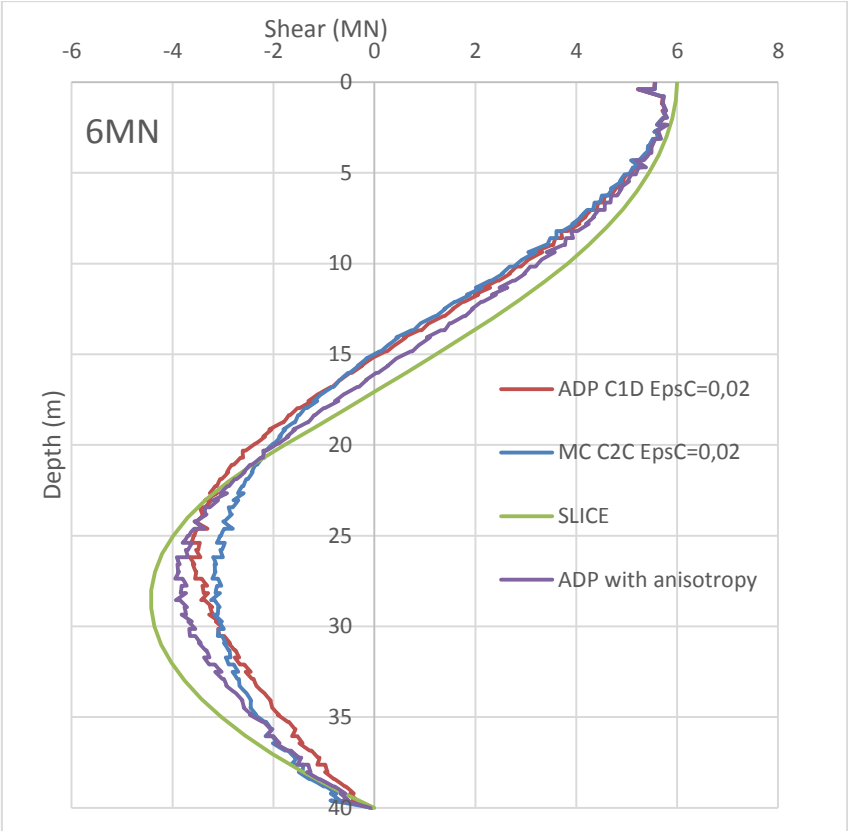


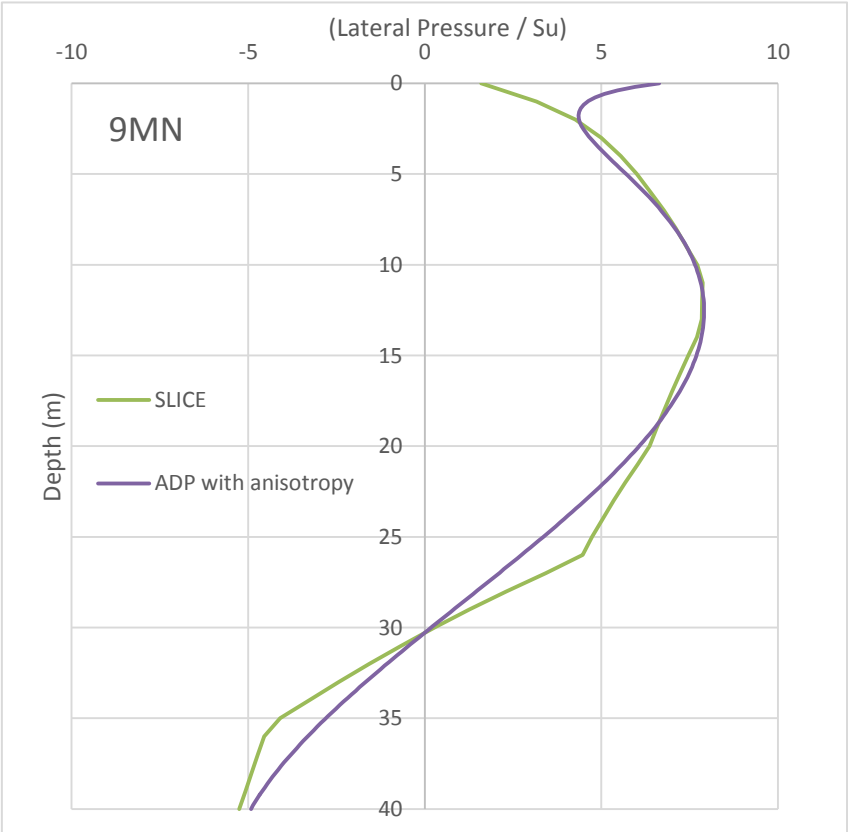
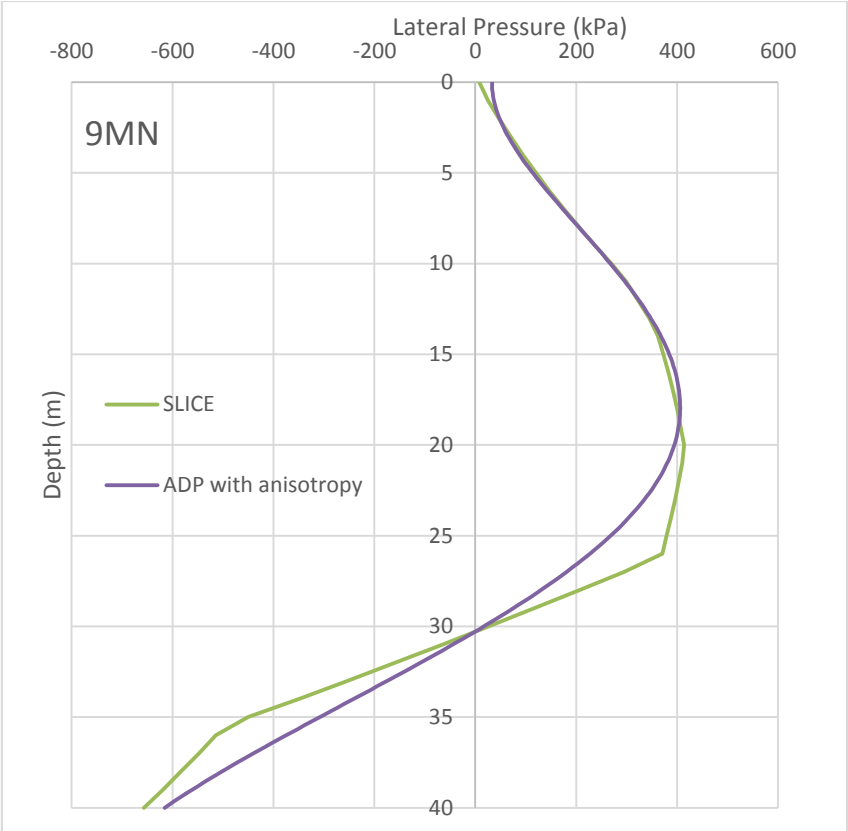


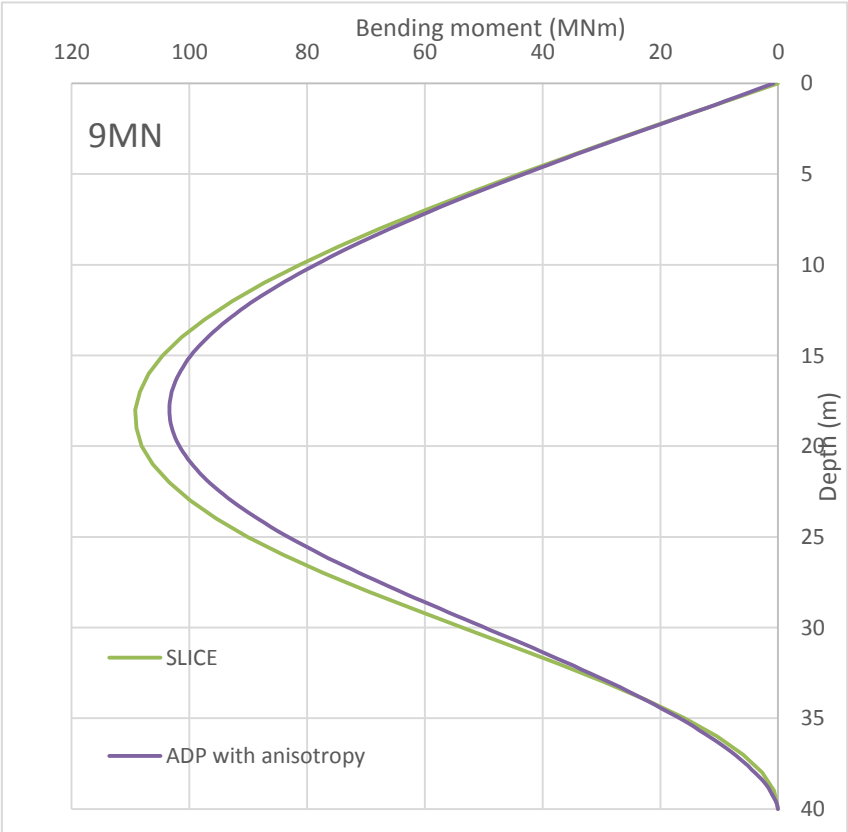
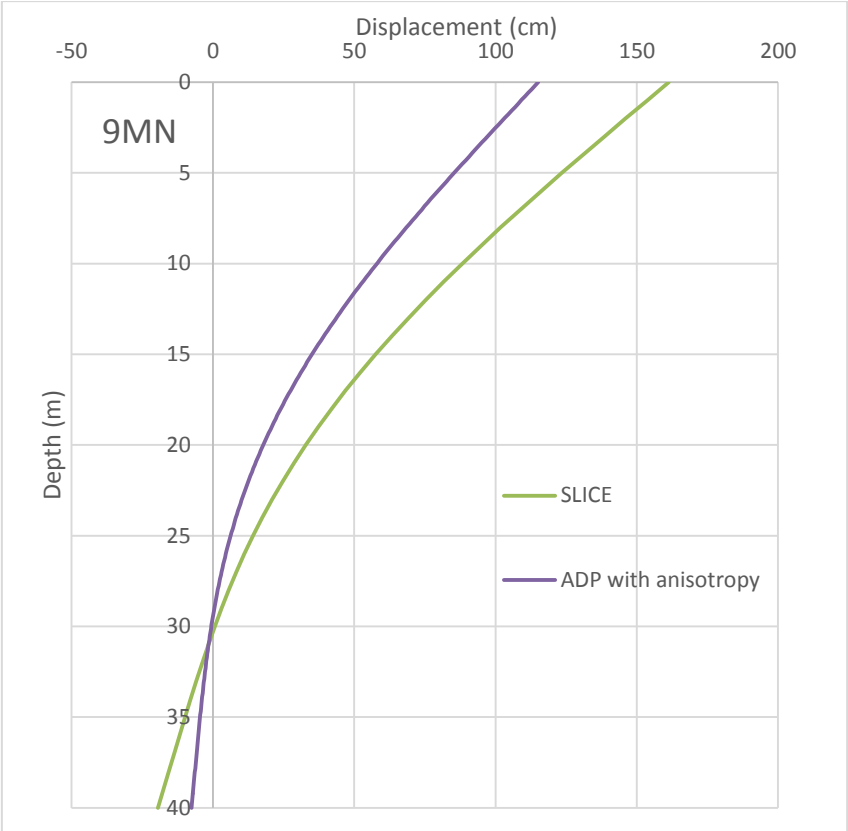


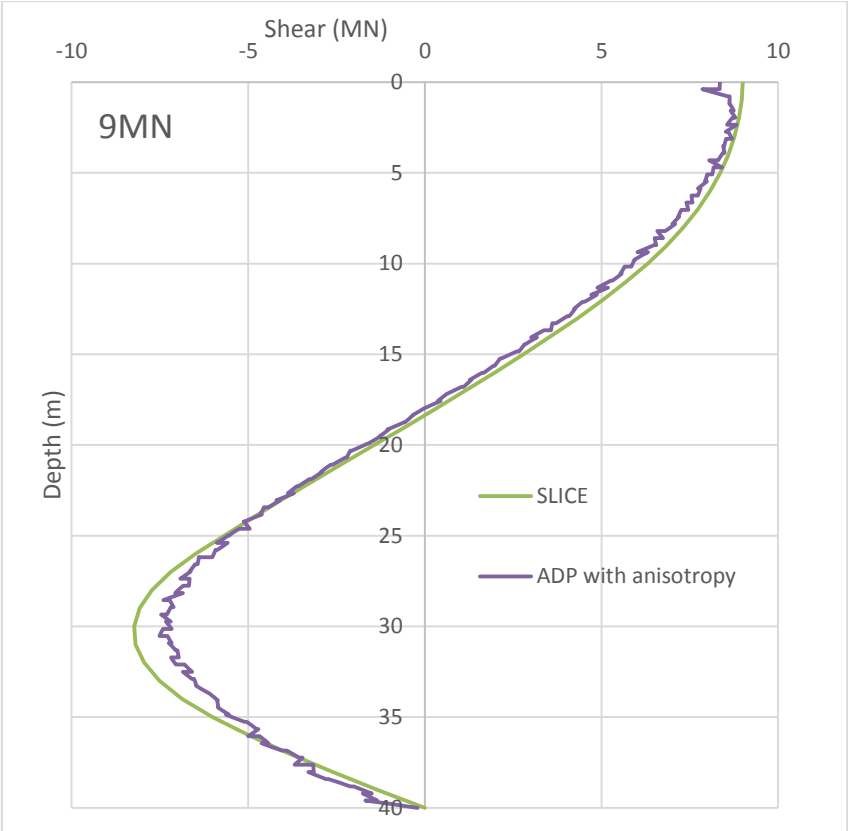




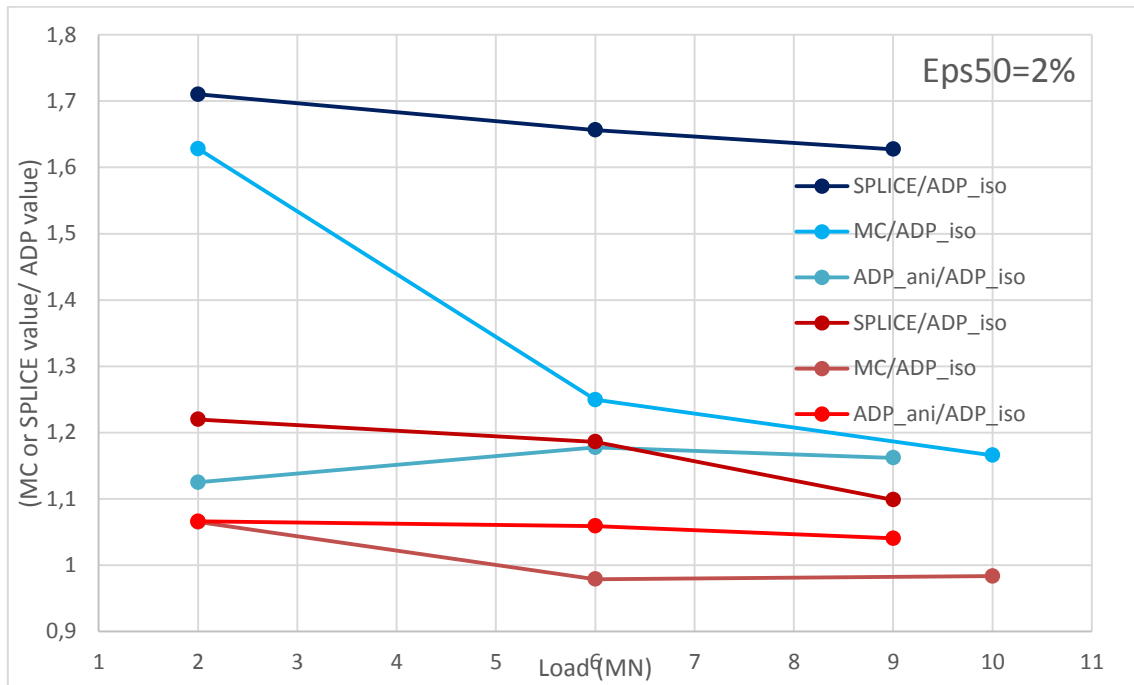




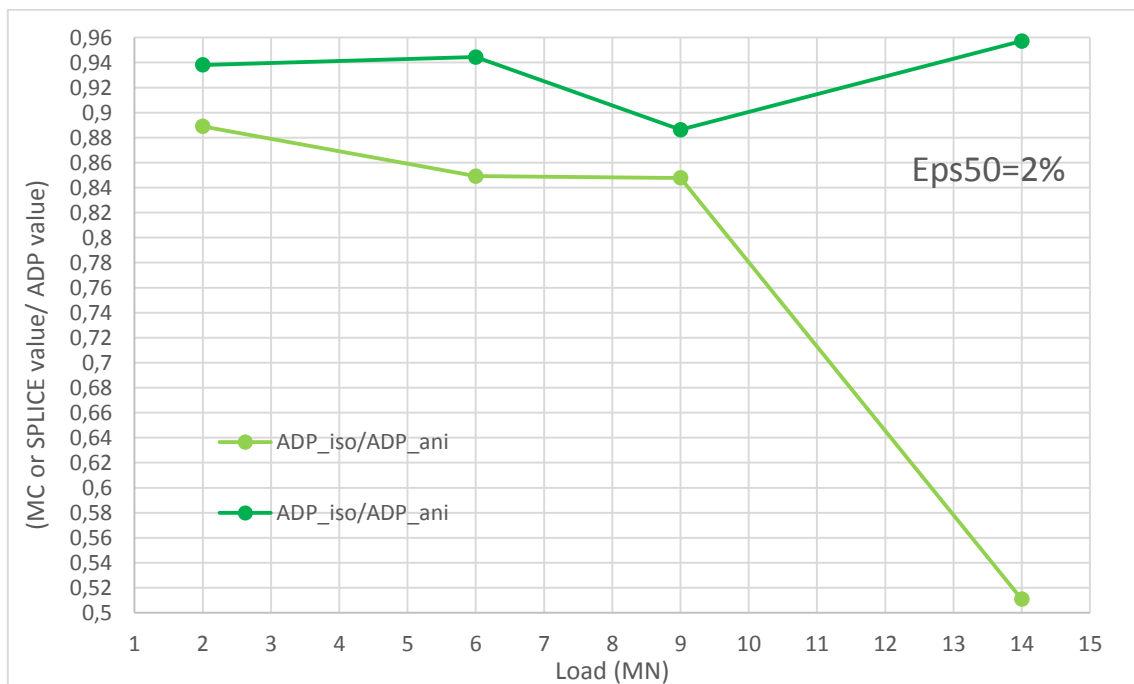




In the first dimensionless graph are plotted the maximum bending moment and the pile head displacement at the seabed. Both these trends are normalized by results calculated by Plaxis3D with isotropic ADP. The normalized results are calculated by SPLICE and Plaxis3D with Mohr-Coulomb and ADP anisotropic output.



Below are presented the same variables calculated with ADP isotropic but normalized by values obtained adopting anisotropic ADP.



A Very relevant consideration could be that the difference shown at 14 MN for the maximum displacement into the second normalized graph, leads to an interception in the first graph between the curves representative of SPLICE and anisotropic ADP, both normalized by isotropic ADP.

However, the consideration above remains a merely theoretical consideration due to the fact that SPLICE does not calculate a solution for such a high load condition.

### Experimental P-y curves

Several points are necessary to draw a curve resistance-deflection. For a certain depth and so for a certain p-y curve, each point is representative of a couple of lateral pressure-deflection. Each point is distinctive of a load, for this reason when a large number of load level is tested it becomes possible to define with good precision the specific p-y curve, representative of a certain soil at a certain depth.

In the next pages are plotted the p-y curves for 5.5-8.5-11.5-14.5-18.5-21.5 meters depth.

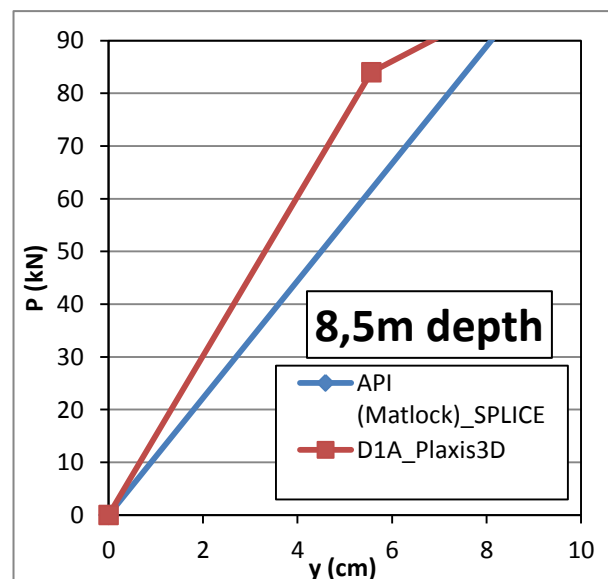
In each graph, three curves are shown: two calculated by Plaxis3D data, from simulations adopting the ADP soil model, relatively with isotropy and anisotropy; and a third curve obtained by SPLICE using the API recommendations i.e. Matlock equation.

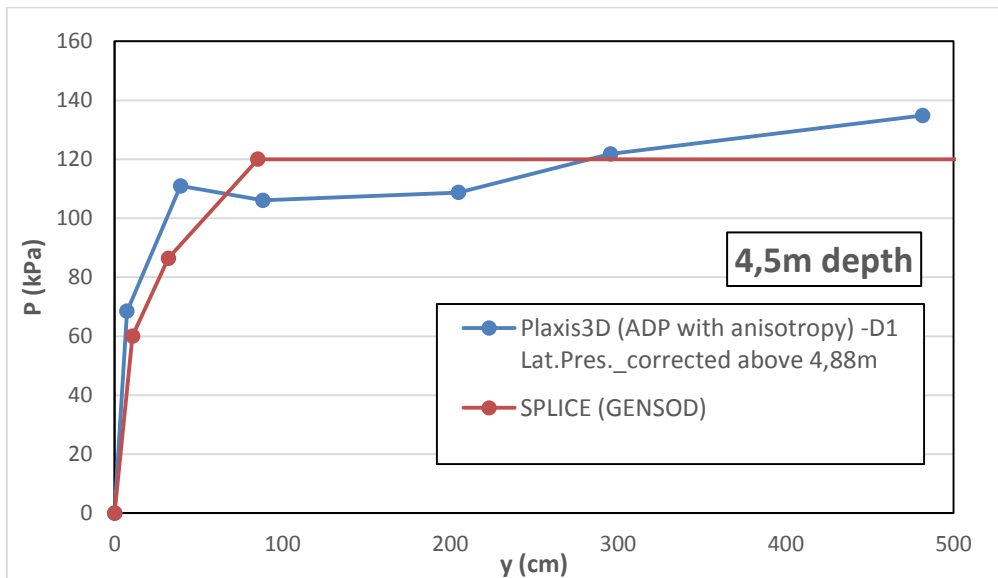
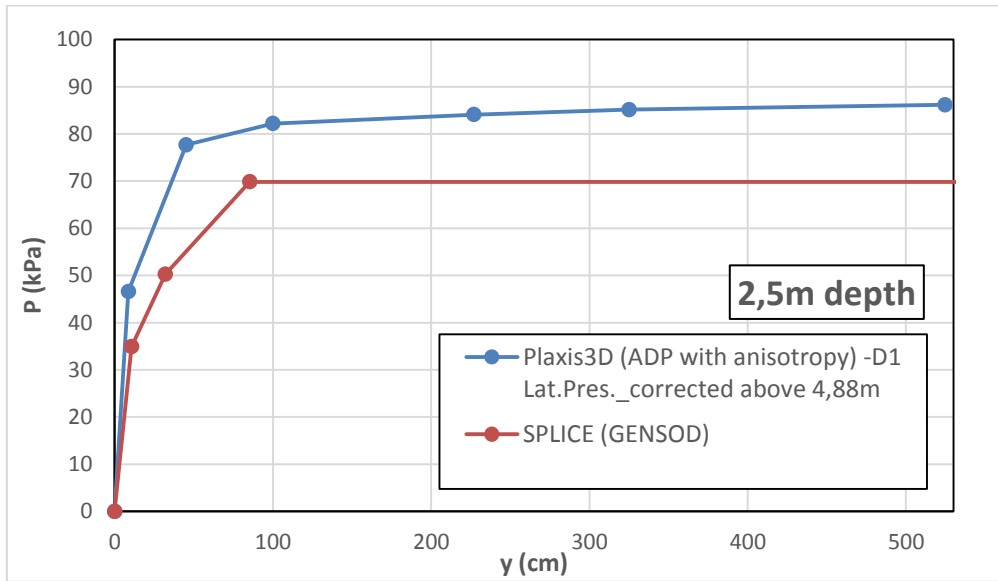
The graphs representative of 2.5 and 4.5 meters depth, present the API curve and a second experimental curve obtained with the lateral pressure corrected by equilibrium, as explained in the last paragraph.

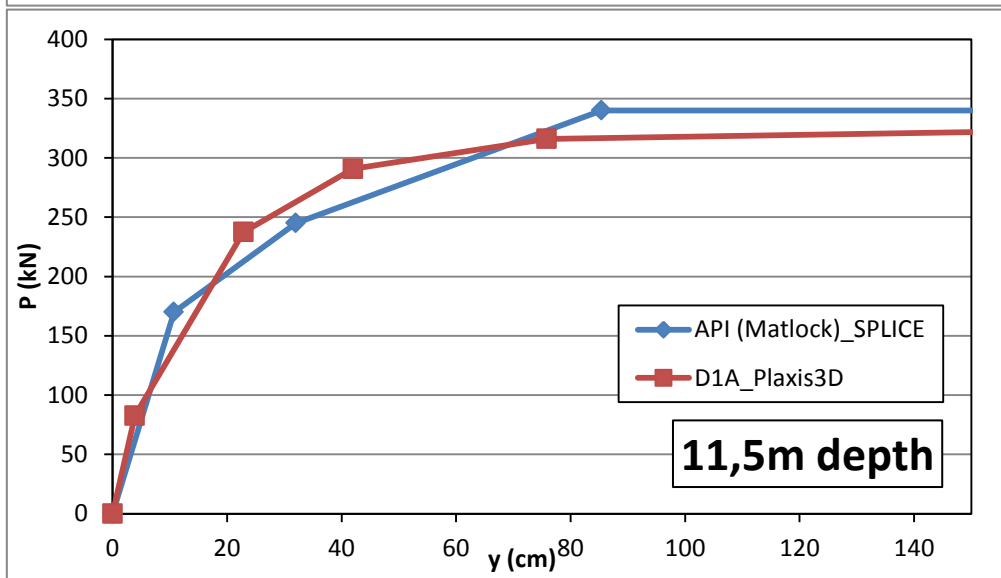
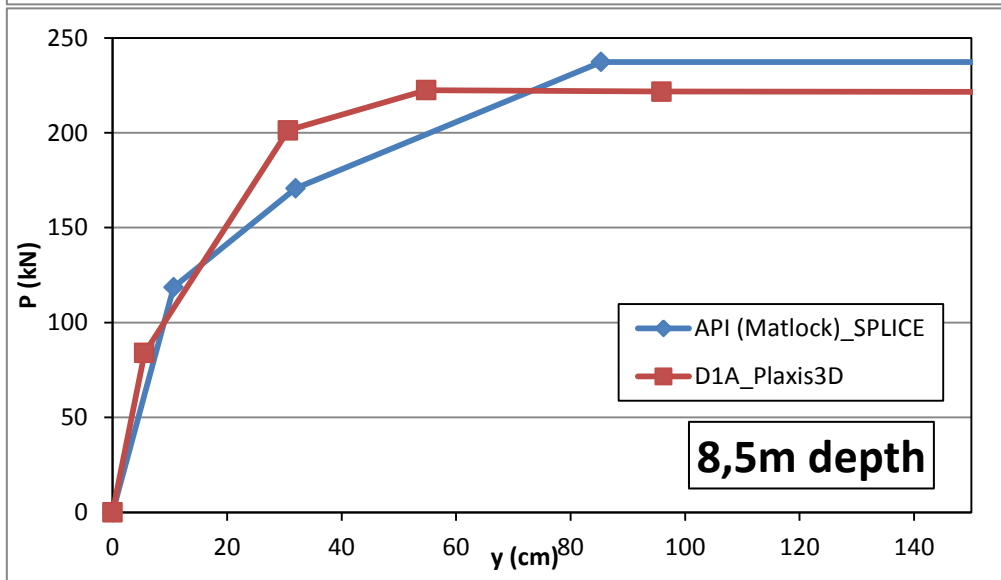
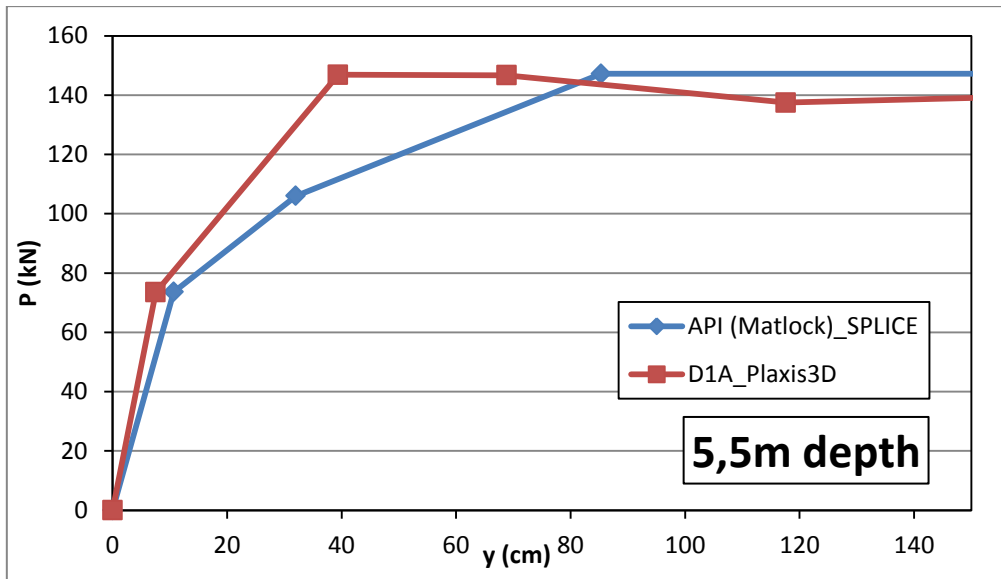
It is clear that the APD soil model gives curves more suitable with the curves calculated from API recommendation if an anisotropic behaviour is defined, this in comparison an isotropic material adopting the ADP soil model.

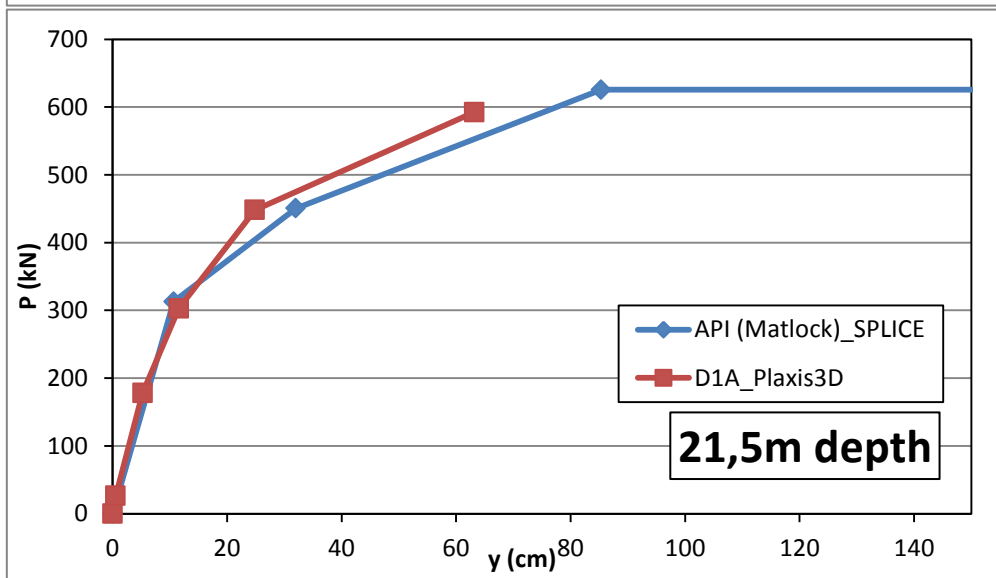
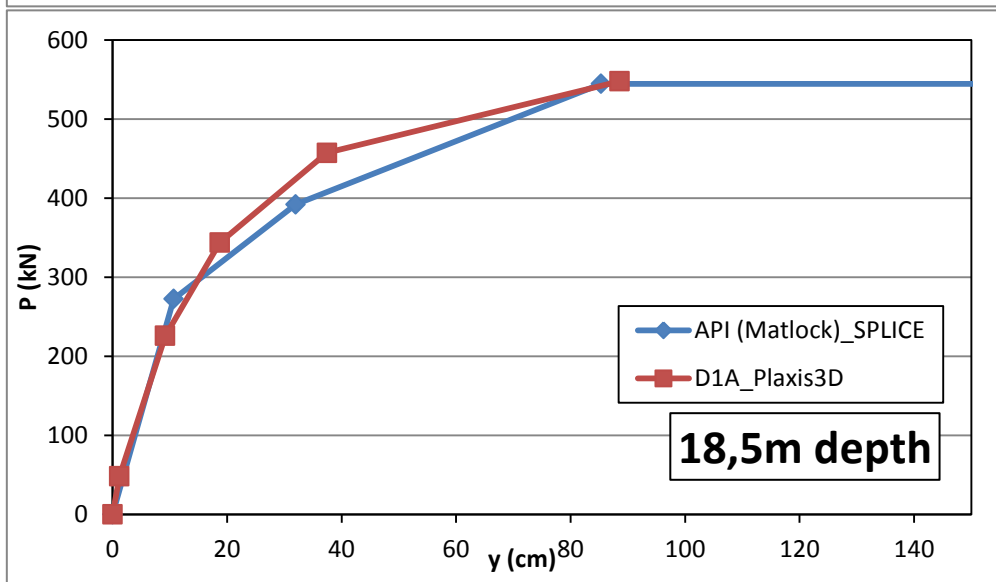
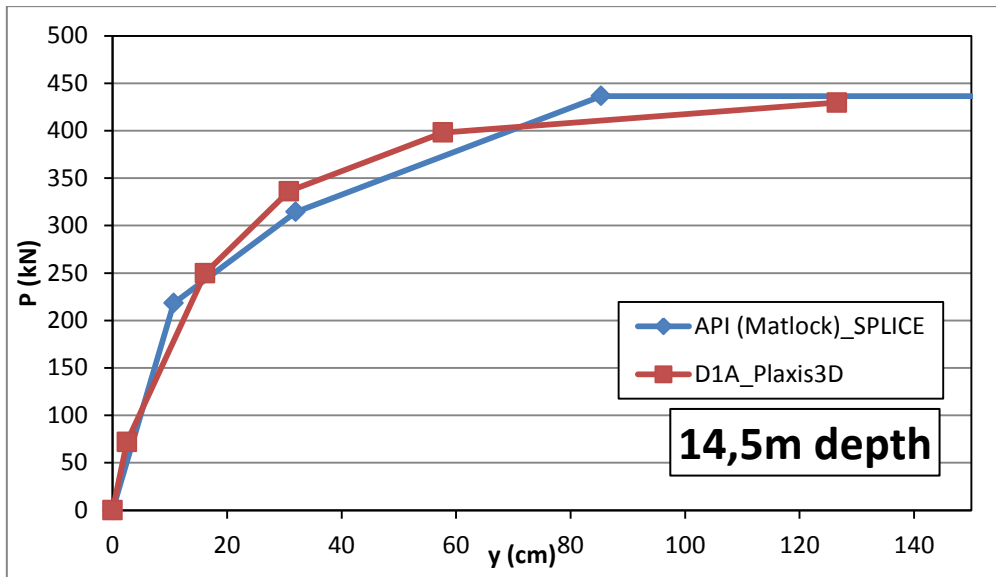
P-y curves calculated from Plaxis3D data (adopting ADP soil model with isotropy) present two main characteristic:

- The ultimate resistance from Plaxis3D data is a little bit higher (+5%) than the ultimate resistance defined by API recommendations i.e. the flat-horizontal part of the curves obtained by Plaxis3D is a little bit higher than the same curve by SPLICE;
- The initial slope of the curve, i.e. the stiffness, is higher for Plaxis3D (detail of the initial different stiffness on the picture at right side).









## SIMPLIFIED ANALYSIS OF A REAL JACKET STRUCTURE

---

To close this master thesis, it was chosen to develop a real case, but simplified, in order to test the obtained p-y curves (during the period, August-December 2013, at Norwegian Geotechnical Institute, in Oslo).

The merely academic use of the following exercise, allows to do very strong assumptions and simplifications.

Objective of this chapter is evaluating the actions on the foundation of a Jacket structure.

The actions calculated are used to verify the piles used to fix the jacket on the seabed.

Little importance is assigned to the structural design of the jacket. Also the fatigue behaviour for the structure and the structural elements have been considered in the simplest way possible: using uniquely a factor on the material resistance. International standard allows this calculation only for inspectable elements, and in the jacket structure herein studied every element is inspectable because it is found in relatively shallow water (for ISO an element below 200 meters depth it is not inspectable with regularity; in this case the mudline is at a depth of 28,7 meter).

To compute the forces acting on the foundation a finite elements software for structural analysis is used (Straus 7). In order to simplify the problem it is used a quasi-static approach for wave and current actions. This procedure is defined into international standard ISO 19902.

The use of this methodology attributes the cyclic action due to wave passage on a system of static forces on the fixed structure.

Metoccean design data and a soil profile are furnished by a senior engineering working in Kvaerner, a Norwegian contractor company.

The soil profile adopted is clay characterized by linear undrained strength, as the soil profile largely used into the parametric analysis run at NGI and was explained in the initial part of this master thesis.

This in order to use the p-y curves above obtained using ADP soil model with anisotropy.

It is modelled a not existing jacket structure, but in order to define an “credible” framework it is used as model the Gudrun jacket (Gudrun is an oil ring between Scotland and Norway, it is property of Statoil company and it was built by Kvaerner Industry).

The original framework of legs, horizontal beams and braces has been largely modified in order to adopt that structure to a relatively shallow seabed.



Once calculated the sum vector for each leg it is supposed an equal subdivision of the force between the three piles that compose the leg foundation.

No specific verifications are done on the leg-pile connection, because normally this part is characterized by very high resistance due to its shape and thickness.

In the picture below are clearly represented the leg-piles connector, with the pile heads housing.



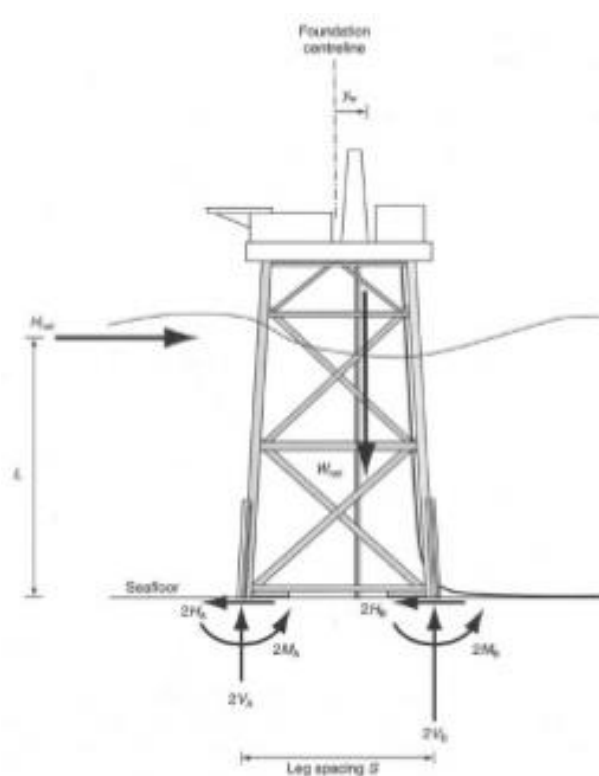
In these pages, it is developed uniquely the in-situ action on the structure, caused by extreme wave plus current and wind conditions.

Dynamic situation is not part of this study.

Also the temporary situations like transport, installation, etc., are not studied, for two reason: without a definitive structure geometry is not possible to study correctly these phase of the structure life and, more important to me, these verifies do not concern the use of P-y curves, objective of this exercise-chapter.

Standard ISO 19902 treats the fixed steel offshore structure and it furnishes a definition of jacket structure: a jacket is a welded tubular space frame with three or more vertical (or near vertical) tubular chords (the legs) and a bracing system between the legs.

The jacket provides support for the foundation piles, conductors, risers and other appurtenances.



The sketch on the left side presents the most simple evaluation of the loads on a jacket structure and the reactions of the foundation. In the case herein treated these forces on the structure base are guaranteed by a pile foundation.

The following example adopts the jacket structure above described and a foundation of three pile for each leg (globally twelve piles).

Each pile is embedded for 40 meters with an outside diameter of 84 inches (2,14 meters) and a wall thickness of 60 mm.

It is used the same piles and the same soil profile used in Norway to define the P-y curves

from Plaxis 3D and API-recommendation in order to simplify the comparison on a real case.

In the Straus numerical model, the desk is simulated like a concentrated mass (of 500 ton) and this point is placed on the top of the structure and it is connected by four rigid links (defined in the plain XR) at the highest columns.

Contact points between legs and seabed are represented by a fixed restrain below each leg.

Obviously, this is a very strong assumption but it leads to precautionary results, which means high actions on the foundation due to the high stiffness of the restrains.

In the reality, the pile settlement reduces a little bit the stiffness of the jacket foundation, also scour and subsidence play an important role in the real behaviour of the pile foundation.

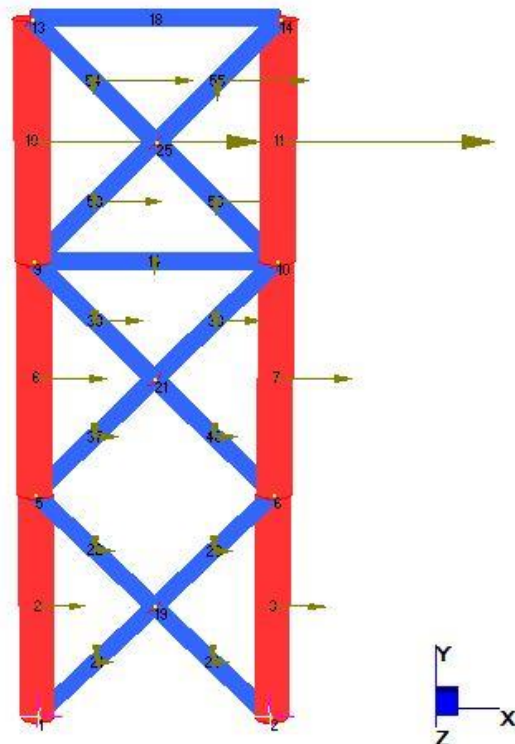
The deck elevation from the water sea level is verified in order to guarantee a safety margin:

$$h_{min} = \sqrt{a^2 + s^2 + t^2} + f = \sqrt{\left(\frac{5}{9} \cdot 15.8\right)^2 + 2^2 + 1^2} + 1 = 10 \text{ m} < (39 - 28.7)\text{m} \quad \textit{Verified}$$

Where:  $a$  is the abnormal wave crest height,  $s$  is the extreme storm surge,  $t$  is the maximum tide relative to the main sea level and  $f$  is the expected sum of subsidence, settlement and sea level rise over the design life of the structure.

In order to avoid to recalculate the structure because of an element too much stressed, it is preferred to define a jacket a little bit over dimensioned.

The steel framework is composed of three levels with equal dimension 13x13x13 (base x width x



height) meters, two levels of horizontal beam are located on the base on the top of the highest framework level (26 and 39 meters).

It is supposed a quasi-static action in the same direction of the x-axis of the jacket structure. This assumption helps me during the force calculation because it reduces the components in two directions and not three for the main part of the braces, this thanks to theme “friendly” orientation.

The assumption of the wave current direction (directed like a jacket axis) simplify the hand-made calculation done with the Morrison equation, because this equation calculate the force setting on a cylindrical member perpendicular to its axis; for the generic brace the axis orientation it has components in X, Y and Z direction.

An oblique beam is put on the plane parallel to the seabed, between second and third level, in order to guarantee sufficient resistance of the jacket framework of actions directed along the diagonal of the structure, so objective of this truss is to avoid the trellis crushing.

### **International Standard ISO 19902**

In this paragraph parts of standard ISO 19902 are reported and briefly analysed in order to explain clearly the passages that lead to the final action on the structure for the exercise presented in these pages. The main concepts are listed below:

- Selecting design metocean parameters and action factors. The reliability of a structure depends on the combination of design actions and design resistances. Design in accordance with ISO 19902 shall be based on a return period of 100 years. Where the data are available and sufficient, the 100 years return period may apply to responses (action effect) of the structure instead of to metocean (meteorological and oceanographic) parameters of design.
- Design action are the product of selected representative actions and associated partial action factors. The recurrence interval for metocean design parameters should be several times the design service life of the structure.
- Aspects to be considered in selecting partial action factors are: use of the structure; structure design service life; time of construction, installation and actions due to environmental condition during operation; earthquakes; ice; exposure level; requirements of regulations and uncertainty of actions associated with metocean parameters.
- Structure can be categorized by various levels of exposure to determine criteria that are appropriate for the intended service of the structure. The levels are determined by consideration of life-safety and of environmental and economic consequences. The structure herein used for the analysis is supposed to be L3 of exposure level (platform unmanned with low consequence in case of collapse).

- Open-ended piles are normally used in foundations for offshore structure. These piles are usually driven into the seabed with impact hammers, which use steam, diesel fuel or hydraulic power as source of energy.
- The foundation shall be designed to carry static, cyclic and transient actions without excessive deformations or vibrations in the structure.
- Special attention shall be given to the effect of cyclic and transient actions on the structural behaviour of the piles, as well as on the strength of the supporting soils.
- The ultimate pile pull out capacity is less than or equal to the total skin friction resistance.
- The pile foundation shall be designed to resist static and cyclic lateral actions. The lateral resistance of the soil near the surface is significant to pile design, and the possible effects of scour on this resistance shall be considered.
- For static lateral actions, the representative unit lateral capacity of soft clay, in unit of force per unit of length has been found to vary between  $8 c_u D$  and  $12 c_u D$ , except at shallow depths where failure occurs in a different mode due to low overburden stress.
- Cyclic actions cause deterioration of the lateral capacity below that for static actions.
- Pile group behaviour: for piles embedded in clays, the group axial capacity can be less than the single isolated pile capacity multiplied by the number of piles in the group. The group settlement in either clay or sand is normally larger than of a single pile subjected to the average action per pile of the pile group.
- Pile group lateral behaviour: for pile with the same pile head fixity conditions and which are embedded in either cohesive or cohesionless soils, the pile group normally experiences greater lateral displacement than those undergone by a single pile subjected to the average action per pile of the corresponding group. The major factors influencing the group displacements and distribution of actions over the piles are the piles spacing, the ratio of the pile penetration to the pile diameter, the pile flexibility relative to the soil, the dimension of the group, and the variations in the shear strength and stiffness modulus of the soil with depth.
- Pile lateral failure: this occurs when the applied actions produce a shear force in a pile that cannot be resisted by the lateral P-y resistance of the upper layers of soil. This results in excessive lateral movement of the piles and, therefore, additional bending moments, which combine with the existing pile axial forces to cause yielding and plastic hinges in the piles. This type of failure will occur if the steel framework is sufficiently stiff and strong against lateral movement and the upper layers of soil are relatively weak.
- Fatigue damage design factors for fatigue of steel components primarily depend on failure consequence and in-service inspectability. A structure with redundancy, capability for in-

service inspection and the possibility for repair/strengthening is preferred, especially for the design of a new structural concept or a conventional structure for new environmental conditions.

## Actions calculation

In the table below are reported the metocean parameters furnished by Kvaerner for a not specified site.

Design wave period (sec)	Design wave height (m)	Seabed depth (m)	Current velocity (m/sec)	Design wind velocity (m/sec)
10.3	15.8	28.7	1.2	42

According to the 2D wave theory the water particle velocity has been calculated in components.

In the following chapter,  $U$  is the component of the local water particle velocity vector normal to the axis of the member and, in this case, it is calculated by components (note:  $\theta_{current-wave} = 10^\circ$ ):

$$u_x = \frac{H}{2} \omega \frac{\cosh(k(z+h))}{\sinh(kh)} \cos(kx - \omega t) + U_{current} \cos \theta_{current-wave}$$

$$u_y = \frac{H}{2} \omega \frac{\sinh(k(z+h))}{\sinh(kh)} \sin(kx - \omega t)$$

Below  $\frac{\partial U}{\partial t}$  is the component of the local water particle acceleration, vector normal to the axis of the member, in this case it is calculated by components:

$$\left(\frac{\partial U}{\partial t}\right)_x = \frac{H}{2} \omega^2 \frac{\cosh(k(z+h))}{\sinh(kh)} \sin(kx - \omega t)$$

$$\left(\frac{\partial U}{\partial t}\right)_y = \frac{H}{2} \omega^2 \frac{\sinh(k(z+h))}{\sinh(kh)} \cos(kx - \omega t)$$

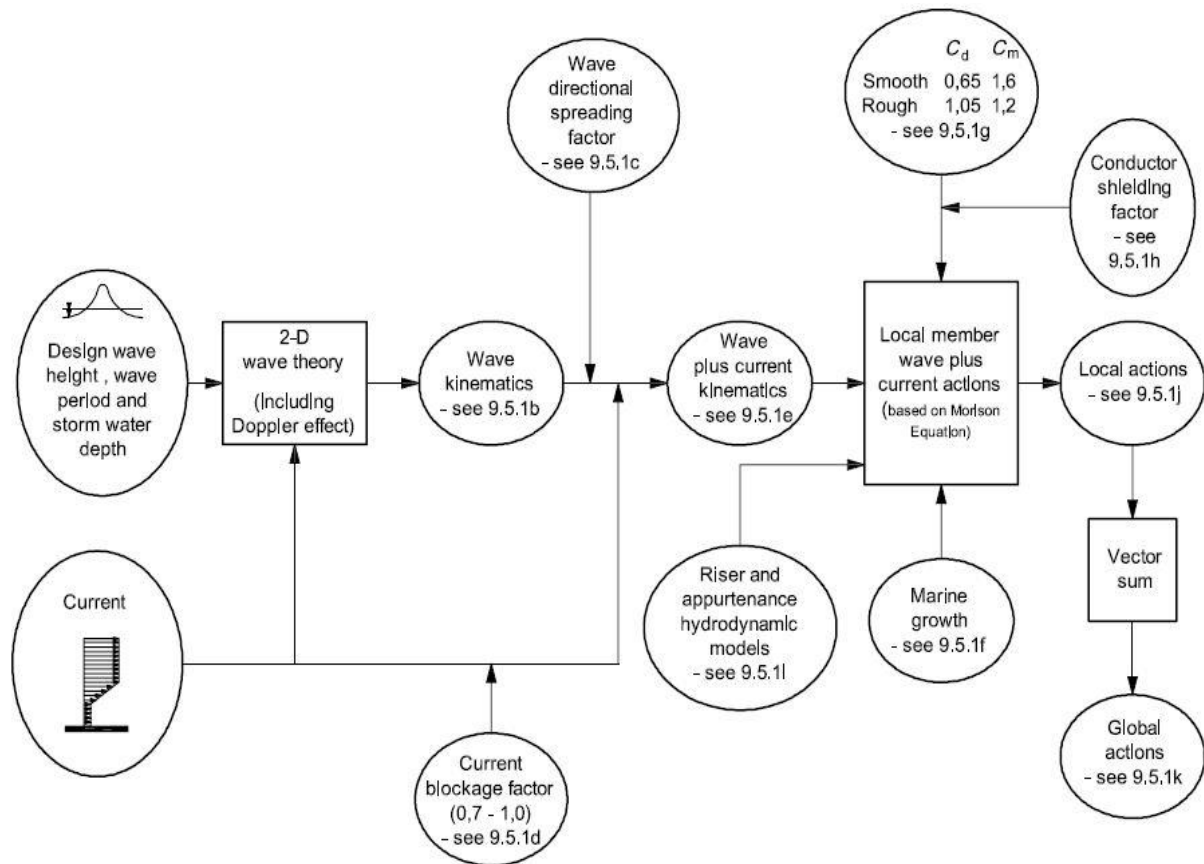
The procedure used to determine the extreme, deterministic, quasi-static global action exerted on the structure caused by waves alone or by waves and current is applicable only to a fixed structure that satisfies the following conditions:

- Negligible distortion of the incident wave by the structure;
- Negligible dynamic structural response.

With the explained method three phase conditions are investigated in order to evaluate the most dangerous load combination. From scientific literature it has been found that the maximum for the global vector sum stays in the range  $(-\frac{\pi}{4} \div 0) \cdot T_{s,wave}$ . In the preliminary proves run in order to evaluate the most complex situation,  $-\frac{\pi}{4}, -\frac{11\pi}{12}, 0$  are tested, corresponding to a time of 7.725, 9.442 and 0 seconds.

Larger actions are found at the time of zero seconds i.e. when the wave crest touches the first leg.

In this page it is reported the scheme, from ISO 19902, representative of the procedure for calculating the quasi-static action caused by wave plus current.



The computation of the action on a cylindrical object (a member) caused by waves, current or a combination of waves and current depends on the ratio of the waves length to the member diameter. When this ratio is large (>5), the member does not significantly modify the incident wave. The action can then be computed as the sum of a hydrodynamic drag action and a hydrodynamic inertia action, as given in following equation:

$$\mathbf{F} = \mathbf{F}_d + \mathbf{F}_i = C_d \cdot \frac{1}{2} \cdot \rho_w \cdot \mathbf{U} \cdot |\mathbf{U}| \cdot A + C_m \cdot \rho_w \cdot V \cdot \frac{\partial \mathbf{U}}{\partial t}$$

Where:

$\mathbf{F}$  is the local action vector per unit length acting normal to the axis of the member;

$\mathbf{F}_d$  is the vector for the drag action per unit length acting normal to the axis of the member in the plane of the member axis and  $\mathbf{U}$ ;

$\mathbf{F}_i$  is the vector for the inertia action per unit length action normal to the axis of the member in the plane of the member axis and

$C_d$  is the hydrodynamic drag coefficient;

$\rho_w$  is the mass density of water;

$A$  is the effective dimension of the cross-sectional area normal to the member axis per unit length (=D for circular cylinder);

$V$  is the displaced volume of the member per unit length

$D$  is the effective diameter of a member ( a circular cylinder), including marine growth;

$U$  is the component of the local water particle velocity vector (due to waves and/or current) normal to the axis of the member;

$|U|$  is the modulus ( the absolute value) of  $U$ ;

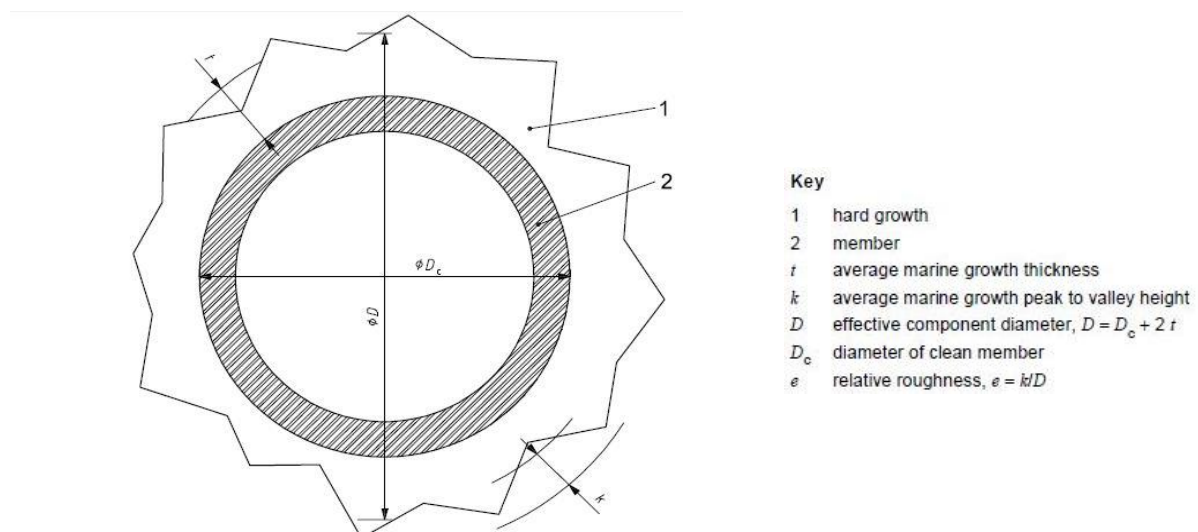
$C_m$  is the hydrodynamic inertia coefficient;

$\frac{\partial U}{\partial t}$  is the component of the local water particle acceleration vector normal to the axis of the member.

Suggested value of drag and inertia coefficients furnished by international standard, for typical situations of smooth and rough member surface.

Surface of the component	$C_d$	$C_m$
smooth	0.65	1.6
rough	1.05	1.2

On the sketch below a member section affected by marine growth is presented.



The components affected by marine growth is classified as “rough”, otherwise “smooth”. In this exercise are considered the smooth elements lower than the water sea level minus half of the design wave height. Above this level, every member is supposed to be affected by marine growth, so the related family of coefficients must be used during the forces calculation i.e. into the Morison equation.

Supposed a platform with vertical walls in normal direction of wind, it is calculated the wind force by the equation:

$$F = \frac{1}{2} \rho_{air} \cdot U_{wind}^2 \cdot C_s \cdot A$$

Where the shape coefficients is set equal to 1.5; like suggested by international standard for flat wall.

The load due to wind results equal to 120 kN, because it is considered a platform with wall dimension of 15x6 meters (15x15 meters of base).

For the finite elements simulation, the deck weight is set equal to 500 tons.

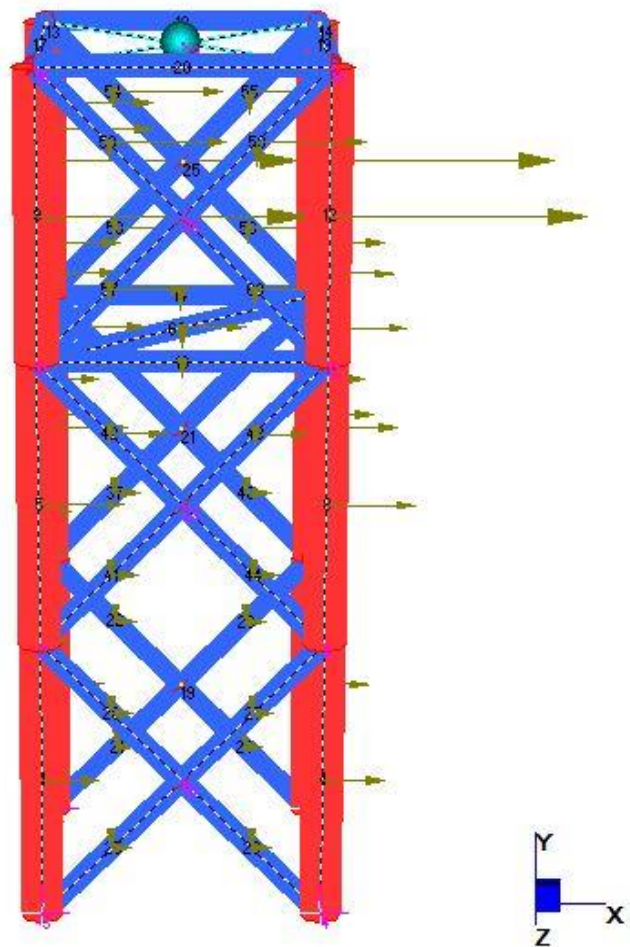
In the picture on the right, the deck is represented by a translation mass on the top of the jacket (blue sphere) connected by rigid link (also blue) to the edge of the column-legs.

Design wind is modelled by a concentrated force on the deck i.e. the translational mass.

The green arrows are representative of the wave plus current action and they are defined for each member into the components along X,Y and Z-axis.

Brace and horizontal beam (outside diameter: 1m, wall thickness: 1inc, steel) are in blue. Legs (outside diameter: 2m, wall thickness: 1inc, steel) are in red.

The white and purple crosses on the legs foot are the fixed restrain imposed.



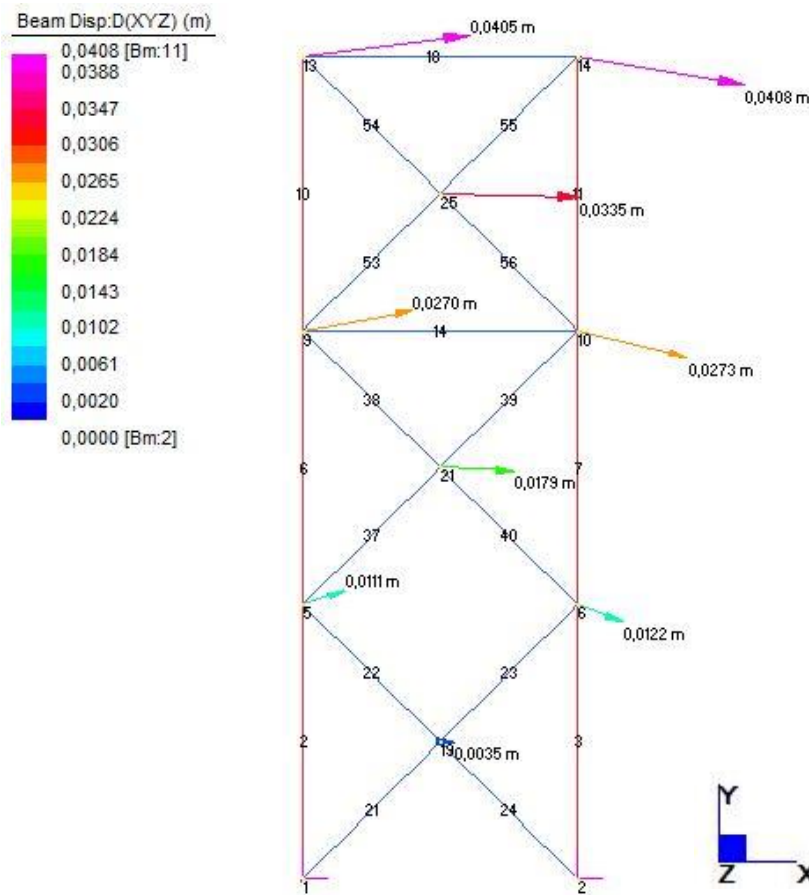
The forces calculated by quasi-static approach are modelled like concentrated forces in the middle of each member.

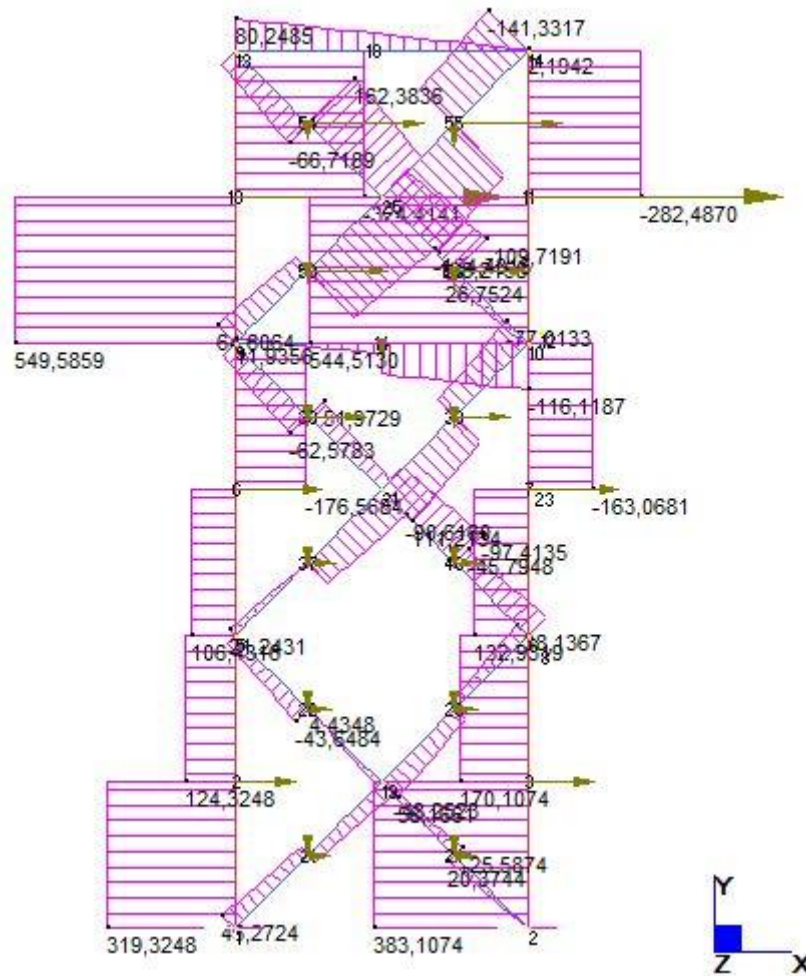
By hand calculation it is evaluated an acceptable leg and brace dimension (outside diameters and wall thickness).

It's important to know that the vertical axis, normally defined like Z-axis also into the equation of this chapter, is named Y-axis instead in Straus 7.

A 3D structure is modelled, but to be clear below are reported only the view into the XY-plane, because it has been supposed that current and wave stays into this plain.

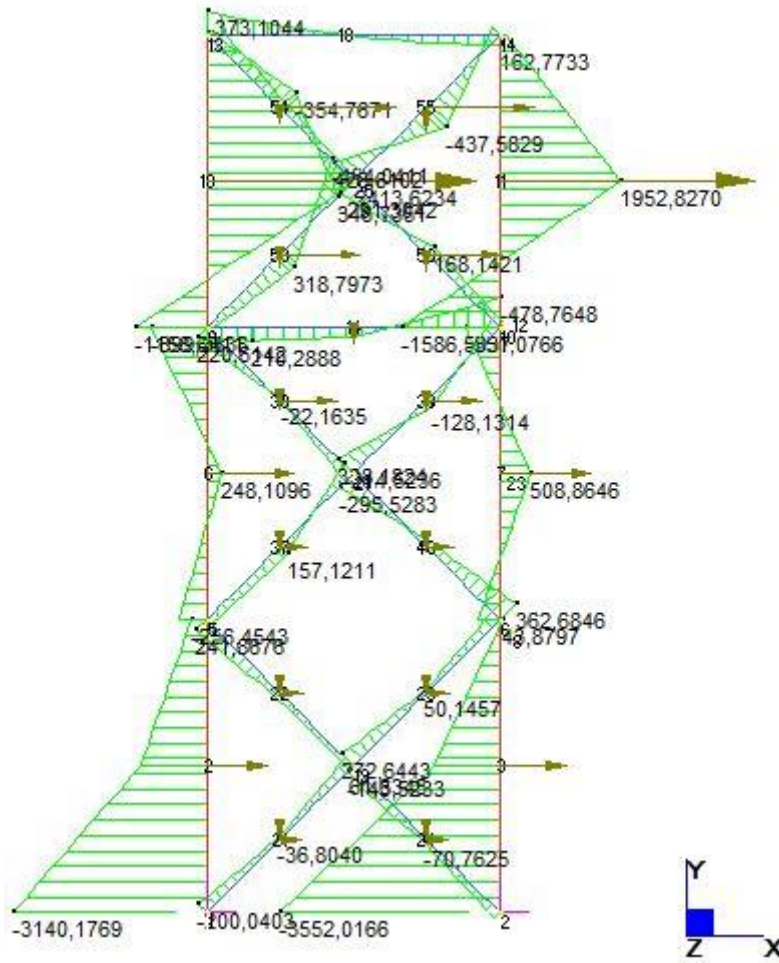
In the picture below are presented the displacements for the nodes.





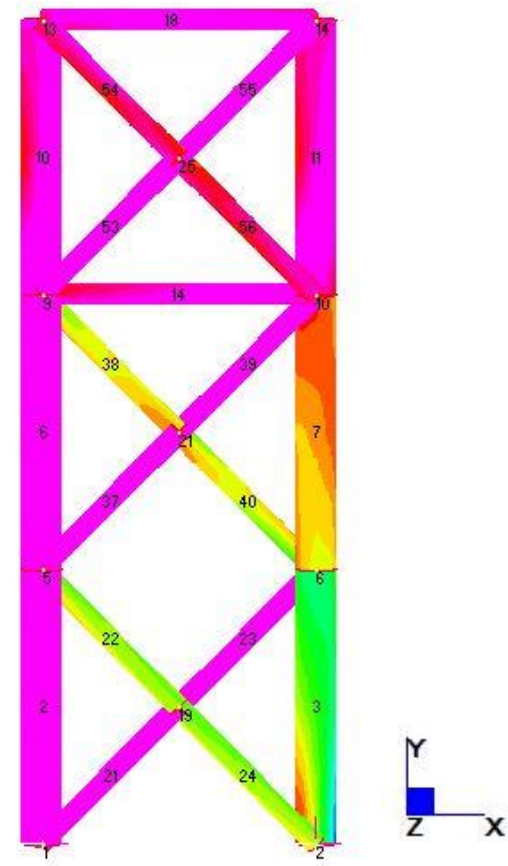
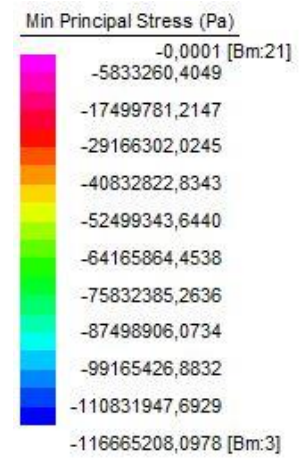
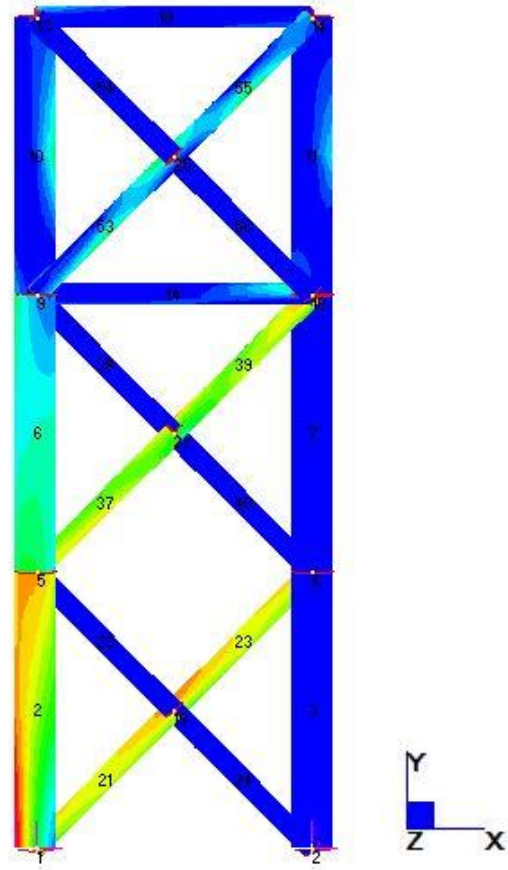
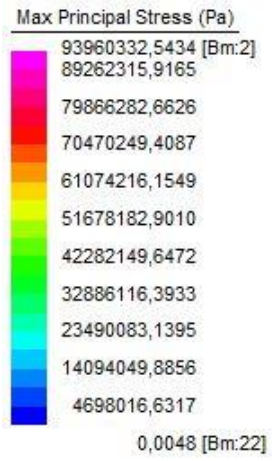
The forces calculated by quasi-static approach are modelled like concentrated forces in the middle of each member.

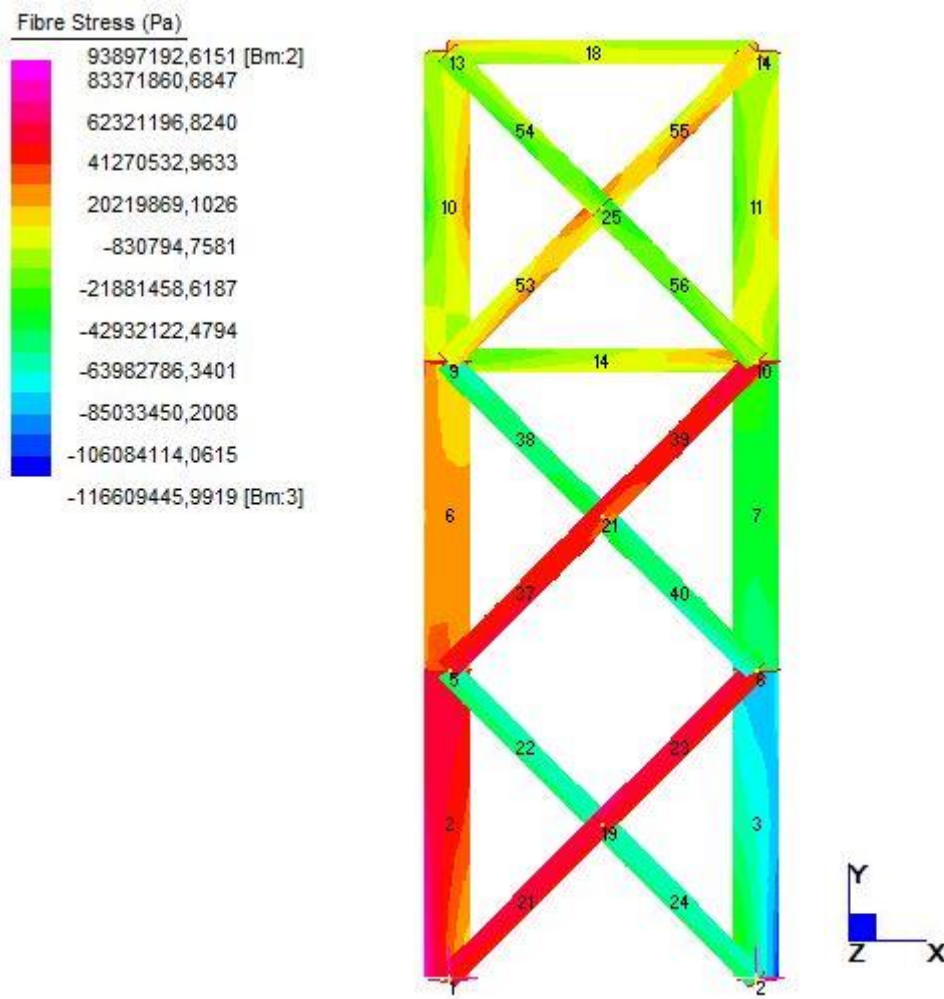
This is the reason of the shear shape and moment diagrams.



In the next pages are shown the distribution of the maximum and the minimum principal stress.

Observing the maximum stress distribution is possible to define the areas subjected to highest tensile stress, while the members in compression are highlighted into the minimum principal stress distribution.





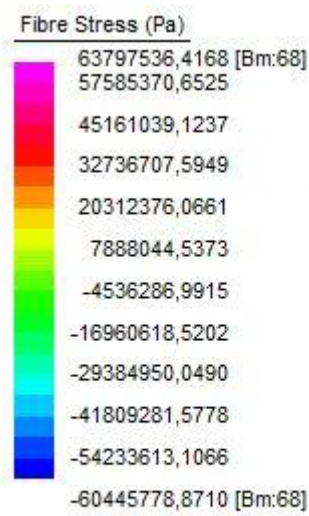
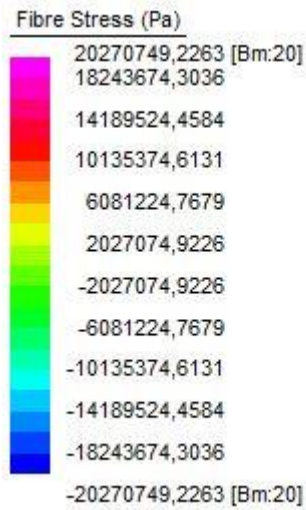
The picture above is representative of the fibre stress for the part of the structure in the XY-plane.

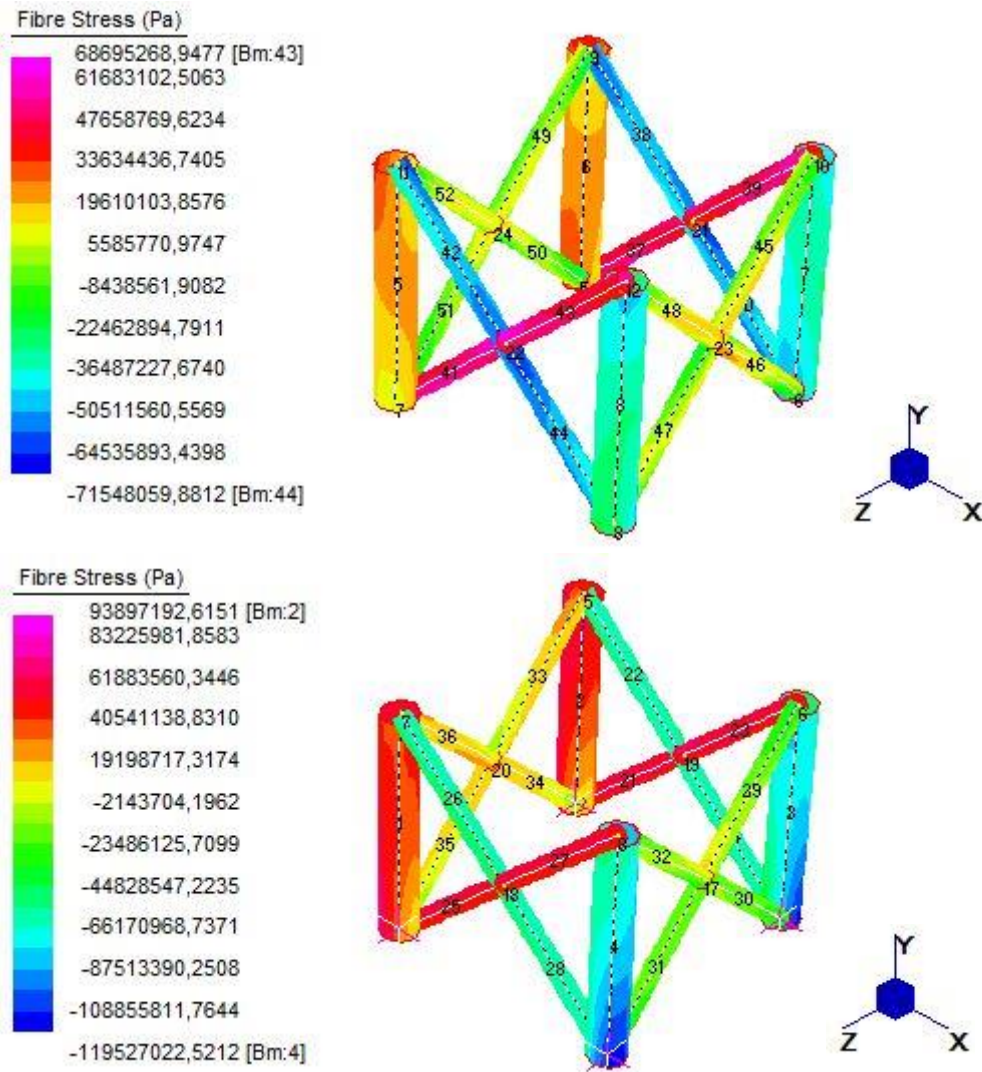
In order to add more information to get the real distribution of stress into the jacket structure, below are reported the fibre stress per each level.

The pictures below confirm the expectation about the more stressed parts of the structure.

The moment, in which the wave crest passes the legs on the YZ-plane, the most stressed elements in tension are the section near the mudline of these legs and the lower bracing. In compression, others legs are more stressed.

Concentrations of stress are visible around each node and in the middle of the highest part of the legs into the YZ-plane.





From the level subdivision above reported it is clear shown that the most stressed elements of this jacket are the lower parts of the legs, because they are very tensioned and compressed depending on the position.

The maximum fibre stress is approximately 94 MPa, using the most simplified approach defined by ISO 19902; the yielding stress (500 MPa) reduced by a safety factor (see table below) must be major of the maximum stress found.

$$\sigma_{max} < \frac{\sigma_{yielding}}{FS_{fatigue}} \xrightarrow{\text{for this simulation}} 94 \text{ MPa} < \frac{500 \text{ MPa}}{5} \text{ Verified}$$

ISO 1990 coefficients table for simplified fatigue approach is below reported.

Failure critical component	Inspectable	Not Inspectable
No	2	5
Yes	5	10

### Piles foundation and P-y curves use

It has been just explained in the previous paragraphs that no cyclic load condition and relative effects are herein considered.

The soil profile adopted is the same largely used in the early chapters and the main characteristics are: linear undrained strength (5 kPa + 3 kPa/m) and Eps50 equal to 2%, unit weight of 20 kN per cubic meter.

Large focus will be put on the pile response of laterally loaded pile, but also a verify about axial capacity must be done. It is verified the axial pile capacity with the most simple approach, for cohesive soils, furnished by ISO 19902:

$$\begin{cases} f = s_u & \text{for } s_u < 24 \text{ kPa} \\ f = \frac{s_u}{2} & \text{for } s_u > 72 \text{ kPa} \end{cases} \quad \text{and linear interpolation between these two option}$$

For safety reasons and in order to verify also the axial extension situation, the pile end bearing capacity is neglected:

$$Q = Q_s + Q_e = f \cdot A_{shaft} + q \cdot A_{end}$$

*assumed no end-bearing capacity*  
 $\xrightarrow{\hspace{1.5cm}} Q \cong 8400 \text{ kN} > \text{every axial load (see table below)}$

The curves resistance-deflection that are herein used have been developed from Plaxis3D 2013 output data and from API recommendations.

From the numerical simulation with Straus 7 these values are found (also a calculation more approximated by excel spreadsheet confirm the values below):

LEG	Vertical Force (kN)	Horizontal Force (kN)	Moment (kNm) in X-direction
<b>Maximum loaded</b>	14694	3551	1178
<b>Minimum loaded</b>	-11345	3280	-1300

This means that the following design load per pile (three piles for each leg is the disposition adopted):

PILE	Vertical Force (kN)	Horizontal Force (kN)	Moment (kNm)
<b>Maximum</b>	5000	1200	400
<b>Minimum</b>	-3800	1100	-450

Also the pile parameters are the same in all parts of this master thesis:

PILE	Length (m)	Outside Diameter (inc/m)	Wall Thickness (mm)	$E_{\text{steel}}$ (GPa)	$E^*$ for the solid section equivalent to real (GPa)
					43
	40	84/2.14	60	210	43

The spreadsheet used to implement the P-y curves and run the simulation comes from a US company, so each input parameter must be converted from the International System of Units into the imperial unit system and vice versa.

In this spreadsheet the curves characteristic of the examined soil profile are defined one by one.

In order to do a comparison of results are run calculations also with curves from API standard.

It seems clear to evaluate that the results from both these methods are very similar and that like expected using the curves obtained by API recommendations conservative results are obtained.

This last observation confirms the prediction done watching Plaxis3D results, just largely commented in the early part of this thesis.

For each variable plotted the trend is almost the same: API curves furnish values larger than Plaxis3D curves, but the curves have the same shape of each other.

In the table below are summarized the maximum values of bending moments and deflection for the pile.

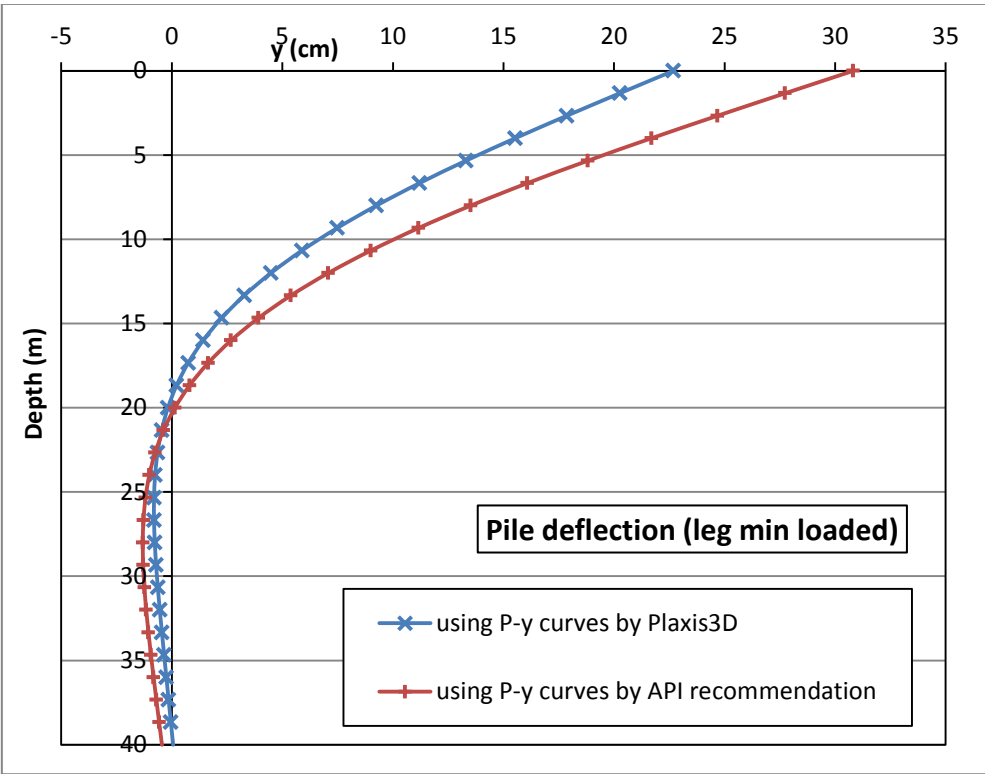
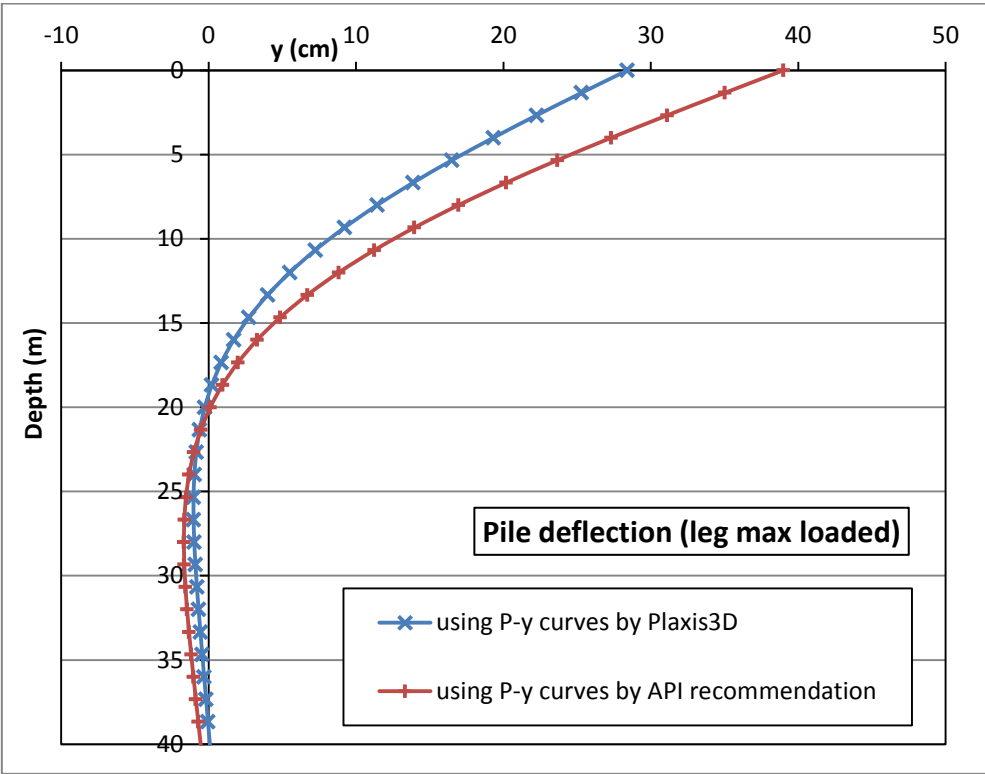
Curves	Leg max loaded		Leg min loaded	
	Head deflection (cm)	Max bending moment (kNm)	Head deflection (cm)	Max bending moment (kNm)
Plaxis3D	28	8589	23	6834
API recommendation	39	10437	31	8206
<b>percentage variation</b>				
	37%	22%	36%	20%

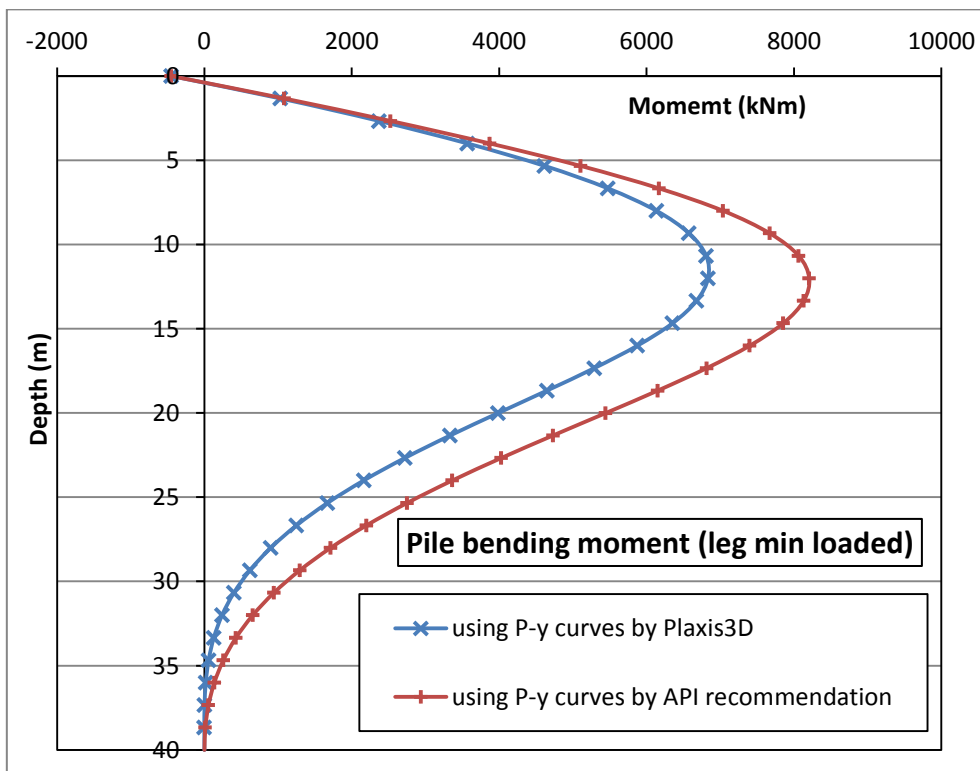
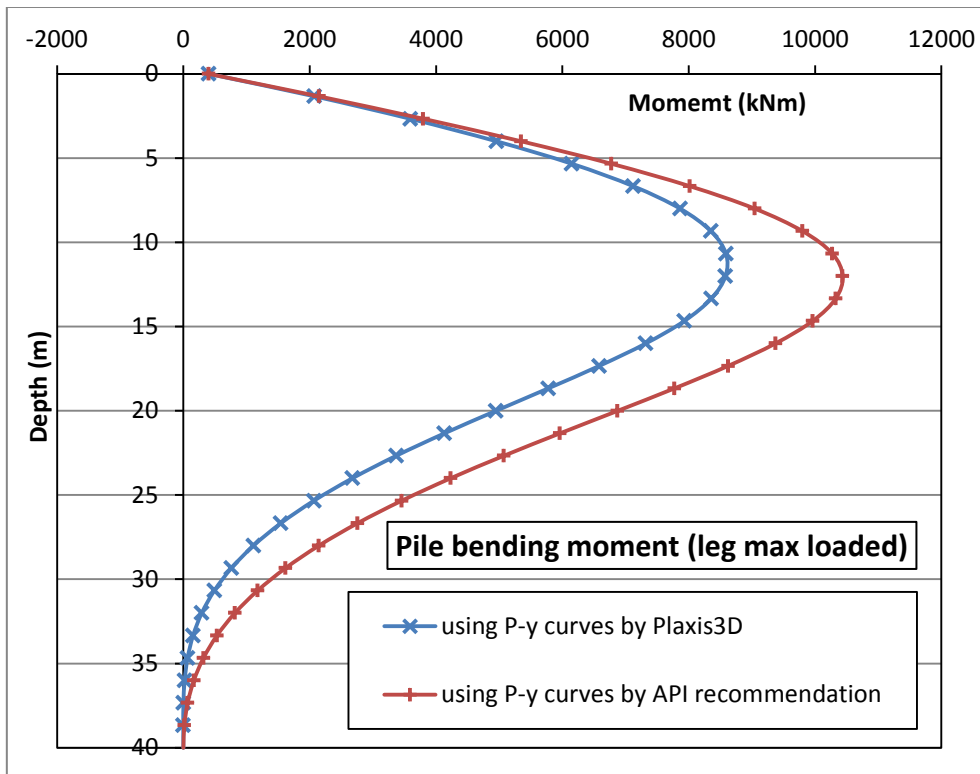
Pile deflection presents a large variation, approximately 35%, than the bending moment, 20% ca.

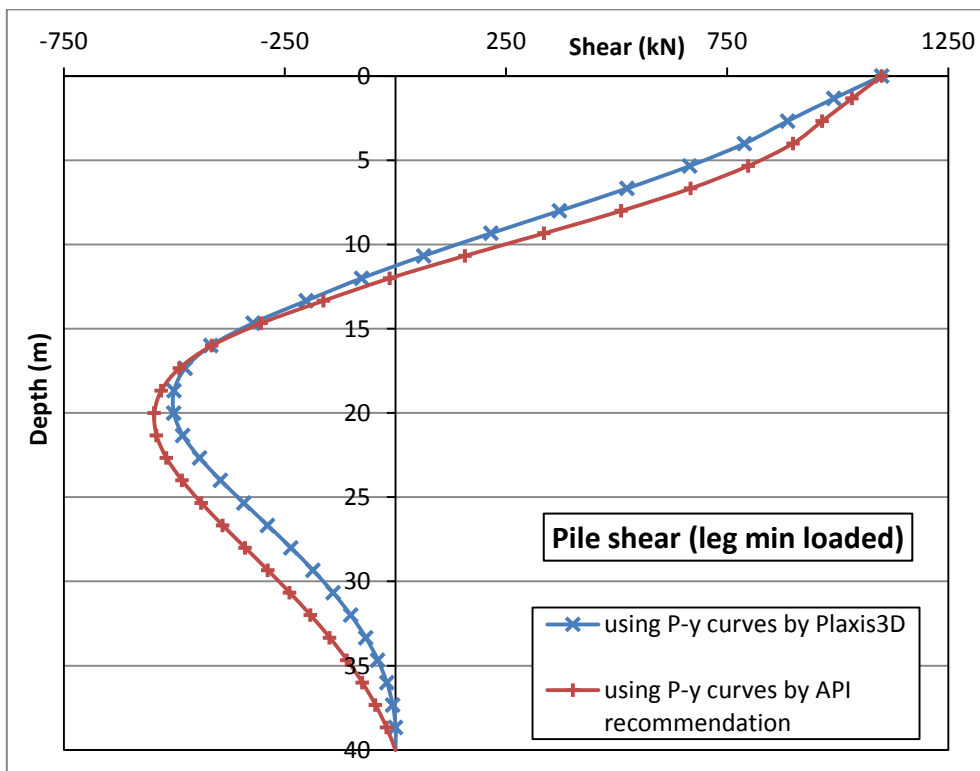
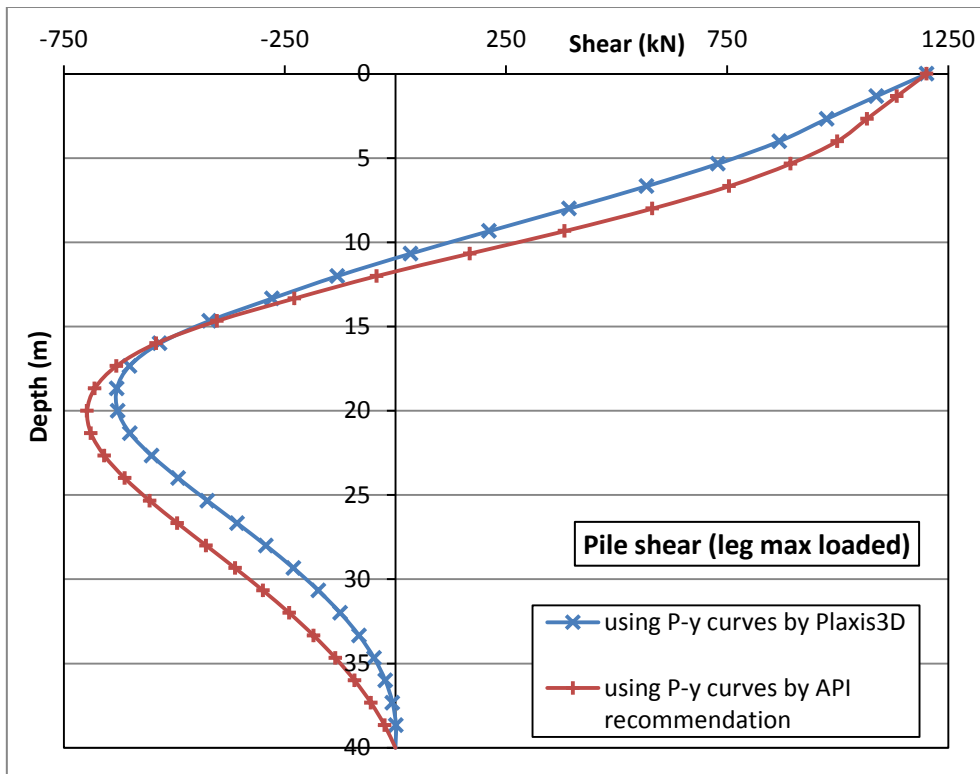
This confirms the observation already done in the initial chapters i.e. Plaxis3D furnishes values smaller than API recommendation for pile deflection and maximum bending moment. It's also confirmed that the signalized trend according to the pile deflection is more variable than the bending moment.

The variation between legs, in the table reported above, shown a very little difference into the percentage variations, so it is possible to observe an increase of the results spreading with the load level reached. Also the last one is an tendency already observed above.

Below are report the pile deflection, shear and bending moment, for the most and the less stressed legs.







## CONCLUSIONS AND OBSERVATIONS

---

During this dissertation, the behaviour of the laterally loaded pile in soft clay has been largely treated.

In addition, the behaviour of groups of two pile (free and fixed) heads has been investigated. These data are put in the appendix in order to avoid simple or wrong interpretations due to the few weeks used to develop these simulations.

To conduct these analyses, the software Plaxis3D 2013 has been used. Several different settings are tested in order to evaluate the sensibility of the model at the parameters variation.

Settings tested have been the interface reduction factor, tensile cut-off and Esp50. It is simple to observe that only Esp50 is a pure geotechnical parameter while the two other parameters listed are more related to the numerical model.

Moreover, a large number of “pure” model settings are analysed. These include model dimension, interface adoption, pile validation and the soil model adopted.

Main result of the huge amount of analysis is a scale of importance for the tested parameters; it is made evaluating the model response related to the parameter variation.

Primary importance must be assigned to soil model adopted and Esp50 value; because changing Esp50 into its typical range of values caused a result fluctuation of almost 30% for each variable of interest.

In the problem treated (short term static lateral load of a pile in soft clay), it has been demonstrated that the best performances are reached adopting NGI-ADP soil model. The best solution for this simulation has been reached defining an ADP soil with anisotropic behaviour. This is the most realistic situation, instead, using an elastic-perfectly plastic soil model, the results are not easy to comment, because the model response becomes stiff.

A secondary influence is observed for the interface reduction factor parameter if it is assumed in its typical engineering range because, for a value between 1 and 0.4, the fluctuation is less than 15%.

To complete the part of the model setting is indispensable to touch two points of fundamental importance: the model dimension along the load direction has a great influence on the result so it

must be set sufficiently large, in order to avoid stiff behaviour of the complex soil-structure. At last, the mesh coarseness must be fine in the zone with high gradients of displacement and stress.

The adoption of the tensile cut-off can affect the result of large variation, but its physical meaning must be evaluated with attention case by case, in reason to avoid “friendly” but wrong results. This because it is not certain a large opening gap behind the pile.

The second part of the dissertation, and declared objective of my working period spent at the Norwegian Geotechnical Institute, has been obtaining the resistance-deflection curves from finite elements analysis (a laterally loaded pile is modelled in Plaxis3D).

Some problems have been found and fixed using Plaxis3D for the case above described. One of them was a shear trend with unrealistic fluctuation along the shallow three meters of the pile (problem attenuated increasing the pile of two meters, one diameter, above the seabed and adopting a rigid plate on the pile head, where the load is applied).

Proving a comparison between displacement field obtained by Plaxis3D and the theoretical failure mechanism of the soil around the pile it is possible to evaluate a correct movement of the soil wedge behind the pile, but it is not possible to highlight a real flow of soil around the pile section, probably because it can be reached only for very high displacements of the pile section, indeed several papers test this behaviour defining a circular disc with imposed (high) displacement into the soil; in that case the soil flow around the pile section is reached.

Indispensable steps to compute the P-y curves from Plaxis3D simulation have been discussed in the specific chapter, but it must be highlighted again that the resistance-deflection curves obtained in this way are stiffer than API standard curves even if they lead to almost the same ultimate resistance.

The last exercise reported in this thesis is representative of a jacket structure under environmental loads.

Wave and current actions are evaluated following the quasi-static approach furnished by international standard ISO 19902. Also wind and structural weight are taken into count.

Once calculated the load acting per each pile, it becomes possible to study the lateral response of the foundation. This analyses are run with a specific spreadsheet.

The axial capacity is largely sufficient to accept the loads transmitted by the legs.

The result obtained by using Plaxis3D or API P-y curves shown the same trends but by 20%-30% bigger adopting the curves recommended by American Petroleum Institute.

This confirms the observation done during the model construction and use.

The method used to obtain the resistance-deflection curves has demonstrated wide possibility for future developments related to the generalization of other soil profiles and to the comparison of curves from field tests of laterally loaded piles with curves obtained by numerical simulations.

-This page intentionally left blank-

## REFERENCE

---

- Hudson M.(1970). *Correlations for design of laterally loaded piles in soft clay*. The U. of Texas at Austin.
- Gustav G., Lars A. and Hans P.J. (2010). *NGI-ADP: Anisotropic shear strength model for clay*.
- John B. Herbich, Editor. *Handbook of Coastal and Ocean Engineering*, Volume 2.
- R. G. Bea, Fellow, ASCE, Z. Jin, C. Valle and R. Ramos (1999). *Evaluation of reliability of platform pile foundations*.
- Hudson M., Wayne B. Ingram, Allen E. Kelley, Dewaine B. (1980). *Field tests of the lateral-load behavior of pile groups in soft clay*.
- Robert G. Dean, Robert A. Dalrymple. *Water wave mechanics for engineers and scientists*.
- V. Padmavathi, E.Saibaba Reddy and M.R. Madhav (2008). *Behaviour of laterally loaded rigid piles in cohesive soils based on kinematic approach*.
- SPLICE manual. NGI, Oslo, Norway.
- Summary report of NGI Strategic Research Project SP2 2011-2013. *Offshore wind turbine foundations*. No.20110001-R-01.
- John A.F. and Kenneth J.K. (1973). *Rational Analysis of the Lateral Performance of Offshore Pile Group*.
- NGI project report No.20092244-00-8-R. *Summary and recommendation practice. Lateral capacity of piles in soft clay*. 2013-01-08.
- Plaxis3D 2013 scientific manual. Plaxis, Delft, Nederland.
- H.Y. Qin, E.Y.N. Oh, W.D. Guo and P.F. Dai (2013). *Upper bound limit analysis of lateral pile capacity*.
- ISO 19901-1. *Petroleum and natural gas industries - Specific requirements for offshore structure*. Part 1: *Metocean design and operating considerations*. First edition 2005-11-15.
- ISO 19902. *Petroleum and natural gas industries – Fixed steel offshore structure*. First edition 2007-12-01.
- V. Zania and O. Hededal (2011). *The effect of soil-pile interface behaviour on laterally loaded piles (paper 1)*. Department of Civil Engineering, Technical University of Denmark.
- V. Zania and O. Hededal (2012). *Friction effects on lateral loading behavior of rigid piles*. Department of Civil Engineering, Technical University of Denmark.
- George G. and Ricardo D., Members, ASCE (1984). *Horizontal response of piles in layered soils*.

- Yit-Jin C., Associate Member, ASCE, Fellow and Fred H.K. (1993). *Undrained strength interrelationships among CIUC, UU, and UC Tests*.
- Youngho K., Sangseom J., Sooil K. (2009). *Characteristics of lateral rigidity of offshore piles in Incheon marine clay*. Department of Civil Engineering, Yonsei University, Seoul, 120-749, Korea.
- L.J. Zhu, Y.M. Cheng and D.B. Yang (2007). *The analysis of instrumented piles under lateral load*. Department of Hydraulic Engineering, Tsinghua University, Beijing, China; Department of civil and Structural Engineering, Hong Kong Polytechnic University, Hong Kong.
- Ke Yang and Robert Liang (2006). *Methods for Deriving p-y Curves from Instrumented Lateral Load Tests*.
- F. Rosquoet, L. Thorel, J. Garnier and M. Khemakhem (2010). *P-y curves on model piles: Uncertainty identification*.
- Todd W. Dunnavant, Associate Member, ASCE, and Michael W. O'Neill (1989). *Experimental p-y Model for Submerged Stiff Clay*.
- James D. Murff, and Jed M. Hamilton, Members, ASCE (1993). *P-Ultimate for Undrained Analysis of Laterally Loaded Piles*.
- P. Jeanjean, BP America Inc. (2009). *Re-Assessment of P-Y Curves for Soft Clays from Centrifuge Testing and Finite Element Modeling*.
- K. Georgiadis, S.W. Sloan, and A.V. Lyamin (2013). *Effect of loading direction on the ultimate lateral soil pressure of two piles in clay*. Georgiadis, K. et al. (2013). *Geotechnique* 63, No. 13, 1170-1175 (<http://dx.doi.org/10.1680/geot.13.T.003>).
- Harry G. Poulos, M. ASCE and Mark F. Randolph (1983). *Pile Group Analysis: A Study of Two Methods*.
- Wei Dong Guo, M. ASCE (2013). *Simple Model for Nonlinear Response of 52 Laterally Loaded Piles*.
- <http://newtonexcelbach.wordpress.com/>.
- [WWW.INTERACTIVEDS.COM.AU](http://WWW.INTERACTIVEDS.COM.AU).

## APPENDIX A – ANALYSIS OF GROUPS OF PILES

In this appendix are reported the results of numerical simulations run with Plaxi3D and compared with SPLICE results.

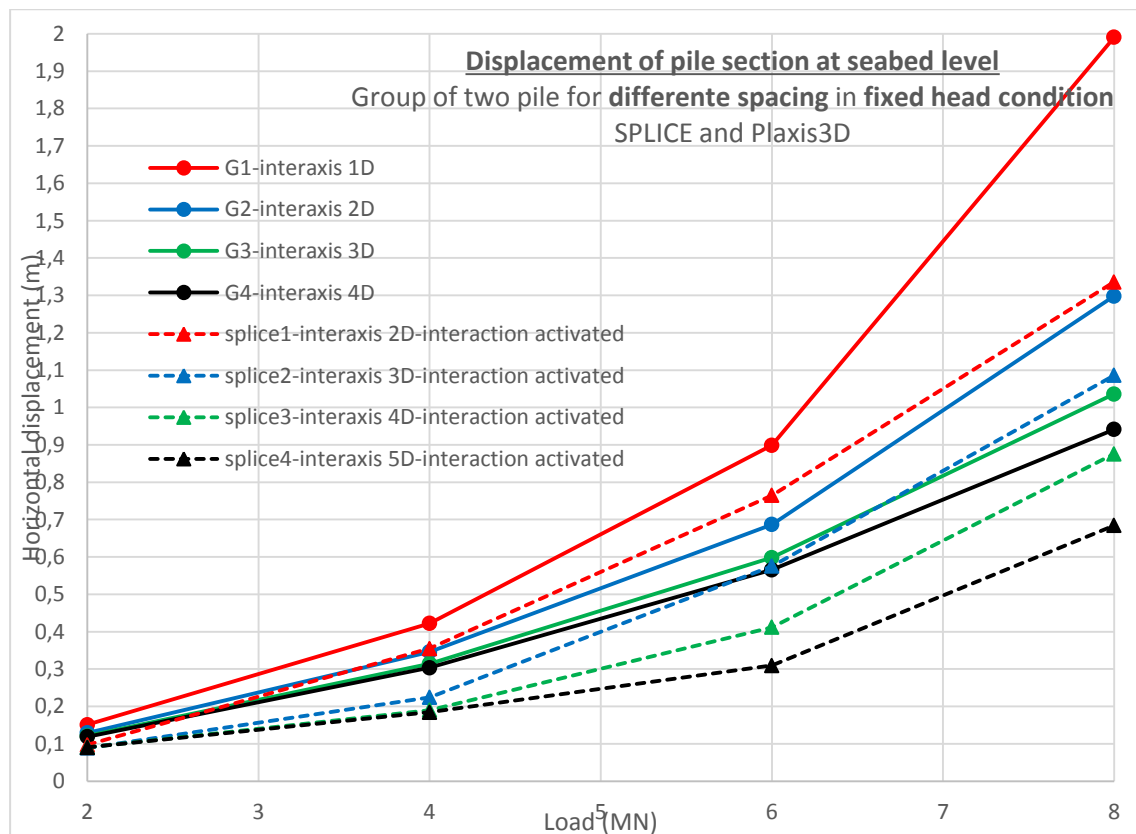
Both fixed and free heads condition are tested. The fixed head condition has been reached connecting the piles heads with a stiff plate.

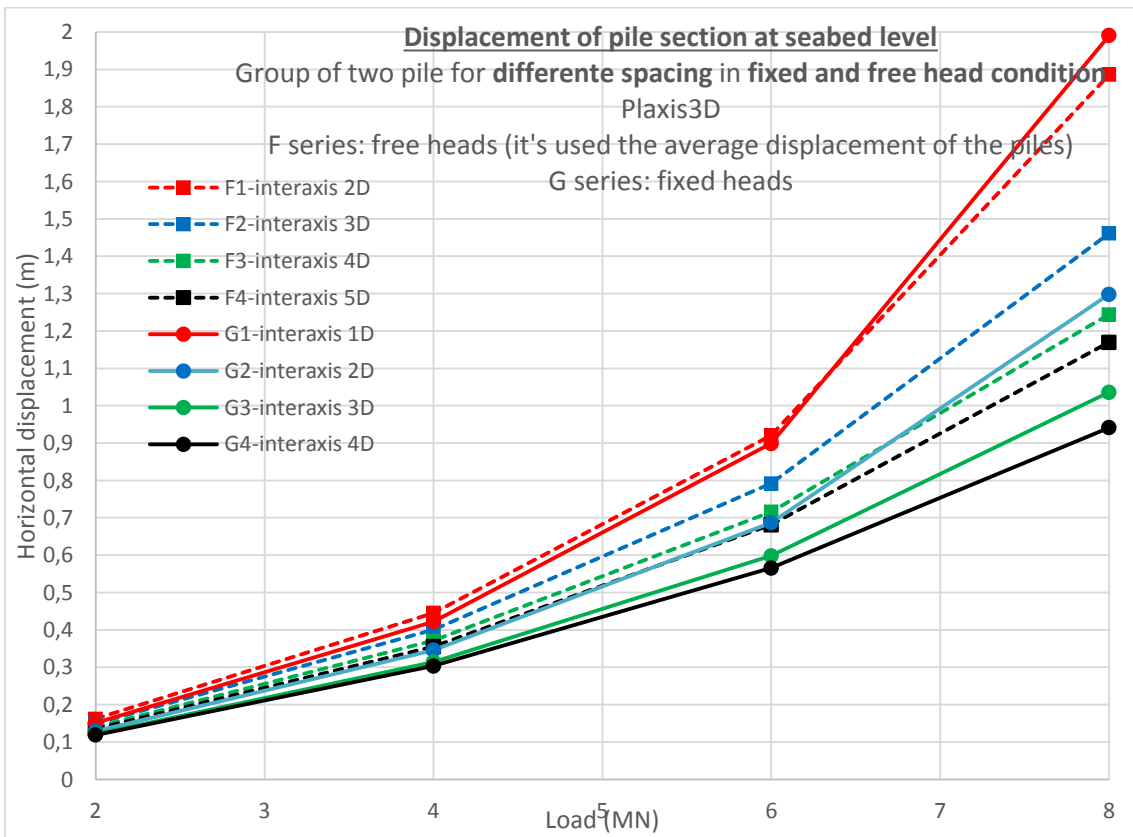
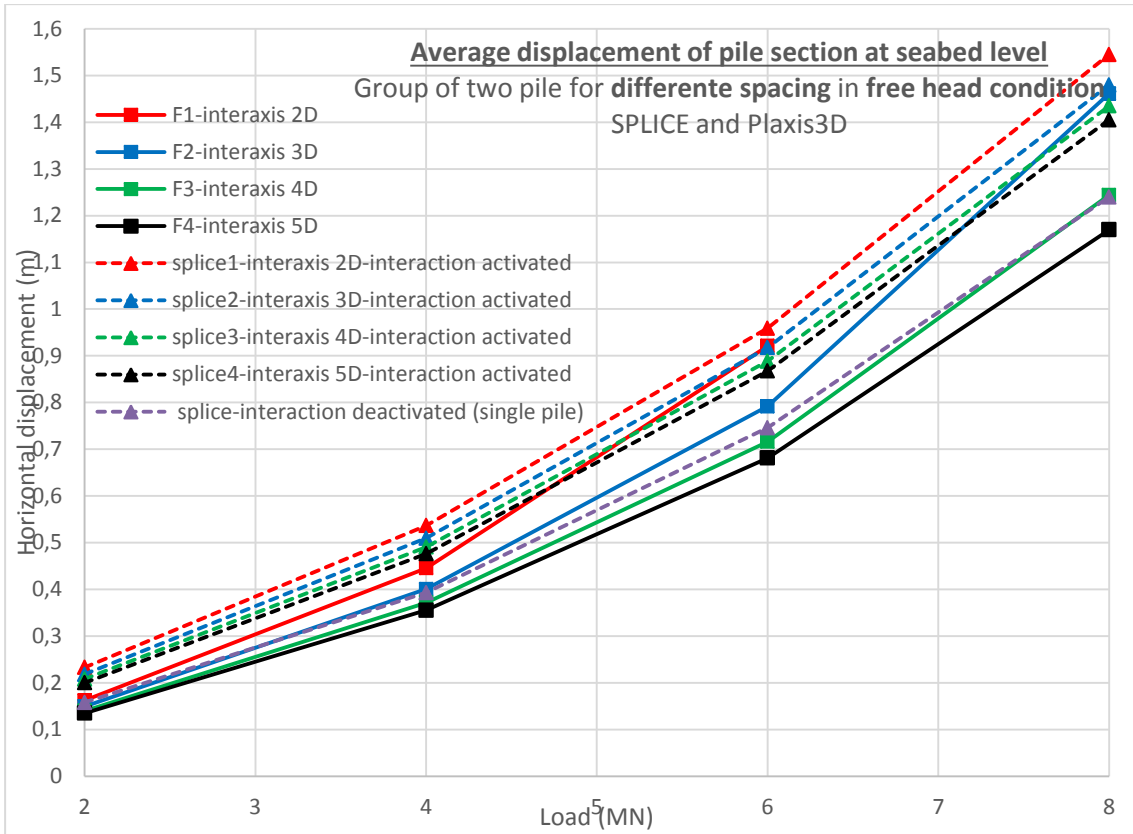
Several series of analysis are run for models with different piles spacing. Interaxis of 2,3,4,5 diameters are tested. These tests are done for both the restrain condition described above.

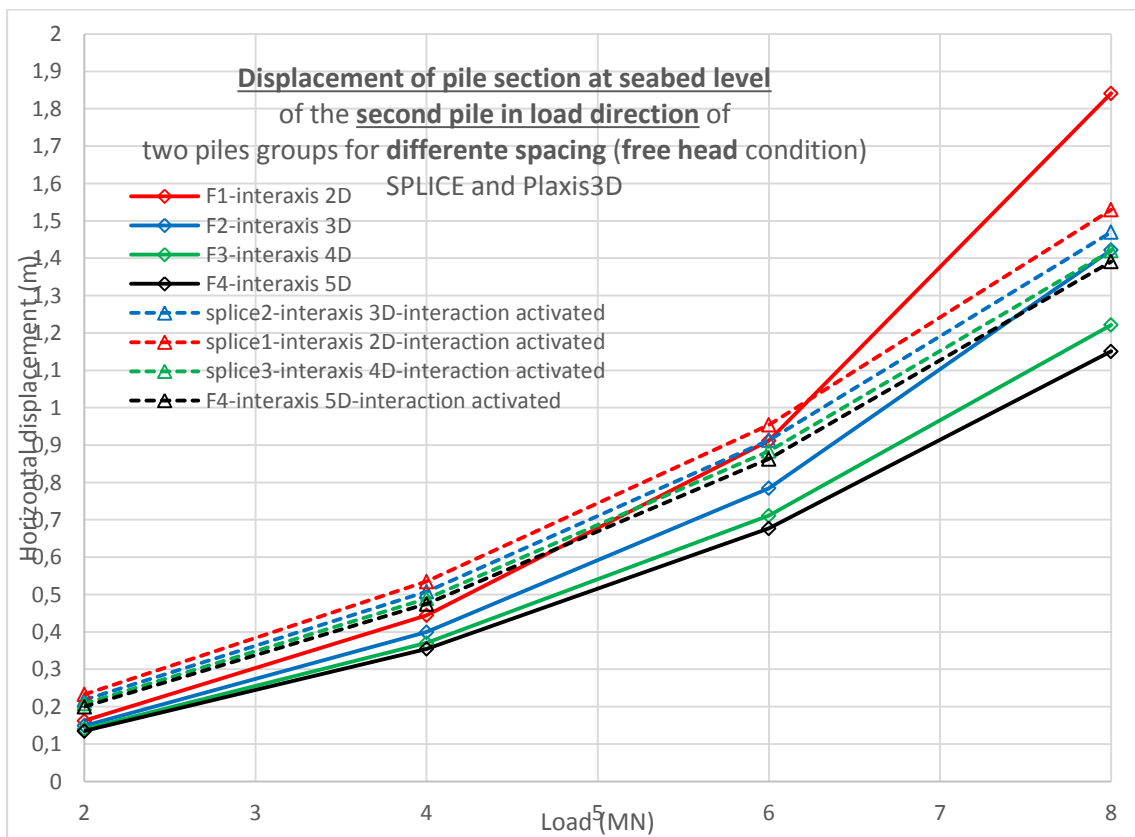
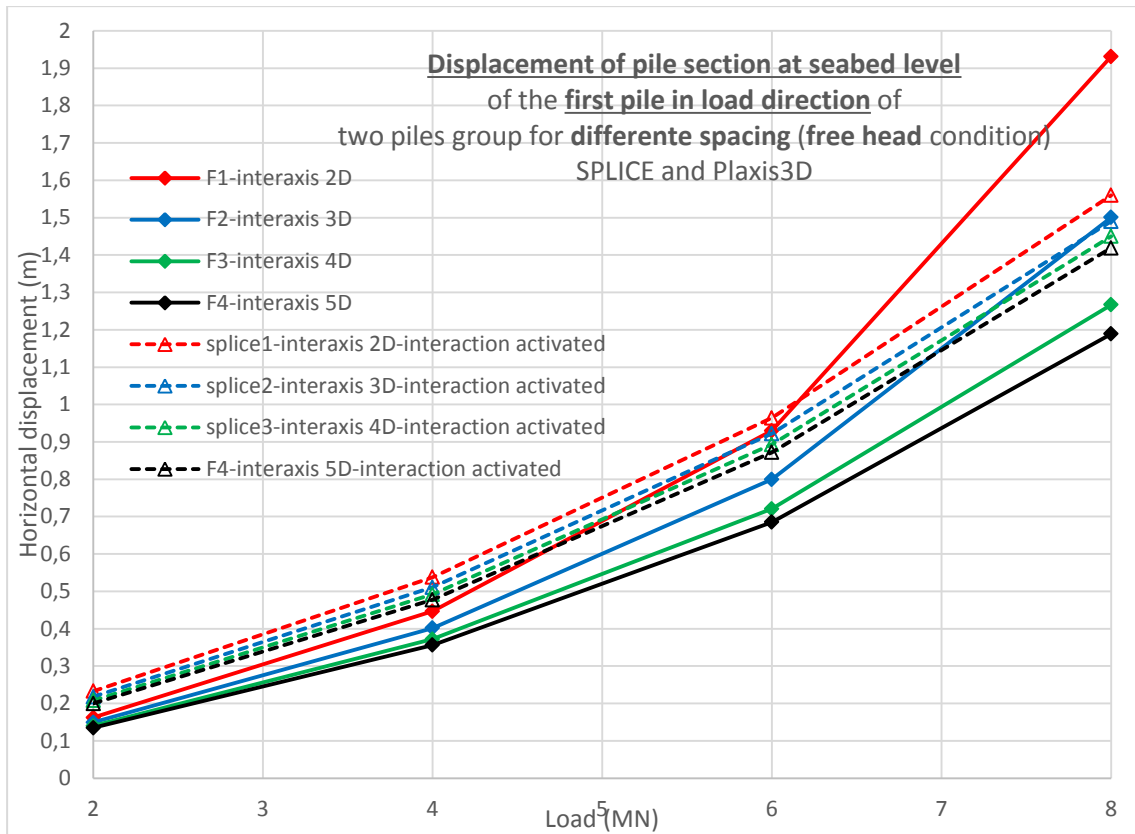
Below the displacements trends and two series of five graphs with two different normalizations are reported.

In the end also a third series is presented. The results are grouped by restrain heads conditions and by the load condition acting on the piles heads.

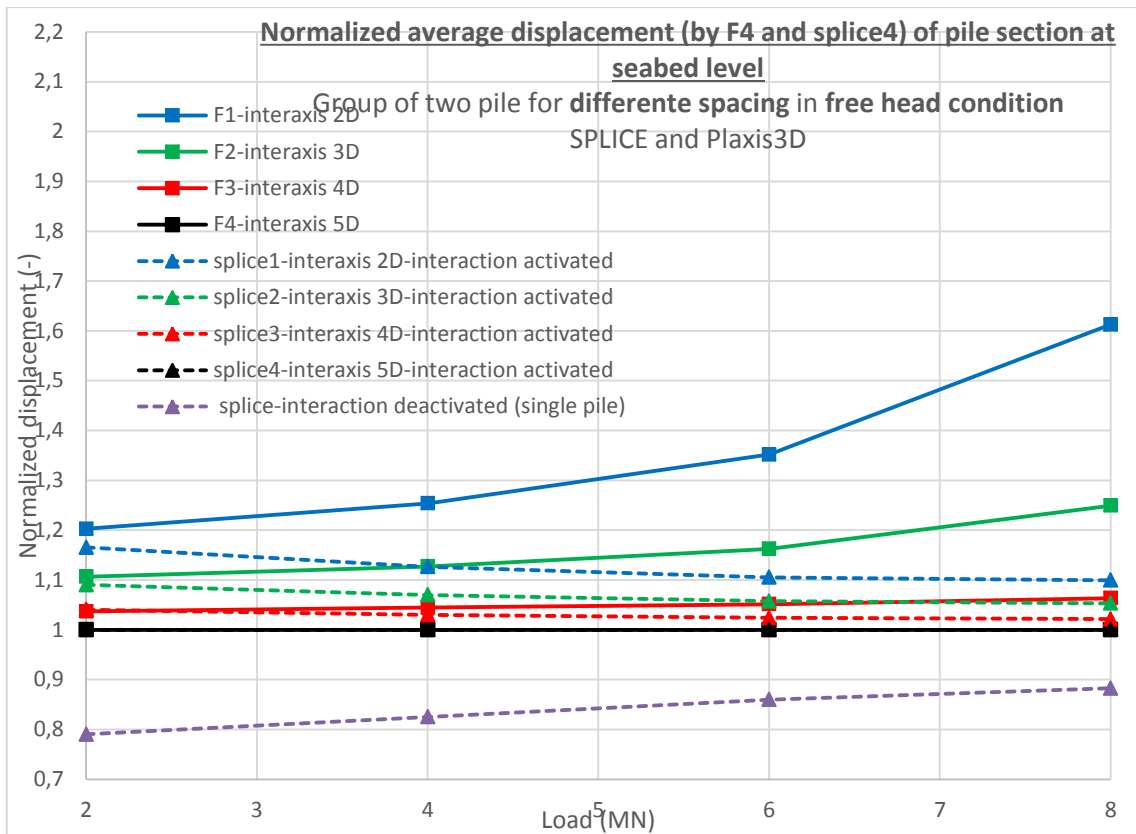
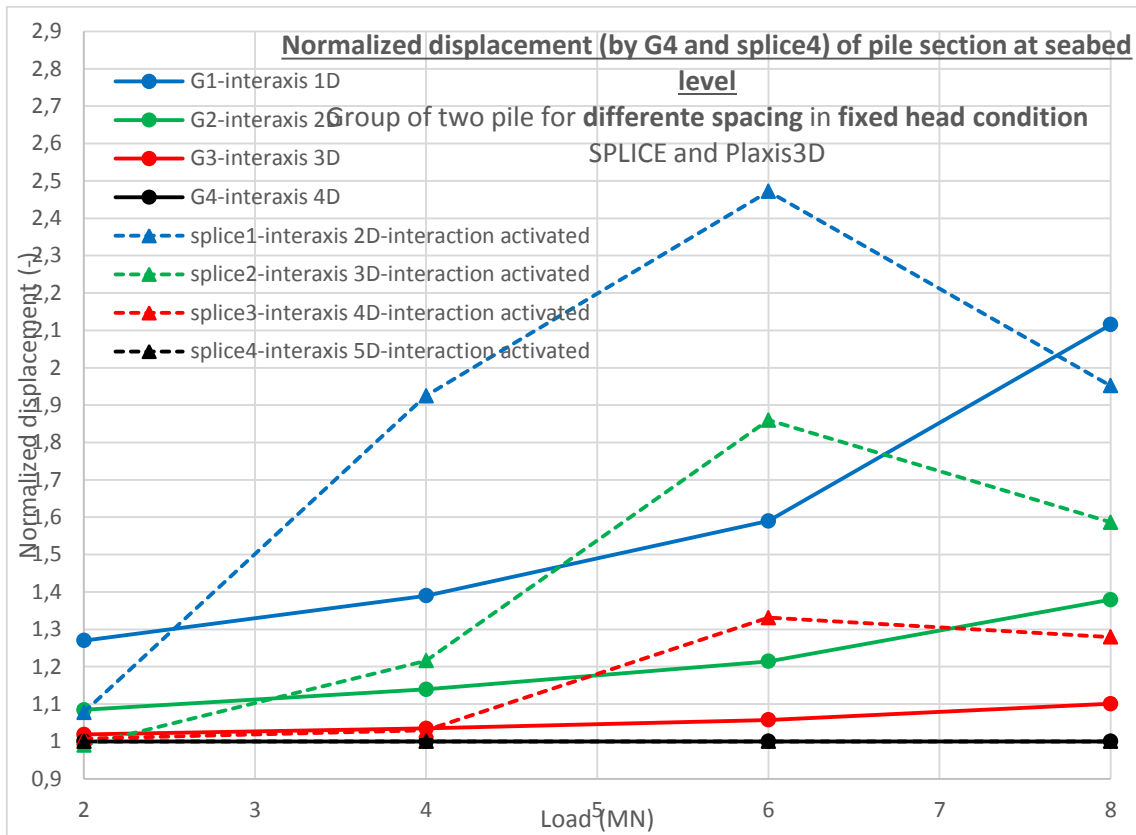
### Head isplacements

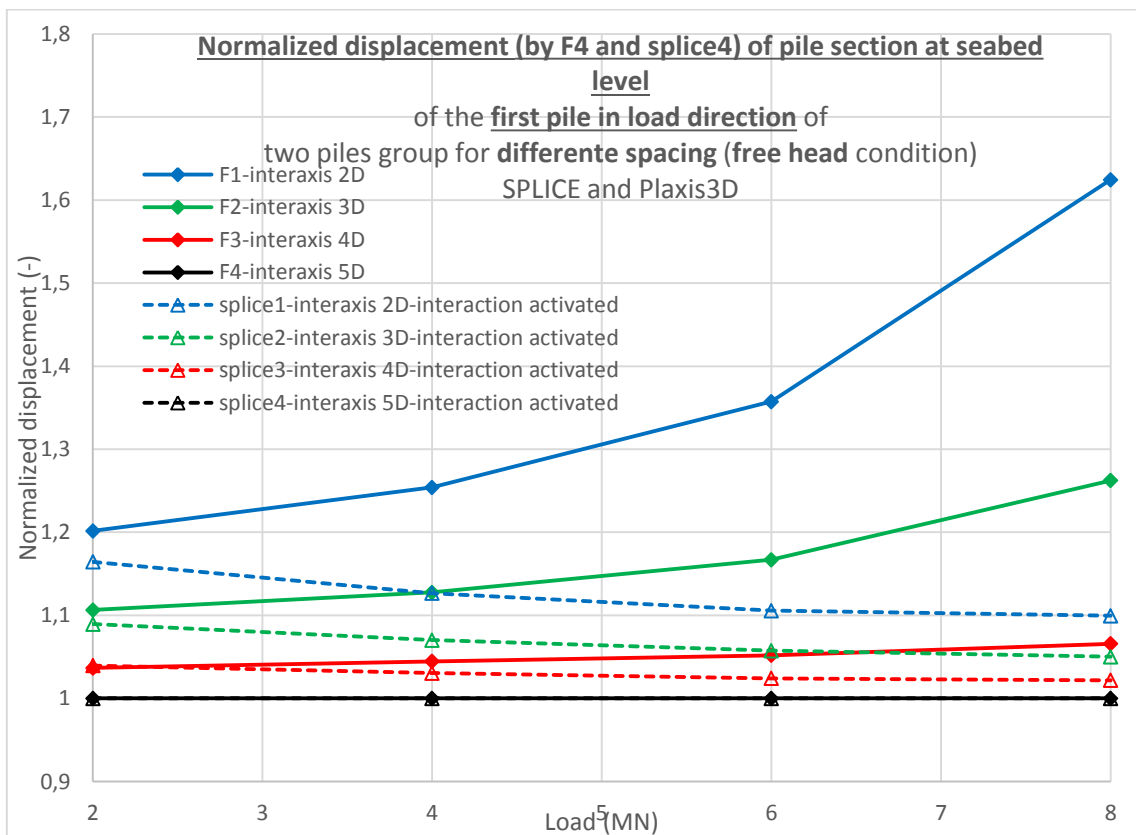
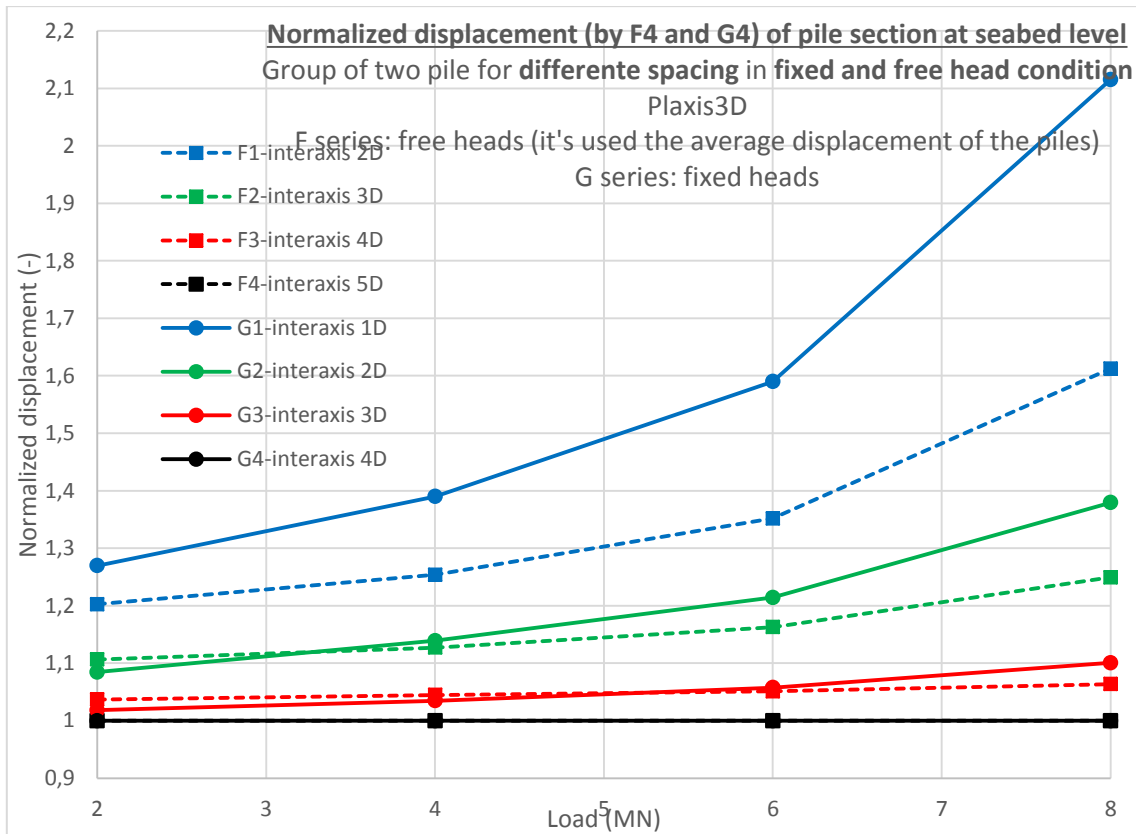


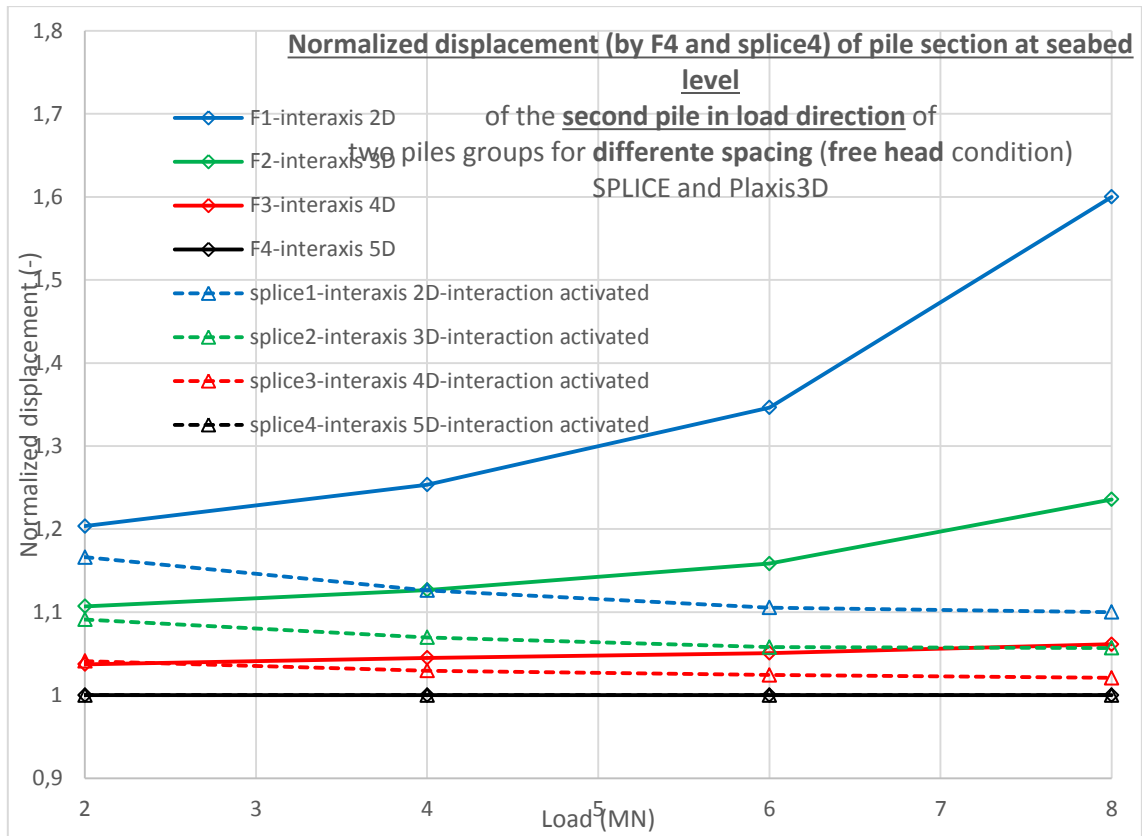




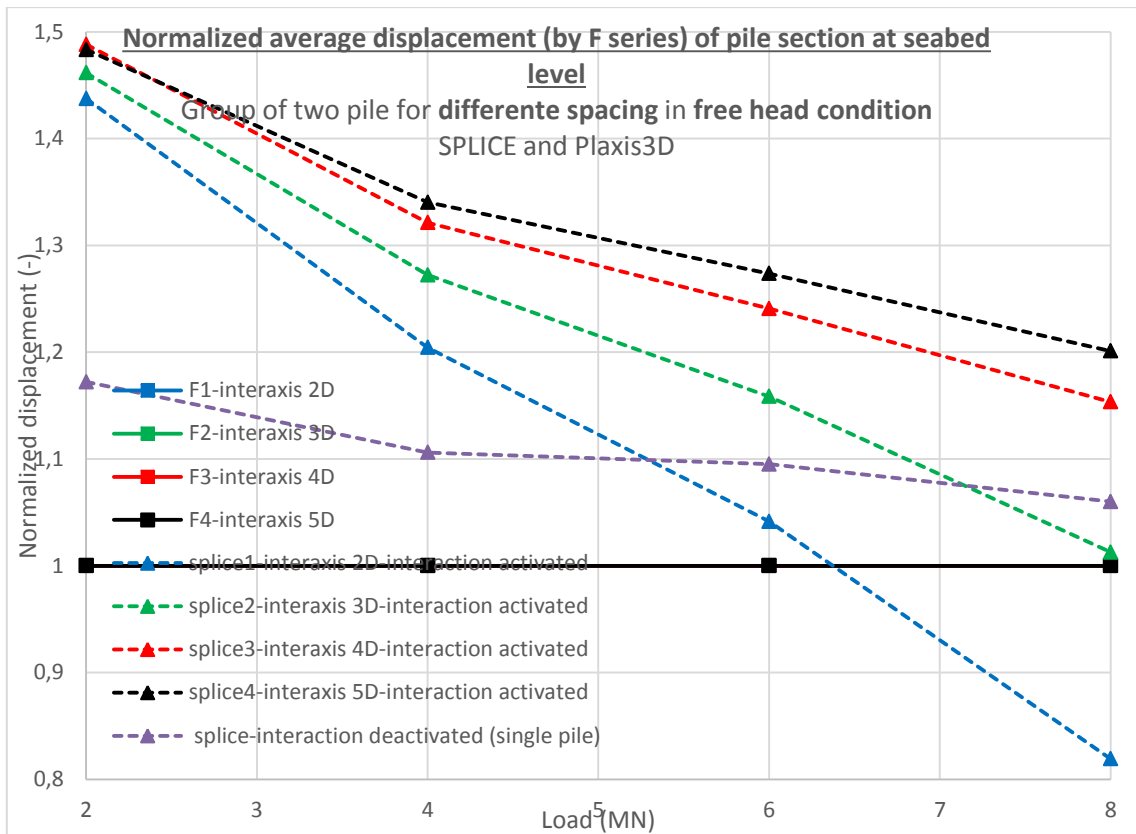
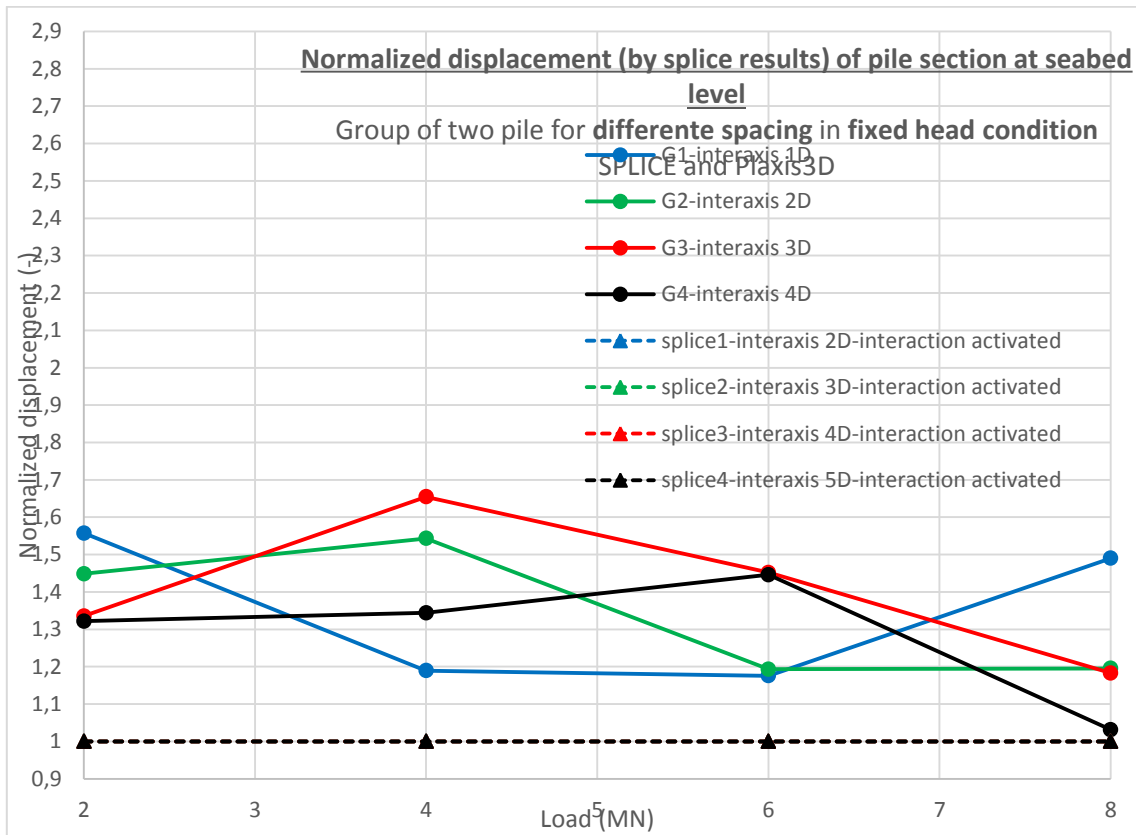
**Normalized head displacements using the maximum interaxis cases (F4-G4)**

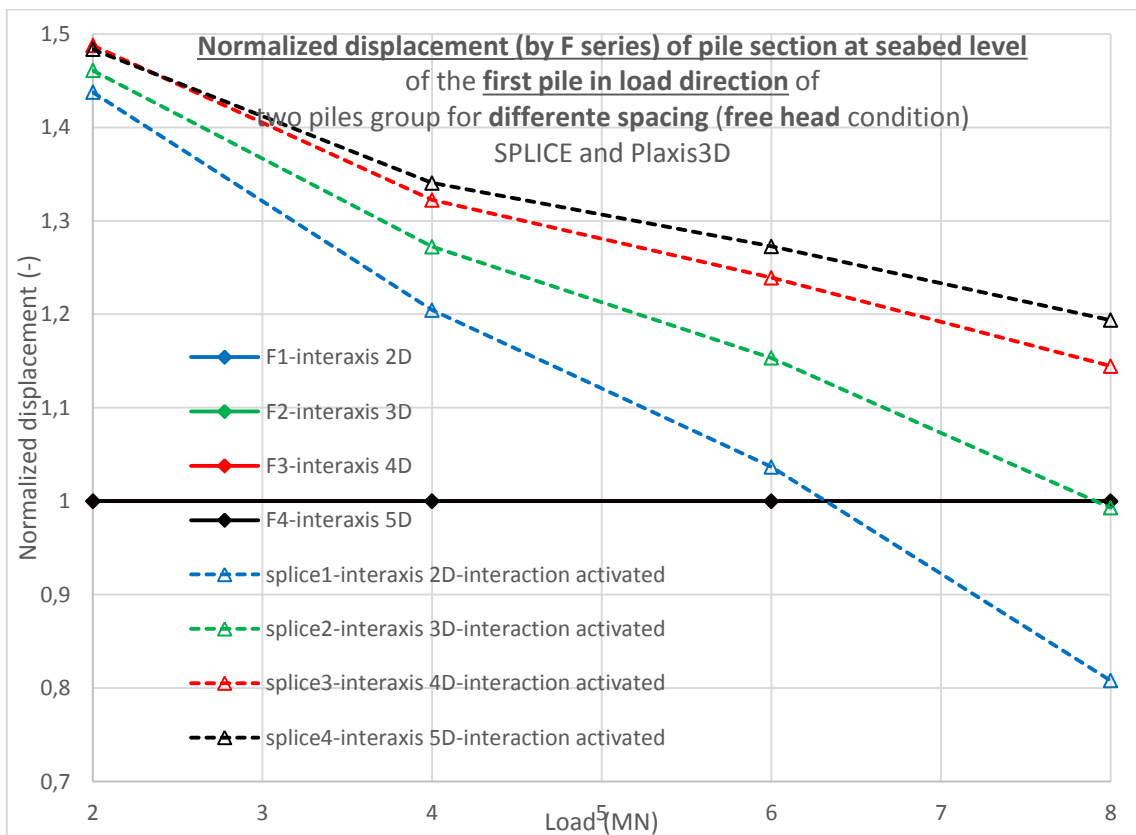
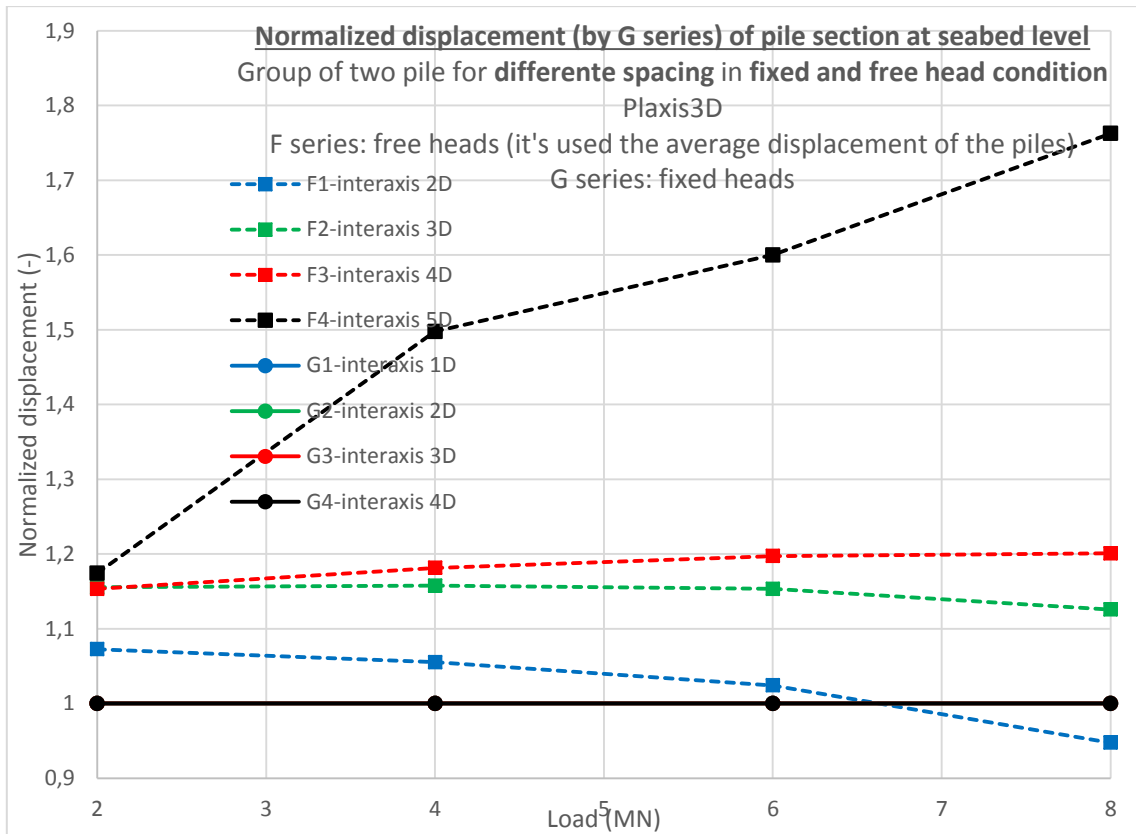


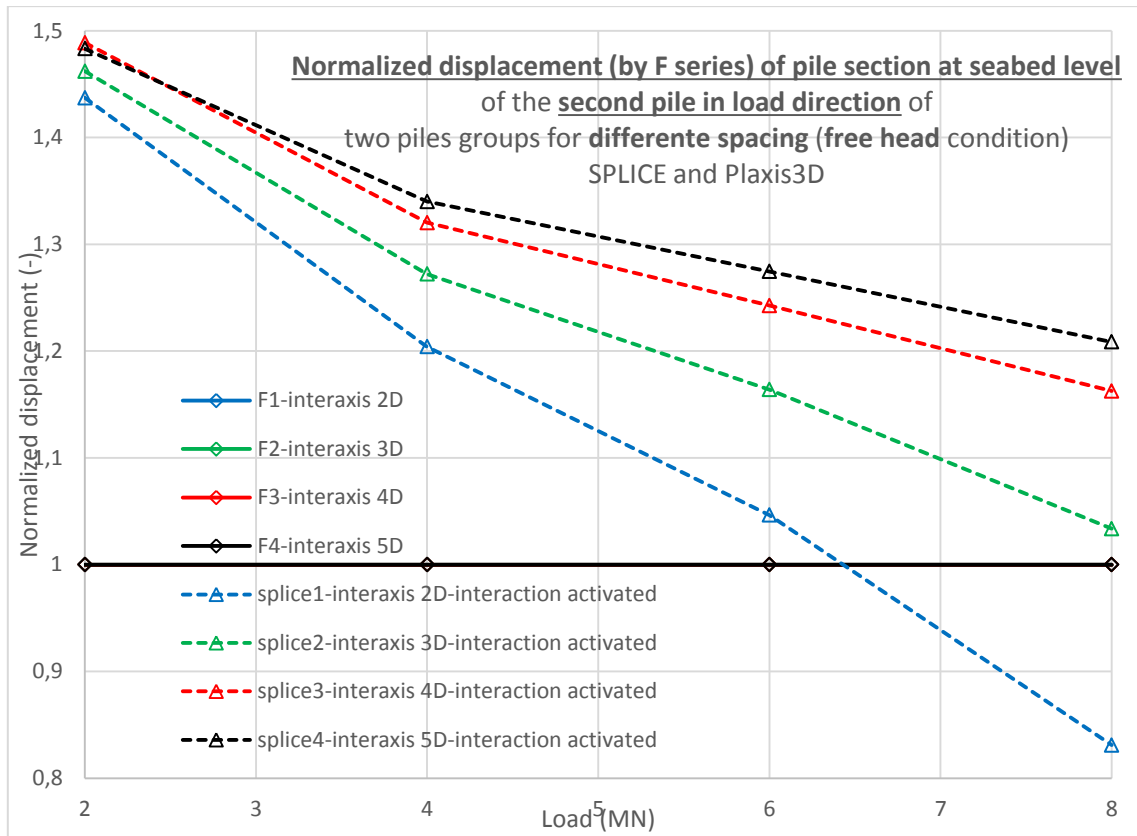




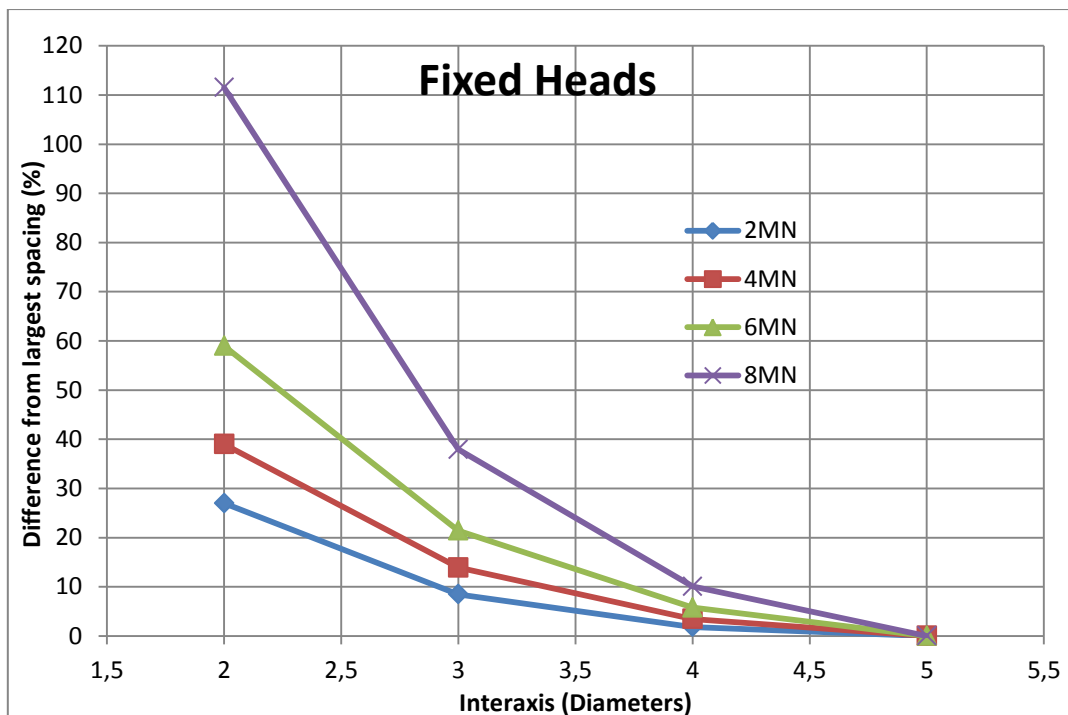
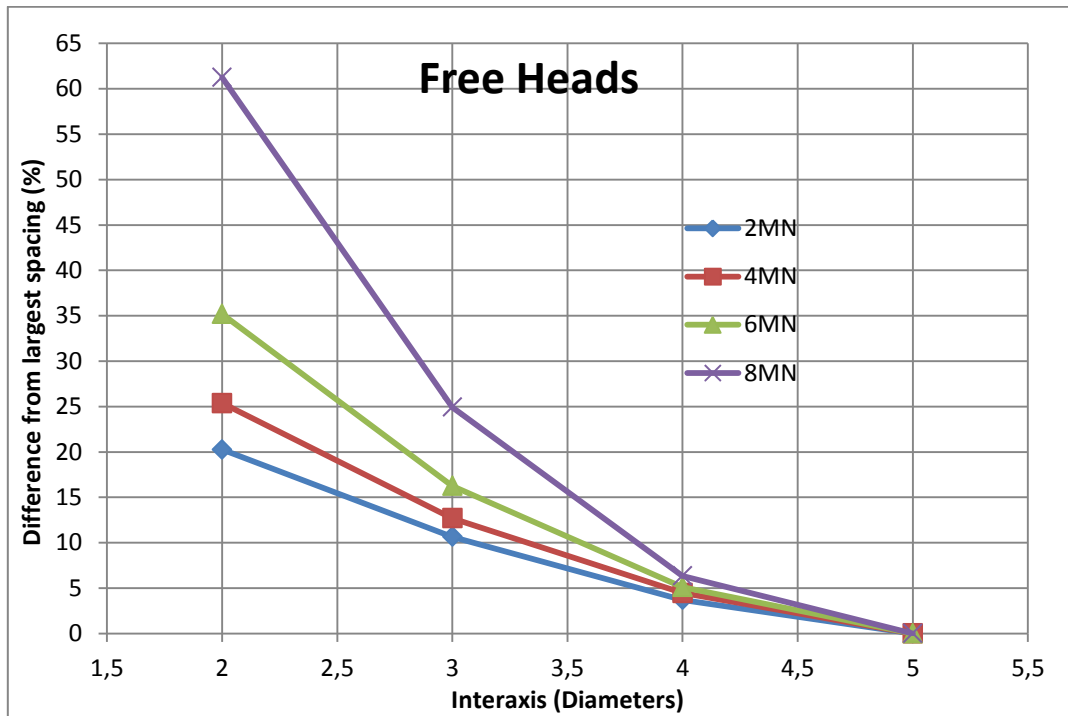
### Normalized head displacements using SPLICE or Plaxis3D results

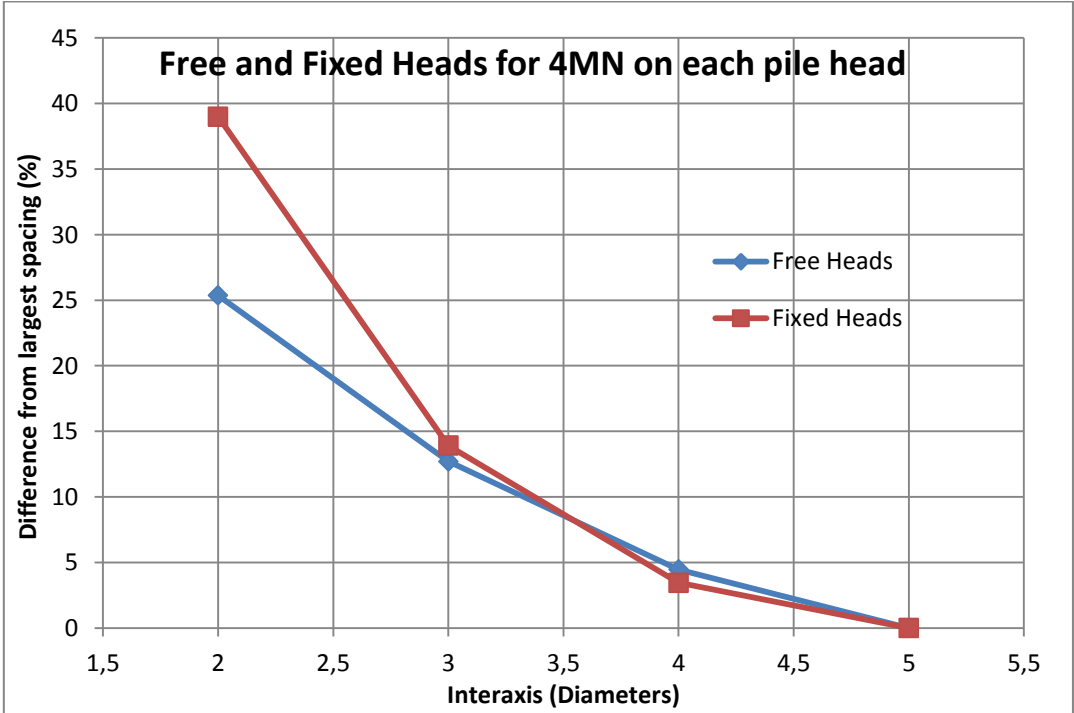
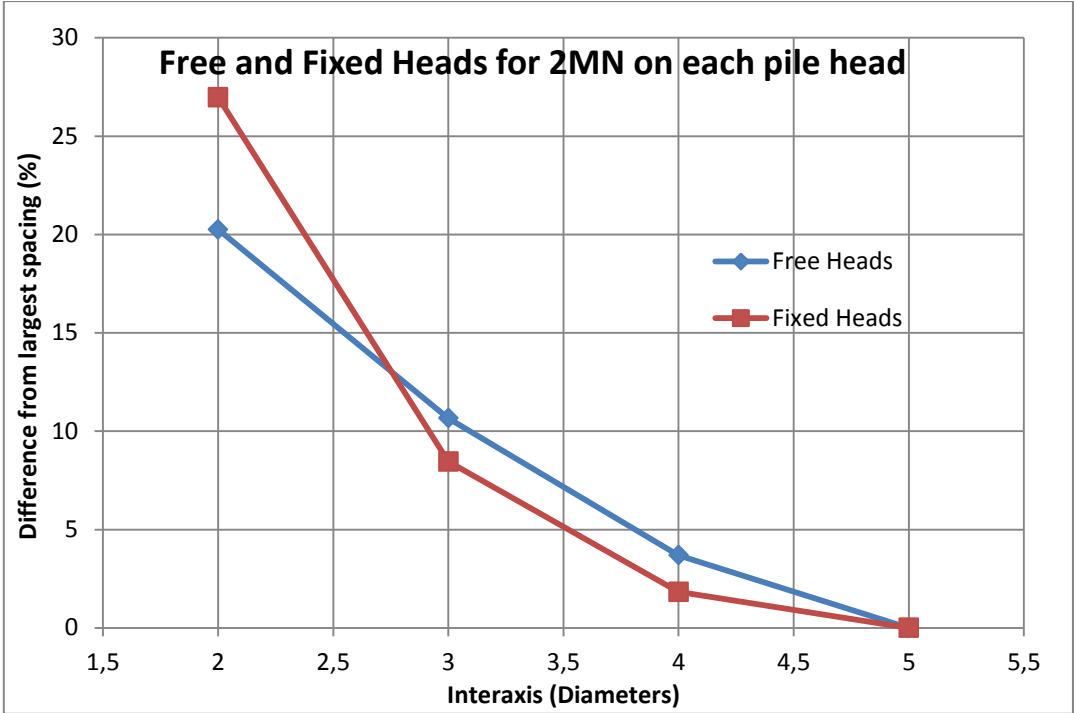


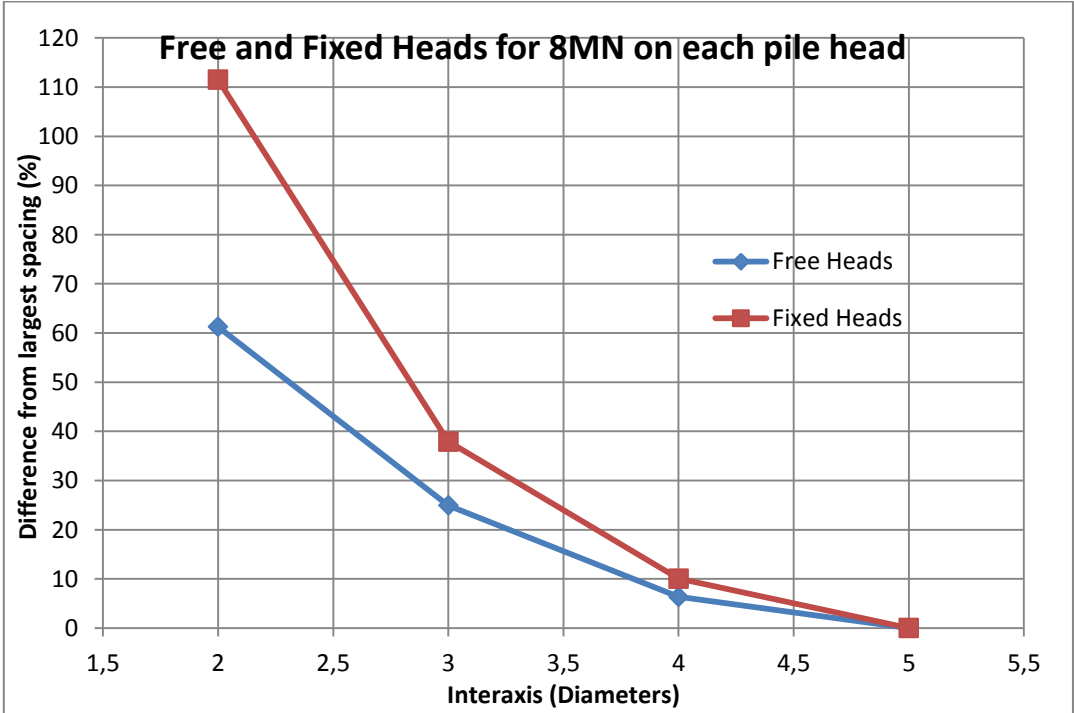
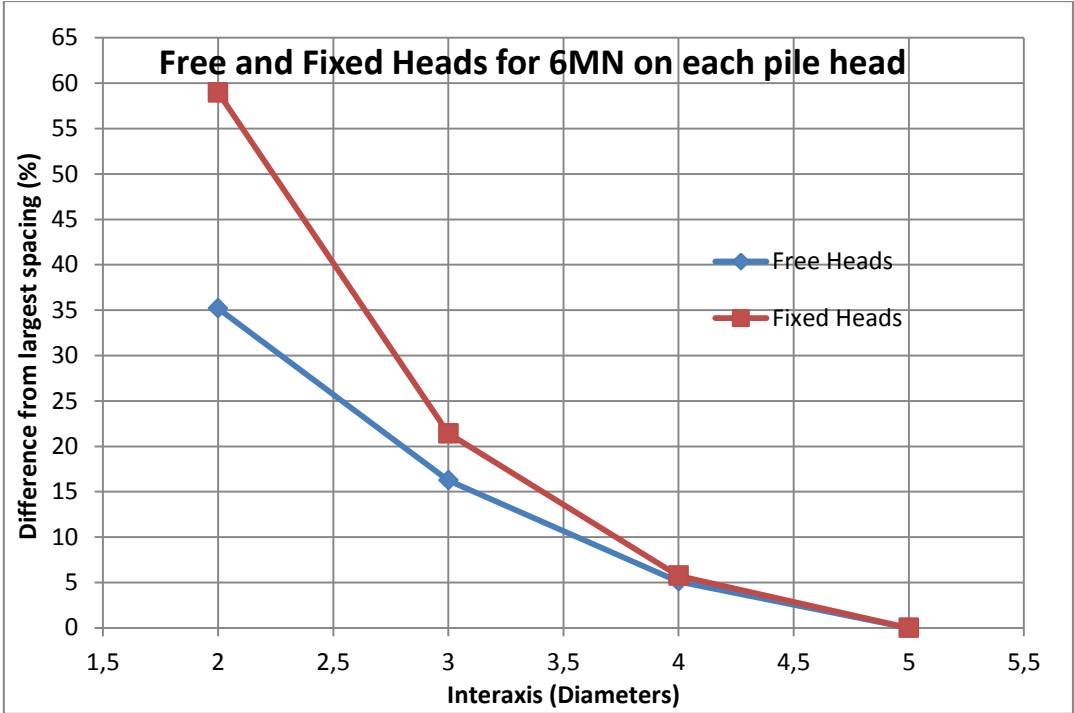


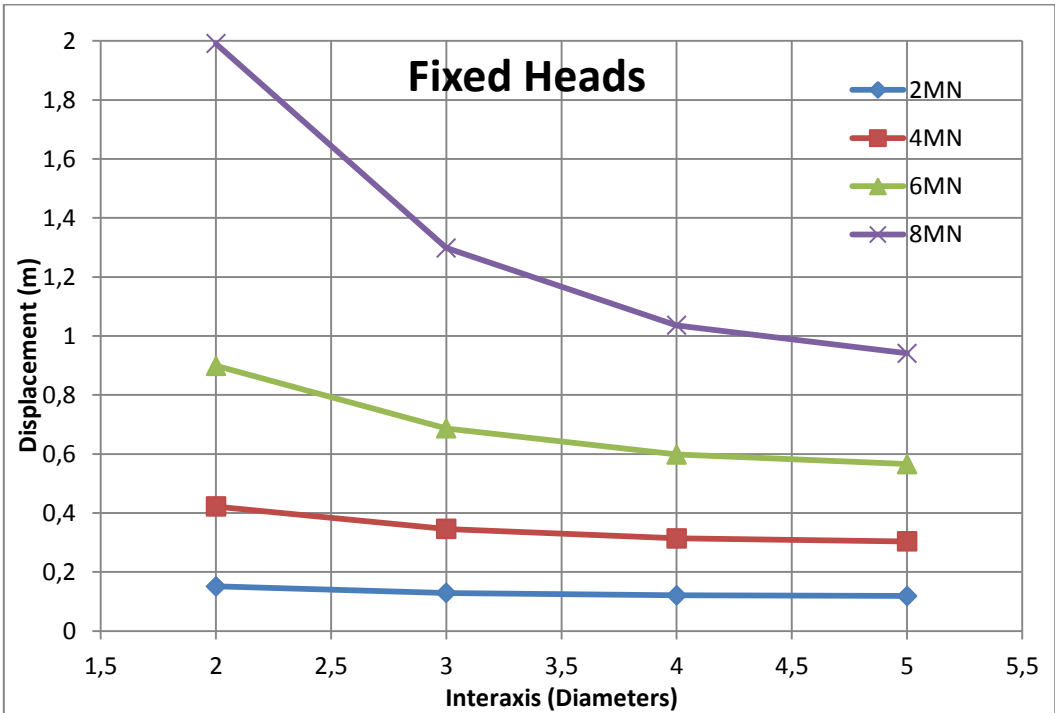
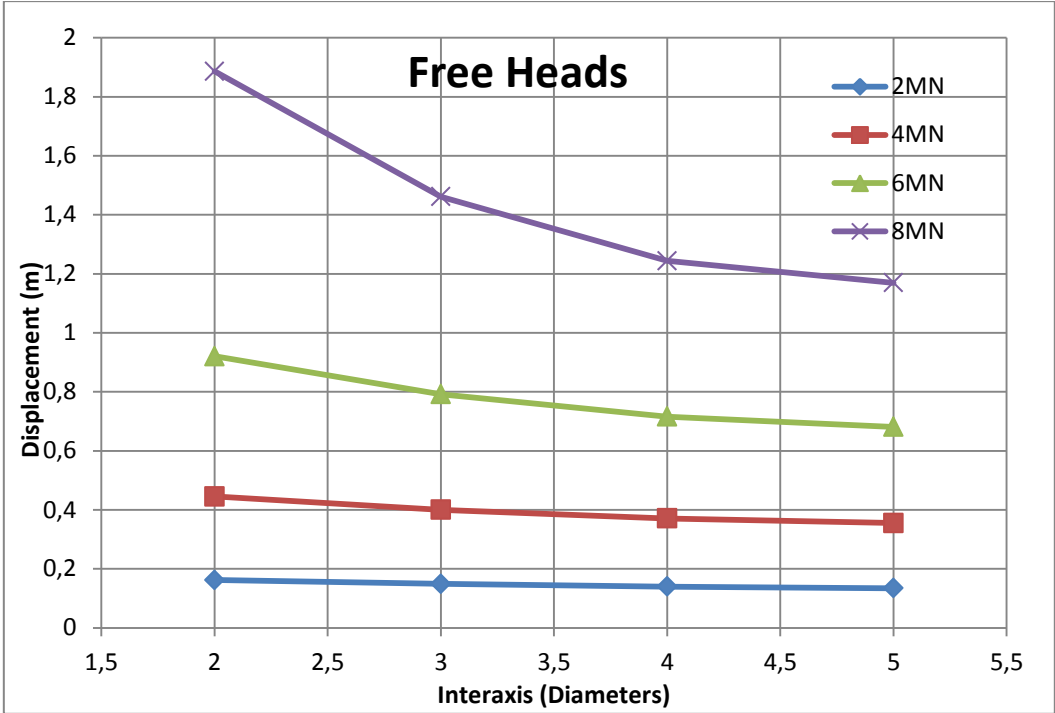


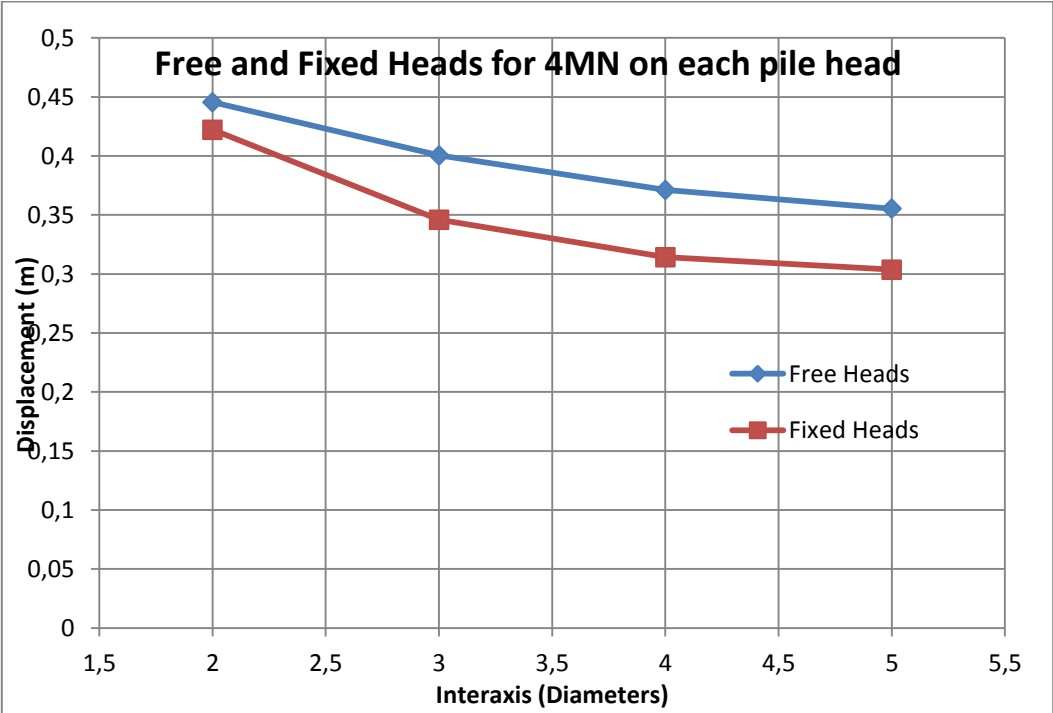
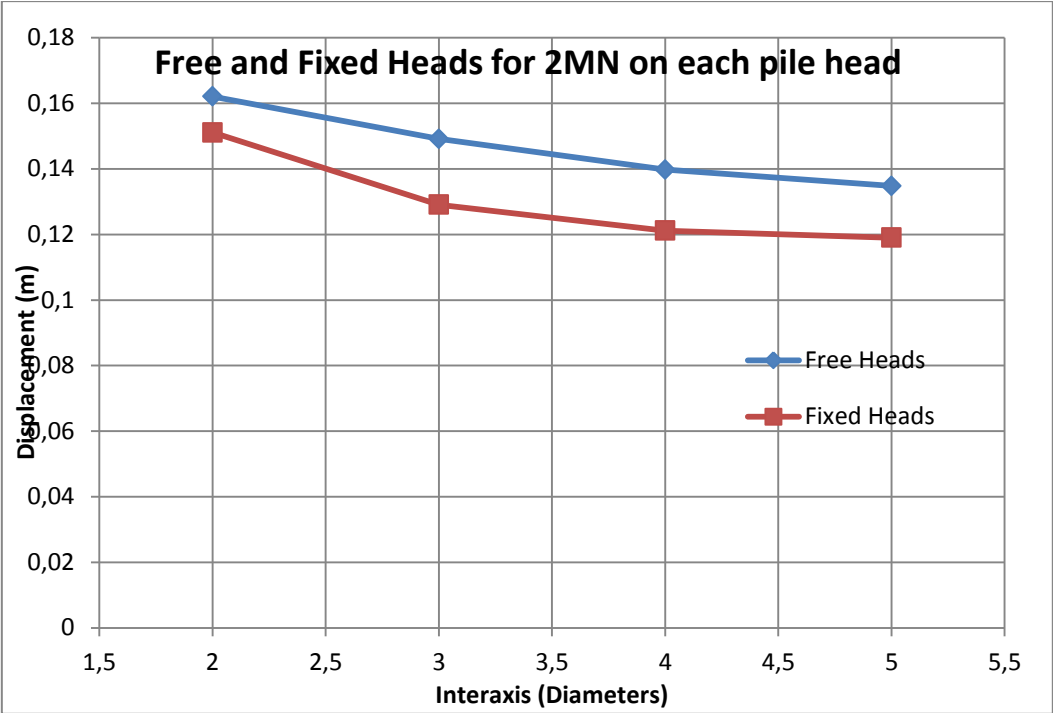
### Head displacements grouped by load

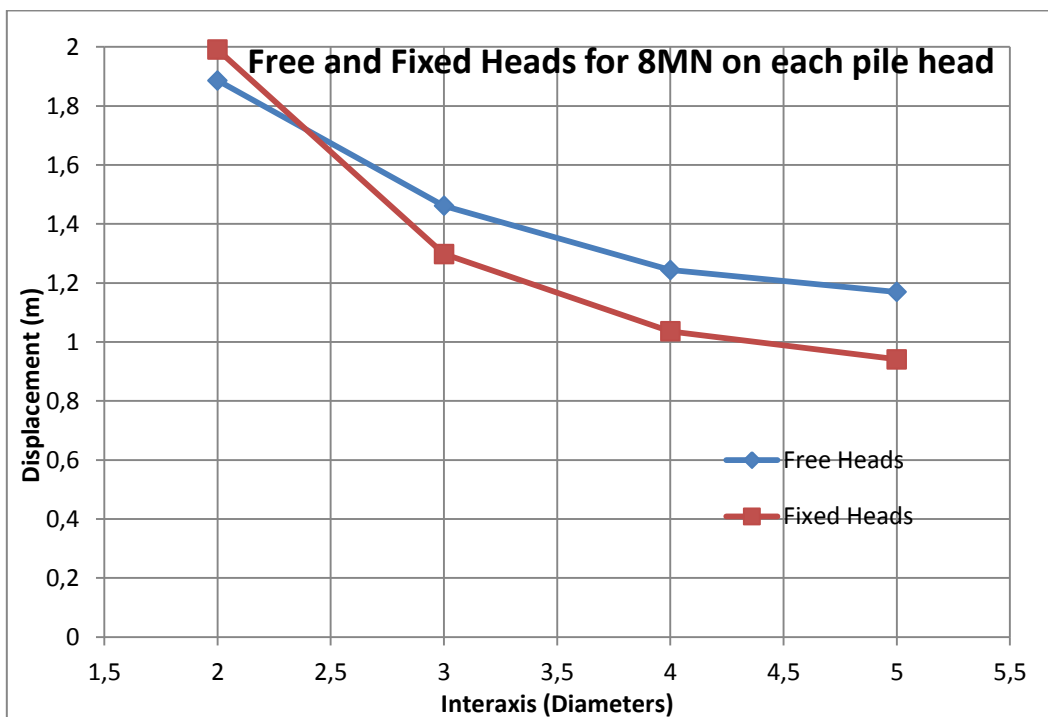
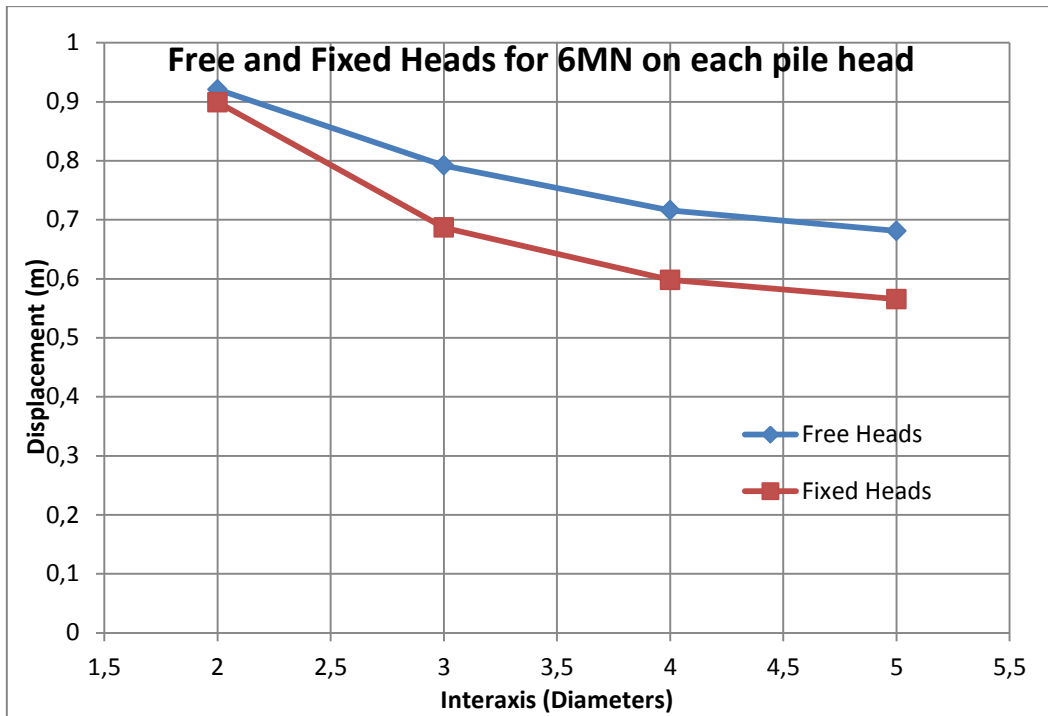












-This page intentionally left blank-